Rosemeyre Amaral Cordeiro

Development of non-viral vectors based on poly(β-amino ester) segments for gene delivery

Coimbra
Junho de 2015

·U· ·C·

UNIVERSIDADE DE COIMBRA

Development of non-viral vectors based on poly(β-amino ester) segments for gene delivery

Rosemeyre Amaral Cordeiro

Thesis submitted in partial fulfillment of the requirements for the degree of Doctor of Philosophy in Chemical Engineering

Supervisors:

Jorge Fernando Jordão Coelho

Arménio Coimbra Serra

Host institution:

Department of Chemical Engineering, Faculty of Sciences and Technology of University of Coimbra

Coimbra

2015

· U C ·

UNIVERSIDADE DE COIMBRA

Financial support:

Acknowledgements

Um trabalho deste âmbito não poderia ser realizado sem a ajuda fulcral de algumas pessoas às quais pretendo manifestar a minha profunda gratidão.

Ao meu orientador, prof. Doutor Jorge Coelho, o meu obrigado por me ter incentivado, confiado e dado a oportunidade de realizar este trabalho de doutoramento, com todas as condições necessárias à sua realização.

Ao meu co-orientador, Doutor Arménio Serra por toda a ajuda e acompanhamento ao longo destes 4 anos. Muito obrigada por todas as sugestões e comentários que foram fundamentais não só no início como durante todo o projecto.

Ao Doutor Henrique Faneca, o meu agradecimento especial pela disponibilidade, simpatia e orientação relativa ao trabalho *in vitro* presente nesta tese.

Ao Doutor Nuno Rocha e à Dina Farinha pela disponibilidade, ajuda e discussão de alguns resultados presentes neste projecto.

Aos meus amigos por terem estado sempre presentes com palavras de apoio e motivação e por todos os momentos bem passados, que tornaram mais fácil ultrapassar todas as dificuldades inerentes a este percurso.

A todos os meus colegas do Grupo de Polímeros agradeço o companheirismo nestes últimos 4 anos.

Ao CIEPQPF e ao CNC um agradecimento especial pela disponibilização dos serviços e laboratórios necessários para a execução das experiências.

E por fim, mas não menos importante, aos meus pais, a minha eterna gratidão pelo esforço, pelo incentivo e por terem sempre apoiado todas as minhas decisões; e às minhas irmãs por estarem sempre presentes ao longo destes anos, mesmo que por vezes longe.

Abstract

Gene therapy has attracted increasing interest over the past few decades as a highly promising therapeutic technique to provide new treatments for a large number of inherited and acquired diseases. However, despite all efforts in this area, the development of a safe and effective delivery of nucleic acids remains a principal challenge to its application in the clinic. In this sense, non-viral vectors have emerged and offer a number of advantages, including facile production, stability, low immunogenicity and toxicity, and higher capacity to carry nucleic acids compared to viral vectors. Nevertheless, current non-viral delivery systems continue far less efficient than viral ones. Among non-viral vectors, cationic polymers have emerged as a promising group for gene delivery.

This thesis is focused on the development of a new and more efficient polymeric non-viral vector based on poly(β-amino ester) (PβAE) and poly[2-(dimethylamino)ethyl methacrylate] (PDMAEMA). The poly[2-(dimethylamino)ethyl methacrylate]-*block*-poly(β-amino ester)-*block*-poly[2-(dimethylamino)ethyl methacrylate] (PDMAEMA-*b*-PβAE-*b*-PDMAEMA) block copolymers were prepared by copper(I)-catalyzed Huisgen azide-alkyne cycloaddition (CuAAC). Their ability to condense and deliver DNA was assessed, firstly, for PDMAEMA$_{8000}$-*b*-PβAE$_{3000}$-*b*-PDMAEMA$_{8000}$ and PDMAEMA$_{3000}$-*b*-PβAE$_{3000}$-*b*-PDMAEMA$_{3000}$ block copolymers in order to study the influence of molecular weight of PDMAEMA segment in transfection capacity. *In vitro* transfection activity was assessed in HeLa and COS-7 cell lines and showed higher activity for polyplexes based on block copolymer prepared with PDMAEMA segment with lower molecular weight (PDMAEMA$_{3000}$-*b*-PβAE$_{3000}$-*b*-PDMAEMA$_{3000}$). In addition, comparing PDMAEMA$_{3000}$-*b*-PβAE$_{3000}$-*b*-PDMAEMA$_{3000}$-based polyplexes transfection results with two of the most used standard transfection reagents, branched PEI 25,000 g.mol^{-1} (bPEI$_{25000}$) and TurboFect^{TM}, revealed higher activity in both cell lines used. However, results also showed that both block copolymer/DNA complexes induced some cytotoxicity for higher nitrogen/phosphate (N/P) ratios. It was hypothesized that could be due to

the residual amounts of copper used during copolymers preparation. To overcome this issue, block copolymers were then prepared by Michael addition reaction (without the need of metal catalysts). In this phase, three block copolymers were prepared differing the molecular weights of central segment (PDMAEMA$_{3000}$-b-PβAE$_{3000}$-b-PDMAEMA$_{3000}$, PDMAEMA$_{3000}$-b-PβAE$_{9000}$-b-PDMAEMA$_{3000}$, PDMAEMA$_{3000}$-b-PβAE$_{12000}$-b-PDMAEMA$_{3000}$). The cell viability after incubation with copolymer/DNA complexes was also assessed in HeLa and COS-7 cell lines, resulting in a notorious increase of cell viability in high N/P ratios. Moreover, *in vitro* transfection assays revealed high transfection activities for all block copolymer tested. From these results, it was concluded that PDMAEMA$_{3000}$-b-PβAE$_{12000}$-b-PDMAEMA$_{3000}$/DNA complexes was the best formulation, showing an increase in transfection activity between 40-fold to 60-fold compared with transfection standard reagents, bPEI$_{25000}$ and TurboFect^{TM}. When compared with the most promising block copolymer synthesized by CuAAC, the PDMAEMA$_{3000}$-b-PβAE$_{12000}$-b-PDMAEMA$_{3000}$ revealed an increase of transfection activity of 5-fold and 9-fold in COS-7 and HeLa cell lines, respectively.

The results presented in this thesis demonstrate that the combination of PDMAEMA and PβAE in a single material disclose interesting physicochemical and biological characteristics making it a very promising material suitable for gene delivery.

Resumo

A terapia génica tem atraído um grande interesse nas últimas décadas como sendo uma técnica altamente promissora para novos tratamentos de um vasto número de doenças hereditárias e não hereditárias. Contudo, apesar de todos os esforços nesta área, o desenvolvimento de uma entrega segura e efectiva continua a ser o principal desafio para a sua aplicação na clínica. Neste sentido, surgem os vectores não-virais que oferecem algumas vantagens, como por exemplo, a fácil produção, estabilidade, baixa imunogenicidade e toxicidade, e grande capacidade de transportar ácidos nucleicos quando comparados com os vectores virais. Todavia, os actuais sistemas de entrega não-virais continuam muito menos eficientes que os virais. Entre os vectores não-virais, os polímeros catiónicos têm surgido como um grupo promissor para a entrega de genes.

O foco desta tese é o desenvolvimento de um novo e mais eficiente vector polimérico não-viral de base poli(ester β-amino) (PβAE) e poli(metacrilato de etilo-2-dimetilamino) (PDMAEMA). Os copolímeros de bloco poli(metacrilato de etilo-2-dimetilamino)-*bloco*-poli(ester β-amino)-*bloco*-poli(metacrilato de etilo-2-dimetilamino) (PDMAEMA-*b*-PβAE-*b*-PDMAEMA) foram preparados por cicloadição de Huisgen azida-alcino catalizada por cobre (I) (CuAAC). A sua habilidade para condensar e entregar DNA foi avaliada, primeiramente, para os copolímeros de bloco PDMAEMA$_{8000}$-*b*-PβAE$_{3000}$-*b*-PDMAEMA$_{8000}$ e PDMAEMA$_{3000}$-*b*-PβAE$_{3000}$-*b*-PDMAEMA$_{3000}$ de modo a estudar a influência do peso molecular do segmento PDMAEMA na capacidade de transfecção. A actividade da transfecção *in vitro* foi avaliada nas linhas celulares HeLa e COS-7 e os poliplexos preparados com o copolímero com segmento de PDMAEMA com menor peso molecular (PDMAEMA$_{3000}$-*b*-PβAE$_{3000}$-*b*-PDMAEMA$_{3000}$) revelaram ter uma maior actividade. Além disso, comparando os resultados da transfecção dos poliplexos de base PDMAEMA$_{3000}$-*b*-PβAE$_{3000}$-*b*-PDMAEMA$_{3000}$ com dois dos mais utilizados padrões de reagentes de transfecção, a PEI ramificada 25,000 g.mol^{-1} (bPEI$_{25000}$) e o TurboFect^{TM}, revelaram uma maior actividade em ambas as linhas celulares

utilizadas. Contudo, os resultados mostraram também que ambos os complexos copolímero/DNA induziam alguma citotoxicidade para maiores razões azoto / fosfato (N/P). Foi hipotetizado que talvez se devesse às quantidades residuais de cobre utilizado aquando da preparação dos copolímeros. Para ultrapassar esta questão, os copolímeros de bloco foram preparados através de reacção de adição de Michael (sem a necessidade de uso de catalizadores metálicos). Nesta fase foram preparados 3 copolímeros de bloco diferindo os pesos moleculares do segmento central (PDMAEMA$_{3000}$-b-PβAE$_{3000}$-b-PDMAEMA$_{3000}$, PDMAEMA$_{3000}$-b-PβAE$_{9000}$-b-PDMAEMA$_{3000}$ e PDMAEMA$_{3000}$-b-PβAE$_{12000}$-b-PDMAEMA$_{3000}$). Após a incubação dos complexos copolímero/DNA a viabilidade celular foi também avaliada nas linhas celulares HeLa e COS-7, resultando num dramático aumento da viabilidade celular nas altas razões de carga copolímero/DNA. Além disso, os ensaios de transfecção *in vitro* revelaram grande actividade de transfecção para todos os copolímeros de bloco testados. A partir destes resultados, concluiu-se que a melhor formulação era para os complexos de base PDMAEMA$_{3000}$-b-PβAE$_{12000}$-b-PDMAEMA$_{3000}$), revelando um aumento na actividade de transfecção entre 40 a 60 vezes superior comparado com os reagentes de transfecção padrão, bPEI$_{25000}$ e TurboFect^{TM}. Quando comparado com o copolímero de bloco mais promissor preparado através de CuAAC, o copolímero de bloco PDMAEMA$_{3000}$-b-PβAE$_{12000}$-b-PDMAEMA$_{3000}$ revelou um aumento da actividade de transfecção de 5 e 9 vezes superior nas linhas celulares COS-7 e HeLa, respectivamente.

Os resultados presentes nesta tese mostram que a combinação do PDMAEMA e PβAE num único material revela características fisico-químicas e biológicas interessantes, fazendo deles promissores materiais para entrega de genes.

List of Publications

Published papers:

RA Cordeiro, N Rocha, JP Mendes, K Matyjaszewski, T Guliashvili, AC Serra and JFJ Coelho. *Synthesis of well-defined poly(2-(dimethylamino)ethyl methacrylate) under mild conditions and its co-polymers with cholesterol and PEG using Fe(0)/Cu(II) based SARA ATRP*. Polymer Chemistry, 2013, 4, 3088-3097, DOI: 10.1039/c3py00190c.

RA Cordeiro, D Farinha, N Rocha, H Faneca, AC Serra and JFJ Coelho. *Novel cationic triblock copolymer of poly[2-(dimethylamino)ethyl methacrylate]-block-poly(β-amino ester)-block-poly[2-(dimethylamino)ethyl methacrylate]: a promising non-viral gene delivery system*. Macromolecular Bioscience, 2015, 15 (2), 215-228, DOI: 10.1002/mabi.201400424.

Published chapters:

AC Fonseca, P Ferreira, **RA Cordeiro**, PV Mendonça, JR Góis, MH Gil and JFJ Coelho. *Drug Delivery Systems for Predictive Medicine: Polymers as Tools for Advanced Applications*. Advances in Predictive, Preventive and Personalised Medicine, Vol. 3. New Strategies to Advance Pre/Diabetes Care: Integrative Approach by PPM. 2013, XVI, p. 399-455, ISBN 978-94-007-5970.

N Rocha, PV Mendonça, JR Góis, **RA Cordeiro**, AC Fonseca, P Ferreira, T Guliashvili, K Matyjaszewski, A Serra and J Coelho. *The Importance of Controlled/Living Radical Polymerization Techniques in the design of Tailor Made Nanoparticles for Drug Delivery Systems*. Drug Delivery Systems: Advanced Technologies Potentially Applicable in Personalised Treatment. Advances in Prediticve, Preventive and Personalised Medicine 4, 2013, XIV, p. 315-357, ISBN 978-94-007-6009-7.

Papers to be published:

RA Cordeiro, D Farinha, H Faneca, AC Serra and JFJ Coelho. *Poly[2-(dimehtylamino)ethyl methacrylate]-block-poly(β-amino ester)-block-poly[2-(dimethylamino)ethyl methacrylate]: the influence of poly(β-amino ester) segment on transfection activity.*

RA Cordeiro, AC Serra and JFJ Coelho. *Poly(β-amino ester)-based non-viral vectors - a promising platform for gene delivery.*

Motivation and Objectives

Over the last decades, the use of nanotechnology approaches for gene delivery, namely nanocarrier systems, has been extensively studied in several areas of medicine. Indeed, the use of the genetic material with no protection in the body can raise problems related mainly to premature degradation, bioavailability, and consequently, fairly efficiency. In this context, it has been reported in the literature different types of gene carriers: viral and non-viral-based. Both have advantages and disadvantages associated. Viral-based carriers have a higher efficiency, however, they present several drawbacks regarding to immunogenecity, difficulty to large production, low loading capacity and high costs of production. The non-viral-based systems, generally, not struggle with these problems but, in return, they have low transfection efficiency and undesirable cytotoxicity. Among them, polymeric-based non-viral vectors have a great potential due to ease and fine tune their physicochemical properties.

Poly(β-amino ester) (PβAE) and poly[2-(dimethylamino)ethyl methacrylate] (PDMAEMA) are two of the most extensively investigated cationic polymers as gene carriers. PβAE is a hydrolytically biodegradable and biocompatible polymer that can be synthesized by Michael addition reaction between primary amine or bis(secondary amine) and diacrylates. PβAE contains easily hydrolyzable esters linkages in their backbone resulting in bis(β-amino acid) and diol fragments. The physicochemical properties of the PβAE, such as charge density, water solubility, crystallinity, and degradation profile, can be adjusted to meet the specific requirements of several applications due to the wide range of amines and diacrylates available as monomers buildings. On the other hand, PDMAEMA could be prepared by a free radical polymerization (FRP) process or by a well-controlled manner through reversible deactivation radical polymerization techniques (RDRP). The use of RDRP techniques permits not only the total control over polymer structure but also polymer functionality, which is impossible by FRP techniques. In spite of both polymers-based polyplexes have relevant values of transfection efficiency, it is not yet enough

to pass to a clinical phase. Thus, it is of prime importance the development of alternative polymeric non-viral vectors that enable the high gene expression to be used efficiently and safely in clinical phase.

This PhD aimed to: (i) the development of novel cationic and biocompatible block copolymers based on PβAE and PDMAEMA; and ii) its use as a non-viral gene delivery system.

1st phase: Synthesis of PDMAEMA-*b*-PβAE-*b*-PDMAEMA

PDMAEMA   PβAE   PDMAEMA-*b*-PβAE-*b*-PDMAEMA

2nd phase: Evaluation of PDMAEMA-*b*-PβAE-*b*-PDMAEMA as gene delivery system

Nucleus
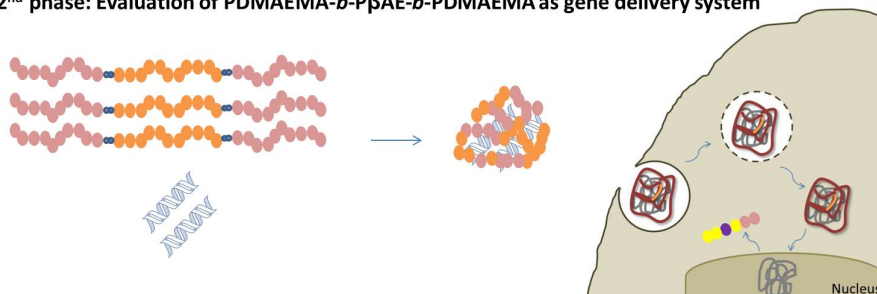
Schematic representation of the work.

Thesis Outline

The main goal of this PhD project was the development of an efficient non-viral vector based on a biocompatible poly[2-(dimethylamino)ethyl methacrylate]-*block*-poly(β-amino ester)-*block*-poly[2-(dimethylamino)ethyl methacrylate] block copolymers using a straightforward synthetic route. The PhD dissertation is organized in five chapters:
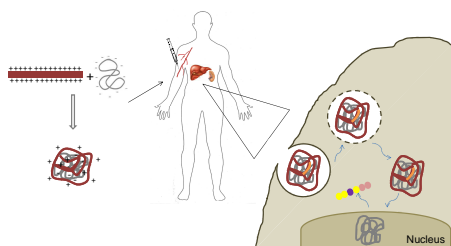

Chapter 1 presents an overview on the importance of polymeric non-viral based gene vectors. In this chapter, special focus is given to the gene carriers based on responsive polymers poly(β-amino ester) and poly[2-(dimethylamino)ethyl methacrylate].
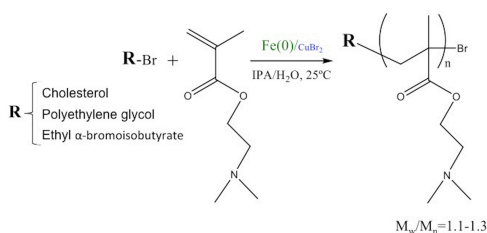
For block copolymer preparation, poly(β-amino ester) was synthesized according to the literature procedures and poly[2-(dimethylamino)ethyl methacrylate] by a new catalytic system known as SARA ATRP. **Chapter 2** describes the synthesis of well-defined poly[2-(dimethylamino)ethyl methacrylate] under mild reaction conditions using Fe(0)/Cu(II) based atom transfer radical polymerization. ATRP of 2-(dimethylamino)ethyl methacrylate was also extended to synthesis of functional bio-relevant polymers with cholesterol and poly(ethylene glycol) segments.
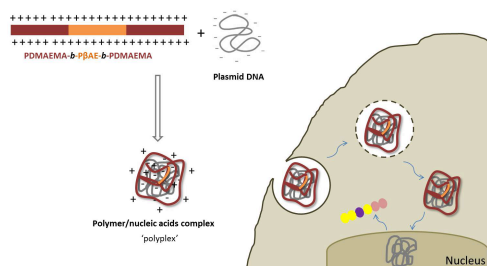
Chapter 3 reports the synthesis and characterization (physicochemical and biological) of a novel dual pH- and temperature-responsive polycationic tri-block copolymer (poly[2-(dimethylamino)ethyl methacrylate]-*block*-poly(β-amino ester)-*block*-poly[2-(dimethylamino)ethyl methacrylate]) prepared by copper(I)-catalyzed Huisgen azide-alkyne 1,3-dipolar cycloaddition click chemistry approach. The preliminary studies for the use of these new block copolymer as a plasmid DNA carrier was assessed.
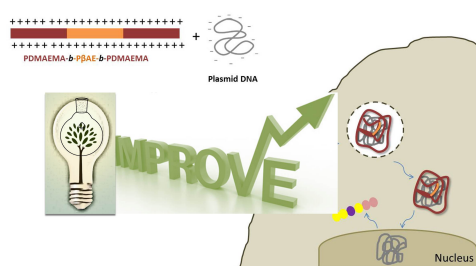
Chapter 4 introduces a new and 'green' procedure based on Michael addition reaction for poly[2-(dimethylamino)ethyl methacrylate]-*block*-poly(β-amino ester)-*block*-poly[2-(dimethylamino)ethyl methacrylate] preparation. It also discusses the influence of the molecular weight of poly(β-amino ester) in physicochemical properties on the block copolymer/nucleic acid complex in *in vitro* transfection assays, and how these parameters can be used to tune the mentioned properties.

Chapter 5 presents the most relevant conclusions from this PhD research, along with further recommendations on future work and some final remarks.

List of Abbreviations

AFM	Atomic force microscopy
APTES	γ-Aminopropyl-triethoxysilane
ARGET	Activators regenerated by electron transfer
ASO	Antisense oligonucleotide
ATRP	Atom transfer radical polymerization
BBiB	α-Bromoisobutyryl bromide
Bcl-2	B-cell lymphoma-like protein 2
bPEI	Branched poly(ethyleneimine)
bpy	2,2'-Bipyridine
BSA	Bovine serum albumin
BTIC	Brain tumor initiating cell line
CHO	Cholesterol
CLSM	Confocal laser scanning microscopy
CME	Clathrin-mediated endocytosis
COS-7	African green monkey kidney fibroblast-like cell line
CRL 1764	Rat fibroblasts cell line
CTA	Chain transfer agent
CuAAC	Copper-catalyzed azide-alkyne cycloaddition
DB	Degree of branching
DC 2.4	Murine dendritic cell line
DCM	Dichloromethane
DDS	Drug delivery system
DHB	2,5-Dihydroxybenzoic acid
DMA	*N,N*-dimethylacetamide
DMAEMA	2-(dimethylamino)ethyl methacrylate
DMAP	4-Dimethylaminopyridine
DMEM-HG	Dulbecco's modified eagle's medium - high glucose
DMF	*N,N*-dimethylformamide
DMSO	Dimethylsulfoxide

DNA	Deoxyribonucleic acid
DOTMA	*N*-[1-(2,3-dioleyloxy)propyl]-*N*,*N*,*N*-trimethylammonium chloride
DP	Degree of polymerization
DT	Degenerative transfer
DT-A DNA	Plasmid DNA that carries the gene for the A segment of the diphtheria toxin
DV	Differential viscometer
eATRP	Electrochemically-mediated atom transfer radical polymerization
EBiB	Ethyl 2-bromoisobutyrate
ECM	Extracellular matrix
EDTA	Ethylenediaminetetraacetic acid
eGFP	Enhanced green fluorescent protein
EPR	Enhanced permeability and retention
EtBr	Ethidium bromide
FTIR-ATR	Fourier transform infrared - attenuated total reflection spectroscopy
FRP	Free radical polymerization
F98	Rat glioma cell line
GB	Glioblastoma
GCV	Prodrug ganciclovir
GFP	Green fluorescent protein
hADSCs	human adipose-derived stem cell line
HEK 293	Human embryonic kidney
HeLa	Human epithelial cervical carcinoma cell line
Hep G2	Human hepatocellular carcinoma cell line
hESCds	Human embryonic stem cell-derived cell line
HIV	Human immunodeficiency virus
hMSCs	Bone marrow-derived human mesenchymal stem cell line
HMTETA	1,1,4,7,10,10-Hexamethyltriethylenetetramine
HSV-tk	Herpes simplex virus type I thymidine kinase
HUVEC	Human umbilical vein endothelial cell line
H446	Human lung carcinoma cell line
ICAR	Initiators for continuous activator regeneration

I.p.	Intraperitoneal
IPA	Propan-2-ol
ITP/RITP	Iodide/reverse iodide transfer polymerization
I.v.	Intravenous
LALLS	Low-angle laser-light scattering
LNCaP	Androgen-sensitive human prostate adenocarcinoma cell line
MALDI-TOF MS	Matrix-assisted laser desorption ionization time-of-flight mass spectroscopy
MCP-1	Monocyte chemotactic protein 1
MDA-MB 231	human triple negative breast cancer cells
miRNA	Micro ribonucleic acid
mPEG	Poly(ethylene glycol) monomethyl ether
NMP	Nitroxide-mediated polymerization
NPC1	Niemann-pick C1 protein
N/P	Nitrogen/phosphate ratio
PβAE	Poly(β-amino ester)
PAA	Poly(acrylic acid)
PBS	Phosphate-buffered saline
PCL	Polycaprolactone
PEG	Poly(ethylene glycol)
PEGDA	Poly(ethylene glycol) diacrylate
PEHO	Poly[3-ethyl-3-(hydroxymethyl)-oxetane]
PEI	Poly(ethyleneimine)
PEM	Polyelectrolyte multi-layers
PDMAEA	Poly[2-(dimethylamino)ethyl acrylate]
PDEAMA	Poly[2-(diethylamino)ethyl methacrylate]
PDMAEMA	Poly[2-(dimethylamino)ethyl methacrylate]
PDMAEMAm	Poly[2-(dimethylamino)ethyl methacrylamide]
PDMAPMA	Poly[3-(dimethylamino)propyl methacrylate]
PDMAPMAm	Poly[3-(dimethylamino)propyl methacrylamide]
pDNA	Plasmid deoxyribonucleic acid

pHSV-tk	Plasmid containing the herpes simplex virus type I thymidine kinase gene
piRNA	Piwi interacting ribonucleic acid
PKCδ	δ Isoform of protein kinase C
PLL	Poly(L-lysine)
PMAA	Poly(methacrylic acid)
PMDETA	(N,N,N',N'',N''-pentamethyldiethylenetriamine)
PNIPAAm	Poly(N-isopropylacrylamide)
PS	Polystyrene
PTFE	Poly(tetrafluoroethylene)
PTMAEMA	Poly[2-(trimethylamino)ethyl methacrylate chloride]
PTX	Paclitaxel
P388 D1	Murine macrophage cell line
RAFT	Reversible addition-fragmentation chain transfer
RALLS	Right-angle laser-light scattering
RDRP	Reversible deactivation radical polymerization
RES	Reticuloendothelial system
RI	Refractive index
RNA	Ribonucleic acid
RNAi	Ribonucleic acid interference
RNase A-R9	Ribonuclease A-R9
SARA	Supplemental activator and reducing agent
SEC	Size-exclusion chromatography
SET-LRP	Single electron transfer living radical polymerization
SFRP	Stable free radical polymerization
shRNA	Short hairpin ribonucleic acid
siRNA	Small interfering ribonucleic acid
sPSS	Sodium poly(styrene sulfonate)
TEA	Triethylamine
THF	Tetrahydrofuran
TMEDA	N,N,N',N'-tetramethylethylenediamine
TMS	Tetramethylsilane

TP53	Tumor protein p53
TPP	Triphenylphosphine
TSA	BALB/c female mouse mammary adenocarcinoma cell line
UCST	Upper critical solution temperature
VP	*N*-vinyl-2-pyrrolidone
^{1}H NMR	Proton nuclear magnetic resonance
^{13}C NMR	Carbon nuclear magnetic resonance
293T	Derived human embryonic kidney cell line
3T3-L1	Mouse embryonic fibroblast cell line
9L	Rat nitrosourea induced gliosarcoma cell line

Nomenclature

$Đ$	Dispersity
dn/dc	Refractive index increment
IC_{50}	Half maximal inhibitory concentration
k_{act}	Activation rate constant
k_{deact}	Deactivation rate constant
m/z	Mass-to-charge ratio
M_n	Number-average molecular weight
M_w	Weight-average molecular weight

Contents

List of Figures

List of Schemes

List of Tables

CHAPTER 1

Introduction

This chapter contains essential information for understanding the subsequent chapters enclosed in this thesis. It does not aim to provide, however, a comprehensive revision of all the subjects herein presented.

The part of this chapter will be submitted to publication: 'Poly(β-amino ester)-based gene delivery materials'.

1.1 Controlled delivery systems

1.1.1 Drug delivery systems

Human pharmaceutical treatments started decades or even centuries ago (for example, aspirin in 1828)[1]. These treatments required repeated administrations to maintain the drug level in the body. Despite the effectiveness of the treatments, drug concentration in the body alternates between therapeutic and sub-therapeutic drug levels between administrations. The difficulty to control the drug concentration within the therapeutic window for a long period of time constitute one of the most important drawback of the conventional way of drugs administration. In this sense, it was developed the so-called drug delivery systems (DDS) where features, such as, the rate and period of time of release can be controlled to reach therapeutic level and enhance the treatment performance[2]. Folkman and Long, in 1964[3], were the pioneers using silicone rubber as a carrier for sustained delivery of low molecular weight compounds in animal tests. After that, and until today, thousands of papers have been reported dealing with this area[4–8]. The use of a DDS aims to promote an efficient delivery of a biologically active compound maintaining the drug concentration in the body within therapeutic level. This goal is achieved using drug carriers, normally polymers (both synthetic and natural) whose physicochemical properties could be tailored in order to improve the DDS efficiency. The use of a good DDS present several advantages, such as, the bioavailability of the drug (controlling the therapeutic payload), the extension of the duration of delivery, protection the drug from biochemical degradation and overcoming solubility issues (mainly for hydrophobic drugs)[9]. However, DDS disadvantages are also well-known, particularly the potencial toxicity of the materials used to produce the carriers and the high cost of final formulations.

Currently, one of the the main focus/challenge in research on DDS is the targeted delivery to specific cells/tissues in response to selected biomarkers in order to enhance the effectiveness of the treatments[9;10].

1.1.2   Gene delivery systems

Gene therapy emerged as a promising method to treat or to eliminate the causes of disease whereas most drug-based approaches only treat symptoms[11]. This strategy could be mainly useful to treat some inherited and acquired diseases involving genetic factors, such as hemophilia, muscular dystrophy, cystic fibrosis, wound healing, cancer, cardiovascular, neurological and infectious diseases[12]. The concept of gene therapy arose during the late 1960s and early 1970s with recent acquired knowledge from *in vitro* transformation of mammalian cells using a virus-based method and with the advent of recombinant DNA technology[13;14]. The *in vitro* and *in vivo* demonstration of the possibility of efficient phenotype correction turned gene therapy a broadly accepted approach to correct genetic defects and diseases, opening the door to studies in human patients[14]. The basic concept of gene therapy is the delivery and transfer of genetic material into specific cells of the patient to alter the expression of existing genes, that will result in either a cure or a slowdown in the progression of the disease[15]. To reach these goals, gene therapy requires technologies capable of gene transfer, in a safe and effective mode, into a wide variety of cells[15;16]. The gene delivery systems, known as vectors, should overcome a number of barriers in order to promote an efficient gene delivery into target cells[15].

The first approved clinical study in gene therapy began in 1989, by Rosenberg[17], where it was studied the first gene-marking protocol of tumor-infiltrating lymphocytes. In 1990, with Blaese[18], it was approved the first clinical trial using a therapeutic gene that was introduced in peripheral blood T lymphocytes of patients with severe combined immunedeficiency. Since that period, numerous human genes, directly associated with diseases states, and different types of vector, available to carrier those genes, have been studied and assessed. However, until nowadays, the safety and/or efficiency of the different gene delivery systems remain the major challenges for their translation to the clinic phase (Figure 1.1).

Glybera® (uniQure), in 2012, became the first gene therapy treatment approved for clinical use in Europe by European Comission[20;21]. Glybera was developed for the treatment of lipoprotein lipase deficiency. The first commercial treatments are expected to be conducted in the first half of 2015 in Germany and the price of a
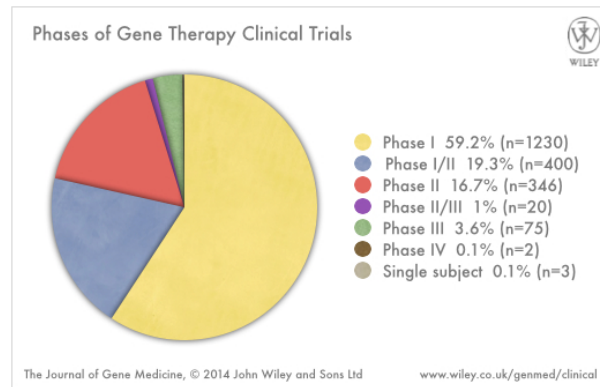
Figure 1.1: Gene therapy clinical trials in different phases in 2014 (provided by the Journal of Gene Medicine[19])

complete treatment will be close to €1.0 million[20;22].

1.1.2.1 Therapeutic agents and gene delivery vectors

In gene therapy strategies, there are two main components, the carrier (gene delivery vector) and the therapeutic agent (nucleic acids). Concerning the therapeutic agent, one of the most widely studied is the plasmid DNA (pDNA) containing therapeutic transgenes. However, RNA interference (RNAi) strategies have been also explored recently for this purpose, mainly small interfering RNAs (siRNAs), microRNAs (miRNAs), short hairpin RNAs (shRNAs), piwi interacting RNAs (piRNAs) and antisense oligonucleotides (ASOs). Although having common properties, pDNA and RNAi face different delivery challenges as a result of differences in the size and stability of the formed nucleic acid complexes and in the location and mechanism of action[23]. Regarding gene delivery vectors, they can be generally divided into viral and non-viral ones (Table 1.1)[24]. Non-viral vectors can be divided into two main groups: physical-based methods (mainly electroporation, microinjection and hydrodynamic injection) and chemical-based vehicles (mainly lipid- and polymer-based)[25].

The main differences between viral and non-viral vector will be discussed below.

1.1.2.2 Viral gene delivery vectors

Viral vectors, as suggested by the name, are systems derived from viruses. They can be divided in two main groups: integrating and non-integrating vectors. Integrat-

Table 1.1: Gene delivery vectors.

Viral vectors	Non-viral vectors	
	Physical methods	**Chemical-based vehicles**
Adenovirus	Electroporation	Lipid-based
Adeno-associated virus		
Lentivirus	Microinjection	Polymer-based
Retrovirus		
Herpes simplex virus	Hydrodynamic injection	
Pox virus		

ing vectors insert the transgene into the recipients genome, while non-integrating normally form an extrachromosomal genetic element[13]. Integrating vectors hold the promise of efficient and lifelong expression of the deficient gene product. On the other hand, a transient but also efficient gene transduction can be reached with non-integrating viral vectors[15]. Examples of integrating vectors are gamma-retroviral vectors that are used to transduce actively dividing cells and lentiviral vectors that transduce actively dividing and non-dividing cells. As non-integrating vectors examples, there are adenoviral vectors and adeno-associated virus that are typically used to transduce quiescent or slowly dividing cells[13]. Viral vectors are the most effective vectors for gene transfer[16], especially for primary cells[26]. The choice of a particular vector includes many factors, such as packing capacity, its host range, its gene expression profile or its tendency to elicit immune responses (Table 1.2)[13].

Table 1.2: Some examples of viral gene delivery vectors[13;16;26].

	Adenovirus	Adeno-associated virus	Vaccinia virus
Genome	dsDNA	ssDNA	dsDNA
Infection/tropism	Dividing and non-dividing cells	Dividing and non-dividing cells	Dividing and non-dividing cells
Host genome interaction	Non-integrating	Non-integrating	Non-integrating
Transgene expression	Transient	Potential long lasting	Transient
Packing capacity	7.5 kb	4.5 kb	25 kb
	Retrovirus	**Lentivirus**	**Herpesvirus**
Genome	ssRNA+	ssRNA+	dsDNA
Infection/tropism	Dividing cells	Dividing and non-dividing cells	Dividing and non-dividing cells
Host genome interaction	Integrating	Integrating	Non-integrating
Transgene expression	Long lasting	Long lasting	Potential long lasting
Packing capacity	8 kb	8 kb	>30 kb

Concerning therapeutic agents, the most commonly RNA viral vectors are de-

rived from retroviruses and can be classified into oncoretroviruses, lentiviruses, and spuma viruses. Regarding DNA viral vectors, the most common are adenovirus, adeno-associated virus and herpesvirus[15].

Retroviruses were the first vectors used in gene therapy clinical trials but, over the years, they have been losing importance due to a not random insertion pattern, preferring the first introns of genes and transcriptional start sites[27]. Actually, adenoviruses has been the most commonly used vector in the clinic trials[19]. The main advantages of this type of vector are: the possibility of carrying a larger DNA load (but still small to accommodate the genes required for certain clinical applications); to be able to infect non-dividing cells; to have a high efficiency of transduction and a high level of gene expression (although this is temporary and decay relatively fast)[27]. Indeed, viral vectors are highly efficient as gene carriers, however they have some weaknesses, namely concerning safety issues. They can cause host immune and inflammatory reactions and they have the potential to form replication-competent virions, as well as to induce tumorigenic mutations and generate active viral particles through recombination. They present also problems related to large-scale manufacture, insert-size limitation of foreign transgenes and expensive production costs[25;28;29]. Recently, strategies that reduce pathogenicity and immunogenicity, promote site-specific integration and allow regulation of transgene expression have been developed and showed to improve their safety concerns[25].

1.1.2.3 Non-viral gene delivery vectors

Non-viral vectors emerged as an alternative to viral ones in cases of viral delivery is problematic or when it is necessary repeated administrations (increasing the risk of an immune response to a viral antigen). Despite being less efficient than viral vectors, non-viral vectors offer several important advantages, such as: low immunogenicity or inflammatory reactions; no insert-size limitation; absence of endogenous virus recombination; construction flexibility; facile fabrication; low production cost; and reproducibility[24;30]. As referred above, non-viral vectors can be sub-divided in two main groups: physical- or chemical-based methods[13]. However, as physical-based methods have inefficient gene transfection, the chemical-based methods are

the most used. Some advantages of chemical-based non-viral vectors are that they could be produced in relatively large amounts and can be designed to be negligibly antigenic, presenting minimal toxic or immunological problems compared to viral ones[15]. Therefore, lipid- and polymer-based complexes formed with nucleic acid have been successfully used to transfer different types of nucleic acids. Until the delivery of the nucleic acid at the target site, complexes need to overcome various extracellular and intracellular barriers[12] (Figure 1.2).
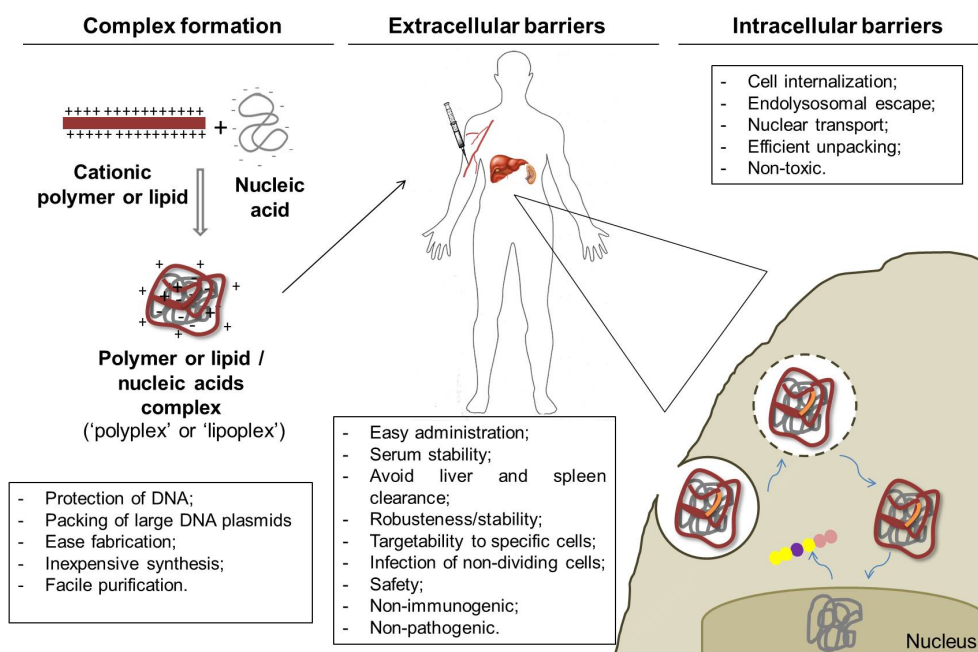
Figure 1.2: Main challenges to be taken into consideration in the design of non-viral vectors.

Following, cationic lipid-based and cationic polymer-based non-viral vectors will be discussed in more detail.

1.1.2.3.1 Cationic lipids

The use of cationic lipids for nucleic acids delivery began in the middle of 1980s[31]. A large variety of different cationic lipids have been synthesized to be used as gene carrier, however, in spite of tidy rational design, the efficiency of transfection remains far away comparatively to viral counterparts[32]. Cationic lipids are amphiphilic molecules constituted by a hydrophilic and positively charged headgroup linked by a spacer (linker) to a hydrophobic lipid anchor (Figure 1.3)[25;28]. The three components influence the final structure of the cationic lipid[25], although it is the charged

headgroup that governs transfection efficiency[28]. The nature (structure and shape of cationic headgroup) and charge density are the two of the main headgroup characteristics that can be used to improve the design of efficient cationic lipids. Some examples of headgroups of cationic lipids are: quaternary ammoniums; primary, secondary, tertiary amines; guanidiniums; heterocyclics; amino acids and peptides[25;28].
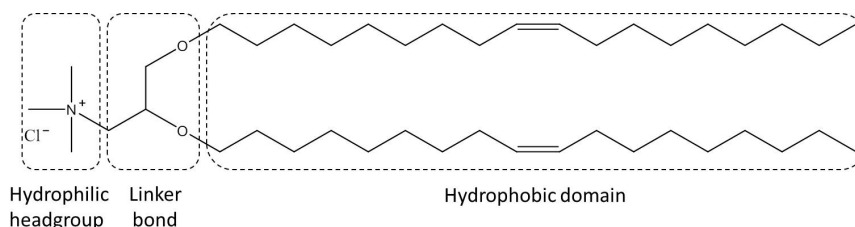
Figure 1.3: Representative structure of a typical cationic lipid (*N*-[1-(2,3-dioleyloxy)propyl]-*N,N,N*-trimethylammonium chloride (DOTMA)).

The polar hydrophilic headgroups interact electrostatically with the negatively charged phosphate groups of the nucleic acids and during the self-assembly process, nucleic acids enwrap with the amphiphilic molecules in a multilamellar fashion. The complexes formed are known as lipoplexes[25;32] (Figure 1.4).
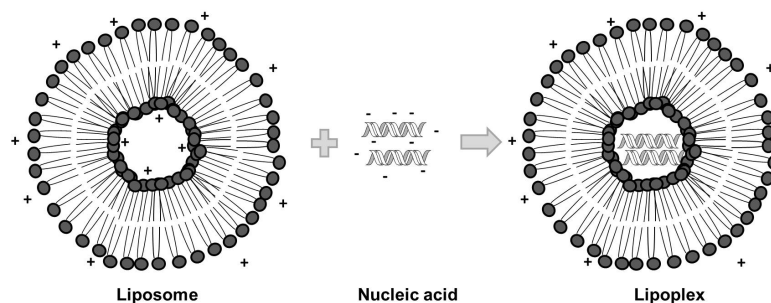
Figure 1.4: Cationic lipids forming micellar structures called liposomes. Liposomes are complexed with nucleic acids to create lipoplexes.

The structure of cationic lipid influences the packing of the plasmids. It is known, that the larger the hydrophilic headgroup the greater is the trend of the cationic lipid to form micelles instead of vesicles[32]. The lipoplex assembly remains to be clarified. The nature of its early interaction with the cell surface has been explained as dependent of electrostatic interactions, before entry into the cells. The major disavantadges of their application *in vivo* are the low transfection efficacy when compared to viral vectors, as mentioned above, relative colloidal instability and high susceptibility towards clustering in circulation[32].

1.1.2.3.2   Cationic polymers

Cationic polymers have attracted growing interest to gene material delivery due to relative facility to fine tune their physicochemical properties using a portfolio of strategies (by varying the chemical composition, molecular weight, or architecture), which can provide multiple functions[29]. In general, the positive charges of cationic polymers (nitrogen atoms) interact electrostatically with the negative charges of nucleic acids (phosphate groups) forming polyelectrolyte complexes particles generally denoted by polyplexes (Figure 1.2). These interactions should be enough to protect genetic material from nucleolytic enzymes but, at the same time, to allow an efficient delivery of the genetic material into target site.

Actually, despite many efforts, the low gene transfection efficiency and the cytotoxicity of the polymeric-based non-viral vectors have greatly limited their clinical applications. The lack of efficiency is, apparently, due to a deficient of capacity to overcome some of the many extra- and intracellular gene delivery obstacles[24] (Figure 1.2). It is known that cationic polymers induce cytotoxicity, however, its mechanism remains not yet fully understood[29]. It is thought that cytotoxicity may be related with the molecular weight and the cationic charge density, which are key parameters for the interaction with cell membranes, and as a consequence, for causing cell damage[29;33]. To address the improvement in transfection efficiency and cytotoxicity various modifications in cationic polymers have been explored, including the introduction of poly(ethylene glycol) (PEG), specific targeting moieties (for instance, sugar molecules, antibodies, aptamers, growth factors, vitamins, transferrin, and hormones)[29;30;34] or hydrophobic segments[29]. From these different strategies, the modification with hydrophobic segments has displayed promising results[29]. It is believed, that the hydrophobic chains affect not only the interaction with cell membrane (favoring endocytosis mechanisms) but also, all gene delivery process (that includes, increased physical encapsulation of genetic materials, enhanced binding to cell membrane, promotion of complex charge inversion, facilitation of gene dissociation from polycation carriers, alleviation of serum inhibition, effects on cytotoxicity and targeting-specificity)[29]. From its first application as non-viral vector in 1965 by Vaheri and Pagano (using diethylaminoethyl functionalized dextran)[35], a large

range of cationic polymers have been used. Among them, chitosan, poly(L-lysine) (PLL), poly[2-(dimethylamino)ethyl methacrylate] (PDMAEMA), poly(ethylenimine) (PEI) and, more recently, poly(β-amino ester) (PβAE) have been the most studied polymers in this application[24;36;37]. Branched PEI (25,000 g.mol^{-1}) (bPEI$_{25000}$) has been considered the gold standard due to its relatively high transfection efficiency[38]. However, it exhibits serious limitations due to its toxicity[39]. Some commercial polymer-based transfection reagents are already available in the market. Examples included TurboFect^{TM} (Fermentas), FuGENE® HD (Promega), iN-fect^{TM} (JH Science), TransIT® (Mirus), GenJet^{TM} (SignaGen® Laboratories), jetPEI^{TM} (PolyPlus Transfection^{TM}), among others, varying depending the type of therapeutic agent used and the type of assay (for example, *in vitro*, *in vivo*, or high throughput screening). In this project, bPEI$_{25000}$ and TurboFect^{TM} will be used for comparison purposes (Chapters 3 and 4)

1.2 Poly(β-amino ester)

1.2.1 Brief historical background of poly(β-amino ester)

Poly(β-amino ester)s, a class of biodegradable cationic polymers, were firstly prepared by Chiellini in 1983[40]. These polymers were based on poly(amidoamine)s developed in 1970 by Ferruti[41], which contain tertiary amines in their backbones and can be synthesized by simple Michael addition reaction. However, the interest in the use of poly(β-amino ester)s rised significantly after its use as transfection reagent at Langer Lab in 2000[42]. The synthesis of this polymer can easily be accomplished without: the preparation of specialized monomers; the use of stoichiometric amounts of coupling reagents, or amine protection strategies prior to polymerization[42].

In fact, poly(β-amino ester) approach exhibited a particularly attractive basis for the development of new polymer-based transfection vectors for several reasons: the polymers contain the required positive charges to complex genetic material; readily degradable linkages (by hydrolysis of ester bonds in the polymer backbones may increase the biodegradability and biocompatibility); and several structures could be synthesized directly from commercially available compounds allowing, in an very

easy way, the possibility to tune polymer properties (for example, buffering capacity)[42].

Besides being used as transfection vector, PβAEs has been also applied in others biomedical areas, such as delivery systems for drugs[43;44] or proteins[45;46], magnetic resonance imaging agents[47;48], or as scaffolds for tissue engineering[49;50].

1.2.2 Synthesis and main physicochemical properties of poly(β-amino ester)s

The PβAEs are easily synthesized by the conjugate addition of a primary amine or bis(secondary amine) and a diacrylate, in a one-step reaction without any side products that needed to be removed through further purification steps. It can be prepared without solvents, catalysts, or complex protecting group strategies[42;51].
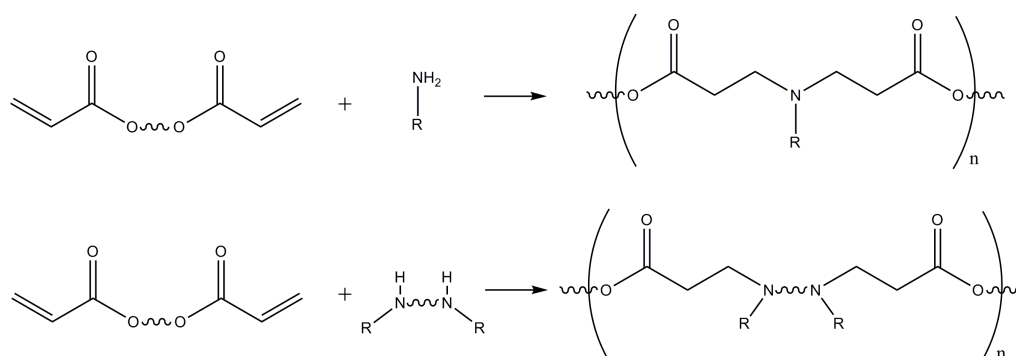
Figure 1.5: Strategies to synthesize poly(β-amino ester)s. The synthesis occurs by the conjugate addition of primary (a) or bis(secondary amine) (b) to diacrylates.

Depending on the excess of monomers during the synthesis, PβAEs can be tailored to have either amine- or diacrylate-terminated chains[52;53].

The synthesis can be carried out either neat (solvent free) or in anhydrous organic solvents to mitigate hydrolytic degradation during synthesis[42;54]. Generally, experiments using solvents occur at lower temperature and over long periods of time compared to solvent-free formulations. Table 1.3 summarizes some different strategies for the synthesis of PβAE and the obtained properties such as molecular weight, polydispersity index ($Đ$), solvent solubility or yield.

The most common solvents used are dimethylsulfoxide (DMSO), chloroform

Table 1.3: Some different strategies for the synthesis of PβAE.

Amine	Diacrylate	Reaction conditions [a]	PβAE's main features	Ref.
N,N'-dimethylethylenediamine Piperazine 4,4'-trimethylenedipiperidine	1,4-butanediol diacrylate	[diamine] = [1,4-butanediol diacrylate] = 0.38 M Anhydrous THF 50 °C, 48 h	$0 < M_n < 30{,}800$ $1.55 < Đ < 2.15$ $0 <$ Yield (%) < 82 Soluble in THF, CH_2Cl_2, $CHCl_3$, MeOH and acidic water	42
N,N'-dimethylethylenediamine Piperazine 4,4'-trimethylenedipiperidine	1,4-butanediol diacrylate	[diamine] = [1,4-butanediol diacrylate] =1.08 M Anhydrous CH_2Cl_2 50 °C, 48 h	$5{,}800 < M_n < 31{,}200$ $2.37 < Đ < 2.83$ $55 <$ Yield (%) < 86 Soluble in THF, CH_2Cl_2, $CHCl_3$, MeOH and acidic water	42
4,4'-trimethylenedipiperidine	1,4-butanediol diacrylate	[diamine] = [1,4-butanediol diacrylate] =1.08 M Anhydrous CH_2Cl_2 50 °C, 48 h	$T_g = 49.8$ °C	55
4,4'-trimethylenedipiperidine	1,4-butanediol diacrylate	[diamine] = [1,4-butanediol diacrylate] =1.08 M Anhydrous CH_2Cl_2 50 °C, 48 h	Slow degradation rate at acidic pH ($t_{1/2} > 10$ h at pH = 5.1, 37 °C) $M_n = 10{,}000$	56
1-butamine 1-aminohexane 2-ethyl-1-hexylamine 2-aminoethanol 4-amino-1-butanol 6-amino-1-hexanol 2-(2-aminoethoxy)ethanol 2-amino-1-butanol 2-dimethylaminoethylamine 3-dimethylaminopropylamine 2-morpholinoethylamine 3-morpholinopropylamine 1-(2-aminoethyl)piperidine 3-(1H-imidazol-1-yl)propan-1-amine 1-cyclopropylmethanamine 1-cyclohexylmethanamine (tetrahydrofuran-2-yl)methanamine Piperazine 4,4'-trimethylenedipiperidine	1,3-butanediol diacrylate 1,4-butanediol diacrylate 1,6-hexanediol diacrylate 2,2'-oxybis(ethane-2,1-diyl) diacrylate Triethylene glycol dimethacrylate 1,3-phenylene diacrylate cyclohexane-1,4-diylbis(methylene) diacrylate	Methylene chloride 45 °C, 5 days	$2{,}000 < M_n < 50{,}000$ $1.16 < Đ < 6.91$	51,57
4,4'-trimethylenedipiperidine	1,4-butanediol diacrylate	THF, 50 °C, 48 h	$M_{n,SEC} = 10{,}000$ $Đ = 2.1$ Yield ~85 % 85% of degradation in 6 days in PBS (pH 7.4) at 37 °C	58
1-(2-aminoethyl)piperazine N-ethylethylenediamine N-methyl-1,3-propanediamine 4-(aminomethyl)piperidine Piperazine	Ethylene diacrylate Poly(ethylene glycol) diacrylate, n = 6, 8 or 14	DMSO, DMA, $CHCl_3$, H_2O, DMF or NMP 35–40 °C, 120–150 h	$85.4 <$ Yield (%) < 92.7 $15{,}680 < M_w < 21{,}360$ $1.28 < Đ < 1.38$ Solubility in water > 0.35 g/mL $15 < T_g$ (°C) < 45 $58.3 < DB < 75.5$	59
1-(2-aminoethyl)piperazine	1,4-butanediol diacrylate	Chloroform, 45 °C, ~72h	$M_w = 5{,}126$ $Đ = 1.52$	60

[a] M_n - number average molar mass, g.mol⁻¹; M_w - weight-average molar mass ; $Đ$ - dispersity; DB - ratio of branched units and terminal units to the total units; DMSO - dimethylsulfoxide; DMA - N,N-dimethylacetamide; $CHCl_3$ - chloroform; DMF - N,N-dimethylformamide; NMP - N-methyl-2-pyrrolidone); MeOH - methanol; THF - tetrahydrofuran; CH_2Cl_2 - dichloromethane

(CHCl$_3$), or dichloromethane (CH$_2$Cl$_2$)[57]. However, others solvents have also been used, such as methanol, *N,N*-dimethylformamide (DMF) or *N,N*-dimethylacetamide (DMA)[59;61–63]. The solvent used has influence on the final molecular weight of the PβAE. For example, the use of CH$_2$Cl$_2$ typically yields higher molecular weight polymer compared to THF[42].

On the other hand, solvent-free polymerizations maximize monomer concentrations, thus favoring the intermolecular addition over intramolecular cyclization reaction[64]. The absence of solvent also allows rising temperature resulting in a higher reaction rate and a lower viscosity of the reacting mixture, assisting to compensate the higher viscosity found on the solvent-free systems. The combination of an increase in monomer concentration and reaction temperature results in a reduction in the reaction time[64]. The solvent-free reactions also allows the generation of higher molecular weight polymers and the solvent removal step during purification process[53;64].

After polymerization, PβAE is precipitated, in cold diethyl ether, hexane[42], ether[65] or ethyl ether[58] and/or then dried under vacuum[57;65]. Frequently, PβAEs are immediately used or stored in cold conditions (4 °C[52;66;67], 0 °C[62], or -20 °C[68–70]). Some PβAEs should be also kept airproof due to its strong moisture absorption ability and easy degradation[71].

Concerning the biodegradation and biocompatibility, generally PβAEs have been shown to possess low cytotoxicity and good biocompatibility[42;52;55;61;72]. Different studies have suggested that PβAEs are significantly less toxic than other available cationic polymers, such as, PEI and PLL[51;64]. Nevertheless, the increase of the number of carbons in the backbone or side chain is associated to the increase of cytotoxicity[73]. PβAE degrade under physiological conditions via hydrolysis of their backbone ester bonds to yield small molecular weight and biologically inert derivatives (β-amino acids)[42;51;55;74]. Some results revealed that the degradation rate of PβAEs is highly dependent on the hydrophilicity of the polymer, wherein the more hydrophilic the polymer is, the faster the degradation process[75;76].

In Table 1.4 are summarized the main characteristic of PβAEs which make them a promising polymeric non-viral vector for gene delivery.

Table 1.4: Summary of the main characteristics of poly(β-amino ester)s which make them a promising gene carrier.
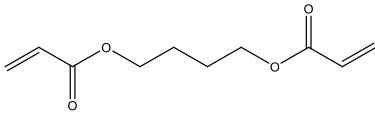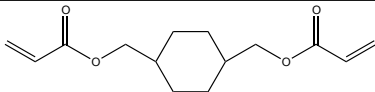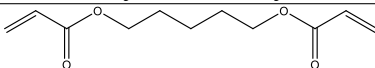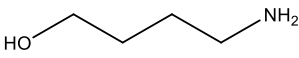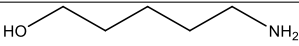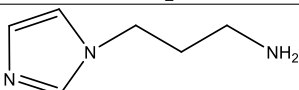
Characteristics of poly(β-amino ester)s suitable for gene carrier
Easy synthesis and commercially available monomers
Facile tune structure using different monomers or easy post-modification chemistry
Absence of byproducts
Good buffer capacity (endossomal escape)
pKa between 5.5 and 7.4 (physiological values)
Easy degradation (hydrolysis of ester bounds in the polymer backbones) into nontoxic byproducts

1.2.3   Combinatorial libraries - a fast and efficient way to evaluate different poly(β-amino ester)s

A fast and efficient way to study relationships between structure and function in a particular material that could be prepared with different reagents is to use combinatorial libraries. Due to promising preliminar results of PβAEs as non-viral vectors, Langer's research group reported a parallel approach for the synthesis of hundreds of PβAEs with different structures and the application of these libraries to a rapid and high throughput identification of new transfection reagents and structure-function trends. For this purpose, major contributions have been reported[52;53;57;66;67;72;75;77;78] not only exploring the possible structure/function relationships, but also imposing an assortment of monomers (amines were denoted by numbers and acrylates by latin alphabet letters) used in order to facilitate cataloging the different PβAEs (Table 1.5 and Tables A.1 and A.2 (Appendix A)).

The first initial library screening was reported in 2001 by Lynn[51]. 140 Different PβAEs from 7 diacrylates and 20 amines were prepared with molecular weights between 2,000 and 50,000 g.mol^{-1}. From this pool polymers, C93 (M$_w$ = 3,180 g.mol^{-1}) and G28 (M$_w$ = 9,170 g.mol^{-1}) revealed transfection levels 4-8 times higher than control experiments employing PEI. At same time, it was observed that for transfection efficiency, high molecular weight was not a relevant parameter. This work was then completed in 2003 by Akinc[57], where biophysical properties and the ability of each polymer/DNA complex to overcome important cellular barriers to gene deliver were investigated. As previous experiments showed, complexes formed from polymers C93 and G28 revealed higher levels of internalization compared to "naked" DNA, displaying 18- and 32-fold more internalization, respectively. In contrast, the major-

Table 1.5: Schematic representation of the most used diacrylates and amines cataloged by Langer lab to prepare PβAEs[52;53;57;67].

Diacrylate	
C	1,4-butanediol diacrylate
G	1,4-cyclohexanediylbis(methylene) diacrylate
JJ	1,5-pentanediol diacrylate
Amine	
28	4-amino-1-butanol
32	5-amino-1-pentanol
93	3-(1H-imidazol-1-yl)propan-1-amine

ity of the polyplexes were found to be uptake-limited. Regarding diameter and zeta potential, out of 10 polymer/DNA complexes with the highest internalization rates, all had diameters lower than 250 nm and 9 had positive zeta potentials. By measuring the cellular pH through fluorescence-based flow cytometry, it was possible to investigate the lysosomal trafficking of the polyplexes. The results demonstrated that complexes based on polymers C93 and G28 were found to have close to neutral pH values, indicating that they were able to avoid acidic lysosomal trafficking. In the same year, Akinc[64] studied the effect of polymer chain end-group, polymer molecular weight and polymer/DNA ratios on *in vitro* gene delivery. For this purpose, 12 different structures were synthesized based only in two different PβAE (C28 prepared from 1,4-butanediol diacrylate and 1-aminobutanol and E28 prepared from 1,6-hexanediol diacrylate and 1-aminobutanol) (Figure 1.6).

These structures were prepared by varying diacrylate/amine stoichiometric ra-
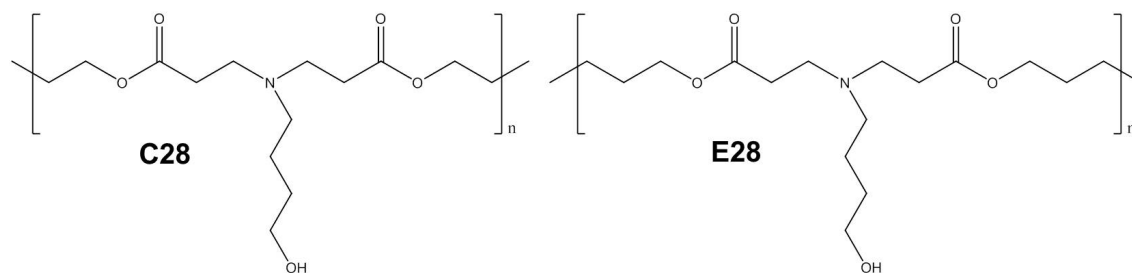
Figure 1.6: Chemical structure of PβAEs C28 and E28.

tios, resulting in PβAEs with either acrylate or amine end-groups and having molecular weights ranging from 3,350 to 18,000 g.mol^{-1}. Polymers were then tested, using high throughput methods, at 9 different polymer/DNA ratios between 10/1 (w/w) and 150/1 (w/w). Concerning terminal groups, it was found that amino-terminated polymers transfected cells more effectively than acrylate-terminated polymers. None of the acrylate terminated PβAEs mediated appreciable levels of transfection activity under any of the assessed conditions. These findings suggest that end-chains of PβAE have crucial importance in transfection activity. Concerning molecular weight effect, highest levels of transfection occurred using the higher molecular weight samples of both amine-terminated C28 ($M_w \sim$ 13,100 g.mol^{-1}) and E28 ($M_w \sim$ 13,400 g.mol^{-1}). Regarding the optimal polymer/DNA ratios for these polymers, it was observed a markedly difference, 150/1 (w/w) for C28 and 30/1 (w/w) for E28. These results highlighted the importance of polymer molecular weight, polymer/DNA ratio, and the chain end-groups in gene transfection activity. Moreover, it has found the fact that two similar polymer structures, differing only by two carbons in the repeating unit, have different optimal transfection parameters emphasizing the usefulness of library screening to perform these optimizations for each unique polymer structure. Meanwhile, in 2003, Anderson[52] described, for the first time, a high-throughput and semi-automated methodology using fluid-handling systems for the synthesis and screening of a library of PβAEs to be used as gene carrier. A crucial feature of these methods was that the whole process of synthesis, storage, and cell-based assays were performed without removing reaction solvent (DMSO). By using these methods, it was possible to synthesize a library of 2350 structurally unique PβAEs in a single day and then test those as transfection reagent at an impressive rate of ∼1,000 per day. Among PβAEs tested, it was identified 46 polymers that

transfect in COS-7 cells as good as or better than PEI. The common characteristic among them was the use of a hydrophobic diacrylate monomer. Moreover, in the hit structures mono- or dialcohol side groups and linear, bis(secondary amines) are over represented. From data obtained with this library, Anderson[67], in 2004, continued his study developing a new polymer library of more than 500 PβAEs using monomers that led higher transfection efficiency in the previous studies and optimizing their polymerization conditions. The top performing polyplexes were assessed by using *in vitro* high-throughput transfection efficiency and cytotoxicity assays at different nitrogen/phosphate (N/P) ratios. As previously observed, the most promising polymers are based on hydrophobic acrylates and amines molecules that possess hydroxyl groups in their structure. Among those, C32 stood out due to higher transfection activity with no associated cytotoxicity. The efficiency to deliver DNA was evaluated in mice after intra-tumoral (i.t.) and intra-muscular (i.m.) injection. The results revealed important differences. While by i.t injection C32 delivered DNA ∼4-fold better than jetPEI®, a commercial polymeric non-viral vector, by i.m. administration transfection was rarely observed. C32 was then assessed for delivery in cells in culture and xenografts derived from androgen-sensitive human prostate adenocarcinoma cells (LNCaP) of plasmid DNA that carries the gene for the A segment of the diphtheria toxin (DT-A DNA). DT-A inhibits protein synthesis resulting in cell death[79]. Recently, it has been used in targeted tumor treatment due to its possibility of conjugation to ligands or antibodies of specific growth factor receptors or antigens overexpressed on cancer cell surface[80]. Results showed that DT-A DNA was successfully delivered and the protein expressed in tumor cells in culture. In human xenografts, the growth was suppressed in 40% of treated tumors. The fact of C32 is non-toxic and it is able to transfect efficiently tumors locally and transfects healthy muscle poorly turned it as a promising carrier for the local treatment of cancer[67].

From here, a panoply of results based in PβAE combinatorial library appeared. In 2005, Anderson[53], prepared a new library of 486 second-generation PβAE based on polymers with 70 different primary structures and with different molecular weights. These 70 polymers were synthesized using monomers previously identified as common to effective gene delivery polymers. This library was then characterized by

molecular weight of polymers, particle size, surface charge, optimal polymer/DNA ratio and transfection efficiency in COS-7 cells of polymer/DNA complexes. Results showed that from 70 polymers with primary structures, 20 possess transfection activities at least about the same of Lipofectamine®2000, one of the most effective commercially available lipid-based transfection reagents. Results also revealed that, in general, the most effective polymers/DNA complexes had <150 nm of particle size and a positive surface charge. Among them, the 2 most effective PβAEs complexed with DNA in smallest particle sizes, 71 nm (C32) and 79 nm (JJ28), and have positive surface charge (over 10 mV). Interestingly, the 9 most effective polymer structures involved the use of amino alcohols, and the chemical structure of the 3 best performing PβAEs (C28, C32 and JJ28) differs by only one carbon. These results show a convergence in chemical structure of the best performing polymers and suggest a common mode of action providing a framework for the design of efficient gene delivery systems.

In 2006, Green[81], synthesized, on a larger scale and at a range of molecular weights, the top 486 of 2350 PβAEs previously assessed[52] and studied their ability to deliver DNA. These PβAEs were tested, firstly, on the basis of transfection efficacy in COS-7 cells in serum-free conditions, and then, the 11 of best-performing PβAEs structures were further analyzed. The transfection conditions were optimized in human umbilical vein endothelial cells (HUVECs) in the presence of serum. In this study, the influence of the factors like polymer structure and molecular weight, and biophysical properties of the polyplexes (such as, particle size, zeta potential, and particle stability throughout time) were studied. The results showed that many of the polyplexes formed have identical biophysical properties in the presence of buffer, but, when in the presence of serum proteins these properties changed differentially, influencing the transfection activity. Concerning to the size, the results showed that in spite of all vectors condensed DNA into small particles below 150 nm in buffer, only a few, such as C32, JJ32 and E28, formed small ($\sim$200 nm) and stable particles in serum. C32, JJ32 and E28 revealed also high transfection activity both in the absence of serum in COS-7 cell line as in the presence of serum in HUVEC cell line. Moreover, C32 transfected HUVECs in the presence of serum significantly better than

jetPEI® and Lipofectamine® 2000. The 3 mentioned PβAEs share a nearly identical structure. The acrylate monomers of these polymers, C, JJ, and E, differ by only their carbon chain lengths (4, 5, and 6 carbons, respectively). Similarly, amines 20, 28, and 32 differ also by only the length of their carbon chain (3, 4, and 5 carbons, respectively). For example, polymers prepared with the same acrylate monomer (C) in which it was varied the length of the carbons chain of the amine monomer resulted in an increased transfection efficacy (C32 (5 carbons) > C28 (4 carbons) > C20 (3 carbons) (Figure 1.7) of these polymers-based polyplexes.
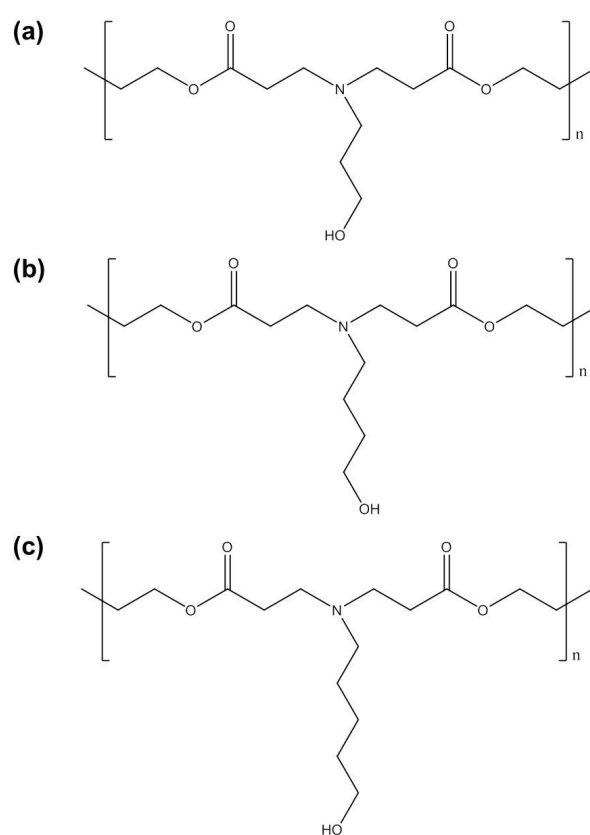
Figure 1.7: Chemical structure of PβAEs C20 (a), C28 (b) and C32 (c).

Interestingly, this study reinforced C32 as the lead PβAE vector and revealed other potential two, JJ28 and E28, which previously showed to be poor vectors. On the other hand, C28 and U28, previously recognized as an efficient transfection reagent, were found to transfect inefficiently HUVEC cells in the presence of serum. By constructing a new library of end-modified PβAE, this research line was continued[78] in order to understand the structure-function relationship of terminal modification of PβAE in transfection activity. For this purpose, it was used 12 dif-

ferent amine capping reagents to end-modify C32, D60 and C20. The choice of these 3 PβAEs was based in their transfection activity: C32, the most effective; D60, an effective transfection reagent with a significantly different structure from C32; and, C20, a relatively poor transfection reagent but with similar structure to C32 differing only in the length of the carbon chain of the amine monomer. The results showed that some PβAEs-based vectors (C32-103 and C32-117 (Figure 1.8)) were able to deliver DNA by approximately two orders of magnitude higher than unmodified C32, PEI (25,000 g.mol^{-1}) or Lipofectamine®2000, and, at levels comparable to adenovirus with high level of infectivity (multiplicity of infection = 100). Once again, it was demonstrated that small structural changes greatly influence the characteristics of gene delivery systems, from biophysical properties (such as, DNA binding affinity, particle size, intracellular DNA uptake) to final protein expression. From these 3 polymers assessed, C20 was the one who transfected cells much less effectively, although it has seen a remarkably improvement with end-modifications. As expected polyplexes based on C32-103 and C32-117 (Figure 1.8) revealed cellular uptake up to five-fold compared to unmodified C32 and, consequently, higher transfection efficiency. Interestingly, and in a general way, terminal modifications of C32 with
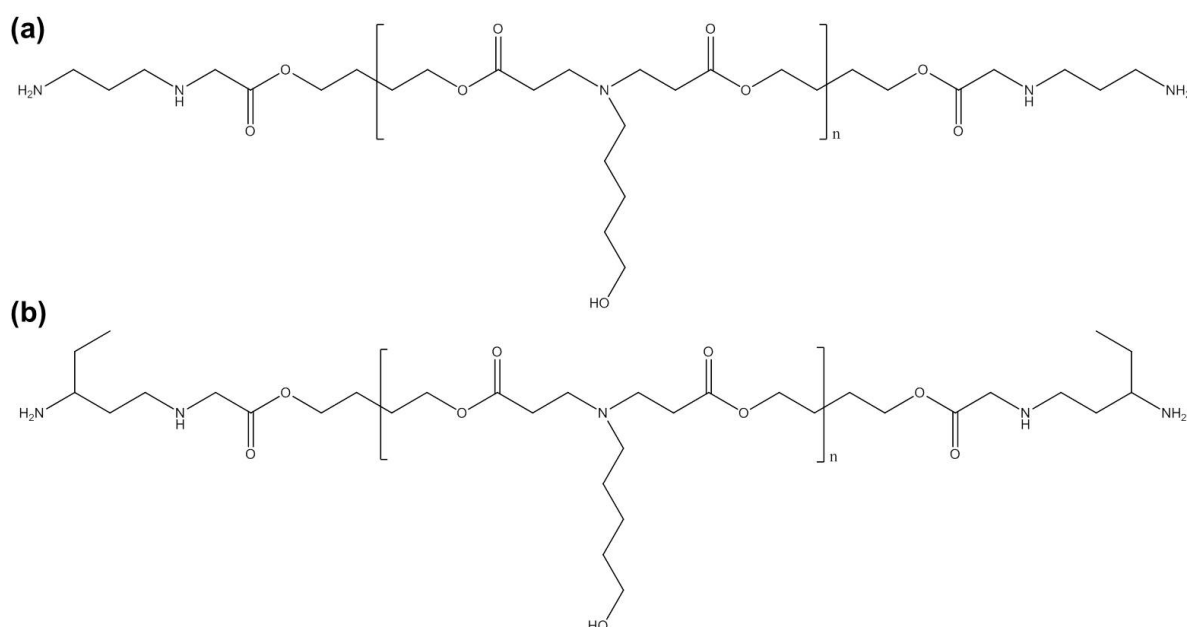
Figure 1.8: Chemical structure of PβAEs C32-103 (a) and C32-117 (b).

primary alkyl diamines were more effective than those with PEG spacers, revealing that a degree of hydrophobicity at the chain ends is an added value for these poly-

mers. Another interesting fact in terminal modification of C32 was that at least a three carbon spacer between terminal amines is necessary to obtain an efficient gene delivery. For example, results showed that C32-103 transfection activity is 130- and 300-fold higher than PβAE C32-102 on the COS-7 and HepG2 cell lines, respectively. As the molecular weight was the same, this result demonstrated the critical role of the chain ends in transfection activity.

In order to better understand the role of the chain ends in transfection efficiency a new library of end-modified C32 was synthesized by Zugates[82] in 2007 using 37 different amine molecules to afford PβAE with different chain ends. In a general way, it was observed that polymers end-capped with hydrophilic amine end groups containing hydroxyls or additional amines led to higher transfection efficiency. On the other hand, terminal-modifications with hydrophobic amines containing alkyl chains or aromatic rings proved to be much less effective. Concerning cytotoxicity, terminal modification with primary monoamine reagents (independently of functional group extending from the amine, such as aromatic, alkyl, hydroxyl, secondary and tertiary amines, and imidazoles functionalities) do not appear to induce any significant cytotoxicity. In contrast, polymers end-capped with primary diamine molecules induced cytotoxicity and were dependent of the spacing between amines and the degree of hydrophobicity[82]. The results showed that, in general, cytotoxicity increased with the increase of the size of the alkyl chain of the amine monomers or the degree of hydrophobicity of the terminal. These significant cell toxicity effects, in large part, could explain the decreasing of the transfection activity of most primary diamine-ended PβAEs at the higher polymer/DNA ratios. The additional charge, in combination with increased hydrophobicity, may be especially harmful to the cell membranes, since both properties are known to disrupt lipid bilayers. Regarding to polyplexes size, PEG-terminated polymers (C32-121 to C32-124) and most polymers terminated with monoprimary amine molecules originated larger particles (between 150 and 220 nm) and weak DNA binding[82]. In contrast, polymers end-capped with primary diamine molecules, except C32-121 and C32-122, condensed DNA in smaller particles (between 85 to 130 nm). Polymers terminated with alkyl primary diamine molecules have shown the highest DNA binding affinity and as-

semble into the smallest polyplexes. Therefore, these results confirmed the importance of the end-modification of PβAEs on transfection efficiency. The research was then complemented by preparing a new polymer library of end-chain modified C32s to prove that hydrophilic amines containing hydroxyl or additional amine groups are the most effective capping agents[77]. Firstly, the polyplexes were tested *in vitro* and results showed, in general, that polymers with hydrophilic terminal groups containing primary or tertiary amines were the most effective, while, those ones with a hydrophobic end group containing either an alkyl chain or an aromatic ring presented the lowest transfection levels. Moreover, it was demonstrated that the amine end-group play an important role on the optimum polymer/DNA ratio. In general, primary diamine-capped polymers reached high quantity of DNA delivery at much lower polymer/DNA ratios compared to mono-amine-ended polymers. For example, C32-108-based polyplexes transfected cells at the same level but at ∼5-fold lower polymer/DNA ratio (20/1 *vs.* 100/1) than C32-based polyplexes. After intraperitoneal (i.p.) administration in mice, *in vivo* results revealed significant gene delivery and sustained protein expression after 1 week. All end-capped C32 polymers, except C32-87, revealed to be more effective than C32 and jetPEI® in whole-body scans. Interestingly, top performers end-capped polymers (C32-103, -116, and -117 (Figure 1.9)) seems apparent convergence in structure.

All PβAE had primary diamine molecules chain ends that contain a three-carbon spacer between amine functionalities differing in the degree and pattern of substitution at the interior carbons. The C32-103, -116, and -117 PβAEs (Figure 1.9) differ slightly in end-group compound but displayed different transfection levels in several organs. C32-117 transfected 5- to 65-fold more efficiently in bladder, spleen, and kidney than C32-103 and -116-based polyplexes. On the other hand, C32-103 and C32-116-based polyplexes transfected 7-fold more in the prostate than C32-117. These results demonstrated that subtle structural differences at the chain ends conduct to significant effects on the organ distribution of polymer/DNA complexes highlighting the critical importance of end-modification of PβAE in gene delivery area. This suggests that C32 end-modification may be a useful strategy in the design of targeted delivery systems allowing the attachment of the targeting agent and, at
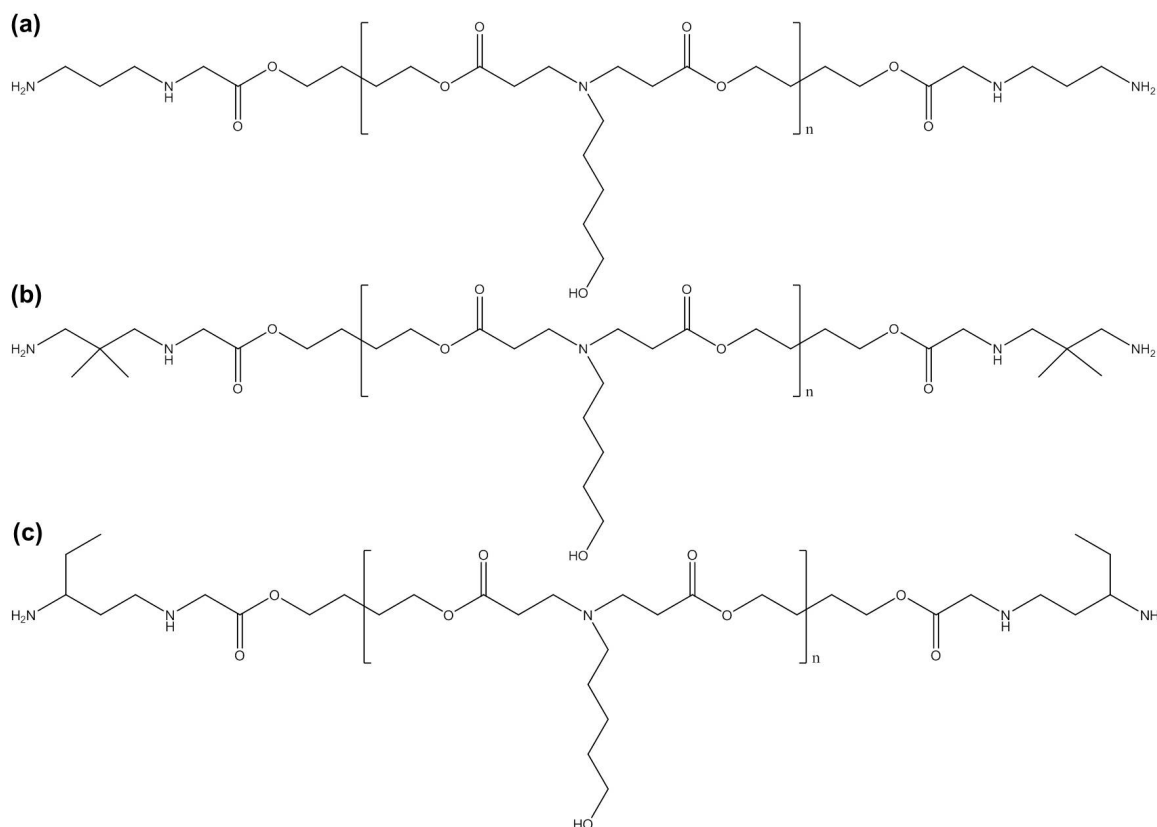
Figure 1.9: Chemical structure of end-modified PβAEs C32-103 (a), C32-116 (b) and C32-117 (c).

the same time, not compromising transfection ability. The *in vivo* results also showed that C32 end-capped polyplexes led to higher expression levels compared to unmodified C32 (4- to 12-fold) and jetPEI® (over 1-fold) in several abdominal organs after i.p. injection. On the other hand, when administered by intravenous (i.v.) route the levels of gene expression was lower compared to levels attained after i.p. administration. The only striking difference was an improvement in lung delivery by C32-117-based polyplexes over C32- ones, but significantly lower than mediated by jetPEI®. One possible explanation for these results may be the serum stability of the polymer/DNA complexes. The high concentration of serum proteins present after i.v. injection may unfavorably interacts with polyplexes lead to limit the gene delivery. The promising results of C32-103-, C32-117- and C32-122-based polyplexes led to further investigation in three different cell lines of human stem cells (human adipose-derived stem cells (hADSCs), human embryonic stem cell-derived cells (hESCds) and bone marrow-derived human mesenchymal stem cells (hMSCs))[83]. The results revealed

a low cytotoxicity and high transfection activity profile. The polyplexes based on these end-modified polymers exhibited good transfection efficiency in hMSCs (27%, C32-122, 20/1 (w/w), 6 μg DNA per well), hADSCs (24%, all three end-modified polymers showed a similar transfection profile, 30/1 (w/w), 3 μg DNA per well) and hESCds (56%, C32-122, 20/1 (w/w), 3 μg DNA per well), with high cell viability (87-97%) achieved in all cell lines tested. When compared to Lipofectamine®2000, the end-modified PβAE-based polyplexes showed significantly higher levels of gene delivery efficiency. This study including these 3 end-modified PβAEs (C32-103, C32-117 (Figure 1.9) and C32-122 (Figure 1.10) was once again extended in order to study the delivery of plasmid DNA containing the gene that encodes vascular endothelial growth factor (pVEGF) gene[84] into hMSC and hESdC cells in order to promote angiogenesis when these tranfected cells were grafted into target tissues. Both cell lines treated with these polyplexes demonstrated good cell viability, hVEGF production and engraftment into target tissues. C32-122-based polyplexes revealed to be the best formulation inducing 2- to 4-fold-higher vessel densities after 2 weeks of s.c. implantation of scaffolds (seeded with stem cells transfected by C32-122 polyplexes (containing pVEGF) than control cells or cells transfected by Lipofectamine® 2000 with the same plasmid. Moreover, it was also observed that after 4 weeks of the i.m. injection of C32-122/pVEGF into mouse ischemic hind limbs an enhanced angiogenesis and limb salvage was found while reducing muscle degeneration and tissue fibrosis[84]. Additionally, Sunshine[85], in 2009, confirmed that the end-group of the polymer can be used as a regulator for cell-type specificity since these small conjugated molecules modulated the gene delivery efficacy of these polymers in a cell-type-specific manner. Different amine-capped C32-based polyplexes were tested in 6 types of cell lines (african green monkey kidney fibroblast-like cells (COS-7), human cervical cancer cells (HeLa), human hepatocellular carcinoma cells (HepG2), human primary endothelial cells (HUVECs), murine dendritic cells (DC 2.4) and human mesenchymal stem cells (hMSC)) revealing different levels of gene expression.
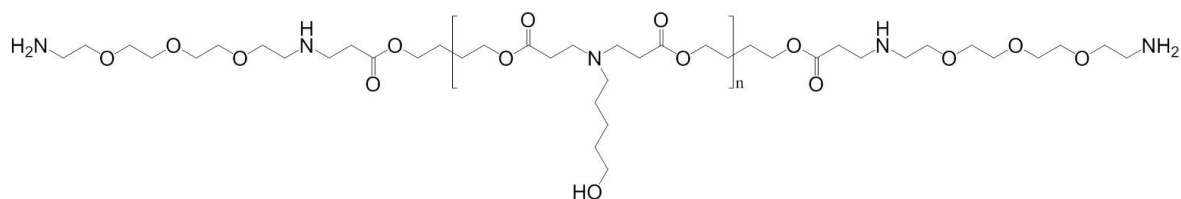
Figure 1.10: Chemical structure of end-modified PβAE C32-122.

Jere *et al.*[86] prepared 16 different PβAEs from poly(ethylene glycol) diacrylate and γ-aminopropyl-triethoxysilane varying the amine/acrylate ratios. *In vitro* studies in 293T and HeLa cells revealed that both transfection activity and cell viability increased with the increase of amine/acrylate ratio, from 0.7/1 to 6/1 ratio. Other interesting result was the uniform pattern of the transfection in the absence and in the presence of serum in culture medium. The most promising PβAE, prepared with 6/1 amine/acrylate ratio and with 16,000 g.mol^{-1}, demonstrated high gene delivery efficiency and low cytotoxicity when compared to PEI (25,000 g.mol^{-1}) and Lipofectamine$^®$. These polyplexes also showed good DNA condensation, even at low PβAE/DNA weight ratio (10/1), resulting into small particle (∼133 nm).

In 2011, Sunshine *et al.*[87] developed a new 320-member polymer library of end-modified PβAEs. The influence in gene delivery efficiency of small changes to the side chains, backbones, and end-groups of the polymers was assessed *in vitro* (COS-7 cell line). In general, it was observed that increasing hydrophobicity of the backbone and side chain of the polymer tended to enhance transfection efficiency. Though, an interesting fact is that the increased hydrophobicity of the backbone reduces the requisite for a hydrophobic side chain, and, likewise, an increased hydrophobicity of the side chain reduced the requisite for a hydrophobic backbone. These observations indicate that there might be some optimal hydrophobicity/hydrophilicity balance for polymeric-based gene delivery. The best formulations exhibited higher transfection efficiency (∼3-fold increased luminescence and ∼2-fold increased transfection percentage) than that obtained with commercially available non-viral alternatives, FuGENE$^®$ HD and Lipofectamine$^®$ 2000. The work was extended[88] to assess the gene delivery efficiency and toxicity of the combinatorial library of PβAEs in retinal pigment epithelial (ARPE-19) cells. Ten formulations exceeded 30% of transfection efficiency. The polyplexes prepared with the polymer 1-(3-aminopropyl)-4-

methylpiperazine end-modified PβAE (synthesized from 1,5-pentanediol diacrylate and 5-amino-1-pentanol (JJ32) at 60/1 w/w polymer/DNA ratio) showed lower cytotoxicity and higher transfection efficiency (44%) than the obtained for PEI (25,000 g.mol^{-1}) (8%), Lipofectamine$^{\circledR}$ 2000 (26%) and X-tremeGENE HP DNA (22%). Subretinal injection of the lyophilized polyplexes resulted in 1.5$\pm$0.7 x10^3-fold and 1.1$\pm$1x10^3-fold increased green fluorescent protein (GFP) expression in neural retina and the retinal pigment epithelium/choroid, respectively, compared to injection of DNA alone. In order to prove that uptake and transfection of linear PβAE-based polyplexes were dependent on polymer end-group structure, but largely independent of polyplexes physicochemical properties the work was complemented[89]. An array of linear PβAEs differing in small changes in side chain, backbone and terminal group of the polymers were synthesized, characterized and assessed their gene delivery efficacy. Regarding to *in vitro* transfection efficiency of the PβAE-based polyplexes in COS-7 cell line, their uptake and transfection ranged between 0-95% and 0-93% of cells, respectively, depending on the basic PβAE structure and the terminal modifications tested. The 5 best polymers achieved higher uptake and transfection efficacy with less toxicity than bPEI control. PβAE acrylate-terminated revealed to be dramatically less efficacious than corresponding small molecule amine-containing end-capped versions, in terms of uptake (1-3% vs. 75-94%) and transfection efficacy (0-1% vs. 20-89%). Nevertheless, there are minimal differences between the obtained polyplexes in terms of particle size, zeta potential, polymer buffering capacity, DNA retardation in gel electrophoresis and cytotoxicity.

In 2011, Tzeng *et al.*[90] tested different end-modified PβAEs-based polyplexes for gene delivery in primary glioblastoma (GB) and GB tumor stem cells. The best formulations revealed low non-specific cytotoxicity and transfection activities of up to 60% in the presence of serum. Interestingly, some PβAEs revealed high transfection efficiency in healthy cells and poor in GB cells while others affected only GB-derived cells and little or nothing the healthy cells. These results show potential for numerous strategies for GB treatment through gene therapy, either using targeted delivery mediated by PβAE structure or using plasmids with differential expression in different cell types. The polyplexes remained stable in normal serum medium and could

also be lyophilized and stored for at least 3 months without loss of efficacy, expanding their practical and clinical potential. This work was then extended in 2012[91] for siRNA delivery into hard-to-transfect human mesenchymal stem cell (hMSC). The results showed that cystamine-terminated PβAEs-based polyplexes caused the most knockdown, with the best formulation achieving 91% knockdown 20 days post-transfection, suggesting that cystamine facilitates especially effective siRNA delivery to hMSCs. Then, the results were validated by transfecting hMSCs with siRNA against B-cell lymphoma-like protein 2 (Bcl-2), an inhibitor of osteogenesis, that resulted in an enhanced osteogenesis over 4 weeks compared to control. The work was complemented in 2013[92] in order to assess the influence in gene delivery of 70 PβAEs-based polyplexes to treat human brain cancer. In addition, nucleic acids with different structures and sizes, such as, siRNA and linear and circular DNAs (from 1.8 to 26 kb) was also evaluated. The most promising formulations delivered DNA with 90% of efficiency in primary human glioblastoma cells with low (<10%) non-specific cytotoxicity, which is much better than that obtained with Lipofectamine® 2000 and X-tremeGENE HP. In what concerns to siRNA delivery, best performer complex caused up to 85% knockdown in these cells while maintaining high viability. The results, from a single dose, persisted for one month and knockdown was higher than the observed for Lipofectamine® 2000. An interesting remark was that the polymer molecular weight was a determining factor of transfection efficacy for some of the polymer structures, however in other structures has no influence on gene delivery efficacy. Another important result that confirmed a previous work[91] revealed that PβAE end-modified with a reducible cystamine functional group greatly improved siRNA delivery but, in general, decreased DNA delivery compared with non-reducible counterparts. These encouraging preliminary results using PβAE libraries to achieve an efficient and specific vector for GB treatment led to an increased interest by researchers. Guerrero-Cázeres *et al.*[93] tested different end-modified PβAEs for delivery pDNA into primary culture of brain tumor initiating cells (BTICs) in 3-D oncosphere. *In vitro* studies revealed that PβAE C28 end-modified with 1-(3-aminopropyl)-4-methylpiperazine (Figure 1.11) was the most effective polymer in all four primary culture BTICs assessed. After local injection in the mouse GB models,

the polyplexes prepared with this end-modified polymer revealed an increased diffusion capacity and selectivity for tumor cells relative to healthy cells. Moreover, it was showed that after lyophilization process these vectors remained fully functional and efficient even after storage during 2 years at -20 °C. These data demonstrated the enormous potential to translate this nanoparticle technology into clinical context. This work was extended in a malignant glioma model to evaluate the efficacy of a therapeutic strategy involving herpes simplex virus type I thymidine kinase (HSV-tk) and the prodrug ganciclovir (GCV)[94]. Different end-modified PβAEs were tested to efficiently deliver the plasmid DNA containing the HSV-tk gene (pHSV-tk). Again, the 1-(3-aminopropyl)-4-methylpiperazine end-modified C28 PβAE (Figure 1.11) was the most effective PβAE. These PβAE/pHSV-tk polyplexes revealed the capacity to kill, in combination with GCV exposure, approximately 100% of cancer cells in two rat glioma cell lines (rat nitrosourea induced gliosarcoma cells (9L) and rat glioma cells (F98)) tested. PβAE/pHSV-tk polyplexes efficiently transfected (∼70%) the referred cell lines had being observed a local activation of the non-toxic pro-drug GCV into a cell-killing drug (cytotoxicity metabolite). After using one single PβAE/pHSV-tk polyplexes infusion *via* convection-enhanced delivery combined with systemic administration of GCV in rats with malignant 9L glioma model no signs of neurotoxicity or paralysis were observed and, at the same time, a significant increase in animal survival was registed. Curiously, this 1-(3-aminopropyl)-4-methylpiperazine end-modified C28 PβAE (Figure 1.11) also revaled high transfection activity in hard-to-transfect human triple negative breast cancer cells (MDA-MB 231) compared to other end-modified PβAEs[95].

Figure 1.11: PβAE prepared from 1,4-butanediol diacrylate and 4-amino-1-butanol (C28) post-polymerization modified with 1-(3-aminopropyl)-4-methylpiperazine (blue).

In 2013, Eltoukhy *et al.*[96] developed 80 amine-end modified PβAE terpolymers with random structure (Figure 1.12) incorporating hydrophobic alkyl side

chains. The top-performing polymer-based polyplexes exhibited significantly enhanced transfection efficiency in HeLa cells compared to Lipofectamine® 2000. The results also showed that the inclusion of alkyl side chains in PβAEs-based polyplexes promoted the stability and resistance to aggregation under physiological conditions. Moreover, the results showed that, at high DNA concentrations and under physiological pH and ionic strength conditions, these hydrophobic PβAE terpolymers, but not PβAEs without alkyl side chains, were able to facilitate interactions with PEG-lipid conjugates and DNA to yield stable particles that maintained their transfection capacity for several hours.

Figure 1.12: Example of a terpolymer PβAE prepared from one diacrylate and two diferent amines (amine 1 and amine 2).

The efficiency of delivery for different nucleic acids was also evaluated for different PβAEs highlighting the importance of these combinatorial libraries. For example, Keeney[97], in 2013, synthesized and tested 18 different PβAEs with different backbone and end-group chemistries for Ubc driven minicircle DNA delivery. Among them, few PβAEs-based polyplexes had the ability to efficiently deliver minicircle DNA *in vitro* in human embryonic kidney 293 and mouse embryonic fibroblasts cells at levels comparable or even superior to Lipofectamine® 2000. *In vivo* results showed that, after i.p. injection, PβAE-based polyplexes formulation led to ~2-fold higher protein expression compared to minicircle DNA alone, which by itself have high level of transgene expression. Another study, also in 2013[98], proposed the design of an array of PβAEs to be used as tumor protein p53 (TP53) gene carrier. *In vitro* results in p53-mutant human lung carcinoma cells (H446) showed that two of the top candidates presented good expression of exogenous protein p53 with functional activity (induction of apoptosis, induction of protein p21 and accumulation of cells in sub-

G1 cell cycle phase). Moreover, after intratumoral injection of subcutaneous H446 xenografts, polyplexes carrying TP53 gene caused marked tumor growth inhibition.

Other interesting study based on combinatorial PβAEs libraries concerned the evaluation of DNA binding and gene delivery efficiency relationship[73]. For this purpose, several PβAEs with different molecular weights and polymer end-groups were synthesized. The *in vitro* transfection results in human breast and brain cancer cells indicated that binding constant (M^{-1}) of PβAE and DNA was biphasic (Hill plot associated with a negative and a positive cooperativity phase) and it had optimal values for transfection efficacy in the range of 1 - 6 x 10^4 M^{-1}. However, in spite of binding constant in this range was required, alone was not sufficient for an effective transfection. It was demonstrated that this range of binding affinity can be independently tuned by PβAEs structure, such as, adding single carbons to the backbone or side-chain structure, varying terminal groups and/or molecular weight control.

After this brief review on the use of combinatorial libraries to evaluate PβAEs as vector, it can be concluded that very small differences in their structures lead to different transfection activity in different types of cells. Thus, from these combinatorial studies, it is possible to select the PβAE structure from an easy and fast way that best fits a particular application.

1.2.4   Polymer architecture

Concerning to the polymer architecture, PβAE can be synthesized as linear, hyperbranched or dendritic forms Figure 1.13.

PβAE dendrimer structure was synthesized for the first time in 2002[99] and had been developed and studied since then[100–104]. However, to the best of our knowledge, its application as gene carrier has not yet been explored. As linear structure had been extensively covered throughout in this literature review, this section will be focused in PβAE-based transfection reagent with hyperbranched structure.

Hiperbranched PβAE has been synthesized since 2002[59], but only in 2005, in two independent research studies by Zhong[76] and Wu[105], it was used for the first time

(a)

(b)

(c)
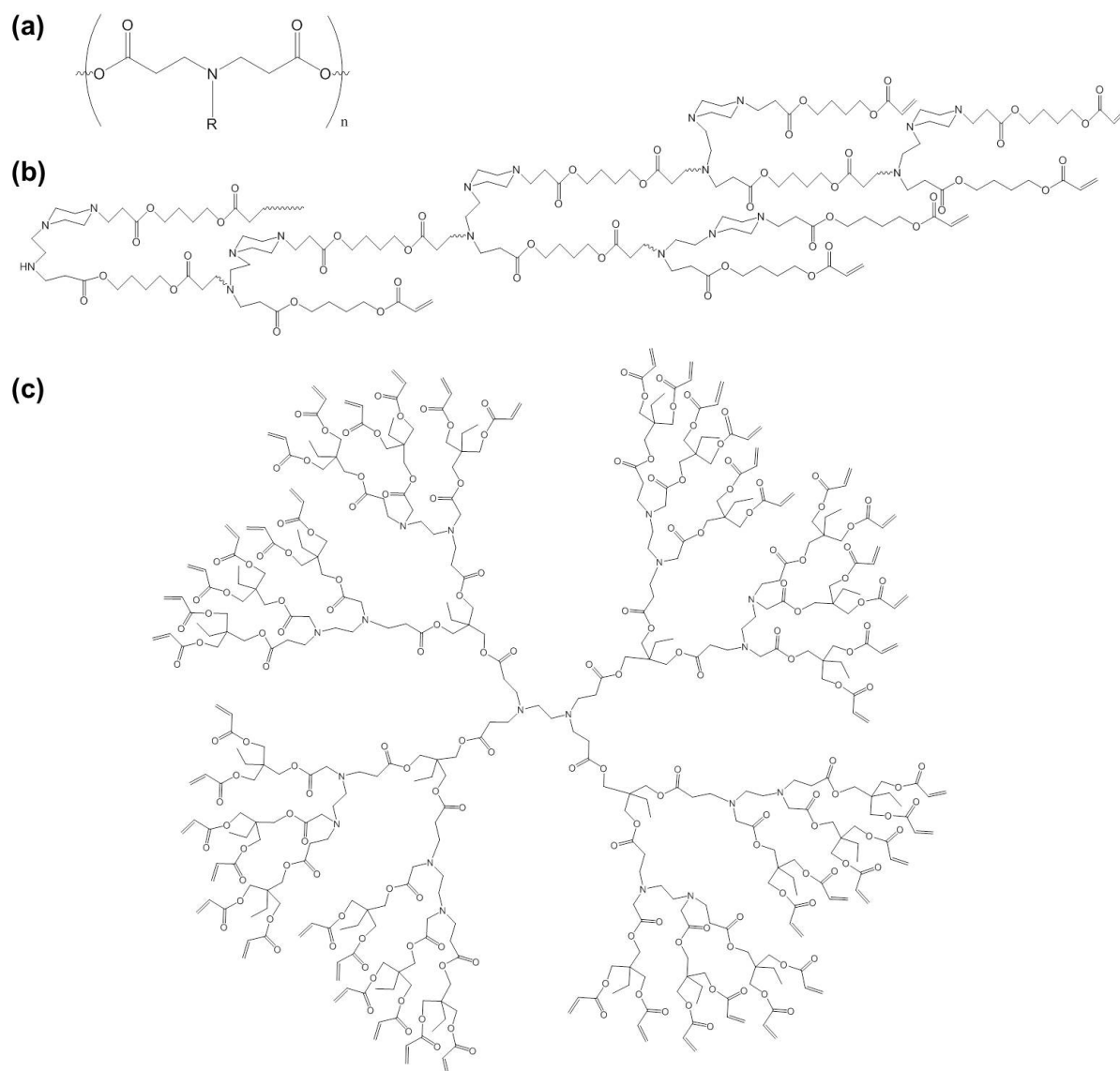
Figure 1.13: Some examples of different structures of PβAE: (a) linear, (b) hyperbranched and (c) dendrimer-like.

as non-viral gene carriers to deliver plasmid DNA.

Zhong *et al.*[76] prepared different hyperbranched PβAE structures by reacting different amines (*N*-methylethylenediamine, 1-(2-aminoethyl)piperazine, (aminomethyl)piperidine) with diacrylates (ethylene glycol diacrylate and 1,4-butanediol diacrylate). The polymers presented a degree of branching of approximately 0.30 and demonstrated interesting properties to be used as gene carrier, such as, water-solubility, degradability in physiological conditions, high buffering capacities between pH 5.1 and 7.4, ability to condense plasmid DNA into small-sized and positively surface charged complexes. *In vitro* studies in COS-7 cell line revealed

good levels of transfection activity even in presence of serum and no (or low) cyto-toxicity. The highest transfection level was observed in polyplexes based on polymer prepared with 1,6-hexanediol diacrylate and 1-(2-aminoethyl)piperazine. The values were higher than or at least comparable to polyplexes based on PEI or PDMAEMA.

Wu *et al.*[105] developed a hyperbranched PβAE based on trimethylol-propane tri-acrylate and 1-(2-aminoethyl)piperazine. The molecular structure had secondary and tertiary amines in the core and primary amines in the periphery, similar to PEI. The polymer was then complexed with pDNA forming stables polyplexes. The *in vitro* transfection studies were assessed in COS-7 and human embryonic kidney (HEK 293) cell lines and revealed comparable transfection efficiency and lower cytotoxi-city when compared to polyplexes prepared with PEI (25,000 g.mol^{-1}). This study was then extended in 2006[106] to understand the effect of terminal amine groups of PβAE based on 1-(2-aminoethyl)piperazine and 1,4-butanediol diacrylate for DNA delivery. Surprisingly, in this case, it was found that amino-end groups had no effect on the hydrolysis rate, cytotoxicity, DNA condensation capability, and *in vitro* DNA transfection activity of the hyperbranched PβAE.

In 2009, Chew *et al.*[107] studied the effect of hydrophilic spacers on branched PβAE-based polyplexes. The polymers were synthesized from three types of trimethylolpropane ethoxylate triacrylates (with three, seven or fourteen ethyleneoxy groups) and 1-(2-aminoethyl)piperazine. The polymer degradation study revealed that it depends on the spacer length and pH. After 14 days, the PβAE degraded more rapidly at pH 7.4 than pH 5.0, and PβAE based on triacrylate with four-teen ethyleneoxy groups degraded faster than one prepared with triacrylate with-out ethyleneoxy groups. Concerning cytotoxicity assays in rat fibroblasts cell line (CRL 1764), all polymers were found to induce lower cytotoxicity than bPEI (25,000 g.mol^{-1}), that increased with the spacer length. On the other hand, transfection assays suggested weaker capacity to transfect when compared to bPEI. This work was expanded to study the effect of the different amines of hyperbranched PβAE on transfection activity[108]. The triacrylate monomer (trimethylolpropane triacry-late) was fixed and different amines (1-(2-aminoethyl)piperazine, 1-(3-aminopropyl) imidazole, *N,N*-dimethylenediamine and hydrazine) were used in polymerization.

All synthesized hyperbranched PβAE polymers presented low cytotoxicity and the polyplexes based on polymers prepared with *N,N*-dimethylenediamine showed better condensation of pDNA and stability at pH 7.4, and higher transfection activity when compared with bPEI (25,000 g.mol^{-1}).

1.2.5 Poly(β-amino ester)-based polyelectrolyte multi-layers for gene delivery

A recent and elegant approach for the use of PβAEs as gene carrier is based on the production of polyelectrolyte multi-layers (PEMs) to promote a localized transfection directly in the affected area. The PEMs were fabricated by alternating PβAE and pDNA layer-by-layer. Two main advantages of this method concern the procedure used for film fabrication that is entirely aqueous and the fact that final thickness of PEMs is ultrathin (from ~10 nm to several hundred nm thick, depending on the number of total layers). In addition, the modular nature of layer-by-layer assembly can also be exploited to combine various layers of diverse therapeutic agents simultaneously or sequentially apart from DNA-cationic polymer combination[109].

The first time that PβAE-based PEMs were used for plasmid DNA delivery occurred in 2004 by Lynn research group[110]. From this pioneer work, the research group developed and tested various biomedical applications using the same method. The PβAE employed in most of their studies was prepared from 1,4-butanediol diacrylate and 4,4'-trimethylenedipiperidine, referred by them as "polymer 1" (Figure 1.14).
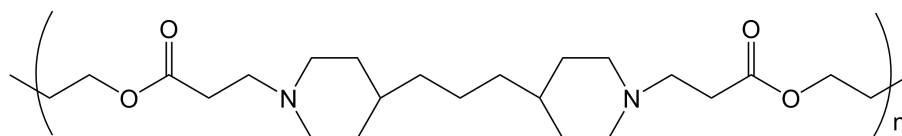
Figure 1.14: Polymer 1 - PβAE prepared from 1,4-butanediol diacrylate and 4,4'-trimethylenedipiperidine.

The first studies were addressed to design and development of PEMs structures and the study of plasmid DNA release profiles. In the first one, Zhang *et al.*[110] fabricated, layer-by-layer, multilayered films with plasmid DNA encoding for enhanced green fluorescent protein (eGFP) and polymer 1 onto the surfaces of planar silicon

and quartz substrates with thickness up to 100 nm. The release of plasmid was evaluated under physiological conditions. After 30 h upon incubation in phosphate-buffered saline (PBS), pDNA was completely released. Additionally, preliminary transfection assays in COS-7 cell line revealed that the released pDNA is transcriptionally viable and promotes the expression of eGFP.

The direct and localized delivery of pDNA by multilayered PEMs was analyzed *in vitro*, by Jewell *et al.* for the first time in 2005[111]. The polymer 1/DNA films had eight bilayers and a thickness of approximately 100 nm, containing 2.7 ($\pm$ 0.8) μg of DNA per cm^2. The films were placed directly on top of COS-7 cells during 48 h and in presence of serum in the culture medium. The cells were analyzed by fluorescence microscopy and those localized under the PEMs film-coated portion of the slides revealed transfection efficiency between 4.6% and 37.9% of the cells. On the other hand, fluorescence was not observed in cells in uncoated portions of the slides. In addition, by atomic force microscopy (AFM) it was observed that the PEMs film topography undergoes significant structural rearrangements upon incubation, exhibiting a surface with particles of polymer 1 and pDNA, that reorganized to form polyplexes.

This work was then detailed by Fredin *et al.*[112] that have carried out a careful surface analysis of erodible multilayered polyelectrolyte films. For this purpose, there were prepared not only PEMs based on polymer 1 and plasmid DNA but also PEMs based on polymer 1 and sodium poly(styrene sulfonate) (sPSS). The observed differences between these two materials in the topography, structures and erosion profiles upon incubation in PBS at 37 °C were significant. PEMs based on sPSS showed a gradual and well-controlled erosion process that occured in a top-down, surface-oriented manner without creating significant roughness, pits, holes or cracks over large micrometer-scale areas of the film, opposed to PEMs containing pDNA that undergoes structural reorganizations to present surface-bound particles ($\sim$50 to 400 nm). Fredin *et al.*[113] continued the study and found out the possibility to manipulate the spinodal dewetting of these materials by varying chemical structure of the polyamines (using polymer 1 and a poly(amido-amine)), film composition and the conditions to which these materials were exposed. Taking advantage of this knowl-

edge acquired by this research group about PEMs for pDNA delivery, Jewell *et al.*[114] studied the surface modification of stainless intravascular stents using these PEMs. The stents were coated uniformly with a PEMs film having approximately 120 nm of thickness (eight bilayers of polymer 1 and pDNA). The mechanical tests mimicking the representative challenges encountered in the course of stent deployment, such as balloon expansion, revealed that PEMs had good properties for this application (did not peel, crack, or delaminate substantially from the surface after exposure). The *in vitro* release of pDNA in phosphate buffer saline at 37 °C revealed a sustainable profile for up to four days. The transfection activity in COS-7 cell line was confirmed without the aid of additional transfection agents. These results were then explored in *in vivo* assays using surface-modified inflatable embolectomy catheter balloons with PEMs in the carotid arteries in rat model of ballon-induce arterial injury developed by Saurer *et al.*[109] in 2011. Ultrathin PEMs based on polymer 1 and pDNA encoding either eGFP or β-galactosidase was used to promote the localized tissue transfection. The results revealed that polymer 1/pDNA films not only supported all mechanical challenges associated to the insertion and inflation of these type of balloons, but also had an efficient delivery of functional pDNA to the vascular wall. Later, in 2013, Saurer *et al.*[115], continued the study, testing stents coated with tetramethylrhodamine end-capped polymer 1/pDNA (encoding eGFP) PEMs to promote uniform and localized *in vivo* delivery of pDNA for vascular tissue. The *in vivo* transfection assays were assessed in pig and rabbits (animal model widely used for the pre-clinical evaluation and testing of drug- and gene-eluting stents) and revealed an uniform transfection of sub-endothelial tissue in the arteries of pigs. Two days after implantation, it was confirmed the expression of eGFP in the stented tissue in both rabbits and pigs. In the same year, Bechler *et al.*[116] developed and tested *in vivo* the catheter balloons coated with polymer 1/pDNA (encoding the δ isoform of protein kinase C (PKCδ)) films in a rat model of vascular injury. PKCδ is a regulator of apoptosis and other important cell processes that has been revealed to decrease intimal hyperplasia in damaged arterial tissue when administered via perfusion using viral vectors. The coated balloons were inserted into injured arteries for 20 min and 3 days after treatment, it was observed a high levels of PKCδ expression in the tissue

treated, confirming an efficient local delivery of pDNA of the PEMs. The results also showed an efficient up-regulation of apoptosis and the production of monocyte chemotactic protein 1 (MCP-1) by PKCδ expression. After 14 days, a reduction of ~60% of intimal hyperplasia was observed in arterial tissue compared to those treated with balloons coated with films without plasmid vectors.

After that, another interesting biomedical applications based on this method was reported. In 2009, Saurer et al.[117] reported polystyrene microspheres (~6 μm) presenting erodible DNA-containing multilayered films on their surfaces. The microparticles were prepared by using alternating and iterative cycles of particle suspension, centrifugation and resuspension in solutions of polymer 1 and pDNA, as shown in Figure 1.15. The smooth and uniform film of microparticles coating sustained the release of transcriptionally active DNA into PBS at 37 °C during approximately three days. The *in vitro* transfection activity of the microparticles coated with polymer 1/pDNA films was assessed in COS-7 cell line and the ability of these particles to be internalized by phagocytic cells was evaluated in murine macrophage cell line (P388 D1). These results demonstrated that these particles could be used to transport and deliver pDNA into phagocytic cells of the immune system.
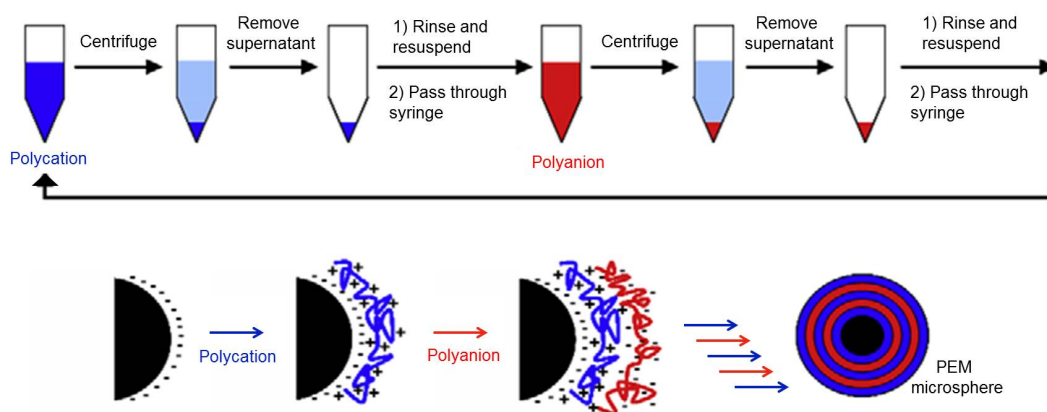
Figure 1.15: Preparation of microspheres based on multilayered polyelectrolyte films (adapted from [117]).

Another interesting approach is the use of this method to coat microneedles. Again, Saurer et al.[118], in 2010, coated microneedles alternating polymer 1/DNA or sodium poly(styrene sulfonate) (sPSS)/ribonuclease (RNase) A-R9 films to the skin treatment. The ultrathin, uniform, and defect-free film coating eroded and consequently released DNA or protein when incubated in PBS at 37 °C or when inserted

into porcine cadaver skin. These microneedles were able to reach and transfer DNA or protein to a depth of ∼500 to 600 μm. These results opened the door to the delivery of different agents of interest in the contexts of vaccine and transdermal drug delivery or a range of other biomedical applications.

In order to tune the release of pDNA, Flessner *et al.*[119], in 2011, developed PEMs that promote rapid release of pDNA by incorporating poly(acrylic acid) (PAA) into polymer 1/pDNA PEMs. The 'tetralayers' of polymer 1/PAA/polymer1/pDNA films eroded more rapidly (∼3-6 h) in PBS at 37 °C than PEMs prepared with 'bilayers' of polymer 1/pDNA (∼2-3 days) and could be used to further fast release of pDNA from surfaces. The results also demonstrated that PAA-containing films released approximately half the amount of pDNA (4 μg) as compared to polymer 1/DNA films (8 μg). The data also suggested different physical erosion profiles of these PEMs that could be correlated with the significant differences in DNA release profiles. The authors also compared the results with PEMs fabricated with bilayers of linear PEI and pDNA and tetralayers of PEI/PAA/PEI/DNA. Again, PAA-containing films released DNA faster and completely (∼3 h) than PEMs based on PEI/pDNA films (not release significant quantity of DNA for up to ∼40 h). These results indicated that incorporation of PAA can also be used to tune and to speed up the release of pDNA from PEMs based on cationic polymers making them significantly more stable.

In 2012, Bechler *et al.*[120] demonstrated *in vitro*, using fluorescence-based techniques, that both polymer 1 and pDNA were released all together (∼58% of DNA was co-localized with polymer) during film erosion, and both film components were internalized by cells growing in the vicinity of the PEMs. For this purpose, polymer 1 was post-polymerization end-functionalized with the fluorescent probes tetramethylrhodamine or Oregon Green 488. This approach permitted simultaneous characterization of polymer 1 and pDNA films erosion in solution and cellular internalization of PEM components providing information about the behaviors and locations of polymer 1.

From 2013, other research groups[121;122] began to use PβAE/pDNA PEMs for gene delivery. Li[121] coated an electrospun polymer 1 with PEMS based on 1-(3-

aminopropyl)-4-methylpiperazine end-capped PβAE (prepared with 1,4-butanediol diacrylate (C) and 4-amino-1-butanol (28)) and pDNA films. The *in vitro* release of the DNA was studied over 24 hours and it was observed a high exogenous gene expression (∼60-80% transfection activity) in primary human glioblastoma 319 cell line. Comparing two different substrates (polymer 1 or a blend of polymer 1 with polycaprolactone (PCL)), the substrates based only on polymer 1 demonstrated to be induce less cytotoxicity and more cell attachment. The combination between electrospun and PEMs based on PβAEs revealed a promising strategy to deliver DNA from a surface.

DeMuth *et al.*[122], developed and tested a PLLA microneedles coated with PEMs based on polymer 1 or PβAE prepared with 4,4'-trimethylenedipiperidine (amine not numbered in PβAE library) and 1,6-hexanediol diacrylate (E) and pDNA that act as a tattoo. These 'multilayer tattoo' DNA vaccines promoted local, continuous and sustained release of polyplexes and adjuvants molecules (that amplify the immune response) from multilayer tattooing in the skin from days to weeks manipulating the film composition. These skin-implanted vaccine multilayers were tested against a human immunodeficiency virus (HIV) antigen. The results showed immune responses comparable to electroporation (a method known to improve performance of DNA vaccines and currently considered a gold standard for experimental DNA vaccine potency) and enhanced memory T-cell generation in mice. An *ex-vivo* assay in macaque (non-human primate) skin showed a 140-fold higher gene expression when compared to intradermal naked DNA injection. In addition, it was observed that these multilayer vaccine microneedles can be stored during weeks at room temperature in a dry-state without loss of efficiency. This polymer film tattoing technique might be the alternative for an efficiency delivery of DNA by a self-administrable and pain-free skin-patch platform.

1.2.6   Poly(β-amino ester)-based copolymers

Despite the first poly(β-amino ester)-based copolymer were described in 2003[58], its use for gene delivery only emerged in 2007[82] and to date the literature is very

scarce. The first copolymers based on PβAE used as gene carrier resulted from end-modification of PβAEs with PEG through a combinatorial library study (see Section *1.2.3. Combinatorial libraries - a fast and efficient way to evaluate different poly(β-amino ester)s*). Among different PβAEs tested, it was seen that PβAE prepared from 1,4-butanediol diacrylate and 5-amino-1-pentanol and posteriorly end-modified with PEG-bis-amine (C32-122) had good gene delivery efficiency[82]. This result was also confirmed in other combinatorial libraries studies[83–85]. Recently[123], C32-122 was used to study the role of Niemann-pick C1 protein (NPC1) in the regulation of endocytic mechanisms influencing nanoparticle trafficking into the cell. The NPC1 is a lysosome membrane involved in various cellular mechanisms (such as, mediates trafficking of cholesterol and in the endosomal escape). The results of the transfection activity of C32-122 PβAE-based polyplexes in NPC1-deficient cells resulted in a dramatic reduction in internalization and transfection efficiency. These polyplexes used cholesterol and dynamin-dependent endocytosis pathways to enter into cells and these were found to be seriously compromised in cells with absence of NPC1. However, when compared with jetPEI® or Lipofectamine® 2000, the absence of NPC1 demonstrated no influence on DNA uptake. Surprisingly, the results showed an enhanced gene uptake ($\sim$3-fold) and transfection activity ($\sim$10-fold) of PβAE-based polyplexes in stably overexpressing the human NPC1 in chinese hamster ovary cells.

Recently, nanoparticles based on two different PβAE-based copolymers, PEI-*b*-PβAE and PEG-*b*-PβAE were used to co-deliver two types of siRNA (Snail siRNA and Twist siRNA) and paclitaxel (PTX). After i.v. administration in 4T1 pulmonary metastatic mice model it was observed a high accumulation and retention of siRNAs and PTX in tumor area. Moreover, 21 days after administration, the results revealed that a combination between Snail and Twist siRNAs and PTX led, simultaneously, to great inhibition of the tumor growth and metastasis[124].

Other type of PβAEs composed of γ-aminopropyl-triethoxysilane (APTES) and poly(ethylene glycol) diacrylate (PEGDA) were developed and studied in a combinatorial mini-library varying amine/diacrylate ratios during polymerization process[86]. These polymers were then assessed for gene delivery in 293T and HeLa cell lines in the presence of and absence of serum. From the screening of mini-library, it was ob-

served that in both cell lines, cell viability and transfection efficiency were increased with the increase of amine/acrylate weight ratio, from 0.7/1 to 6/1 APTES/PEG. In addition, the transfection pattern revealed uniform both in absence as in presence of serum. The polyplexes based on PβAE prepared from amine/acrylate ratio of 6/1, with average size of 133 nm, revealed high transfection activity and low cytotoxicity compared to Lipofectamine and PEI (25,000 g.mol^{-1}).

1.3   Poly[2-(dimethylamino)ethyl methacrylate]

PDMAEMA was recently reviewed as gene carrier[37] covering the main aspect that can influence transfection efficiency, such as molecular weight, polyplex size, pH, ionic strength, temperature, viscosity, polymer/plasmid ratio, the presence of stabilisers.

1.3.1   Synthesis and main physicochemical properties of poly[2-(dimethylamino)ethyl methacrylate]

PDMAEMA, a dual-responsive polymer (temperature and pH), has been widely used in gene delivery area[125–127] since its first use as a gene transfection system in 1996 by Cherng[128]. PDMAEMA can be prepared by radical polymerization based methods (Figure 1.16).

Figure 1.16:   Schematic representation of poly[2-(dimethylamino)ethyl methacrylate] (PDMAEMA) by radical polymerization.

van de Wetering et al.[129], in 1999, compared toxicity and the transfection activity of polyplexes based on PDMAEMA with other cationic polymers: poly[3-

(dimethylamino)propyl methacrylate] (PDMAPMA); poly[2-(dimethylamino)ethyl methacrylamide] (PDMAEMAm); poly[3-(dimethylamino)propyl methacrylamide] (PDMAPMAm); poly[2-(trimethylamino)ethyl methacrylate chloride] (PTMAEMA); poly[2-(diethylamino)ethyl methacrylate] (PDEAMA) and poly[2-(dimethylamino)ethyl acrylate] (PDMAEA). It was found that PDMAEMA had a higher transfection efficiency, but also, the highest cytotoxicity comparing to the other cationic polymers assessed. However, nowadays, PDMAEMA has been generally referred to possess low cytotoxicity and good biocompatibility[37]. Nevertheless, polymers with high molecular weights induce more cytotoxicity than those with low molecular weights even though, the resulting polyplexes are smaller and more efficient. The primary mode of toxicity has been reported to be induced by cellular membrane destabilization[125]. Also, to circumvent the low degradation profile, PDMAEMA was designed with reducible/cleavable bonds[126;130] (Figure 1.17).
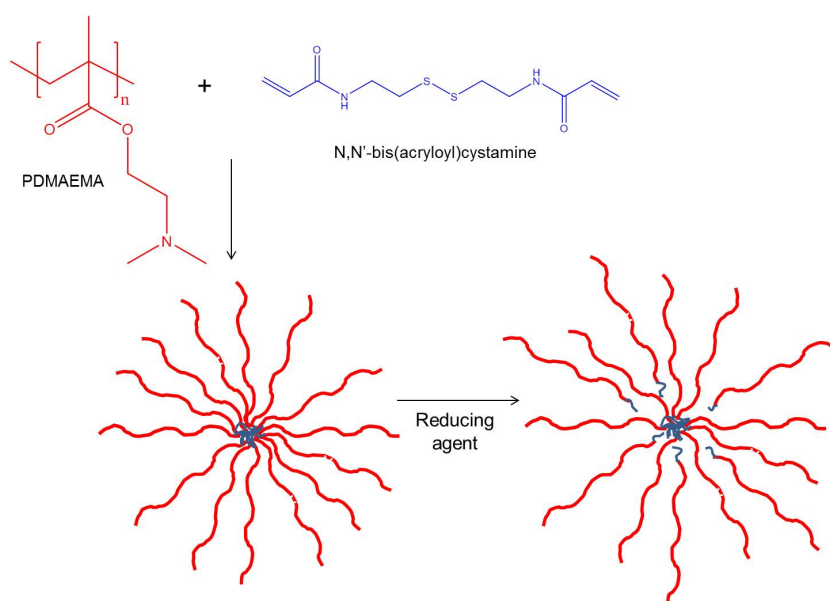
Figure 1.17: An example of a PDMAEMA with cleavable bonds. The disruption is caused by the reduction of disulfide bonds (adapted from[130]).

In Table 1.6 are summarized the main characteristics of PDMAEMA, which make it a promising polymeric non-viral vector for gene delivery.

Table 1.6: Summary of the main characteristics of poly[2-(dimethylamino)ethyl methacrylate].

Characteristics of poly[2-(dimethylamino)ethyl methacrylate] suitable for gene carrier
Easy synthesis and commercially available monomer
Possibility to control over polymer structure (such as molecular weight and architecture)
Lack of byproducts
Good buffer capacity (endossomal escape)
pKa between 5.5 and 7.4 (physiological values)
Lower cytotoxicity (half maximal inhibitory concentration (IC$_{50}$) = $\sim$40 μg/ml)

1.3.2 Polymer architecture

PDMAEMA, like PβAE, can be synthesized with different structures, such as, linear, star-shaped, highly-branched or comb/brush-shaped (Figure 1.18).
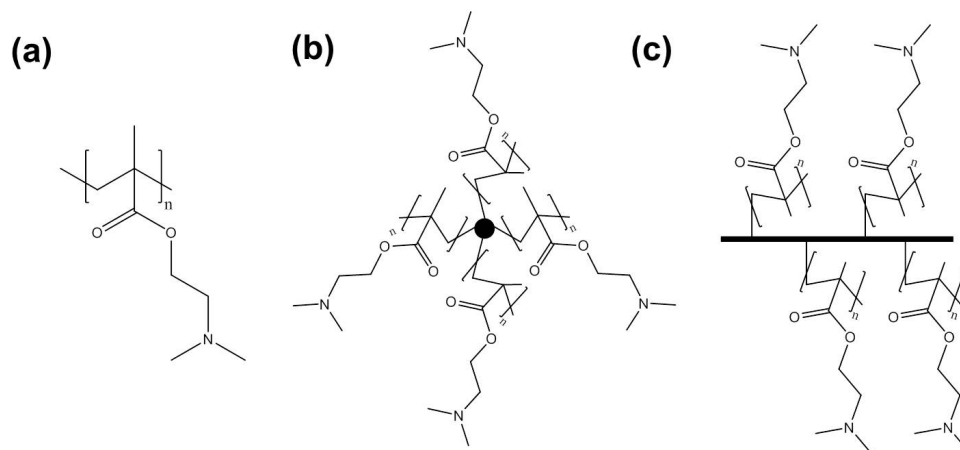
Figure 1.18: Some examples of different structures of PDMAEMA: (a) linear, (b) star-shaped and (c) comb/brush-shaped.

Star-shaped PDMAEMAs were introduced for the first time as gene delivery system by Georgiou[131] in 2004. In this study, star-shaped PDMAEMAs were coupled with ethylene glycol dimethacrylate. From star-shaped prepared, varying degree of polymerization (DP) of the arms from 10 to 100, it was observed that transfection efficiency decreased with the increase of the DP, being the best results obtained for stars with arms having DP equal to 10. In 2006[132], the study was extended in order to investigate the influence of the different star polymers structures (heteroarm, star block, and statistical star) based on PDMAEMA (DP 15) and poly(methacrylic acid) (PMAA) (DP 5). Regarding their cytotoxicity, all star-shaped polymers induced lower cytotoxicity compared to DMAEMA star homopolymer and SuperFect®. Among

the different star-shaped polymers tested, the PDMAEMA$_{15}$-*star*-PMAA$_5$ ampholyte was the one that provided higher transfection efficiency, although lower than the value observed for SuperFect$^{®}$ at its optimal conditions. Recently[133], the differences in gene delivery efficiency between a linear, a highly-branched and a star-shaped PDMAEMA vectors have been compared. For all structures tested, no differences in capacity to compact DNA and cellular uptake efficacy were observed. However, regarding transfection efficiency, star-shaped polymers demonstrated to be better than other PDMAEMAs structures. When compared to branched PEI, star-shaped PDMAEMA reached almost similar levels of transfection efficiency. An interesting fact was the observation that, for both PEI and PDMAEMA, linear structure revealed lower transfection efficiency when compared to its branched structures. Concerning to cytotoxicity, highly branched and linear PDMAEMAs were the most cytotoxic structures. Moreover, in general, star-shaped PDMAEMA-based polyplexes induced lower cytotoxicity than linear, branched or star-shaped PEI-based ones. Other study that evaluates the influence of the linear and star-shaped PDMAEMAs with different molecular weights (from 16,000 to 150,000 g.mol^{-1}) on the cytotoxicity and transfection efficiency was designed by Synatschke in 2011[134]. A mini-library of linear and star-shaped topology with 3- or 5-arms was developed. Results showed that at a given molecular weight, the cytotoxicity decreased with the increasing number of arms. Surprisingly, for all topologies a negligible transfection efficiency for polymers with molecular weight below 20,000 g.mol^{-1} was observed. The comparison of transfection efficiency among different architectures assessed was difficult to establish due to high variance of results. But, concerning star-shaped polymers, the results showed that the transfection efficiency is not necessarily improved with an increase of molecular weight. Considering both cytotoxicity and transfection activity, it was concluded that polymers with a branched topology and an intermediate molecular weight were the most promising candidates as gene delivery carriers.

1.3.3   Poly[2-(dimethylamino)ethyl   methacrylate]-based   copolymers

In recent years, the use of PDMAEMA-based copolymers with different structures has been widely used for gene delivery[130;135–139]. Preparation of copolymers based on PDMAEMA has been one of the strategies adopted to reduce its cytotoxicity without sacrificing the transfection efficiency[37]. Among the most studied structures, poly(ethylene glycol)-*block*-poly[2-(dimethylamino)ethyl methacrylate] has been one of the most used[140–144]. For example, Lin *et al.*[145], prepared PEG-PDMAEMA block copolymers with or without an acid-labile linkage between PEG and PDMAEMA blocks. The copolymers prepared with acid-labile linkage revealed higher transfection efficiency than PEG-PDMAEMA and PDMAEMA homopolymer. In addition, polyplexes based on PEG-PDMAEMAs copolymers presented lower cytotoxicity and higher particle stability than those prepared with PDMAEMA homopolymer. However, studies showed that in spite of a reduction in cytotoxicity by using PEG-PDMAEMA copolymers, the transfection efficiency decreased most probably due to the steric stabilization effect of a PEG corona[146]. This weakness was mitigated by introducing a hydrophobic segment, such as PCL, between the PDMAEMA and PEG blocks. The results showed an enhancement of about 15 times on transfection efficiency of PEG-PCL-PDMAEMA comparing to PEG-PDMAEMA copolymers[147]. Lin *et al.*[148] studied the effect of structural differences in transfection efficiency of blocked and grafted PEG-PCL-PDMAEMA copolymers. *In vitro* and *in vivo* results revealed that PEG-*block*-(PCL-*graft*-PDMAEMA)-based polyplexes have higher transfection efficiency comparing to PEG-*block*-PCL-*block*-PDMAEMA-based ones. The results also showed that polyplexes prepared with grafted copolymer have higher zeta potential, which could explain the higher efficiency (probably greater cellular uptake and endosome escape ability). Other interesting study was developed by Lim *et al.*[149] that prepared a poly(DMAEMA-*co*-N-vinyl-2-pyrrolidone) (VP)-*block*-PEG-galactose copolymer. This copolymer was complexed with plasmid DNA and the particles were coated with KALA, a cationic pH sensitive and endosomolytic peptide, in order to generate a positively charged surface. The results revealed that the inclusion of PEG segment and galactose moiety increase the transfection activity, with values

close to that obtained with Lipofectamine$^{®}$ Plus, even in the presence of serum. The inclusion of a reducible linking agent inside the copolymer chain has been shown to decrease the cytotoxicity of the materials. For instance, it was recently demonstrated that the inclusion of dibromomaleimide-based linking agent in statistical copolymers of oligo(ethylene glycol)methyl ether and DMAEMA reduced significantly its cytotoxicity when compared to non-reducible ones. Moreover, it was also showed that the inclusion of this reducible linking agent did not affect the transfection activity being observed comparable values for reducible and non-reducible copolymers[150]. In 2009, Xu *et al.*[151], compared the transfection efficiency of comb-shaped copolymers prepared by long hydroxypropyl cellulose backbones and short PDMAEMA side chains with high molecular weight PDMAEMA homopolymers. The comb-shaped copolymer-based polyplexes revealed higher transfection activity and lower cytotoxicity than the ones prepared with high molecular weight homopolymers. × Yu *et al.*[152] synthesized hyperbranched multiarm PDMAEMA-based copolymers with hydrophobic cores of poly[3-ethyl-3-(hydroxymethyl)-oxetane] (PEHO) and assessed the influence of topological architectures of these copolymers in transfection activity. PEHO-*g*-PDMAEMA revealed better transfection activity comparing to PDMAEMA homopolymer and branched PEI. Results also showed that for high degrees of branching (DB) of PEHO cores, higher transfection efficiency of PEHO-*g*-PDMAEMA-based polyplexes was observed. Interestingly, it was found that this DB-dependence was not related with the buffering capacity, DNA binding ability or cytotoxicity, but rather associated with the self-assembly ability of the copolymers with pDNA. Copolymers with higher DB condense more efficiently pDNA into smaller polyplexes, which can protect it more efficiently from enzymatic degradation and may facilitate their uptake by cells. Table 1.7 presents some examples of PDMAEMA-based copolymers used as transfection reagent.

Table 1.7: Examples of copolymers based on PDMAEMA used as gene carrier.

Copolymer	Architecture	Cargo	Ref.
PDMAEMA-*b*-PCL-*b*-PDMAEMA	Linear	siRNA and paclitaxel	[153]
PEG-*b*-PDMAEMA-*b*-PEG	Hyperbranched	pDNA	[145]
PEG-*b*-P(CL-*co*-DLLA)-*g*-PDMAEMA	Comb	siRNA	[154]
PCL-*b*-PDMAEMA	Dendritic	pDNA	[155]
PHEMA-*b*-PDMAEMA	Brush	pDNA	[156]
PHEMA-*b*-PDMAEMA-*b*-PEG-*b*-PDMAEMA-*b*-PHEMA	Linear	pDNA	[157]
P(DMAEMA-*co*-NVP)-*b*-PEG	Linear	pDNA	[149]
Lignin-*b*-PDMAEMA	Hyperbranched	pDNA	[158]
PVP-*g*-PDMAEMA-*b*-PMMA	Comb	pDNA	[159]

1.4 Reversible deactivation radical polymerization

1.4.1 Radicalar methods

Free radical polymerization (FRP) is a widely versatile type of polymer chain growth. It is a robust method that can be applied in a large variety of monomers and it is less sensitive to solvents (*e.g.*, tolerant to protic compounds, such as water) or presence of impurities (stringent purification of reagents is not required)[160]. FRP method is mainly composed by 3 steps: initiation, propagation and termination (Table 1.8).

Table 1.8: Free radical polymerization main steps.

	Reaction [a]
Initiation	$I \rightarrow 2R^\bullet$
	$R^\bullet + M \rightarrow P_1{}^\bullet$
Propagation	$P_n{}^\bullet + M \rightarrow P_{n+1}{}^\bullet$
Termination	$P_n{}^\bullet + P_m{}^\bullet \rightarrow P_{n+m}$
	$P_n{}^\bullet + P_m{}^\bullet \rightarrow P_n + P_m$

[a]Where I represents the initiator, $R^\bullet$ the initial radical, M the monomer and $P^\bullet$ the polymer growing chain [161;162]

Initiation step is started with the production of radicals $R^\bullet$ resulting from the homolytic decomposition of the initiator. The radical will react with a monomer unit, initiating the chain propagation. A succession of rapid (~ 1 s) monomer additions allows the polymer chain to growth in a step known as propagation. The polymerization process ends with termination steps, when a bimolecular reaction occurs in-

volving radicals, by combination or disproportionation, resulting in the deactivation of the radical propagating chain ends[161].

1.4.2   Problems

The average lifetime of propagation chain is in the range of 1 s wherein hundreds of monomer units are added to the generated radical before the termination process[161]. Because this step is so fast, the possibility of implementing a process of design and synthesis of well-controlled complex macromolecular architecture (macromolecular engineering), in order to improve the polymer properties (such as, controlled molecular weight, polydispersity index, composition or macromolecular architecture), is not feasible under this conditions. Furthermore, the addition of other monomers or functionalization groups, to produce pure block copolymers or end-functional polymers, respectively, is also unattainable[163;164].

1.4.3   Reversible deactivation radical polymerization

Reversible deactivation radical polymerization (RDRP) emerged as a method to overcome the main limitations of conventional FRP, including, poor control over the molecular weight, molecular weight distribution (dispersity), composition, topology, architecture and chain-end functionalities[165]. The concept of living polymerization came up for the first time in the middle of the 1960s by Szwarc[166;167], where block copolymers were prepared with controlled compositions using anionic polymerization technique. The RDRP methods have been extensively studied since 1995 and significant progresses have been achieved[168]. The basic principle involving RDRP techniques is the dynamic equilibrium between growing radicals and dormant species based on a fast and reversible activation/deactivation equilibrium of the growing radicals (keeping its concentration very low during the polymerization)[169]. Comparing to FRP, one major difference is the nature of the steady state concentration of radicals, that in RDRP results from ratio of the rate of activation and deactivation processes, and for FRP it is the balance between initiation and termination rates. As the initiation step in RDRP systems is very fast compared to propagation, polymer chains grow approximately at the same time[170]. Moreover, in RDRP the number of

polymer growing chains is much higher compared with FRP and the rates of termination and chain transfer to monomer per chain are much lower than in FRP, making the impact of termination negligible reactions[171]. These differences allow the synthesis of polymers with well-defined topology, composition and functionality, as well as the synthesis of block copolymers, which are not possible through FRP. The polymer molecular weight increases linearly with the conversion and the polymers possess active chain-ends (livingness), which allow being reinitiated with further monomer supply or functionalized with functional molecules or even other macromolecules[170] (Figure 1.19).
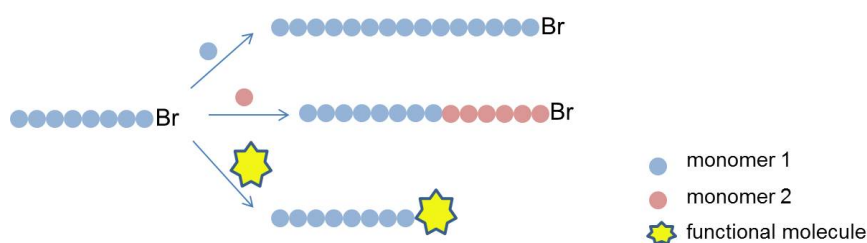
Figure 1.19: Examples of the modification possibilities from active chain-ends of the polymers prepared by RDRP.

1.4.3.1   Main RDRP methods

Depending on the strategy used to mediate this dynamic equilibrium, the main RDRP techniques can be divided in two main groups: reversible activation/deactivation of radicals (persistent radical effect) or reversible chain transfer (degenerative transfer process - DT) (Table 1.9).

Table 1.9: Main RDRP methods[168;170;172].

Persistent Radical Effect	**Stable Free Radical Polymerization (SFRP)** • Nitroxide-Mediated Polymerization (NMP) **Metal Catalyzed Reversible Deactivation Radical Polymerization** • Atom Transfer Radical Polymerization (ATRP) • Single Electron Transfer Living Radical Polymerization (SET-LRP)
Degenerative Transfer	**Degenerative Transfer Process (DT)** • Reversible Addition-Fragmentation Chain Transfer (RAFT) • Iodide/Reverse Iodide Transfer Polymerization (ITP/RITP)

The common concept is that reactive growing radical species is transiently and

reversely converted into the dormant state *via* the formation of the covalent termi-nal[164]. In persistent radical effect methods the steady state is established by balanc-ing activation and deactivation rates. During the activation step in persistent radical effect the growing radicals are formed by atom exchange and, consequently, as the activation step itself generates a propagating radical. Therefore, the use of a conven-tional radical initiators is not required[169;170]. In degenerative transfer, the initiation is slow and termination is fast with a steady state of growing radicals. The constant rate of propagation is lower than the constant rate of chain transfer between the ac-tive radicals and dormant species[169–171]. The concentration of chain transfer agent (CTA) is much larger compared to radical initiators. In this sense, the chain transfer agent acts as the dormant species. Thus, the CTA structure and its suitability to the monomer that is being polymerized plays an important role in the quality of the control achieved in the degenerative processes methods[169;170].

In the degenerative transfer, the most studied methods are: reversible addition-fragmentation chain transfer (RAFT) polymerization and iodine/reverse iodine transfer polymerization (ITP/RITP) (iodine atom transfer). The persistent radical effect category can be subdivided in two main techniques: stable free radical poly-merization, also known as nitroxide-mediated polymerization (NMP); and metal cat-alyzed reversible deactivation radical polymerization which includes atom transfer radical polymerization (ATRP) and single electron transfer living radical polymer-ization (SET-LRP)[170;168;172].

Among all RDRP tecnhiques, ATRP is one the most commonly explored method due to its efficiency, simplicity, high tolerance to monomer functionality and com-mercial availability of required initiators and catalysts[164;173]. As it is a metal cat-alyzed RDRP method, and as the name suggests, the catalyst plays an important role, and therefore, it has been investigated the use of various catalysts such as iron, ruthenium, copper, and other metals on polymerization[174]. The combination of tran-sition metal and ligand has strong influence in the catalytic features of the complex. Therefore, the development and study of the transition metal complexes for ATRP methods has been the subject of a large number of studies[164].

1.4.3.2   Atom Transfer Radical Polymerization

The concept of ATRP is based on the generation of a fast transition metal complex that mediates the equilibrium between dormant (macroinitiators P_n-X, where X represents a halogen or pseudohalogen) and active species (macroradical, $P^\bullet$). A lower oxidation state transition metal complex (Mt^m/L where Mt^m represents the transition metal species in oxidation state m and L is a ligand) activates the dormant species acting as an activator to intermittently form growing radicals ($P_n{}^\bullet$). The deactivator or persistent radical is represented by the transition metal complexes in the higher oxidation state coordinated with halide ligands X-Mt^{m+1}/L (Scheme 1.1).

$$P_n\text{-X} \; + \; Mt^m/L \quad \underset{k_{\text{deact}}}{\overset{k_{\text{act}}}{\rightleftharpoons}} \quad P_n{}^\bullet \; + \; \text{X-}Mt^{m+1}/L$$

Scheme 1.1: General mechanism of ATRP.

In the ATRP systems, research has been focused to assess several transition metal complexes in an attempt to perform the polymerization of a large range of monomers functionalities. The metal halide and ligand compose the transition-metal complex. The role of the ligand around the center metal is important in the solubility of the complex in the reaction medium as well as in the reactivity of the redox reaction via the adjustment of the redox potential of the metal[164;175]. The copper based complexes with nitrogen-based ligands are the most often used in ATRP. The unavoidable radical - radical termination process accompanied ATRP mechanism, resulting in the build up of small excess of X-Cu(II)/L deactivator (persistent radical effect)[176].

Among ATRP techniques, different variations exist, such as activators regenerated by electron transfer (ARGET), initiators for continuous activator regeneration (ICAR), electrochemically mediated ATRP (*e*ATRP), supplemental activator and reducing agent (SARA) ATRP and photochemically mediated ATRP. The development of these ATRP variations allowed the reduction of the amounts of transition metal complexes to tiny quantities (<100 ppm) in the presence of various reducing agents (including zero-valent metals[177;178], organotin complexes[179;180], ascorbic acid[179], glu-

cose[179] or sulfites[181;182]). The metal contamination of the resultant polymers is one of the most significant disadvantages of the ATRP techniques. This aspect is crucial on polymers that will be used in biomedical and electronic applications.

1.4.3.2.1 Challenges - SARA ATRP as polymerization technique for biomedical applications

Despite the advances and remarkable advantages of ATRP prepared materials, there are some limitations that remain to be overcome. The main issue, as previously mentioned, is the residual content of metal complex in the product. Besides cytotoxicity issue, other concerns, such as, product color, environmental legislative conformity, process complexity and cost need also to be considered[183]. Thus, new challenges emerge aiming to develop new catalytic systems employing lower concentration of toxic catalysts and new polymerization systems using eco-friendly solvents and commercial available products.

Therefore, SARA ATRP, which uses zero-valent transition metals[178;184] as both reducing agents and supplemental activators, has been one of the most used new ATRP technique. When Cu(0) is used, it slowly generates radical and Cu(I)X by a supplemental activator, and it slowly regenerates Cu(I)X species as a reducing agent[185]. In addition, this method can be performed using environmentally friendly solvents/solvent mixtures (such as alcohol or alcohol/water mixtures) at room temperature[186]. Therefore, the development of this polymerization technique emerges as a promising RDRP technique to prepare tailor-made and well-controlled polymers for biomedical applications.

1.4.3.2.2 RDRP and macromolecular engineering

RDRP, and in particularly ATRP, as mentioned above, is used as a method to prepare tailor made polymers being a powerful tool in the control of polymer structures consequently providing specific characteristics to the end products. Moreover, the complete control in polymer synthesis allows to obtain complex and very well-defined architectures. Additionally, the initiator used in ATRP method can provide specific end-groups on the polymer chain(s) (Figure 1.20). Generally, with a functional initiator one chain-end of the polymer is an alkyl halide, whereas the other

can be a predetermined functional group[187]. These features turn possible the easy preparation of functional polymers, for example, with structures and combination of polymers, that are otherwise inaccessible using FRP methods[188].
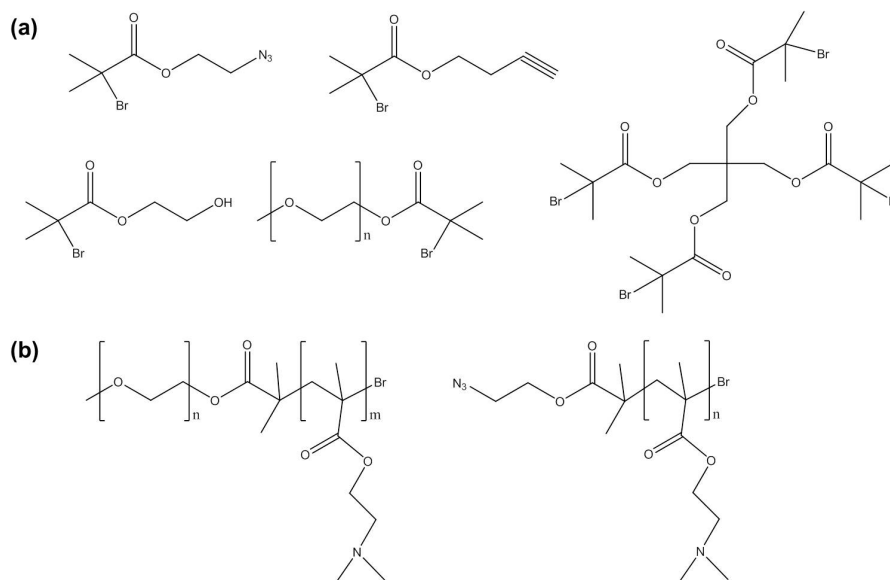

Figure 1.20: Examples of functional RDRP initiators (a) and two examples of PDMAEMA synthesized from these functional initiators.

1.4.4 Click chemistry

1.4.4.1 General considerations

The advent of RDRP allowed the controlled polymerization of functional monomers or end-funcionalized polymers. However, in spite of recent advances in RDRP methods that have facilitated access to (co)polymers with well-defined and complex architectures with precise functional groups, some interesting macromolecules are not possible to be synthesized by these robust polymerization techniques requiring post-polymerization modification methods. Some of these post-polymerization reactions are frequently inefficient and can conduct to side reactions with other groups within the polymer[189]. Because of that, it was necessary to develop versatile and specific chemical reactions that can facilitate access to nearly any polymeric structure rather by the simplest, cleanest, and more effective means possible[189;190]. Accordingly, these reactions, denominated as click chemistry reactions, are also characterized by high yields with little or no by-products, tolerance of a broad range of functional

groups, and by their mild reaction conditions[191;192]. In addition, there are also known to require simple or no purification procedure of the product, use easily accessible reagents, insensitive to water or oxygen, require no solvent or a benign one (like water) or an easily removed solvent and go rapidly to full conversion[191;193]. The combination of click chemistry reactions with RDRP methods has been particularly profitable for exploring complex structure materials with unique properties while oversimplify their preparation. These procedures allowed the preparation of (co)polymers with advanced macromolecular topologies and increased functionality obtaining materials with unique properties. Some examples of click chemistry reactions are copper(I)-catalyzed and strain-promoted azide-alkyne cycloadditions, thiol-ene reactions and Diels-Alder cycloadditions. Among them, Huisgen 1,3-dipolar cycloaddition of alkynes to azides and Michael additions click reactions are two of the most studied[189;194;195].

1.4.4.2   Copper-catalyzed azide-alkyne cycloaddition

Copper-catalyzed Huisgen 1,3-dipolar cycloaddition of terminal alkynes to azides, also known as, copper-catalyzed azide-alkyne cycloaddition (CuAAC) (Figure 1.21), is a well-established and most representative approach of click chemistry[190;196]. The utility of the CuAAC has been demonstrated for the synthesis and modification of polymers with a wide range of composition, functionality, architecture, and intended purpose[197;198].

The copper catalyst dramatically increases the rate of the azide-alkyne cycloaddition[192;193;196]. Indeed, in the absence of a proper catalyst the reaction is fairly slow because alkynes are poor 1,3-dipole acceptors. On the other hand, in the presence of copper (I), that can bind to terminal alkynes, the reaction becomes very fast, efficient and regioselective[200]. Some of the advantages of the CuCAAC are that can be performed at room temperature in various solvents and it is tolerant to several functional groups[200]. In addition, azide-based click reactions has particular interest because azide group is easy to introduce into macromolecules having halogen chain ends without dramatically changing their physicochemical properties[196].

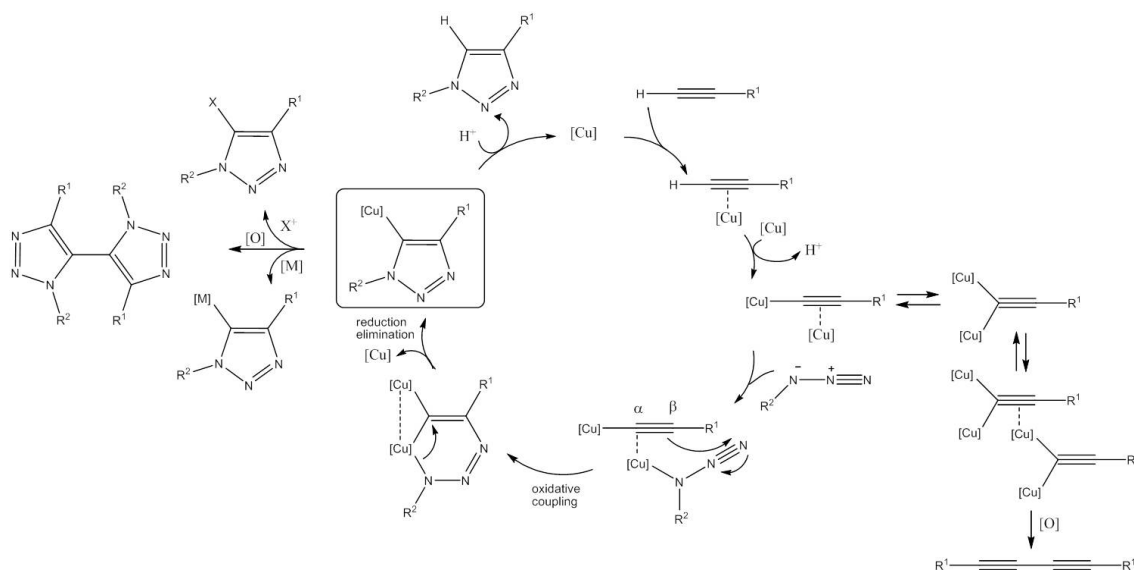One of the most important feature of the CuAAc reaction is its unique bioorthog-

Figure 1.21: Proposed mechanism for copper-catalyzed Huisgen 1,3-dipolar cycloaddition. [Cu] denotes a copper fragment that varies in the number of ligands and oxidation states (adapted from [199]).

onality, since the alkyne and azide are not biologically present and do not react with biological functionalities. This issue has special interest for site-specifically attaching biomolecules, such as peptides, proteins, polysaccharides, and even entire viruses and cells [193].

The combination of ATRP and CuAAC was firstly reported independently in 2005 by Hest and Opsten [201], Weichenhan [202] and Matyjaszewski [203], and become very popular due to the fact that both reactions can be catalyzed by the same copper complexes. The most popular approach of click living ATRP chain end resulting in the conversion of the living R-halide (such as, R-Br or R-Cl) chain end into R-N$_3$ by nucleophilic substitution before a CuAAC reaction can be conducted [191;204] (Figure 1.22).
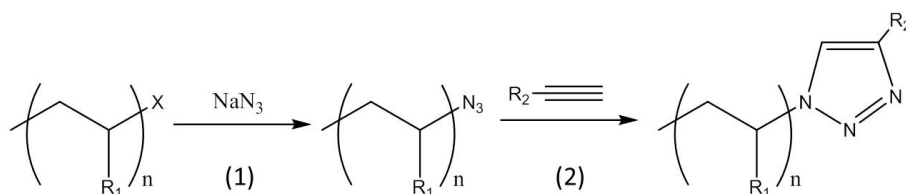

Figure 1.22: Schematic representation of the transformation of a halide chain-end into azide (1) and subsequent CuAAC reaction with alkyne-functionalized molecules (2).

This azidation procedure is generally carried out using a wide excess of NaN$_3$

in N,N-dimethylformamide (DMF) and, requires high temperature in the case of chloride-terminated polymers[204;191].

1.4.4.3   Michael addition

The Michael addition reaction, named for Arthur Michaels, belongs to a larger class of conjugate additions and consists in a nucleophilic addition between a carbanion (or another nucleophile) and an α,β-unsaturated carbonyl compound[205;206]. This addition leads to the formation of C-C bonds. A schematic Michael addition reaction is represented in Figure 1.23.
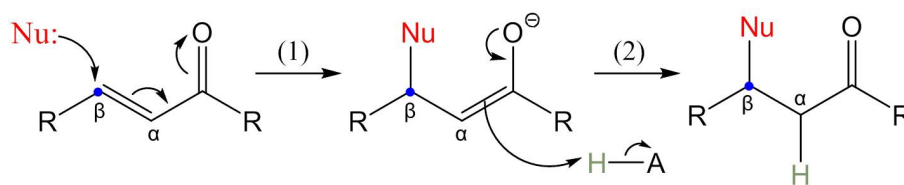
Figure 1.23: General schematic representation of the Michael addition reaction.

The nucleophile is an electron-withdrawing group, such as acyl or cyano groups, and attacks C_β resulting in an enol or enolate intermediate (carbanion) (step 1). Normally, this carbanion collapses and the C_α is protonated (step 2). The substituents on the nucleophile known as a Michael donor while substituents on the activated alkene are the Michael acceptor[205].

The Michael addition reaction has been used for polymerization reactions due to mild conditions reactions needed, a high functional group tolerance, a large variety of polymerizable monomers and functional precursors with a favorable reaction rates and high conversions[206]. Some examples of polymers synthesized by this method are: poly(amido amine); poly(amino ester); poly(ester sulfide); poly(imido sulfide); poly(aspartamide); poly(enone sulfide); poly(imido ether); poly(amino quinone) or poly(enamine ketone)[206]. And recently, it has been applied for post-polymerization modifications and coupling of biological and synthetic polymers[82;207;208].

1.5   Final remarks

To sum up the information contained in this introduction, it is crucial the design and the development of more efficient and safe gene carrier. For this purpose, polymer-based vectors appear as a promising carriers. Their low immunocytotoxicity and facility to tune their properties by facile synthesis procedures make them attractive materials for gene delivery. However, their transfection activity are still significantly lower when compared to viral vectors. Moreover, some polymers present some cytotoxicity.

In this direction, the subsequent chapters include the experimental approaches and results regarding the development of a new copolymer based on PDMAEMA and PβAE, two of the most used cationic polymers in gene therapy. The main purpose is to validate the hypothesis that the combination of both polymers would be advantageous for gene delivery. The influence of PβAE segment in transfection activity would be the last focus of the work.

Bibliography

[1] V. Fuster and J.M. Sweeny. Aspirin a historical and contemporary therapeutic overview. *Circulation*, 123(7):768–778, 2011.

[2] K. Jain. Drug delivery systems - an overview. In KewalK. Jain, editor, *Drug Delivery Systems*, volume 437 of *Methods in Molecular Biology*, pages 1–50. Humana Press, 2008.

[3] J. Folkman and D.M. Long. The use of silicone rubber as a carrier for prolonged drug therapy. *Journal of Surgical Research*, 4(3):139–142, 1964.

[4] J. Kost and R. Langer. Responsive polymeric delivery systems. *Advanced Drug Delivery Reviews*, 64, Supplement(0):327–341, 2012.

[5] A. Rösler, G.W.M. Vandermeulen, and H.A. Klok. Advanced drug delivery devices via self-assembly of amphiphilic block copolymers. *Advanced Drug Delivery Reviews*, 64, Supplement(0):270–279, 2012.

[6] T.M. Allen and P.R. Cullis. Liposomal drug delivery systems: from concept to clinical applications. *Advanced Drug Delivery Reviews*, 65(1):36–48, 2013. Advanced Drug Delivery: Perspectives and Prospects.

[7] A. Kumari, S.K. Yadav, and S.C. Yadav. Biodegradable polymeric nanoparticles based drug delivery systems. *Colloids and Surfaces B: Biointerfaces*, 75(1):1–18, 2010.

[8] R.A. Siegel. Stimuli sensitive polymers and self regulated drug delivery systems: a very partial review. *Journal of Controlled Release*, 190(0):337–351, 2014. 30th Anniversary Special Issue.

[9] D. Patra, S. Sengupta, W. Duan, H. Zhang, R. Pavlick, and A. Sen. Intelligent, self-powered, drug delivery systems. *Nanoscale*, 5:1273–1283, 2013.

[10] D.J.A. Crommelin and A.T. Florence. Towards more effective advanced drug delivery systems. *International Journal of Pharmaceutics*, 454(1):496–511, 2013.

[11] A. Mountain. Gene therapy: the first decade. *Trends in Biotechnology*, 18(3):119–128, 2000.

[12] D.W. Pack, A.S. Hoffman, S. Pun, and P.S. Stayton. Design and development of polymers for gene delivery. *Nature Reviews Drug Discovery*, 4(7):581–593, 2005.

[13] C. Sheridan. Gene therapy finds its niche. *Nature Biotechnology*, 29(2):121–128, 2011.

[14] T. Friedmann. A brief history of gene therapy. *Nature Genetics*, 2(2):93–98, 1992.

[15] I.M. Verma and M.D. Weitzman. Gene therapy: twenty-first century medicine. *Annual Review of Biochemistry*, 74(1):711–738, 2005.

[16] J.N. Warnock, C. Daigre, and M. Al-Rubeai. Introduction to viral vectors. In Otto-Wilhelm Merten and Mohamed Al-Rubeai, editors, *Viral Vectors for Gene Therapy*, volume 737 of *Methods in Molecular Biology*, pages 1–25. Humana Press, 2011.

[17] S.A. Rosenberg, P. Aebersold, K. Cornetta, A. Kasid, R.A. Morgan, R. Moen, E.M. Karson, M.T. Lotze, J.C. Yang, S.L. Topalian, M.J. Merino, K. Culver, A.D. Miller, R.M. Blaese, and W.F. Anderson. Gene transfer into humans - immunotherapy of patients with advanced melanoma, using tumor-infiltrating lymphocytes modified by retroviral gene transduction. *New England Journal of Medicine*, 323(9):570–578, 1990.

[18] R.M. Blaese, K.W. Culver, A.D. Miller, C.S. Carter, T. Fleisher, M. Clerici, G. Shearer, L. Chang, Y.W. Chiang, P. Tolstoshev, J.J. Greenblatt, S.A. Rosenberg, H. Klein, M. Berger, C.A. Mullen, W.J. Ramsey, L. Muul, R.A. Morgan, and W.F. Anderson. T-Lymphocyte-directed gene-therapy for ADA-SCID - initial trial results after 4 years. *Science*, 270(5235):475–480, 1995.

[19] The Journal of Gene Medicine. Gene therapy trials wordwide, February 2015. http://www.abedia.com/wiley/phases.php.

[20] C. Morrison. $ 1-million price tag set for Glybera gene therapy. *Nature Biotechnology*, 33(3):217–218, 2015.

[21] uniQure, November 2014. http://www.uniqure.com/home/.

[22] Reuters. Germany poised to say yes to 1.1m euros a patient gene therapy drug, November 2014. http://www.theguardian.com/society/2014/nov/27/worlds-most-expensive-medicine-glybera-sale-1million-price.

[23] Y.K. Kim, C. Zhang, C.S. Cho, M.H. Cho, and H.L. Jiang. Poly(amino ester)s-based polymeric gene carriers in cancer gene therapy. *InTech*, 2013.

[24] Y. Yue and C. Wu. Progress and perspectives in developing polymeric vectors for *in vitro* gene delivery. *Biomaterials Science*, 1:152–170, 2013.

[25] H. Faneca, A.L. Cardoso, S. Trabulo, S. Duarte, and MCP de Lima. Cationic liposome-based systems for nucleic acid delivery: from the formulation development to therapeutic applications. In *Drug Delivery Systems: Advanced Technologies Potentially Applicable in Personalised Treatment*, pages 153–184. Springer Netherlands, 2013.

[26] Y.C. Hu. Viral gene therapy vectors. In *Gene Therapy for Cartilage and Bone Tissue Engineering*, SpringerBriefs in Bioengineering, pages 17–31. Springer Berlin Heidelberg, 2014.

[27] M.L. Edelstein, M.R. Abedi, and J. Wixon. Gene therapy clinical trials worldwide to 2007 - an update. *The Journal of Gene Medicine*, 9(10):833–842, 2007.

[28] D. Zhi, S. Zhang, S. Cui, Y. Zhao, Y. Wang, and D. Zhao. The headgroup evolution of cationic lipids for gene delivery. *Bioconjugate Chemistry*, 24(4):487–519, 2013.

[29] Z. Liu, Z. Zhang, C. Zhou, and Y. Jiao. Hydrophobic modifications of cationic polymers for gene delivery. *Progress in Polymer Science*, 35(9):1144–1162, 2010.

[30] T.G. Park, J.H. Jeong, and S.W. Kim. Current status of polymeric gene delivery systems. *Advanced Drug Delivery Reviews*, 58(4):467–486, 2006.

[31] P.L. Felgner, T.R. Gadek, M. Holm, R. Roman, H.W. Chan, M. Wenz, J.P. Northrop, G.M. Ringold, and M. Danielsen. Lipofection: a highly efficient, lipid-mediated DNA-transfection procedure. *Proceedings of the National Academy of Sciences*, 84(21):7413–7417, 1987.

[32] Z. ur Rehman, I.S. Zuhorn, and D. Hoekstra. How cationic lipids transfer nucleic acids into cells and across cellular membranes: recent advances. *Journal of Controlled Release*, 166(1):46–56, 2013.

[33] D. Fischer, Y. Li, B. Ahlemeyer, J. Krieglstein, and T. Kissel. *In vitro* cytotoxicity testing of polycations: influence of polymer structure on cell viability and hemolysis. *Biomaterials*, 24(7):1121–1131, 2003.

[34] J.H. Jeong, S.W. Kim, and T.G. Park. Molecular design of functional polymers for gene therapy. *Progress in Polymer Science*, 32(11):1239–1274, 2007.

[35] A. Vaheri and J.S. Pagano. Infectious poliovirus RNA: a sensitive method of assay. *Virology*, 27(3):434–436, 1965.

[36] A. Aied, U. Greiser, A. Pandit, and W. Wang. Polymer gene delivery: overcoming the obstacles. *Drug Discovery Today*, 18:1090–1098, 2013.

[37] S. Agarwal, Y. Zhang, S. Maji, and A. Greiner. PDMAEMA based gene delivery materials. *Materials Today*, 15(9):388–393, 2012.

[38] U. Lungwitz, M. Breunig, T. Blunk, and A. Göpferich. Polyethylenimine-based non-viral gene delivery systems. *European Journal of Pharmaceutics and Biopharmaceutics*, 60(2):247–266, 2005.

[39] L. Parhamifar, A.K. Larsen, A.C. Hunter, T.L. Andresen, and S.M. Moghimi. Polycation cytotoxicity: a delicate matter for nucleic acid therapy-focus on polyethylenimine. *Soft Matter*, 6:4001–4009, 2010.

[40] G. Galli, M. Laus, A. Santeangeloni, P. Ferruti, and E. Chiellini. Thermotropic poly(β-aminoester)s containing azoxy groups. *Makromolekulare Chemie - Rapid Communications*,

4(10):681–686, 1983.

[41] F. Danusso and P. Ferruti. Synthesis of tertiary amine polymers. *Polymer*, 11(2):88–113, 1970.

[42] D.M. Lynn and R. Langer. Degradable poly(β-amino esters): synthesis, characterization, and self-assembly with plasmid DNA. *Journal of the American Chemical Society*, 122(44):10761–10768, 2000.

[43] J. Chen, J. Ouyang, J. Kong, W. Zhong, and M.M. Xing. Photo-cross-linked and pH-sensitive biodegradable micelles for doxorubicin delivery. *ACS Applied Materials & Interfaces*, 5(8):3108–3117, 2013.

[44] W. Song, Z. Tang, M. Li, S. Lv, H. Yu, L. Ma, X. Zhuang, Y. Huang, and X. Chen. Tunable pH-sensitive poly(β-amino ester)s synthesized from primary amines and diacrylates for intracellular drug delivery. *Macromolecular Bioscience*, 12(10):1375–1383, 2012.

[45] Y. Zhang, R. Wang, Y. Hua, R. Baumgartner, and J. Cheng. Trigger-responsive poly(β-amino ester) hydrogels. *ACS Macro Letters*, 3(7):693–697, 2014.

[46] M. Keeney, H. Waters, K. Barcay, X. Jiang, Z. Yao, J. Pajarinen, K. Egashira, S.B. Goodman, and F. Yang. Mutant MCP-1 protein delivery from layer-by-layer coatings on orthopedic implants to modulate inflammatory response. *Biomaterials*, 34(38):10287–10295, 2013.

[47] M.L. Viger, J. Sankaranarayanan, C. de Gracia Lux, M. Chan, and A. Almutairi. Collective activation of MRI agents via encapsulation and disease-triggered release. *Journal of the American Chemical Society*, 135(21):7847–7850, 2013.

[48] G.H. Gao, H. Heo, J.H. Lee, and D.S. Lee. An acidic pH-triggered polymeric micelle for dual-modality MR and optical imaging. *Journal of Materials Chemistry*, 20:5454–5461, 2010.

[49] D.L. Safranski, D. Weiss, J.B. Clark, B.S. Caspersen, W.R. Taylor, and K. Gall. Effect of poly(ethylene glycol) diacrylate concentration on network properties and *in vivo* response of poly(β-amino ester) networks. *Journal of Biomedical Materials Research Part A*, 96A(2):320–329, 2011.

[50] D.L. Safranski, D. Weiss, J.B. Clark, W.R. Taylor, and K. Gall. Semi-degradable poly(β-amino ester) networks with temporally controlled enhancement of mechanical properties. *Acta Biomaterialia*, 10(8):3475–3483, 2014.

[51] D.M. Lynn, D.G. Anderson, D. Putnam, and R. Langer. Accelerated discovery of synthetic transfection vectors: parallel synthesis and screening of a degradable polymer library. *Journal of the American Chemical Society*, 123(33):8155–8156, 2001.

[52] D.G. Anderson, D.M. Lynn, and R. Langer. Semi-automated synthesis and screening of a large library of degradable cationic polymers for gene delivery. *Angewandte Chemie*, 42(27):3153–3158, 2003.

[53] D.G. Anderson, A. Akinc, N. Hossain, and R. Langer. Structure/property studies of polymeric gene delivery using a library of poly(β-amino esters). *Molecular Therapy*, 11(3):426–434, 2005.

[54] D.M. Lynn, D.G. Anderson, A. Akinc, and R. Langer. *Degradable poly (β-amino ester)s for gene delivery*. CRC Press: New York, 2004.

[55] D.M. Lynn, M.M. Amiji, and R. Langer. pH-Responsive polymer microspheres: rapid release of encapsulated material within the range of intracellular pH. *Angewandte Chemie International Edition*, 40(9):1707–1710, 2001.

[56] E. Vázquez, D.M. Dewitt, P.T. Hammond, and D.M. Lynn. Construction of hydrolytically-degradable thin films via layer-by-layer deposition of degradable polyelectrolytes. *Journal of the American Chemical Society*, 124(47):13992–13993, 2002.

[57] A. Akinc, D.M. Lynn, D.G. Anderson, and R. Langer. Parallel synthesis and biophysical characterization of a degradable polymer library for gene delivery. *Journal of the American Chemical Society*, 125(18):5316–5323, 2003.

[58] A. Potineni, D.M. Lynn, R. Langer, and M.M. Amiji. Poly(ethylene oxide)-modified poly(β-amino ester) nanoparticles as a pH-sensitive biodegradable system for paclitaxel delivery. *Journal of Controlled Release*, 86(2-3):223–234, 2003.

[59] C. Gao, W. Tang, and D. Yan. Synthesis and characterization of water-soluble hyperbranched poly(ester amine)s from diacrylates and diamines. *Journal of Polymer Science Part A: Polymer Chemistry*, 40(14):2340–2349, 2002.

[60] Y. Liu, D. Wu, Y. Ma, G. Tang, S. Wang, C. He, T. Chung, and S. Goh. Novel poly(amino ester)s obtained from Michael addition polymerizations of trifunctional amine monomers with diacrylates: safe and efficient DNA carriers. *Chemical Communications*, pages 2630–2631, 2003.

[61] R. Arote, T.H. Kim, Y.K. Kim, S.K. Hwang, H.L. Jiang, H.H. Song, J.W. Nah, M.H. Cho, and C.S. Cho. A biodegradable poly(ester amine) based on polycaprolactone and polyethylenimine as a gene carrier. *Biomaterials*, 28(4):735–744, 2007.

[62] R.B. Arote, S.K. Hwang, M.K. Yoo, D. Jere, H.L. Jiang, Y.K. Kim, Y.J. Choi, J.W. Nah, M.H. Cho, and C.S. Cho. Biodegradable poly(ester amine) based on glycerol dimethacrylate and polyethylenimine as a gene carrier. *The Journal of Gene Medicine*, 10(11):1223–1235, 2008.

[63] J. Zhang, N.J. Fredin, and D.M. Lynn. Erosion of multilayered films fabricated from degradable polyamines: characterization and evidence in support of a mechanism that involves polymer hydrolysis. *Journal of Polymer Science Part A: Polymer Chemistry*, 44(17):5161–5173, 2006.

[64] A. Akinc, D.G. Anderson, D.M. Lynn, and R. Langer. Synthesis of poly(β-amino ester)s optimized for highly effective gene delivery. *Bioconjugate Chemistry*, 14(5):979–988, 2003.

[65] P. Xu, S.Y. Li, Q. Li, J. Ren, E.A. Van Kirk, W.J. Murdoch, M. Radosz, and Y. Shen. Biodegradable cationic polyester as an efficient carrier for gene delivery to neonatal cardiomyocytes. *Biotechnology and Bioengineering*, 95(5):893–903, 2006.

[66] D.M. Brey, I. Erickson, and J.A. Burdick. Influence of macromer molecular weight and chemistry on poly(β-amino ester) network properties and initial cell interactions. *Journal of Biomedical Materials Research Part A*, 85A(3):731–741, 2008.

[67] D.G. Anderson, W.D. Peng, A. Akinc, N. Hossain, A. Kohn, R. Padera, R. Langer, and J.A. Sawicki. A polymer library approach to suicide gene therapy for cancer. *Proceedings of the National Academy of Sciences of the United States of America*, 101(45):16028–16033, 2004.

[68] G.T. Zugates, D.G. Anderson, S.R. Little, I.E.B. Lawhorn, and R. Langer. Synthesis of poly(β-amino ester)s with thiol-reactive side chains for DNA delivery. *Journal of the American Chemical Society*, 128(39):12726–12734, 2006.

[69] A.A. Eltoukhy, D.J. Siegwart, C.A. Alabi, J.S. Rajan, R. Langer, and D.G. Anderson. Effect of molecular weight of amine end-modified poly(β-amino ester)s on gene delivery efficiency and toxicity. *Biomaterials*, 33(13):3594–3603, 2012.

[70] R.B. Shmueli, M. Ohnaka, A. Miki, N.B. Pandey, R. Lima e Silva, J.E. Koskimaki, J. Kim, A.S. Popel, P.A. Campochiaro, and J.J. Green. Long-term suppression of ocular neovascularization by intraocular injection of biodegradable polymeric particles containing a serpin-derived peptide. *Biomaterials*, 34(30):7544–7551, 2013.

[71] C.B. Wu, J.Y. Hao, and X.M. Deng. A novel degradable poly(β-amino ester) and its nano-complex with poly(acrylic acid). *Polymer*, 48(21):6272–6285, 2007.

[72] J.J. Green, R. Langer, and D.G. Anderson. A combinatorial polymer library approach yields insight into nonviral gene delivery. *Accounts of Chemical Research*, 41(6):749–759, 2008.

[73] C.J. Bishop, T.M. Ketola, S.Y. Tzeng, J.C. Sunshine, A. Urtti, H. Lemmetyinen, E. Vuorimaa-Laukkanen, M. Yliperttula, and J.J. Green. The effect and role of carbon atoms in poly(β-amino ester)s for DNA binding and gene delivery. *Journal of the American Chemical Society*, 135(18):6951–6957, 2013.

[74] D. Shenoy, S. Little, R. Langer, and M. Amiji. Poly(ethylene oxide)-modified poly(β-amino ester) nanoparticles as a pH-sensitive system for tumor-targeted delivery of hydrophobic drugs. 1. *In vitro* evaluations. *Molecular Pharmaceutics*, 2(5):357–366, 2005.

[75] D.G. Anderson, C.A. Tweedie, N. Hossain, S.M. Navarro, Van Vliet K.J. Brey, D.M., R. Langer, and J.A. Burdick. A combinatorial library of photocrosslinkable and degradable materials. *Advanced Materials*, 18(19):2614–2618, 2006.

[76] Z. Zhong, Y. Song, J.F.J. Engbersen, M.C. Lok, W.E. Hennink, and J. Feijen. A versatile family of degradable non-viral gene carriers based on hyperbranched poly(ester amine)s. *Journal of Controlled Release*, 109(1-3):317–329, 2005.

[77] G.T. Zugates, W. Peng, A. Zumbuehl, S. Jhunjhunwala, Y.H. Huang, R. Langer, J.A. Sawicki, and D.G. Anderson. Rapid optimization of gene delivery by parallel end-modification of poly(β-amino ester)s. *Molecular Therapy*, 15(7):1306–1312, 2007.

[78] J.J. Green, G.T. Zugates, N.C. Tedford, Y.H. Huang, L.G. Griffith, D.A. Lauffenburger, J.A. Sawicki, R. Langer, and D.G. Anderson. Combinatorial modification of degradable polymers enables transfection of human cells comparable to adenovirus. *Advanced Materials*, 19(19):2836+, 2007.

[79] R.J. Collier. Understanding the mode of action of diphtheria toxin: a perspective on progress during the 20th century. *Toxicon*, 39(11):1793–1803, 2001.

[80] S. Potala, S.K. Sahoo, and R.S. Verma. Targeted therapy of cancer using diphtheria toxin-derived immunotoxins. *Drug Discovery Today*, 13(17â18):807–815, 2008.

[81] J.J. Green, J. Shi, E. Chiu, E.S. Leshchiner, R. Langer, and D.G. Anderson. Biodegradable polymeric vectors for gene delivery to human endothelial cells. *Bioconjugate Chemistry*, 17(5):1162–1169, 2006.

[82] G.T. Zugates, N.C. Tedford, A. Zumbuehl, S. Jhunjhunwala, C.S. Kang, L.G. Griffith, D.A. Lauffenburger, R. Langer, and D.G. Anderson. Gene delivery properties of end-modified poly(β-amino ester)s. *Bioconjugate Chemistry*, 18(6):1887–1896, 2007.

[83] F. Yang, J.J. Green, T. Dinio, L. Keung, S.W. Cho, H. Park, R. Langer, and D.G. Anderson. Gene delivery to human adult and embryonic cell-derived stem cells using biodegradable nanoparticulate polymeric vectors. *Gene Therapy*, 16(4):533–546, 2009.

[84] F. Yang, S.W. Cho, S.M. Son, S.R. Bogatyrev, D. Singh, J.J. Green, Y. Mei, S. Park, S.H. Bhang, B.S. Kim, R. Langer, and D.G. Anderson. Genetic engineering of human stem cells for enhanced angiogenesis using biodegradable polymeric nanoparticles. *Proceedings of the National Academy of Sciences*, 107(8):3317–3322, 2010.

[85] J. Sunshine, J.J. Green, K.P. Mahon, F. Yang, A.A. Eltoukhy, D.N. Nguyen, R. Langer, and D.G. Anderson. Small-molecule end-groups of linear polymer determine cell-type gene-delivery efficacy. *Advanced Materials*, 21(48):4947–4951, 2009.

[86] D. Jere, M.K. Yoo, R. Arote, T.H. Kim, M.H. Cho, J.W. Nah, Y.J. Choi, and C.S. Cho. Poly(amino ester) composed of poly(ethylene glycol) and aminosilane prepared by combinatorial chemistry as a gene carrier. *Pharmaceutical Research*, 25(4):875–885, 2008.

[87] J.C. Sunshine, M.I. Akanda, D. Li, K.L. Kozielski, and J.J. Green. Effects of base polymer hydrophobicity and end-group modification on polymeric gene delivery. *Biomacromolecules*, 12(10):3592–3600, 2011.

[88] J.C. Sunshine, S.B. Sunshine, I. Bhutto, J.T. Handa, and J.J. Green. Poly(β-amino ester)-nanoparticle mediated transfection of retinal pigment epithelial cells *in vitro* and *in vivo*. *PLoS ONE*, 7(5):e37543, 05 2012.

[89] J.C. Sunshine, D.Y. Peng, and J.J. Green. Uptake and transfection with polymeric nanoparticles are dependent on polymer end-group structure, but largely independent of nanoparticle physical and chemical properties. *Molecular Pharmaceutics*, 9(11):3375–3383, 2012.

[90] S.Y. Tzeng, H. Guerrero-Cázares, E.E. Martinez, J.C. Sunshine, A. Quiñones-Hinojosa, and J.J. Green. Non-viral gene delivery nanoparticles based on poly(β-amino esters) for treatment of glioblastoma. *Biomaterials*, 32(23):5402–5410, 2011.

[91] S.Y. Tzeng, B.P. Hung, W.L. Grayson, and J.J. Green. Cystamine-terminated poly(β-amino ester)s for siRNA delivery to human mesenchymal stem cells and enhancement of osteogenic differentiation. *Biomaterials*, 33(32):8142–8151, 2012.

[92] S.Y. Tzeng and J.J. Green. Subtle changes to polymer structure and degradation mechanism enable highly effective nanoparticles for siRNA and DNA delivery to human brain cancer. *Advanced Healthcare Materials*, 2(3):468–480, 2013.

[93] H. Guerrero-Cázares, S.Y. Tzeng, N.P. Young, A.O. Abutaleb, A. Quiñones-Hinojosa, and J.J.

Green. Biodegradable polymeric nanoparticles show high efficacy and specificity at DNA delivery to human glioblastoma *in vitro* and *in vivo*. *ACS Nano*, 8(5):5141–5153, 2014.

[94] A. Mangraviti, S.Y. Tzeng, K.L. Kozielski, Y. Wang, Y. Jin, D. Gullotti, M. Pedone, N. Buaron, A. Liu, D.R. Wilson, S.K. Hansen, F.J. Rodriguez, G.D. Gao, F. DiMeco, H. Brem, A. Olivi, B. Tyler, and J.J. Green. Polymeric nanoparticles for nonviral gene therapy extend brain tumor survival in vivo. *ACS Nano*, 9(2):1236–1249, 2015. PMID: 25643235.

[95] J. Kim, J.C. Sunshine, and J.J. Green. Differential polymer structure tunes mechanism of cellular uptake and transfection routes of poly(β-amino ester) polyplexes in human breast cancer cells. *Bioconjugate Chemistry*, 25(1):43–51, 2014.

[96] A.A. Eltoukhy, D. Chen, C.A. Alabi, R. Langer, and D.G. Anderson. Degradable terpolymers with alkyl side chains demonstrate enhanced gene delivery potency and nanoparticle stability. *Advanced Materials*, 25(10):1487–1493, 2013.

[97] M. Keeney, S.G. Ong, A. Padilla, Z. Yao, S. Goodman, J.C. Wu, and F. Yang. Development of poly(β-amino ester)-based biodegradable nanoparticles for nonviral delivery of minicircle DNA. *ACS Nano*, 7(8):7241–7250, 2013.

[98] C.D. Kamat, R.B. Shmueli, N. Connis, C.M. Rudin, J.J. Green, and C.L. Hann. Poly(β-amino ester) nanoparticle delivery of TP53 has activity against small cell lung cancer in vitro and in vivo. *Molecular Cancer Therapeutics*, 12(4):405–415, 2013.

[99] Y. Sha, L. Shen, and X. Hong. A divergent synthesis of new aliphatic poly(ester-amine) dendrimers bearing peripheral hydroxyl or acrylate groups. *Tetrahedron Letters*, 43(51):9417–9419, 2002.

[100] Y. Wang, G. Quelever, and L. Peng. The seemingly trivial yet challenging synthesis of poly(aminoester) dendrimers. *Current Medicinal Chemistry*, 19(29):5011–5028, 2012.

[101] S. Khoee and K. Hemati. Synthesis of magnetite/polyamino-ester dendrimer based on PCL/PEG amphiphilic copolymers via convergent approach for targeted diagnosis and therapy. *Polymer*, 54(21):5574–5585, 2013.

[102] H. Akiyama, K. Miyashita, Y. Hari, S. Obika, and T. Imanishi. Synthesis of novel polyesteramine dendrimers by divergent and convergent methods. *Tetrahedron*, 69(33):6810–6820, 2013.

[103] W. Han, B. Lin, H. Yang, and X. Zhang. Synthesis of novel poly(ester amine) dendrimers by Michael addition and acrylate esterification. *Designed Monomers and Polymers*, 16(1):67–71, 2013.

[104] C. Bouillon, A. Tintaru, V. Monnier, L. Charles, G. Quéléver, and L. Peng. Synthesis of poly(amino)ester dendrimers via active cyanomethyl ester intermediates. *The Journal of Organic Chemistry*, 75(24):8685–8688, 2010.

[105] D. Wu, Y. Liu, X. Jiang, L. Chen, C. He, S.H. Goh, and K.W. Leong. Evaluation of hyperbranched poly(amino ester)s of amine constitutions similar to polyethylenimine for DNA delivery. *Biomacromolecules*, 6(6):3166–3173, 2005.

[106] D. Wu, Y. Liu, X. Jiang, C. He, S.H. Goh, and K.W. Leong. Hyperbranched poly(amino ester)s with different terminal amine groups for DNA delivery. *Biomacromolecules*, 7(6):1879–1883, 2006.

[107] S.A. Chew, M.C. Hacker, A. Saraf, R.M. Raphael, F.K. Kasper, and A.G. Mikos. Biodegradable branched polycationic polymers with varying hydrophilic spacers for nonviral gene delivery. *Biomacromolecules*, 10(9):2436–2445, 2009.

[108] S.A. Chew, M.C. Hacker, A. Saraf, R.M. Raphael, F.K. Kasper, and A.G. Mikos. Altering amine basicities in biodegradable branched polycationic polymers for nonviral gene delivery. *Biomacromolecules*, 11(3):600–609, 2010.

[109] E.M. Saurer, D. Yamanouchi, B. Liu, and D.M. Lynn. Delivery of plasmid DNA to vascular tissue in vivo using catheter balloons coated with polyelectrolyte multilayers. *Biomaterials*, 32(2):610–618, 2011.

[110] J. Zhang, L.S. Chua, and D.M. Lynn. Multilayered thin films that sustain the release of functional DNA under physiological conditions. *Langmuir*, 20(19):8015–8021, 2004.

[111] C.M. Jewell, J. Zhang, N.J. Fredin, and D.M. Lynn. Multilayered polyelectrolyte films promote the direct and localized delivery of DNA to cells. *Journal of Controlled Release*, 106(1-2):214–223, 2005.

[112] N.J. Fredin, J. Zhang, and D.M. Lynn. Surface analysis of erodible multilayered polyelectrolyte films: nanometer-scale structure and erosion profiles. *Langmuir*, 21(13):5803–5811, 2005.

[113] N.J. Fredin, J. Zhang, and D.M. Lynn. Nanometer-scale decomposition of ultrathin multilayered polyelectrolyte films. *Langmuir*, 23(5):2273–2276, 2007.

[114] C.M. Jewell, J. Zhang, N.J. Fredin, M.R. Wolff, T.A. Hacker, and D.M. Lynn. Release of plasmid DNA from intravascular stents coated with ultrathin multilayered polyelectrolyte films. *Biomacromolecules*, 7(9):2483–2491, 2006.

[115] E.M. Saurer, C.M. Jewell, D.A. Roenneburg, S.L. Bechler, J.R. Torrealba, T.A. Hacker, and D.M. Lynn. Polyelectrolyte multilayers promote stent-mediated delivery of DNA to vascular tissue. *Biomacromolecules*, 14(5):1696–1704, 2013.

[116] S.L. Bechler, Y. Si, Y. Yu, J. Ren, B. Liu, and D.M. Lynn. Reduction of intimal hyperplasia in injured rat arteries promoted by catheter balloons coated with polyelectrolyte multilayers that contain plasmid DNA encoding PKC delta. *Biomaterials*, 34(1):226–236, 2013.

[117] E.M. Saurer, C.M. Jewell, J.M. Kuchenreuther, and D.M. Lynn. Assembly of erodible, DNA-containing thin films on the surfaces of polymer microparticles: toward a layer-by-layer approach to the delivery of DNA to antigen-presenting cells. *Acta Biomaterialia*, 5(3):913–924, 2009.

[118] E.M. Saurer, R.M. Flessner, S.P. Sullivan, M.R. Prausnitz, and D.M. Lynn. Layer-by-layer assembly of DNA- and protein-containing films on microneedles for drug delivery to the skin. *Biomacromolecules*, 11(11):3136–3143, 2010.

[119] R.M. Flessner, Y. Yu, and D.M. Lynn. Rapid release of plasmid DNA from polyelectrolyte multilayers: a weak poly(acid) approach. *Chemical Communications*, 47:550–552, 2011.

[120] S.L. Bechler and D.M. Lynn. Characterization of degradable polyelectrolyte multilayers fabricated using DNA and a fluorescently-labeled poly(β-amino ester): shedding light on the role of

the cationic polymer in promoting surface-mediated gene delivery. *Biomacromolecules*, 13(2):542–552, 2012.

[121] C. Li, S.Y. Tzeng, L.E. Tellier, and J.J. Green. (3-Aminopropyl)-4-methylpiperazine end-capped poly(1,4-butanediol diacrylate-co-4-amino-1-butanol)-based multilayer films for gene delivery. *ACS Applied Materials & Interfaces*, 5(13):5947–5953, 2013.

[122] P.C. DeMuth, Y. Min, B. Huang, J.A. Kramer, A.D. Miller, D.H. Barouch, P.T. Hammond, and D.J. Irvine. Polymer multilayer tattooing for enhanced DNA vaccination. *Nature Materials*, 12(4):367–376, 2013.

[123] A.A. Eltoukhy, G. Sahay, J.M. Cunningham, and D.G. Anderson. Niemann-Pick C1 affects the gene delivery efficacy of degradable polymeric nanoparticles. *ACS Nano*, 8(8):7905–7913, 2014. PMID: 25010491.

[124] S. Tang, Q. Yin, J. Su, H. Sun, Q. Meng, Y. Chen, L. Chen, Y. Huang, W. Gu, M. Xu, H. Yu, Z. Zhang, and Y. Li. Inhibition of metastasis and growth of breast cancer by pH-sensitive poly(β-amino ester) nanoparticles co-delivering two siRNA and paclitaxel. *Biomaterials*, 48(0):1–15, 2015.

[125] J.M. Layman, S.M. Ramirez, M.D. Green, and T.E. Long. Influence of polycation molecular weight on poly(2-dimethylaminoethyl methacrylate)-mediated DNA delivery *in vitro*. *Biomacromolecules*, 10(5):1244–1252, 2009.

[126] Y.Z. You, D.S. Manickam, Q.H. Zhou, and D. Oupicky. Reducible poly(2-dimethylaminoethyl methacrylate): synthesis, cytotoxicity, and gene delivery activity. *Journal of Controlled Release*, 122(3):217–225, 2007.

[127] S.E. Averick, E. Paredes, A. Irastorza, A.R. Shrivats, A. Srinivasan, D.J. Siegwart, A.J. Magenau, H.Y. Cho, E. Hsu, A.A. Averick, J. Kim, S. Liu, J.O. Hollinger, S.R. Das, and K. Matyjaszewski. Preparation of cationic nanogels for nucleic acid delivery. *Biomacromolecules*, 13(11):3445–3449, 2012.

[128] J.Y. Cherng, P. van de Wetering, H. Talsma, D.J.A. Crommelin, and W.E. Hennink. Effect of size and serum proteins on transfection efficiency of poly((2-dimethylamino)ethyl methacrylate)-plasmid nanoparticles. *Pharmaceutical Research*, 13(7):1038–1042, 1996.

[129] P. van de Wetering, E.E. Moret, N.M.E. Schuurmans-Nieuwenbroek, M.J. van Steenbergen, and W.E. Hennink. Structure-activity relationships of water-soluble cationic methacrylate/methacrylamide polymers for nonviral gene delivery. *Bioconjugate Chemistry*, 10(4):589–597, 1999.

[130] F. Dai, P. Sun, Y. Liu, and W. Liu. Redox-cleavable star cationic PDMAEMA by arm-first approach of ATRP as a nonviral vector for gene delivery. *Biomaterials*, 31(3):559–569, 2010.

[131] T.K. Georgiou, M. Vamvakaki, C.S. Patrickios, E.N. Yamasaki, and L.A. Phylactou. Nanoscopic cationic methacrylate star homopolymers: synthesis by group transfer polymerization, characterization and evaluation as transfection reagents. *Biomacromolecules*, 5(6):2221–2229, 2004.

[132] T.K. Georgiou, L.A. Phylactou, and C.S. Patrickios. Synthesis, characterization, and evaluation

as transfection reagents of ampholytic star copolymers: effect of star architecture. *Biomacro-molecules*, 7(12):3505–3512, 2006.

[133] A. Schallon, V. Jérôme, A. Walther, C.V. Synatschke, A.H.E. Müller, and R. Freitag. Performance of three PDMAEMA}-based polycation architectures as gene delivery agents in comparison to linear and branched PEI}. *Reactive and Functional Polymers*, 70(1):1–10, 2010.

[134] C.V. Synatschke, A. Schallon, V. Jérôme, R. Freitag, and A.H.E. Müller. Influence of polymer architecture and molecular weight of poly(2-(dimethylamino)ethyl methacrylate) polycations on transfection efficiency and cell viability in gene delivery. *Biomacromolecules*, 12(12):4247–4255, 2011. PMID: 22007721.

[135] X. Qian, L. Long, Z. Shi, C. Liu, M. Qiu, J. Sheng, P. Pu, X. Yuan, Y. Ren, and C. Kang. Star-branched amphiphilic PLA-*b*-PDMAEMA copolymers for co-delivery of miR-21 inhibitor and doxorubicin to treat glioma. *Biomaterials*, 35(7):2322–2335, 2014.

[136] H. Cheng, H. Deng, L. Zhou, Y. Su, S. Yu, X. Zhu, Y. Zhou, and D. Yan. Improvement of gene delivery of PDMAEMA by incorporating a hyperbranched polymer core. *Journal of Controlled Release*, 152, Supplement 1(0):e187–e188, 2011.

[137] W. Tian, J. Kong, Z. Zheng, W. Zhang, and C. Mu. Temperature-responsive property of star poly((N,N-dimethylamino)ethyl methacrylate) with hyperbranched core: effect of core-shell architecture and β-cyclodextrin grafted via covalent bond or ionic electrostatic attraction. *Soft Materials*, 11(3):272–280, 2013.

[138] S. Venkataraman, W.L. Ong, Z.Y. Ong, S.C.J. Loo, P.L.R. E., and Y.Y. Yang. The role of PEG architecture and molecular weight in the gene transfection performance of PEGylated poly(dimethylaminoethyl methacrylate) based cationic polymers. *Biomaterials*, 32(9):2369–2378, 2011.

[139] B. Newland, H. Tai, Y. Zheng, D. Velasco, A. Di Luca, S.M. Howdle, C. Alexander, W. Wang, and A. Pandit. A highly effective gene delivery vector - hyperbranched poly(2-(dimethylamino)ethyl methacrylate) from in situ deactivation enhanced ATRP. *Chemical Communications*, 46:4698–4700, 2010.

[140] C. Zhu, M. Zheng, F. Meng, F.M. Mickler, N. Ruthardt, X. Zhu, and Z. Zhong. Reversibly shielded DNA polyplexes based on bioreducible PDMAEMA-SS-PEG-SS-PDMAEMA triblock copolymers mediate markedly enhanced nonviral gene transfection. *Biomacromolecules*, 13(3):769–778, 2012.

[141] Y. Qian, Y. Zha, B. Feng, Z. Pang, B. Zhang, X. Sun, J. Ren, C. Zhang, X. Shao, Q. Zhang, and X. Jiang. PEGylated poly(2-(dimethylamino) ethyl methacrylate)/DNA polyplex micelles decorated with phage-displayed TGN peptide for brain-targeted gene delivery. *Biomaterials*, 34(8):2117–2129, 2013.

[142] Y. Qiao, Y. Huang, C. Qiu, X. Yue, L. Deng, Y. Wan, J. Xing, C. Zhang, S. Yuan, A. Dong, and J. Xu. The use of PEGylated poly [2-(N,N-dimethylamino) ethyl methacrylate] as a mucosal DNA delivery vector and the activation of innate immunity and improvement of HIV-1-specific

immune responses. *Biomaterials*, 31(1):115–123, 2010.

[143] D.J. Gary, J. Min, Y. Kim, K. Park, and Y.Y. Won. The effect of N/P ratio on the in vitro and in vivo interaction properties of PEGylated poly[2-(dimethylamino)ethyl methacrylate]-based siRNA complexes. *Macromolecular Bioscience*, 13(8):1059–1071, 2013.

[144] C.E. Nelson, J.R. Kintzing, A. Hanna, J.M. Shannon, M.K. Gupta, and C.L. Duvall. Balancing cationic and hydrophobic content of PEGylated siRNA polyplexes enhances endosome escape, stability, blood circulation time, and bioactivity in vivo. *ACS Nano*, 7(10):8870–8880, 2013.

[145] S. Lin, F. Du, Y. Wang, S. Ji, D. Liang, L. Yu, and Z. Li. An acid-labile block copolymer of PDMAEMA and PEG as potential carrier for intelligent gene delivery systems. *Biomacromolecules*, 9(1):109–115, 2008.

[146] U. Rungsardthong, M. Deshpande, L. Bailey, M. Vamvakaki, S.P. Armes, M.C. Garnett, and S. Stolnik. Copolymers of amine methacrylate with poly(ethylene glycol) as vectors for gene therapy. *Journal of Controlled Release*, 73(2-3):359–380, 2001.

[147] X. Yue, Y. Qiao, N. Qiao, S. Guo, J. Xing, L. Deng, J. Xu, and A. Dong. Amphiphilic methoxy poly(ethylene glycol)-*b*-poly(epson-caprolactone)-*b*-poly(2-dimethylaminoethyl methacrylate) cationic copolymer nanoparticles as a vector for gene and drug delivery. *Biomacromolecules*, 11(9):2306–2312, 2010.

[148] D. Lin, Y. Huang, Q. Jiang, W. Zhang, X. Yue, S. Guo, P. Xiao, Q. Du, J. Xing, L. Deng, Z. Liang, and A. Dong. Structural contributions of blocked or grafted poly(2-dimethylaminoethyl methacrylate) on PEGylated polycaprolactone nanoparticles in siRNA delivery. *Biomaterials*, 32(33):8730–8742, 2011.

[149] D.W. Lim, Y.I. Yeom, and T.G. Park. Poly(DMAEMA-NVP)-*b*-PEG-galactose as gene delivery vector for hepatocytes. *Bioconjugate Chemistry*, 11(5):688–695, 2000.

[150] J.K.Y. Tan, J.L. Choi, H. Wei, J.G. Schellinger, and S.H. Pun. Reducible, dibromomaleimide-linked polymers for gene delivery. *Biomaterials Science*, 3:112–120, 2015.

[151] F.J. Xu, Y. Ping, J. Ma, G.P. Tang, W.T. Yang, J. Li, E.T. Kang, and K.G. Neoh. Comb-shaped copolymers composed of hydroxypropyl cellulose backbones and cationic poly((2-dimethyl amino)ethyl methacrylate) side chains for gene delivery. *Bioconjugate Chemistry*, 20(8):1449–1458, 2009.

[152] S. Yu, J. Chen, R. Dong, Y. Su, B. Ji, Y. Zhou, X. Zhu, and D. Yan. Enhanced gene transfection efficiency of PDMAEMA by incorporating hydrophobic hyperbranched polymer cores: effect of degree of branching. *Polymer Chemistry*, 3:3324–3329, 2012.

[153] C. Zhu, S. Jung, S. Luo, F. Meng, X. Zhu, T.G. Park, and Z. Zhong. Co-delivery of siRNA and paclitaxel into cancer cells by biodegradable cationic micelles based on PDMAEMA-PCL-PDMAEMA triblock copolymers. *Biomaterials*, 31(8):2408–2416, 2010.

[154] S. Han, Q. Cheng, Y. Wu, J. Zhou, X. Long, T. Wei, Y. Huang, S. Zheng, J. Zhang, L. Deng, X. Wang, X.J. Liang, H. Cao, Z. Liang, and A. Dong. Effects of hydrophobic core components in amphiphilic PDMAEMA nanoparticles on siRNA delivery. *Biomaterials*, 48(0):45–55, 2015.

[155] Y. Liu, C. Lin, J. Li, Y. Qu, and J. Ren. *In vitro* and *in vivo* gene transfection using biodegradable and low cytotoxic nanomicelles based on dendritic block copolymers. *Journal of Materials Chemistry B*, 3:688–699, 2015.

[156] X. Jiang, M.C. Lok, and W.E. Hennink. Degradable-brushed pHEMA-pDMAEMA synthesized via ATRP and click chemistry for gene delivery. *Bioconjugate Chemistry*, 18(6):2077–2084, 2007.

[157] F.J. Xu, H. Li, J. Li, Z. Zhang, E.T. Kang, and K.G. Neoh. Pentablock copolymers of poly(ethylene glycol), poly((2-dimethyl amino)ethyl methacrylate) and poly(2-hydroxyethyl methacrylate) from consecutive atom transfer radical polymerizations for non-viral gene delivery. *Biomaterials*, 29(20):3023–3033, 2008.

[158] X. Liu, H. Yin, Z. Zhang, B. Diao, and J. Li. Functionalization of lignin through ATRP grafting of poly(2-dimethylaminoethyl methacrylate) for gene delivery. *Colloids and Surfaces B: Biointerfaces*, 125(0):230–237, 2015.

[159] Y. Song, T. Zhang, X. Song, L. Zhang, C. Zhang, J. Xing, and X.J. Liang. Polycations with excellent gene transfection ability based on PVP-g-PDMAEMA with random coil and micelle structures as non-viral gene vectors. *Journal of Materials Chemistry B*, 3:911–918, 2015.

[160] G. Moad and D.H. Solomon. 1 - Introduction. In Graeme MoadDavid H. Solomon, editor, *The Chemistry of Radical Polymerization (Second Edition)*, pages 1 – 9. Elsevier Science Ltd, Amsterdam, second edition edition, 2005.

[161] B. Yamada and P. Zetterlund. 3 General chemistry of radical polymerization. *Handbook of Radical Polymerization*, page 117, 2002.

[162] K.F. O'Driscoll. Free radical polymerization kinetics - revisited. *Pure and Applied Chemistry*, 53(3):617–626, 1981.

[163] K. Matyjaszewski. *General Concepts and History of Living Radical Polymerization*, pages 361–406. John Wiley & Sons, Inc., 2003.

[164] Z. Xue, D. He, and X. Xie. Iron-catalyzed atom transfer radical polymerization. *Polymer Chemistry*, pages –, 2014.

[165] M.A. Tasdelen, M.U. Kahveci, and Y. Yagci. Telechelic polymers by living and controlled/living polymerization methods. *Progress in Polymer Science*, 36(4):455–567, 2011.

[166] M. Szwarc. Living polymers. *Nature*, 178(4543):1168–1169, 1956.

[167] M. Szwarc, M. Levy, and R. Milkovich. Polymerization initiated by electron tranfer to monomer. a new method of formation of block copolymers. *Journal of the American Chemical Society*, 78(11):2656–2657, 1956.

[168] M. Destarac. Controlled radical polymerization: industrial stakes, obstacles and achievements. *Macromolecular Reaction Engineering*, 4(3-4):165–179, 2010.

[169] K. Matyjaszewski. *Controlled radical polymerization: state-of-the-art in 2011*, chapter 2, pages 1–13.

[170] W.A. Braunecker and K. Matyjaszewski. Controlled/living radical polymerization: features, developments, and perspectives. *Progress in Polymer Science*, 32(1):93–146, 2007.

[171] F. Schué. Controlled/living radical polymerization: progress in ATRP, NMP and RAFT: ACS symposium series no 768 edited by: Krzysztof matyjaszewski american chemical society, washington, dc, september 2000 pp 484, isbn 0-8412-3707-7. *Polymer International*, 51(4):370–370, 2002.

[172] K. Matyjaszewski. Controlled radical polymerization: state of the art in 2008. In *ACS symposium series*, volume 1023, pages 3–13. Oxford University Press, 2009.

[173] A.C. Fonseca, P. Ferreira, R.A. Cordeiro, P.V. Mendonça, J.R. Góis, M.H. Gil, and J.F.J. Coelho. Drug delivery systems for predictive medicine: polymers as tools for advanced applications. In *New Strategies to Advance Pre/Diabetes Care: Integrative Approach by PPPM*, pages 399–455. Springer, 2013.

[174] M. Kamigaito. Recent developments in metal-catalyzed living radical polymerization. *Polymer journal*, 43(2):105–120, 2011.

[175] K. Matyjaszewski and J. Xia. Atom transfer radical polymerization. *Chemical Reviews-Columbus*, 101(9):2921–2990, 2001.

[176] H. Fischer. The persistent radical effect: a principle for selective radical reactions and living radical polymerizations. *Chemical Reviews*, 101(12):3581–3610, 2001.

[177] N. Rocha, P.V. Mendonça, J.P. Mendes, P.N. Simões, A.V. Popov, T. Guliashvili, A.C. Serra, and J.F.J. Coelho. Facile synthesis of well-defined telechelic alkyne-terminated polystyrene in polar media using ATRP with mixed Fe/Cu transition metal catalyst. *Macromolecular Chemistry and Physics*, 214(1):76–84, 2013.

[178] C.M.R. Abreu, P.V. Mendonça, A.C. Serra, J.F.J. Coelho, A.V. Popov, and T. Guliashvili. Accelerated ambient-temperature ATRP of methyl acrylate in alcohol-water solutions with a mixed transition-metal catalyst system. *Macromolecular Chemistry and Physics*, 213(16):1677–1687, 2012.

[179] W. Jakubowski and K. Matyjaszewski. Activators regenerated by electron transfer for atom-transfer radical polymerization of (meth)acrylates and related block copolymers. *Angewandte Chemie*, 118(27):4594–4598, 2006.

[180] W. Jakubowski, K. Min, and K. Matyjaszewski. Activators regenerated by electron transfer for atom transfer radical polymerization of styrene. *Macromolecules*, 39(1):39–45, 2006.

[181] J. Tonnar, P. Lacroix-Desmazes, and B. Boutevin. Living radical ab initio emulsion polymerization of n-butyl acrylate by reverse iodine transfer polymerization (RITP): use of persulfate as both initiator and oxidant. *Macromolecules*, 40(17):6076–6081, 2007.

[182] C.M.R. Abreu, P.V. Mendonça, A.C. Serra, A.V. Popov, K. Matyjaszewski, T. Guliashvili, and J.F.J. Coelho. Inorganic sulfites: efficient reducing agents and supplemental activators for atom transfer radical polymerization. *ACS Macro Letters*, 1(11):1308–1311, 2012.

[183] J.P. Rao and K.E. Geckeler. Polymer nanoparticles: preparation techniques and size-control parameters. *Progress in Polymer Science*, 36(7):887–913, 2011.

[184] Y. Zhang, Y. Wang, and K. Matyjaszewski. ATRP of methyl acrylate with metallic zinc, magnesium, and iron as reducing agents and supplemental activators. *Macromolecules*, 44(4):683–685,

2011.

[185] T. Guliashvili, P.V. Mendonça, A.C. Serra, A.V. Popov, and J.F.J. Coelho. Copper-mediated controlled/"living" radical polymerization in polar solvents: insights into some relevant mechanistic aspects. *Chemistry - A European Journal*, 18(15):4607–4612, 2012.

[186] C.M.R. Abreu, A.C. Serra, A.V. Popov, K. Matyjaszewski, T. Guliashvili, and J.F.J. Coelho. Ambient temperature rapid SARA ATRP of acrylates and methacrylates in alcohol-water solutions mediated by a mixed sulfite/Cu(II)Br$_2$ catalytic system. *Polymer Chemistry*, 4:5629–5636, 2013.

[187] V. Coessens, T. Pintauer, and K. Matyjaszewski. Functional polymers by atom transfer radical polymerization. *Progress in Polymer Science*, 26(3):337–377, 2001.

[188] H. Gao and K. Matyjaszewski. Synthesis of functional polymers with controlled architecture by CRP of monomers in the presence of cross-linkers: from stars to gels. *Progress in Polymer Science*, 34(4):317–350, 2009.

[189] B.S. Sumerlin and A.P. Vogt. Macromolecular engineering through click chemistry and other efficient transformations. *Macromolecules*, 43(1):1–13, 2010.

[190] J.F. Lutz and H. Schlaad. Modular chemical tools for advanced macromolecular engineering. *Polymer*, 49(4):817–824, 2008.

[191] N. Akeroyd and B. Klumperman. The combination of living radical polymerization and click chemistry for the synthesis of advanced macromolecular architectures. *European Polymer Journal*, 47(6):1207–1231, 2011.

[192] J.E. Hein and V.V. Fokin. Copper-catalyzed azide-alkyne cycloaddition (CuAAC) and beyond: new reactivity of copper(I) acetylides. *Chemical Society Reviews*, 39:1302–1315, 2010.

[193] N.K. Devaraj and J.P. Collman. Copper catalyzed azide-alkyne cycloadditions on solid surfaces: applications and future directions. *QSAR & Combinatorial Science*, 26(11-12):1253–1260, 2007.

[194] H.C. Kolb, M.G. Finn, and K.B. Sharpless. Click chemistry: diverse chemical function from a few good reactions. *Angewandte Chemie International Edition*, 40(11):2004–2021, 2001.

[195] J.E. Moses and A.D. Moorhouse. The growing applications of click chemistry. *Chemical Society Reviews*, 36:1249–1262, 2007.

[196] V. Hong, N.F. Steinmetz, M. Manchester, and M.G. Finn. Labeling live cells by copper-catalyzed alkyne-azide click chemistry. *Bioconjugate Chemistry*, 21(10):1912–1916, 2010.

[197] J.F. Lutz. 1,3-Dipolar cycloadditions of azides and alkynes: a universal ligation tool in polymer and materials science. *Angewandte Chemie International Edition*, 46(7):1018–1025, 2007.

[198] M. Meldal. Polymer "clicking" by CuAAC reactions. *Macromolecular Rapid Communications*, 29(12-13):1016–1051, 2008.

[199] B. Schulze and U.S. Schubert. Beyond click chemistry - supramolecular interactions of 1,2,3-triazoles. *Chemical Society Reviews*, 43:2522–2571, 2014.

[200] V.V. Rostovtsev, L.G. Green, V.V. Fokin, and K.B. Sharpless. A stepwise Huisgen cycloaddition process: copper(I)-catalyzed regioselective "ligation" of azides and terminal alkynes. *Ange-*

wandte Chemie, 114(14):2708–2711, 2002.

[201] J.A. Opsteen and J.C.M. van Hest. Modular synthesis of block copolymers via cycloaddition of terminal azide and alkyne functionalized polymers. *Chemical Communications*, pages 57–59, 2005.

[202] J.F. Lutz, H.G. Börner, and K. Weichenhan. Combining atom transfer radical polymerization and click chemistry: a versatile method for the preparation of end-functional polymers. *Macro-molecular Rapid Communications*, 26(7):514–518, 2005.

[203] N.V. Tsarevsky, B.S. Sumerlin, and K. Matyjaszewski. Step-growth "click" coupling of telechelic polymers prepared by atom transfer radical polymerization. *Macromolecules*, 38(9):3558–3561, 2005.

[204] A.J. de Graaf, E. Mastrobattista, C.F. van Nostrum, D.T.S. Rijkers, W.E. Hennink, and T. Ver-monden. ATRP, subsequent azide substitution and 'click' chemistry: three reactions using one catalyst in one pot. *Chemical Communications*, 47:6972–6974, 2011.

[205] R. Morrison and R. Boyd. Química orgânica. *Fundação Calouste Gulbenkian*, (12th ed.):1102–1103, 1995.

[206] B.D. Mather, K. Viswanathan, K.M. Miller, and T.E. Long. Michael addition reactions in macro-molecular design for emerging technologies. *Progress in Polymer Science*, 31(5):487–531, 2006.

[207] W. Chen, H. Yang, R. Wang, R. Cheng, F. Meng, W. Wei, and Z. Zhong. Versatile synthesis of functional biodegradable polymers by combining ring-opening polymerization and post-polymerization modification via Michael-type addition reaction. *Macromolecules*, 43(1):201–207, 2010.

[208] N. Segovia, P. Dosta, A. Cascante, V. Ramos, and S. Borrós. Oligopeptide-terminated poly(β-amino ester)s for highly efficient gene delivery and intracellular localization. *Acta Biomaterialia*, 10(5):2147–2158, 2014.

CHAPTER 2

Synthesis of well-defined PDMAEMA under mild

conditions using Fe(0)/Cu(II) based SARA ATRP

2.1   Abstract

Atom transfer radical polymerization (ATRP) of 2-(dimethylamino)ethyl methacrylate (DMAEMA) with mixed transition metal catalytic system consisting of Fe(0) and small amounts of $CuBr_2$/PMDETA (*N,N,N',N'',N''*-pentamethyldiethylenetriamine) in water-isopropanol mixtures at 60 °C and 25 °C is reported and compared with commonly used CuBr/PMDETA-mediated ATRP systems. The obtained kinetics of polymerization showed that, in addition to the environmental attractiveness of this catalytic system, Fe/Cu mixed transition metal mediated ATRP of DMAEMA monomer provides a significantly improved control of polymer chain growth, forming PDMAEMA of low dispersity values at several conversions. The controlled character of ATRP of DMAEMA was confirmed by the linear increase of molecular weights with monomer conversion, narrow molecular weight distributions, and re-initiation/chain extension experiments. The molecular structure of the obtained polymer(s) was confirmed by ^{1}H nuclear magnetic resonance spectroscopy and matrix-assisted laser desorption ionization time-of-flight mass spectroscopy. The developed system for ATRP of DMAEMA was also extended to synthesis of functional bio-relevant polymers with cholesterol and poly(ethylene glycol) segments.

2.2   Introduction

Reversible deactivation radical polymerization (RDRP)[1;2] emerged in the mid-1990s to overcome major limitations of conventional free radical polymerization, such as poor control over the molecular weight, molecular weight distribution (dispersity), topology, composition, architecture and chain-end functionalities. One of the most often used methods to prepare a wide range of polymers with controlled molecular architecture is atom transfer radical polymerization (ATRP). ATRP is based on creation of a fast transition metal-complex-mediated equilibrium between dormant (macroinitiators P_n-X, where X represents a halogen or pseudohalogen) and active species (macroradical, $P^\bullet$). The dormant species are activated by a lower oxidation state transition metal complex (Mt^m/L, where Mt^m represents the transition metal species in oxidation state *m* and L is a ligand), acting as an activator to intermittently

form growing radicals ($P_n^\bullet$), and transition metal complexes in the higher oxidation state, coordinated with halide ligands X-Mt^{m+1}/L that act as the deactivator or persistent radical. The reverse reaction (k_{deact}) occurs when the deactivator reacts with the propagating radical to re-form the dormant species and the activator (Scheme 2.1).

$$P_n\text{-}X \ + \ Mt^m/L \ \underset{k_{\text{deact}}}{\overset{k_{\text{act}}}{\rightleftarrows}} \ P_n^\bullet \ + \ X\text{-}Mt^{m+1}/L$$

$$\xrightarrow{\quad K_p \quad M \quad} \ \xrightarrow{k_t} \ P_n\text{-}P_n$$

Scheme 2.1: General mechanism of ATRP.

Several transition metals have been used in ATRP, including Cu, Ru, Fe, Ni, Mo, and Os. Copper-based catalysts are the most broadly applied and are presently superior in terms of performance and cost[1;3;4]. However, an intensive research has been carried out in order to address environmental regulations/requirements, focused on diminishing the total amount of transition metals used in an ATRP to ppm levels[5–10]. This is particularly important since the need for low levels of metal contamination in the final product presents challenges of complete removal of the metal from the polymer[11]. Therefore, it is of primary importance to develop and understand the use of versatile catalysts systems that can be selected for well-controlled polymerization of a wide variety of monomers, are environmentally friendly (*i.e.*, use non-toxic metal(s)/solvent(s)), are sustainable, employing common low cost metals, and when targeting biomedical applications.

Shortly after the development of ATRP, successful Fe-based ATRP systems were reported[12;13] as was the use of zero-valent metals to reduce the higher oxidation state metal complex and increase the rate of reaction[14]. This procedure has received increasing attention and, recently, the use of mixed transition-metal catalysts involving zero-valent metals (Fe(0), Zn(0) and Mg(0)) as initial activators together with very small amounts of CuBr$_2$/Me$_6$TREN (tris[2-(dimethylamino)ethyl]amine) or CuBr$_2$/PMDETA (*N,N,N',N'',N''*-pentamethyldiethylenetriamine) as deactivator complexes has been reported for ambient temperature ATRP of methyl acrylate[15–17], methyl methacrylate[15] and styrene[15].

The use of the RDRP method to prepare tailor made polymers has been proved to be a powerful tool[18;19]. Here, the synthesis of stimuli-responsive polymers for biomedical applications can serve as a good example[20–27]. Dual-responsive polymers based on poly(2-(dimethylamino)ethyl methacrylate) (PDMAEMA) are among the most used, mainly in the gene delivery area[28–31], due to their lower cytotoxicity and higher transfection efficiency compared to poly(ethyleneimine) (PEI)[32;33], considered as a standard for this purpose. PDMAEMA has also been used as the hydrophilic segment in amphiphilic block copolymers to stabilize micellar systems in water[34]. The temperature[35] and pH-responsive character[16] of PDMAEMA are particularly useful for the preparation of responsive micellar structures in biomedical applications[36–39].

The first synthesis of PDMAEMA by ATRP, reported in 1998[40], was carried out in polar media and room temperature to form polymers with low dispersity ($\mathcal{Đ}$). PDMAEMA has also been polymerized *via* ATRP in aqueous media[41] and in bulk[42]. Further studies on ATRP of DMAEMA in methanol-water mixtures have shown that improved chain growth control can be achieved when *p*-toluenesulfonyl chloride[43] and chloroacetylated *β*-cyclodextrins[44] are used as initiators. More recently, DMAEMA has been polymerized at high temperatures with CuBr and PMDETA, forming polymers with narrow molecular weight distributions[45;46]. However, the kinetic data using PMDETA as a ligand that was scarcely reported in the literature did not show any significant differences between the dispersities of polymers prepared with several amine based ligands (2,2′-bipyridine (bpy), *N,N,N′,N′*-tetramethylethylenediamine (TMEDA), *N,N,N′,N″,N″*-pentamethyldiethylenetriamine (PMDETA) or 1,1,4,7,10,10-hexamethyltriethylenetetramine (HMTETA))[40].

Block copolymers with PDMAEMA segments are of interest for biomedical use[18]. ATRP of DMAEMA initiated from poly(ethylene glycol) (PEG) initiators has been proposed due to the compatibility of PEG with biological systems[42;47]. The ATRP of DMAEMA initiated with hydrophobic macroinitiators, such as with poly(*n*-butyl methacrylate)[48], poly(fluorene)[49] and polycaprolactone (PCL), has also been studied, typically forming block copolymers with broad molecular weight distributions.

Cholesterol (CHO) based initiators were used for the preparation of the PDMAEMA-based self-assembled system in gene carrying applications, due to the combination of the cationic nature of PDMAEMA and the lipid nature of cholesterol[50]. However, ATRP of DMAEMA using a cholesteryl-2-bromoisobutyrate initiator has not yet been reported.

In this Chapter, the influence of solvent and temperature on the kinetics of ATRP of DMAEMA with a PMDETA/CuBr catalyst was evaluated as it provides a facile procedure for the preparation of PDMAEMA-based block copolymers suitable for self-assembled structures. However, considering the relevance of PDMAEMA for biomedical applications, the overall objective was to identify an alternative ATRP catalytic system for polymerization of DMAEMA, based on a more biocompatible catalyst system comprising Fe(0) and very low amounts of $CuBr_2$ deactivator. ATRP of DMAEMA was initiated using initiators of biomedical relevance, such as PEG and cholesterol. In this work, the successful ambient temperature ATRP of DMAEMA in a mixture of alcohol-water with Fe(0)/$CuBr_2$/PMDETA catalyst under mild reaction conditions, relevant for some biomedical applications, was reported.

2.3 Experimental

2.3.1 Materials

DMAEMA (Aldrich, 98%) was passed over a sand/alumina column before use in order to remove radical inhibitors. Copper(I) bromide (CuBr) (Fluka, +98%), copper(II) bromide ($CuBr_2$) (Acros, +99% extra pure, anhydrous), deuterated chloroform ($CDCl_3$) (Euriso-top, +1% TMS), 2-propanol (IPA) (Fisher Chemical), tetrahydrofuran (THF) (Fisher Chemical), ethyl 2-bromoisobutyrate (EBiB) (Aldrich, 98%), PS standards (Polymer Laboratories) (Acros, 99%, ~70 mesh), PMDETA (Aldrich, 99%), HMTETA (Aldrich, 97%), iron powder (Fe(0)), cholesterol (CHO) (Sigma-Aldrich, 95%), α-bromoisobutyryl bromide (BBiB) (Aldrich, 98%) and magnesium sulfate (Sigma-Aldrich, +97%) were used as received. Milli-Q water (Milli-Q®, Millipore, resistivity >18 MΩ cm) was obtained by reverse osmosis. High-performance liquid chromatography (HPLC) THF (Panreac, HPLC grade) was filtered under reduced

pressure before use. Dichloromethane (DCM) (Fisher Scientific, +99.6%) was dried and distilled over calcium hydride. Poly(ethylene glycol) monomethyl ether (mPEG) (Aldrich, M_n 5,000 g.mol^{-1}) was dried by azeotropic distillation with toluene. Triethylamine (TEA) (Sigma-Aldrich, 96%) was distilled and stored over molecular sieves. 4-Dimethylaminopyridine (DMAP) (Sigma-Aldrich, +99%) was recrystallized from toluene. Me$_6$TREN[51] and bromo-telechelic mPEG macroinitiator (mPEG-Br)[52] were synthesized according to procedures described in the literature.

2.3.2   Methods

2.3.2.1   Synthesis of cholesteryl-2-bromoisobutyrate (CHO-Br)

Cholesteryl-2-bromoisobutyrate was synthesized through an adaption of the synthesis of Br-PEG-Br in the literature[53]. 4-Dimethylaminopyridine (4.5 g, 37.5 mmol), dry dichloromethane (50 mL) and triethylamine (3.5 mL, 25 mmol) were placed into a 500 mL flask. A solution with 2-bromoisobutyryl bromide (7.7 mL, 62.5 mmol) and dry dichloromethane (50 mL) was added dropwise. When the addition was finished, a solution of cholesterol (CHO) (4.8 g, 12.4 mmol) and dry dichloromethane (250 mL) were added dropwise over a period of 30 min, in a dry ice bath. The resulting solution was further refluxed under nitrogen. After 24 h, there was a yellow dispersion, which was further washed with sodium chloride saturated aqueous solution. Magnesium sulphate was then added, and the final solution was filtered and concentrated. The cholesteryl-2-bromoisobutyrate (CHO-Br) product was recovered by precipitation in ethanol, leading to a white precipitated that was collected and dried in vacuum. The crude product was purified by recrystallization in ethyl acetate/ethanol (95/5, v/v). The ^{1}H NMR and FTIR-ATR spectra are shown in Figures B.1 and B.2 (*Appendix B - Supporting Information*), respectively.

2.3.2.2   Typical procedure for the $[Fe(0)]_0/[CuBr]_0/[PMDETA]_0 = 1/0.1/1.1$ catalyzed ATRP of DMAEMA

A typical procedure for the $[CuBr]_0/[PMDETA]_0 = 1/1$ catalyzed ATRP of DMAEMA was followed as reported in the literature[45].

A mixture of DMAEMA (6.0 mL, 35.61 mmol), Fe(0) (44.2 mg, 0.79 mmol) and CuBr$_2$

(17.7 mg, 0.079 mmol) was placed in a Schlenk tube reactor. The sample was first stirred and then frozen in liquid nitrogen. Subsequently, a mixture of EBiB (154.3 mg, 0.79 mmol), PMDETA (150.8 mg, 0.87 mmol), IPA (5.4 mL) and Milli-Q water (0.6 mL) (previously bubbled with nitrogen for about 15 minutes) was added, under nitrogen atmosphere, to the reactor. The Schlenk tube reactor containing the reaction mixture was deoxygenated with four freeze-vacuum-thaw cycles and purged with nitrogen prior to being placed in a pre-heated oil bath at the reaction temperature with magnetic stirring. Aliquot samples were taken during the polymerization using an airtight syringe and purging the side arm of the Schlenk tube reactor with nitrogen. The samples were analyzed by ^{1}H NMR spectroscopy to determine the monomer conversion and by SEC to determine the molecular weight and molecular weight distribution of the polymer samples. PDMAEMA was precipitated in *n*-hexane, re-dissolved in THF and passed through a silica column to remove the metal catalysts. The sample was concentrated under reduced pressure and then re-precipitated in *n*-hexane. The final product was obtained by drying overnight under vacuum at 40 °C.

2.3.2.3   Size exclusion chromatography

Size-exclusion chromatography (SEC) analysis was performed using high performance size-exclusion chromatography (HPSEC); Viscotek (ViscotekTDAmax) with a differential viscometer (DV); right-angle laser-light scattering (RALLS, Viscotek); low-angle laser-light scattering (LALLS, Viscotek) and refractive index (RI) detectors. The column set consisted of a PL 10 mm guard column (50 × 7.5 mm^2) followed by one Viscotek T200 column (6 μm), one MIXED-E PLgel column (3 μm) and one MIXED-C PLgel column (5 μm). A HPLC dual piston pump was set with a flow rate of 1 mL.min^{-1}. The eluent (HPLC THF) was previously filtered through a 0.2 μm filter. The system was also equipped with an on-line degasser. The tests were conducted at 30 °C using an Elder CH-150 heater. Before injection (100 μL), the samples were filtered through a poly(tetrafluoroethylene) (PTFE) membrane with 0.2 μm pore. The system was calibrated with narrow PS standards. The dn/dc of PDMAEMA in THF was assumed to be 0.084 mL.g^{-1}, in accordance with previ-

ously reported data[54]. The number-average molecular weight ($M_{n,SEC}$) and $Đ$ of the synthesized polymers were determined by multidetector calibration using OmniSEC software version: 4.6.1.354. For PDMAEMA block copolymers, $M_{n,SEC}$ and $Đ$ values were determined by conventional calibration with PS standards between 1,820 and 96,000 g.mol^{-1}.

2.3.2.4   Nuclear magnetic resonance spectroscopy

400 MHz ^{1}H nuclear magnetic resonance (NMR) spectra of samples of the reaction mixture were recorded on a Bruker Avance III 400 MHz spectrometer, with a 5 mm TXI triple resonance detection probe, in CDCl$_3$ with tetramethylsilane (TMS) as an internal standard. Conversion of monomers was determined by integration of monomer and polymer peaks using MestReNova software version: 6.0.2-5475.

2.3.2.5   Matrix-assisted laser desorption ionization time-of-flight mass spectroscopy

The PDMAEMA samples were dissolved in THF at a concentration of 10 mg.mL^{-1} for the matrix-assisted laser desorption ionization time-of-flight mass spectroscopy (MALDI-TOF MS) analysis and 2,5-dihydroxybenzoic acid (DHB) and α-cyano-4-hydroxycinnaminic acid (HCCA) were used as the matrix. The dried-droplet sample preparation technique was used to obtain 1/1 ratio (sample/matrix); an aliquot of 1 μL of each sample was directly spotted on the MTP AnchorChip TM 600/384 TF MALDI target, Bruker Daltonik (Bremen, Germany) and, before being dried 1 μL of matrix solution in THF was added and the sample was allowed to dry at room temperature to allow matrix crystallization. External mass calibration was performed with a peptide calibration standard (PSCII) for the range 700-3,000 (nine mass calibration points); 0.5 μL of the calibration solution and the matrix previously mixed in an Eppendorf tube (1/2, v/v) were applied directly on the target and allowed to dry at room temperature. Mass spectra were recorded using an Autoflex III smartbeam MALDI-TOF-MS mass spectrometer Bruker Daltonik (Bremen, Germany) operating in the linear positive ion mode. Ions were formed upon irradiation by a smartbeam laser using a frequency of 200 Hz. Each mass spectrum was produced by averaging

2,500 laser shots collected across the whole sample spot surface by screening in the range *m/z* 1,500-17,850. The laser irradiance was set to 35-40% (relative scale 0-100) arbitrary units according to the corresponding threshold required for the applied matrix systems.

2.3.2.6   Fourier transform infrared spectroscopy

Infrared attenuated total reflection (FTIR-ATR) spectroscopy (Jasco, model 4000, UK) was performed at 64 scans and with a 4 cm^{-1} resolution between 500 and 3,500 cm^{-1}.

2.4   Results and discussion

The first report on ATRP of DMAEMA employed CuBr complexed with various nitrogen based ligands: 2,2'-bipyridine, PMDETA, 1,1,4,7,10,10-hexamethyltriethylenetetramine (HMTETA) and *N,N,N',N'*-tetramethylethylenediamine (TMEDA)[40]. Due to its commercial availability and relatively low cost, PMDETA remains an attractive ligand for ATRP and, recently, this ligand has been used for the synthesis of PDMAEMA based polymeric materials[45;46;51]. However, no kinetic data were reported, and in most cases, the polymerizations were stopped at low conversions to avoid significant deviation from the living character.

Figure 2.1 presents the kinetics of ATRP of DMAEMA performed at 60 °C in the presence of THF or IPA solvents.

The results show that reasonable control over molecular weight was achieved when THF was used as the solvent. However, monomer conversion was limited to approximately 55% and it was not possible to decrease the final value of *Đ* even for polymer samples taken at low conversions, as reported by other authors for the same reaction system[45]. When IPA was used as solvent the initial rate of polymerization was higher than that in THF, but final monomer conversion in IPA was nearly complete. For both solvents, the deviation from the linear behavior of the $\ln[M]_0/[M]$ *vs.* polymerization time curve indicates that the concentration of active chains was strongly reduced, suggesting that termination is taking place during polymerization. In THF, this deviation from the living character starts at lower conversions (40-50%)
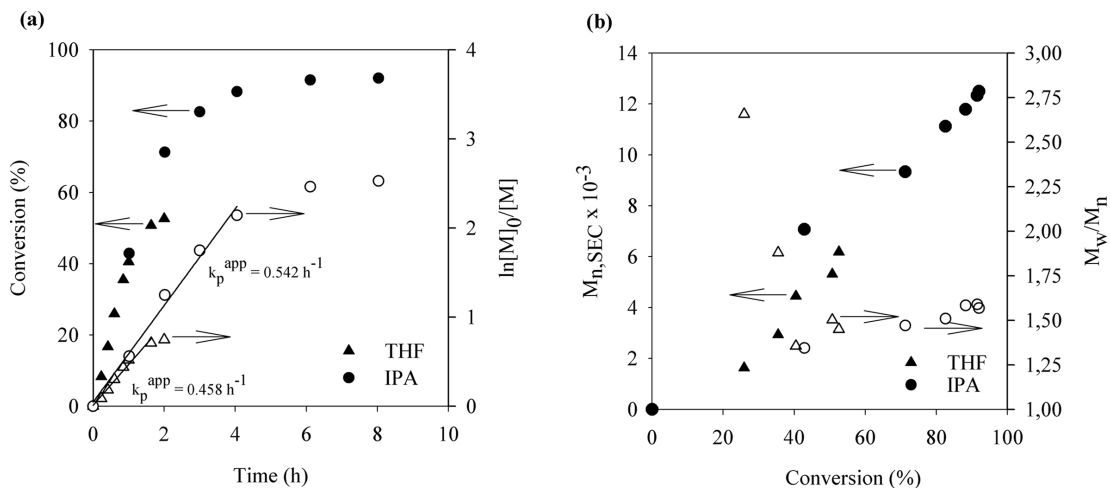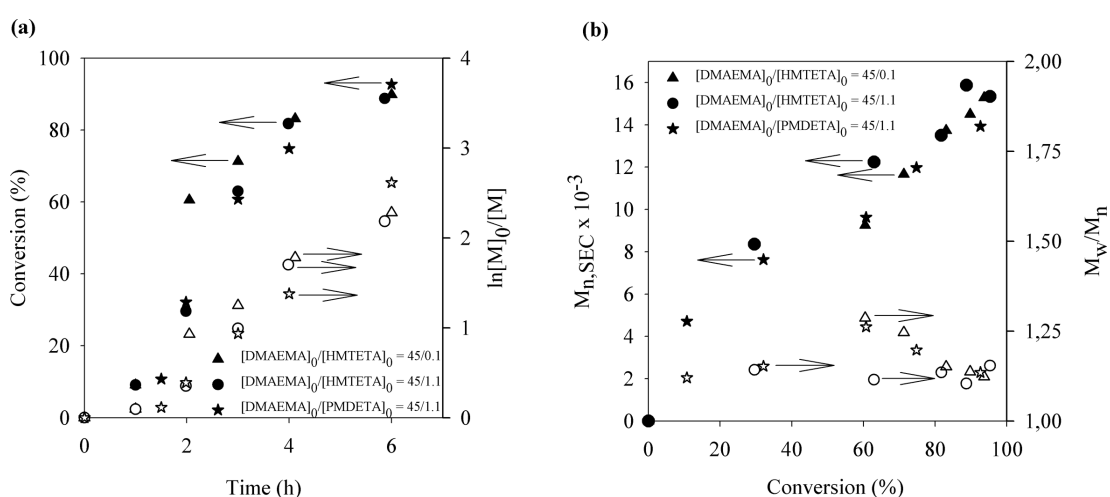
Figure 2.1: **(a)** Kinetic plots of conversion and $\ln[M]_0/[M]$ *vs.* time and **(b)** plot of number average molecular weights ($M_{n,SEC}$) and $Đ$ (M_w/M_n) *vs.* conversion (%) for ATRP of DMAEMA at 60 °C. Conditions: $[DMAEMA]_0/[solvent] = 1/1.25$ (v/v); $[DMAEMA]_0/[EBiB]_0/[CuBr]_0/[PMDETA] = 50/1/1/1$ (molar), in THF or IPA.

as compared to IPA (60-70%). This is concurrent with the increase of the $Đ$ values with the monomer conversion (Figure 2.1 (b)).

SEC traces of PDMAEMA prepared in IPA at 60 °C at different reaction times (and, thus, at different conversions) are provided in Figure 2.2.
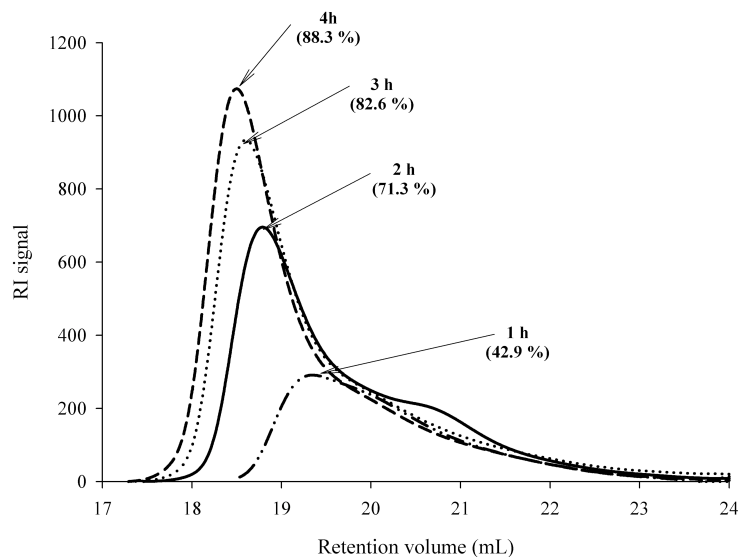
Figure 2.2: SEC traces of PDMAEMA samples taken at different reaction times. Conditions: $[DMAEMA]_0/[IPA] = 1/1.25$ (v/v); $[DMAEMA]_0/[EBiB]_0/[CuBr]_0/[PMDETA] = 50/1/1/1$ (molar); T = 60 °C.

The overlap of the trace tailing for higher retention volumes suggests that there is a significant contribution of chain breaking reactions, which can explain the pro-

gressive increase in the $Đ$ values as monomer conversion increases.

It has been reported that the addition of small amounts of water to a CuBr-catalyzed ATRP in IPA media can improve the level of control attained in polymerization and significantly decrease the $Đ$ values[55]. Additionally, it has been suggested that an increase in the rate of ATRP of DMAEMA in the presence of water could reduce undesired Cu(I)-catalyzed transesterification reactions of DMAEMA with alcohols, avoiding the need of use of high temperatures[56]. Therefore, the effect of using 10% of water in IPA medium at 60 °C and 25 °C was evaluated (Figure 2.3 and Figure 2.4, respectively). The results confirmed that the presence of water can effectively increase the polymerization rate at 60 °C, but a decrease in the $Đ$ values could only be achieved when the polymerization temperature was reduced to 25 °C.

In addition, a catalytic system based on Fe(0) was studied as an alternative for ATRP of DMAEMA using CuBr. The use of zero-valent metals, namely Fe(0), in the presence of small amounts of $CuBr_2$ deactivator for ATRP under ambient temperature conditions using different solvents was previously reported for different monomers[15;16], but, to the best of our knowledge, there are no reports available in the literature regarding DMAEMA. The stringent control reported with this catalytic system combined with the attractive environmental characteristics of water/alcohols media suggests that this may be an interesting system for the ATRP of monomers that are used in biomedical applications, since iron is a biocompatible metal and, thus, polymer purification processes are less demanding and the alcohol-based solvent media is preferable.

In Figure 2.3, the results of the ATRP of DMAEMA mediated with the Fe/Cu mixed transition metal system and CuBr/PMDETA alone is compared (60 °C in IPA/H_2O media). The kinetic plots show that when water was added to the CuBr-mediated ATRP, the rate of polymerization significantly increased, but deviates significantly from optimum control, leading to formation of polymers with high $Đ$ values. Interestingly, when the same solvent and temperature conditions were applied on the ATRP of DMAEMA catalyzed by $Fe(0)/CuBr_2/PMDETA$, higher monomer conversion and low $Đ$ values were observed.

The effect of ATRP temperature on the livingness of polymerization was also ex-
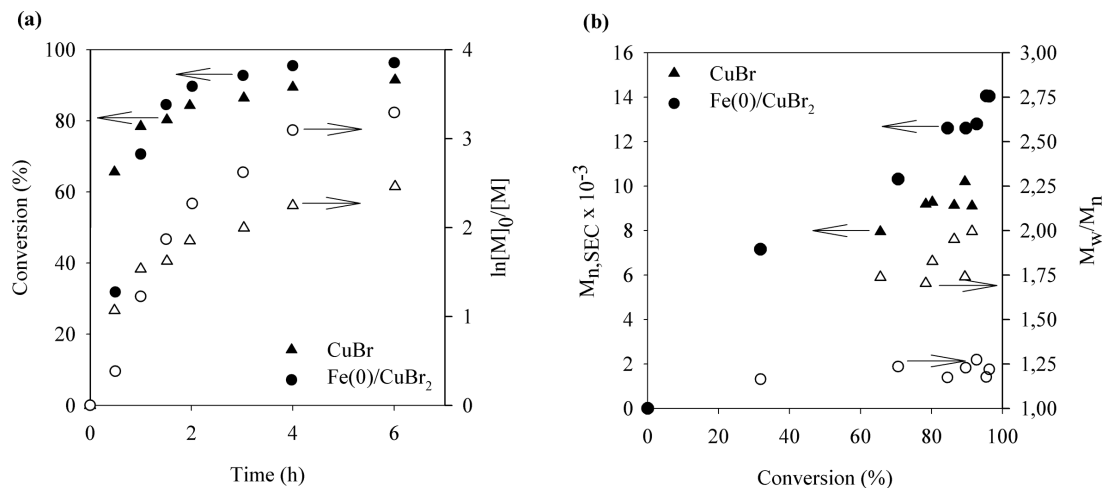
Figure 2.3: **(a)** Kinetic plots of conversion and $\ln[M]_0/[M]$ *vs.* time and **(b)** plot of number average molecular weights ($M_{n,SEC}$) and Đ (M_w/M_n) *vs.* conversion (%) for ATRP of DMAEMA at 60 °C in IPA/H_2O. Conditions: $[DMAEMA]_0/[IPA]/[H_2O] = 1/0.9/0.1$ (v/v); $[DMAEMA]_0/[EBiB]_0/[CuBr]_0$ or $[Fe(0)]_0/[CuBr_2]_0)/[PMDETA] = 45/1/(1$ or $1/0.1)/(1$ or $1.1)$ (molar).

amined (for both catalytic systems - CuBr and Fe(0)/CuBr$_2$). Figure 2.4 presents the kinetic data of the ATRP of DMAEMA in IPA/H_2O (9/1 (v/v)) at room temperature using these catalysts.
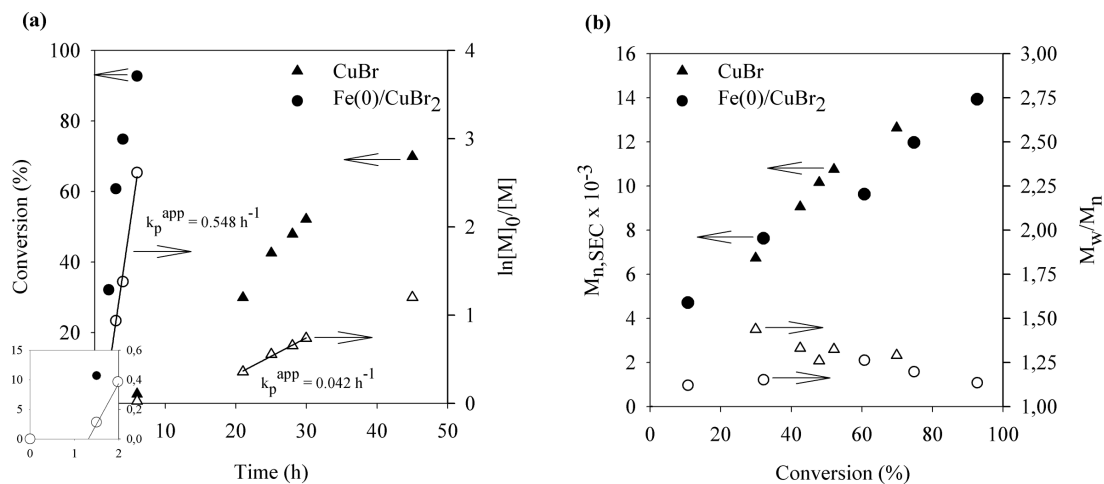
Figure 2.4: **(a)** Kinetic plots of conversion and $\ln[M]_0/[M]$ *vs.* time and **(b)** plot of number average molecular weights ($M_{n,SEC}$) and Đ (M_w/M_n) *vs.* conversion (%) for ATRP of DMAEMA at 25 °C in IPA/H_2O. Conditions: $[DMAEMA]_0/[IPA]/[H_2O] = 1/0.9/0.1$ (v/v); $[DMAEMA]_0/[EBiB]_0/[Fe(0)]_0/[CuBr_2]_0$ or $[CuBr]_0)/[PMDETA] = 45/1/(1/0.1$ or $1/(1.1$ or $1))$ (molar).

For both systems, as expected, there was a very significant decrease in the polymerization rate. Moreover, an induction period was also observed, which delayed the progress of the polymerization. For the Fe(0)/CuBr$_2$ catalytic system, the induc-

tion period is slightly higher than one hour, as indicated by the inset graph in Figure 2.4. This period was significantly longer for the CuBr-catalyzed system, leading, in combination with the much slower polymerization rate, to very long polymerization times. After the induction period, a linear dependence of the $\ln[M]_0/[M]$ on the polymerization time was observed, and low Đ values could be observed at all conversions. The lower Đ values, when compared to the polymerizations that were carried out at higher temperatures, indicate that an improved level of control over PDMAEMA chain growth was achieved. The rate of polymerization with the Fe(0)-based catalytic system was more than ten times faster than for the CuBr mediated system, achieving nearly full conversion of DMAEMA in only a few hours, while forming PDMAEMA with low Đ values. In fact, for the Fe(0)-mediated DMAEMA's ATRP, very low Đ values were obtained even for monomer conversions as high as 93%, which suggests that deviations from "living" polymerization conditions are negligible.

Figure 2.4 also highlights the fact that the Fe(0)-based catalyst system significantly improved the level of control over the chain growth process when compared to the CuBr/(THF and IPA) systems (Figure 2.1), which are typically reported in the literature[45;46;51] for the preparation of PDMAEMA segments. This is indicated by the linearity of the conversion and narrow molecular weight distribution curves (compare Figures 2.2 and 2.5) after the induction period, and the fact that polymers displaying low dispersities are obtained even at high conversions. The observed induction period may be attributed to the significant rate of deactivation at the beginning of the polymerization due to the presence of Cu(II), whereas the deviation from linearity in CuBr systems at high monomer conversion reflects a significant decrease of active species[57]. Improved control in Fe(0)/CuBr$_2$ supplemental activator and reduction system allowed achieving low dispersities at all conversions and significantly decreased the tailing observed in molecular weight distribution curves (Figure 2.5). In addition to excellent control over reaction kinetics, the low cost and environmental attractiveness of the materials used provide a great opportunity for preparing PDMAEMA-based materials with well-defined structure under industrially relevant conditions.
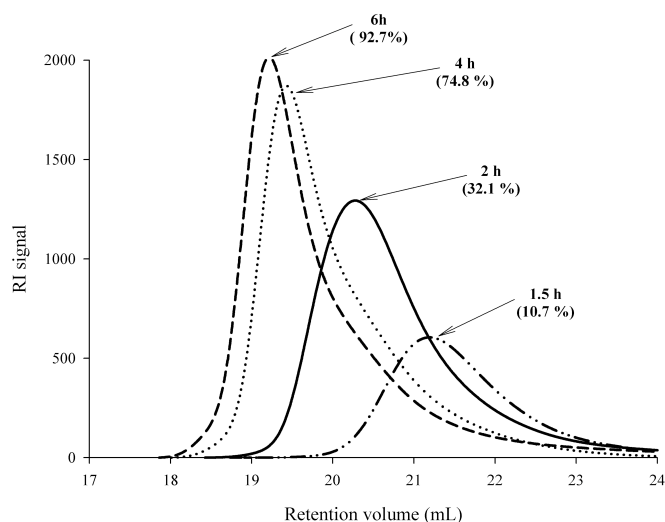
Figure 2.5: SEC traces of PDMAEMA samples taken at different reaction times. Conditions: $[DMAEMA]_0/[IPA]/[H_2O]$ = 1/0.9/0.1 (v/v); $[DMAEMA]_0/[EBiB]_0/[Fe(0)]_0/[CuBr_2]_0/[PMDETA]$ = 45/1/1/0.1/1 (molar); T = 25 °C.

Since HMTETA has been suggested to be an excellent ligand for ATRP of DMAEMA[40], the effect of this ligand in the $Fe(0)/CuBr_2/IPA/H_2O$ polymerization system at 25 °C was further evaluated. Additionally, the use of lower amounts of ligand was also evaluated. Figure 2.6 shows that the use of either HMTETA or PMDETA as ligands has little effect on the kinetics of ATRP of DMAEMA under these reaction conditions.
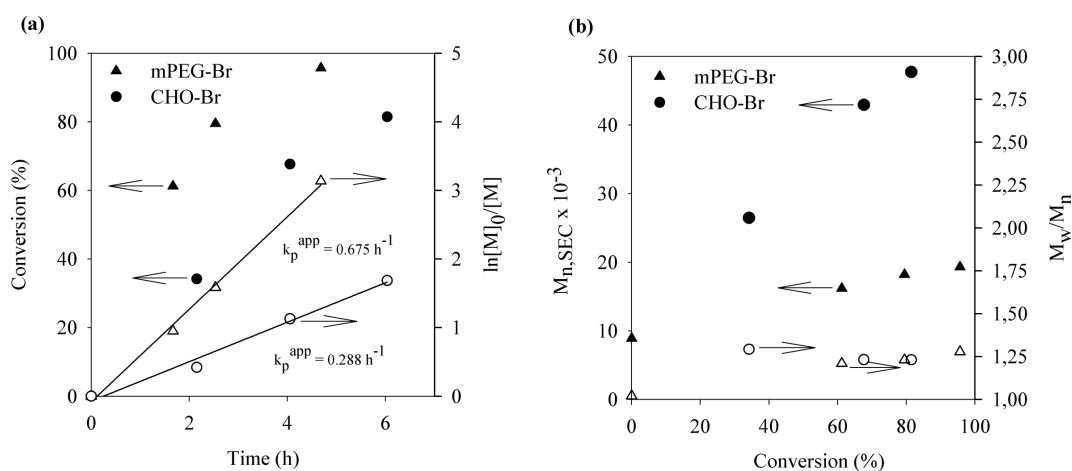

Figure 2.6: (a) Kinetic plots of conversion and $\ln[M]_0/[M]$ *vs.* time and **(b)** plot of number average molecular weights ($M_{n,SEC}$) and Đ (M_w/M_n) *vs.* conversion (%) for ATRP of DMAEMA at 25 °C in IPA/H_2O. Conditions: $[DMAEMA]_0/[IPA]/[H_2O]$ = 1/0.9/0.1 (v/v); $[DMAEMA]_0/[EBiB]_0/[Fe(0)]_0/[CuBr_2]_0/[ligand]$ = 45/1/1/0.1/x (molar).

The commercial availability of PMDETA makes this ligand a more suitable choice. It is also noteworthy that the use of very low amounts of the ligand provides accurate control over the ATRP of DMAEMA, and may be further optimized.

2.4.1 ^{1}H NMR and MALDI-TOF analyses

The molecular structure of PDMAEMA obtained using the $[Fe(0)]_0/[CuBr_2]_0/[PMDETA]$ catalyst system in isopropanol/water (9/1 (v/v)) at 25 °C was characterized by ^{1}H NMR and MALDI-TOF MS analyses. Figure 2.7 presents the ^{1}H NMR spectrum of the PDMAEMA samples. The peaks observed at 4.07 ppm (e) (2H, -OCH_2CH$_2$N-), 2.58 ppm (f) (2H, -OCH$_2$CH_2N-), 2.35-2.20 ppm (g) (6H, -N(CH_3)$_2$), 2.00-1.75 ppm (c) (2H, -CCH_2C-) and 1.00-0.80 ppm (d) (3H, -CCH_3Br) are in agreement with the expected PDMAEMA chemical structure[58]. Additionally, the methyl (CH_3CH$_2$O-) protons (a) from the EBiB initiator at 1.42 ppm can be observed in Figure 2.7 which allows one to estimate the number-average molecular weight. On the basis of the integral ratio of peaks f and a, M$_n$ = 7,745 g.mol^{-1} was calculated. The amount of active chain ends could not be determined from ^{1}H NMR analysis, since the protons in the PDMAEMA unit adjacent to the Br chain end do not have a distinct signal that allows integration as a single unit.

Re-initiation experiments were performed to evaluate the livingness of PDMAEMA chains prepared with the Fe(0)/CuBr$_2$/PMDETA catalyst system in IPA/H$_2$O at 25 °C. Low molecular weight tailing observed in SEC curves with increasing monomer conversion was attributed to the loss of bromine chain ends (that increases with high conversions) (Figure 2.5). Therefore, re-initiation of PDMAEMA was carried out using samples taken at different monomer conversions, 57% and 88%, to evaluate the effect of polymerization time on retained chain end functionality. Figure 2.8 presents the SEC traces of original and re-initiated PDMAEMA samples.

The results show that PDMAEMA samples could be re-initiated, but not completely. The estimated percentage of re-initiation was calculated to be 77% and 65%, respectively, on the basis of ratio of the RI signals area, for samples taken at 57% and 88% of monomer conversion. Therefore, the fraction of polymers successfully re-
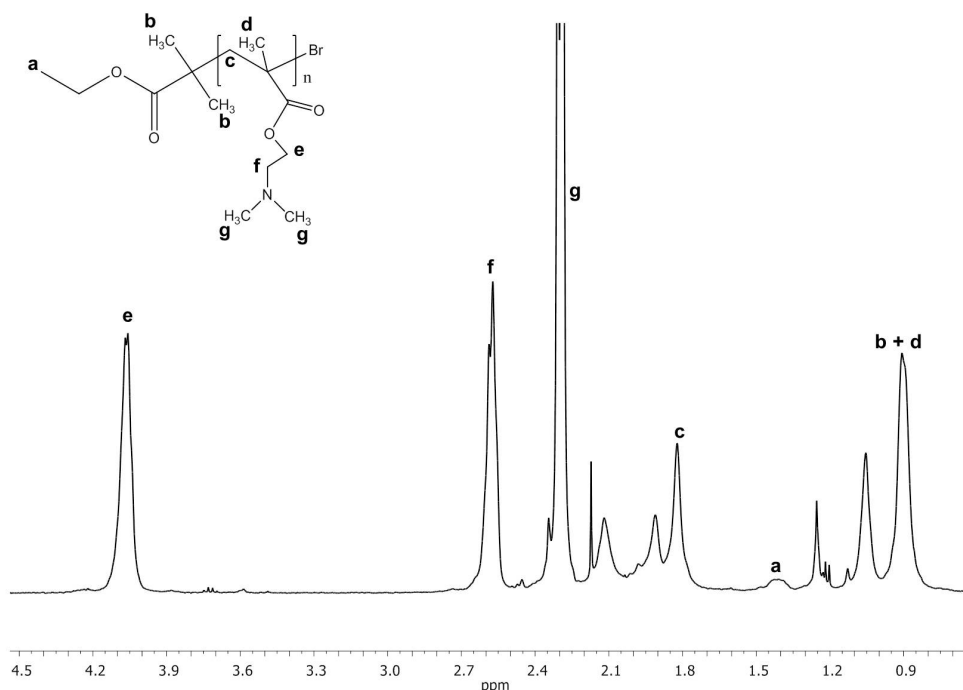
Figure 2.7: ^{1}H NMR spectrum (CDCl$_3$, 400 MHz) of PDMAEMA (M$_{n,SEC}$ = 11,239 g.mol^{-1}, Đ = 1.21).   Conditions: [DMAEMA]$_0$/[IPA]/[H$_2$O] = 1/0.9/0.1 (v/v); [DMAEMA]$_0$/[EBiB]$_0$/[Fe(0)]$_0$/[CuBr$_2$]$_0$/[PMDETA] = 45/1/1/0.1/1.1 (molar); T = 25 °C.
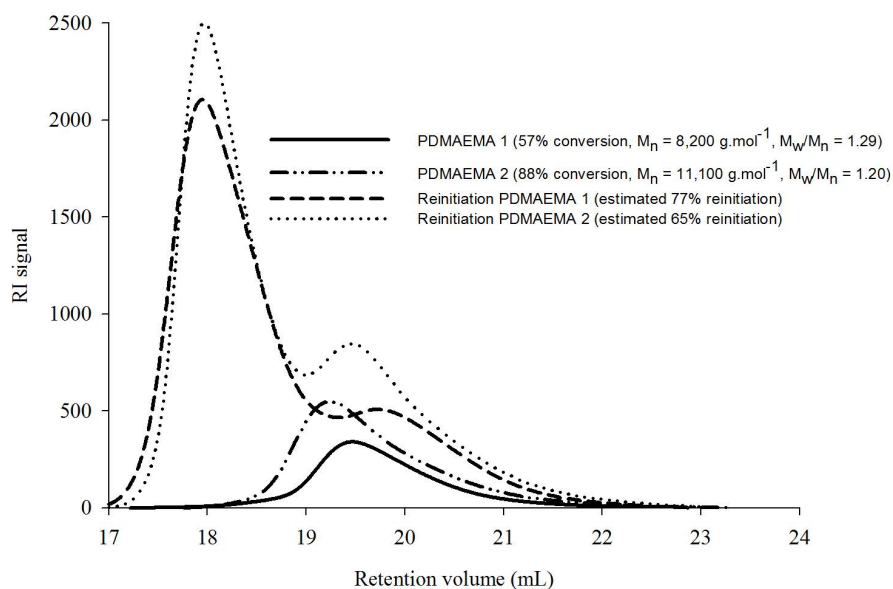
Figure 2.8: SEC traces of PDMAEMA samples stopped at different monomer conversion values and of products of further reinitiation of those samples.   Conditions: [DMAEMA]$_0$/[IPA]/[H$_2$O] = 1/0.9/0.1 (v/v); T = 25 °C; for PDMAEMA macroinitiator preparation: [DMAEMA]$_0$/[EBiB]$_0$/[Fe(0)]$_0$/[CuBr$_2$]$_0$/[PMDETA] = 45/1/0.1/1/1.1 (molar) (samples taken at 57% and 88% conversions); for reinitiation experiments: [DMAEMA]$_0$/[PDMAEMA]$_0$/[Fe(0)]$_0$/[CuBr$_2$]$_0$/[PMDETA] = 225/1/0.1/1/1.1 (molar).

initiated decreased with the conversion values at which PDMAEMA macroinitiators were taken. This result corroborates the idea that the increasing tailing observed in the SEC curves obtained for PDMAEMA with higher monomer conversion is related to the loss of active chain ends functionality as the reaction progresses. It should be further noted that PDMAEMA's re-initiation occurred at an extent that is significantly greater than that for other reported systems[59].

In MALDI-TOF MS experiments, two types of matrices, HCCA and DHB, were tested but only the latter gave a clearly resolved spectrum (Figure 2.9).
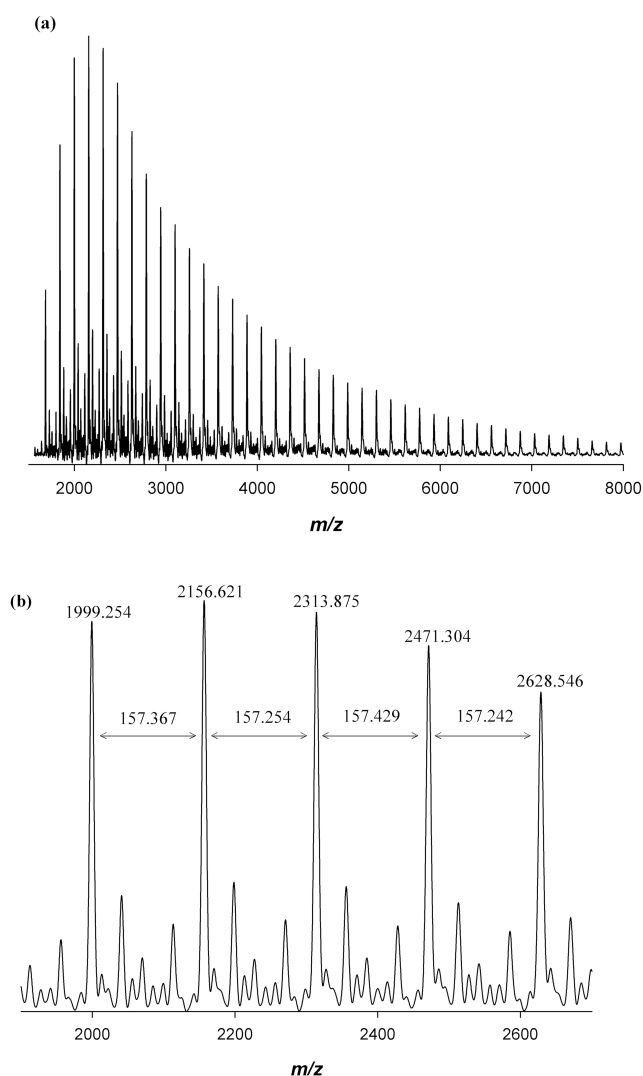
Figure 2.9:   MALDI-TOF MS **(a)** in the linear mode (using DHB as matrix) of PDMAEMA-Br; **(b)** Enlargement of the MALDI-TOF MS from m/z 1,900 to 2,700 of PDMAEMA-Br.   Conditions: $[DMAEMA]_0/[IPA]/[H_2O]$ = 1/0.9/0.1 (v/v); $[DMAEMA]_0/[EBiB]_0/[Fe(0)]_0/[CuBr_2]_0/[PMDETA]$ = 45/1/0.1/1/1.1 (molar); T = 25 °C.

The MALDI-TOF MS of PDMAEMA-Br in the linear mode with *m/z* ranging from 1,500 to 8,000 and its enlargement of the 1,900-2,700 range are shown in Figure 2.9 (a) and (b), respectively. As expected, the series of main peaks are separated by an interval corresponding to a DMAEMA repeating unit (157.21 mass units). Regarding the *m/z* values, the identified peaks present a loss of HBr in the polymer structure which has been reported in MALDI-TOF MS of acrylate-based polymers produced by ATRP[60–62]. The highest intensity peak (*m/z* 2,156.6) corresponds to a DP = 13 DMAEMA repeating units polymer ($EBiB + (DMAEMA)_n - HBr = 195.05 + 157.21 \times 13 - (1.01 + 79.90) = 2,157.87$).

2.4.2 Preparation of high molecular weight PDMAEMA

The Fe(0)-mediated ATRP catalyst system in IPA/H_2O at room temperature was further used to prepare high molecular weight PDMAEMA. Figure 2.10 presents the kinetic profile of ATRP of DMAEMA targeting a DP of 500.
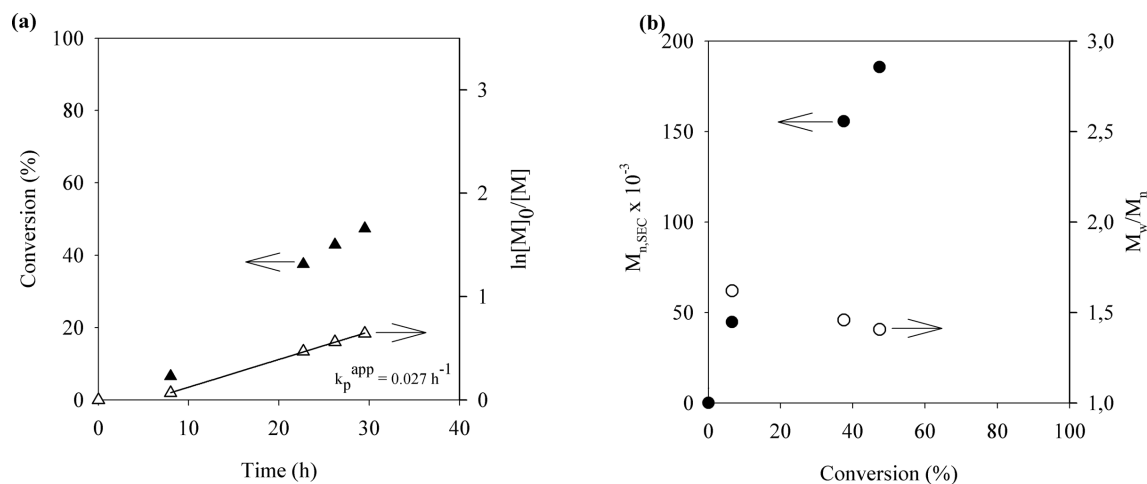
Figure 2.10: (a) Kinetic plots of conversion and $\ln[M]_0/[M]$ *vs.* time and **(b)** plot of number average molecular weights ($M_{n,SEC}$) and Đ (M_w/M_n) *vs.* conversion (%) for ATRP of DMAEMA at 25 °C in IPA/H_2O. Conditions: $[DMAEMA]_0/[IPA]/[H_2O]$ = 1/0.9/0.1 (v/v); $[DMAEMA]_0/[EBiB]_0/[Fe(0)]_0/[CuBr_2]_0/[PMDETA]$ = 500/1/1/0.1/1 (molar).

As expected, comparing with low targeting DPs (Figure 2.4 and Figure 2.6), the rate of polymerization is significantly decreased, by about a factor of 20. Moreover, the induction period increased to approximately 5 h compared to the induction period of 1.4 h observed for a DP of 45. However, after 30 h the monomer conversion reached 47%, and a PDMAEMA of approximately M_n = 186,000 g.mol⁻¹ was ob-

tained. These results demonstrate that this catalyst system can be used to prepare high molecular weight PDMAEMA at reasonable monomer conversions. The final dispersity ($Đ = 1.41$) is higher than that for the low molecular weight PDMAEMA, but it is still an acceptable result, if one considers the very high monomer to initiator ratios that were used in this polymerization.

The molecular weight distributions, determined from SEC analysis, for both DP 45 and DP 500 polymerizations are compared in Figure 2.11 and provide evidence of the possibility to use this catalytic system to prepare PDMAEMA's segments with narrow M_w distributions over a wide range of molecular weight values.
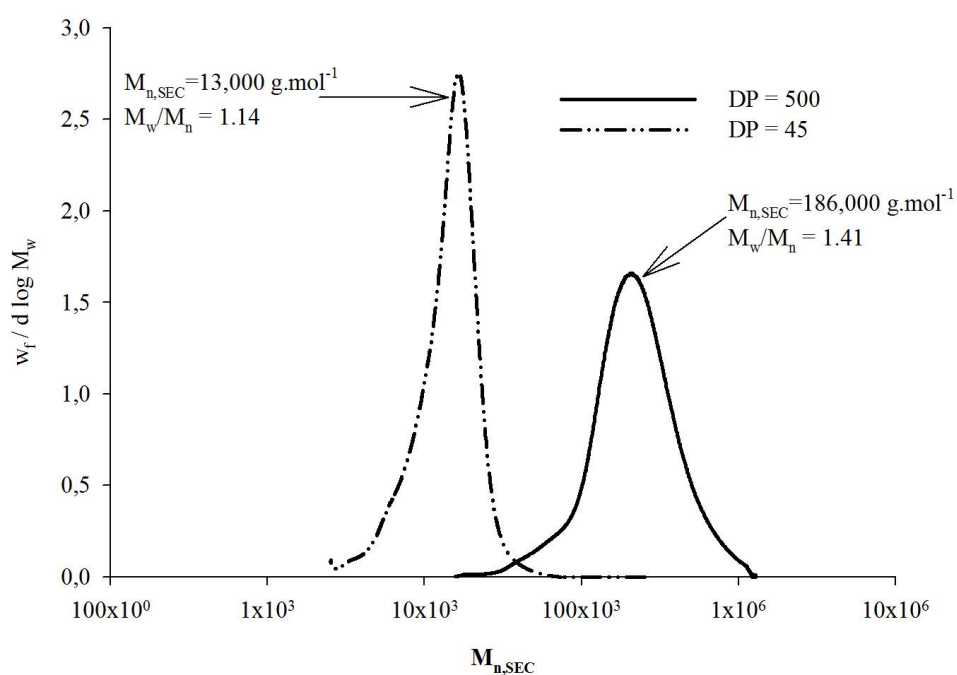
Figure 2.11: Molecular weight distribution for PDMAEMA samples obtained with Fe(0)/CuBr$_2$/PMDETA in IPA/H$_2$O at 25 °C for DP 45 and 500.

2.4.3 DMAEMA ATRP initiated with biocompatible mPEG and CHO segments

The utility of the ATRP of DMAEMA mediated by Fe(0)/CuBr$_2$/PMDETA in IPA/H$_2$O was expanded by use of a hydrophilic, biocompatible mPEG-Br initia-

tor and a hydrophobic, CHO-Br initiator. It should be noted that ATRP initiated with mPEG-Br was carried out at 50 °C, since the initiator is poorly soluble in IPA at 25 °C. The procedure used to prepare the CHO-Br initiator was an adaptation from a PEG-Br synthesis method used in the published literature[53] and is provided in the *Appendix B - Supporting Information* in addition to ^{1}H NMR (Figure B.1) and FTIR-ATR (Figure B.2) spectra.

The kinetics using mPEG and cholesterol based initiators is presented in Figure 2.12.

Figure 2.12: (a) Kinetic plots of conversion and $\ln[M]_0/[M]$ *vs.* time and **(b)** plot of number average molecular weights ($M_{n,SEC}$) and Đ (M_w/M_n) *vs.* conversion (%) in IPA/H_2O using mPEG-Br or CHO-Br as ATRP initiators. Conditions: $[DMAEMA]_0/[IPA]/[H_2O]$ = 1/0.9/0.1 (v/v); $[DMAEMA]_0/[initiator]_0/[Fe(0)]_0/[CuBr_2]_0/[PMDETA]$ = 90/1/1/0.1/1 (molar).

The kinetics of both polymerization reactions indicate that the polymerizations proceed with only small deviations from linear kinetics. The induction period seems to be negligible for ATRP of DMAEMA on the mPEG-Br initiated experiment, which can be attributed to the higher reaction temperature. Comparing mPEG-Br initiated DMAEMA ATRP with the reaction initiated with EBiB carried out at 60 °C using the Fe(0)/CuBr$_2$ catalytic system (Figure 2.3), mPEG-Br provides an enhanced level of control of ATRP over the full range of monomer conversion. However, towards the end of the polymerization, Đ increased slightly to values close to 1.30. The ATRP of DMAEMA initiated from CHO-Br proceeds at a slower rate than the reaction initiated with mPEG-Br. This observation can be attributed to the lower temperature used and to the lower solubility of CHO-Br in the reaction medium. The poor CHO-Br solubility was expected to lead to poor initiation efficiency and it may explain the

much higher M_n values that were determined by the SEC of samples taken during this polymerization, as shown in Figure 2.12 (b).

In spite of the solubility issues, ATRP of DMAEMA initiated with PEG-Br or CHO-Br displayed the characteristics of well-controlled copolymerization using the much more environmentally friendly catalytic system and a solvent medium than the systems traditionally used for ATRP. Figure 2.13 compares the molecular weight distribution of the PDMAEMA initiated with EBiB with those of the polymers initiated with mPEG-Br and CHO-Br. The curves support the narrow molecular weight distribution obtained with this catalytic system for any of the products.

······ EBiB-PDMAEMA, Mn = 14,000 g.mol^{-1}, Đ = 1.13
——— PEG-PDMAEMA, Mn = 10,000 g.mol^{-1}, Đ = 1.36
– – – CHO-PDMAEMA, Mn = 48,000 g.mol^{-1}, Đ = 1.23

1×10^3 10×10^3 100×10^3 1×10^6

$M_{n,SEC}$
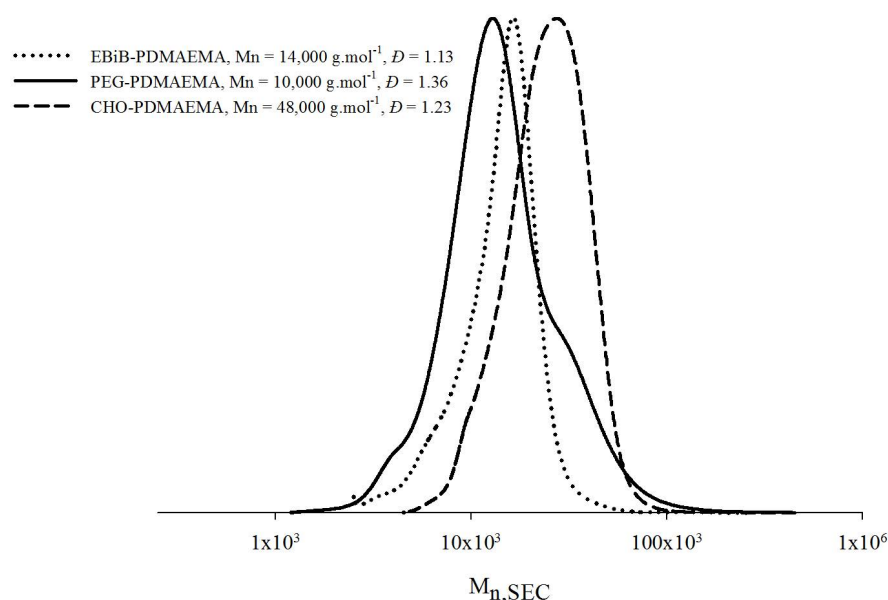
Figure 2.13: SEC traces of PDMAEMA using mPEG-Br, CHO-Br or EBiB as ATRP initiators. Conditions: $[DMAEMA]_0/[IPA]/[H_2O]$ = 1/0.9/0.1 (v/v); $[DMAEMA]_0/[initiator]_0/[Fe(0)]_0/[CuBr_2]_0/[PMDETA]$ = 90/1/1/0.1/1 (molar).

^{1}H NMR analysis of the polymers was carried in order to compare the integrals of the macroinitiator with those of PDMAEMA. Figure 2.14 presents the ^{1}H NMR spectra of PEG-PDMAEMA (A) and CHO-PDMAEMA (B) prepared at 25 °C with the Fe(0)/CuBr$_2$/PMDETA catalyst system. As mentioned above, relative intensities of the signals at 4.07 ppm (a), 2.58 ppm (b), 2.35-2.20 ppm (c), 2.00-1.75 ppm (d) and 1.10-0.80 ppm (e) are in agreement with the expected PDMAEMA chemical structure

and are visible in both spectra.
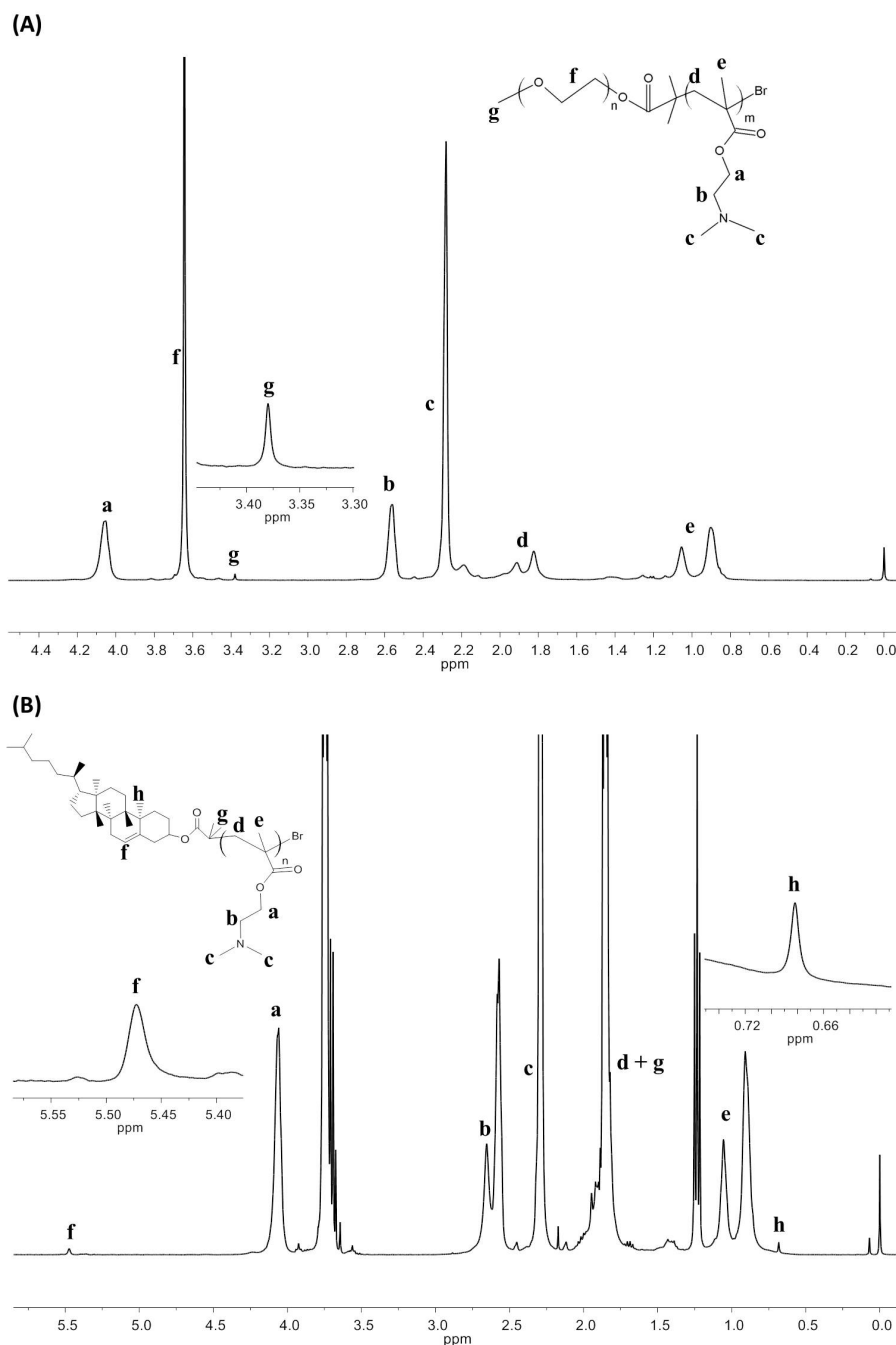
Figure 2.14: ^{1}H NMR spectrum (CDCl$_3$, 400 MHz) of PDMAEMA-based polymers: **(A)** mPEG-*b*-PDMAEMA and **(B)** CHO-PDMAEMA. Conditions: [DMAEMA]$_0$/[IPA]/[H$_2$O] = 1/0.9/0.1 (v/v); [DMAEMA]$_0$/[initiator]$_0$/[Fe(0)]$_0$/[CuBr$_2$]$_0$/[PMDETA] = 90/1/1/0.1/1 (molar).

In the ^{1}H NMR spectrum of PEG-PDMAEMA (Figure 2.14 (A)), the sharp signal at 3.65 ppm (f) was attributed to the ethylene protons of the ethylene glycol (-O(CH_2)$_2$O-) and the signal at 3.35 ppm (g) belonged to methyl protons of a CH_3O-

unit in PEG. In the ^{1}H NMR spectrum of CHO-PDMAEMA (Figure 2.14 (B)), the signals at 5.45 (f) and 1.85 (g) ppm correspond to -C*H*=C- and (C*H*$_3$)$_2$-C- units of the cholesterol initiator, respectively (*Appendix B - Supporting Information*). Since, mPEG's number-average molecular weight is known, 5,000 g.mol^{-1} (DP 113), the average number DP of the PDMAEMA segment on the basis of ^{1}H NMR analysis is estimated to be 89, giving a final product of M$_n$ = 19,000 g.mol^{-1}. Integration of cholesteryl and PDMAEMA signals (respectively, (f) and (a)) gives an estimation of the number-average molecular weight of CHO-*b*-PDMAEMA as 109,653 g.mol^{-1}. Differences from the values estimated based on the SEC system can be attributed to the difficulty of comparing PDMAEMA and cholesteryl segments due to the very low intensity of ^{1}H signals of cholesteryl segments.

The kinetic parameters obtained for the different catalytic systems and conditions used for the DMAEMA's polymerizations are summarized in Table 2.1.

The results presented in Table 2.1 evidence that, independently of the polymerization conditions (solvent and temperature), when compared to CuBr, the Fe(0)/CuBr$_2$-mediated catalyst system allows the DMAEMA's ATRP to reach very high conversions, while affording PDMAEMA with low *Đ* values. Polymerization control decreased for the preparation of high molecular weight PDMAEMA with PEG and CHO segments, but still with acceptable *Đ* values.

Table 2.1: Molar mass and *Đ* of PDMAEMA obtained by ATRP (monomer/solvent ratio 1:1 (v/v)).

ATRP system	Molar ratio	Solvent	T (°C)	Conv. (%)	M$_n$^{a}	*Đ*
DMAEMA/EBiB/CuBr/PMDETA	50/1/1/1	THF	60	52	6,185	1.45
DMAEMA/EBiB/CuBr/PMDETA	50/1/1/1	IPA	60	92	12,499	1.57
DMAEMA/EBiB/CuBr/PMDETA	45/1/1/1/1	IPA/H$_2$O^b	60	96	12,078	1.47
DMAEMA/EBiB/CuBr/PMDETA	45/1/1/0.1/1.1	IPA/H$_2$O^b	60	83	10,325	1.25
DMAEMA/EBiB/Fe(0)/CuBr$_2$/PMDETA	45/1/1/0.1/1.1	IPA/H$_2$O^b	60	96	14,035	1.22
DMAEMA/EBiB/Fe(0)/CuBr$_2$/PMDETA	45/1/1/0.1/1.1	IPA/H$_2$O^b	25	93	14,016	1.13
DMAEMA/EBiB/Fe(0)/CuBr$_2$/HMTETA	45/1/1/0.1/1.1	IPA/H$_2$O^b	25	90	14,499	1.14
DMAEMA/EBiB/Fe(0)/CuBr$_2$/HMTETA	45/1/1/0.1/0.1	IPA/H$_2$O^b	25	89	15,877	1.10
DMAEMA/EBiB/Fe(0)/CuBr$_2$/PMDETA	500/1/1/0.1/1.1	IPA/H$_2$O^b	25	47	185,635	1.41
DMAEMA/mPEG-Br/Fe(0)/CuBr$_2$/PMDETA	90/1/1/0.1/1.1	IPA/H$_2$O^b	50	96	19,282	1.28
DMAEMA/CHO-Br/Fe(0)/CuBr$_2$/PMDETA	90/1/1/0.1/1.1	IPA/H$_2$O^{b,c}	25	81	47,716	1.23

^{a}g.mol^{-1}

^{b}IPA/water = 9/1 (v/v)

^{c}monomer/solvent = 1/2 (v/v)

2.5   Conclusions

To conclude, it was reported on the ATRP of DMAEMA, using the environmentally friendly Fe(0)-mediated catalytic system, containing residual amounts of copper and economically attractive PMDETA ligand in isopropanol/water medium. The PDMAEMA obtained had relatively narrow molecular weight distribution. When compared to the conventionally used CuBr-mediated catalyst system, the new catalytic system resulted in greater polymerization rates, higher monomer conversion, and significantly lower dispersity values at all conversions. Improved control was achieved when the polymerization temperature was decreased from 60 °C to 25 °C, while maintaining reasonable polymerization rates; no significant differences were found when HMTETA was used as the ligand. The Fe(0)/CuBr$_2$/PMDETA catalyst system could be further used to prepare high molecular weight PDMAEMA and biorelevant PEG-*b*-PDMAEMA and CHO-*b*-PDMAEMA polymers of narrow molecular weight distributions.

2.6   Acknowledgements

Bibliography

[1] K. Matyjaszewski. Atom transfer radical polymerization (ATRP): current status and future perspectives. *Macromolecules*, 45(10):4015–4039, 2012.

[2] W.A. Braunecker and K. Matyjaszewski. Controlled/living radical polymerization: features, developments, and perspectives. *Progress in Polymer Science*, 32(1):93–146, 2007.

[3] F. di Lena and K. Matyjaszewski. Transition metal catalysts for controlled radical polymerization. *Progress in Polymer Science*, 35(8):959–1021, 2010.

[4] K. Matyjaszewski and J. Xia. Atom transfer radical polymerization. *Chemical Reviews-Columbus*, 101(9):2921–2990, 2001.

[5] T. Guliashvili, P.V. Mendonça, A.C. Serra, A.V. Popov, and J.F.J. Coelho. Copper-mediated controlled/"living" radical polymerization in polar solvents: insights into some relevant mechanistic aspects. *Chemistry - A European Journal*, 18(15):4607–4612, 2012.

[6] N.V. Tsarevsky, K. Matyjaszewski, et al. "Green" atom transfer radical polymerization: from process design to preparation of well-defined environmentally friendly polymeric materials. *Chemical Reviews-Columbus*, 107(6):2270–2299, 2007.

[7] K. Matyjaszewski, W. Jakubowski, K. Min, W. Tang, J. Huang, W.A. Braunecker, and N.V. Tsarevsky. Diminishing catalyst concentration in atom transfer radical polymerization with reducing agents. *Proceedings of the National Academy of Sciences*, 103(42):15309–15314, 2006.

[8] W. Jakubowski, K. Min, and K. Matyjaszewski. Activators regenerated by electron transfer for atom transfer radical polymerization of styrene. *Macromolecules*, 39(1):39–45, 2006.

[9] W. Jakubowski and K. Matyjaszewski. Activators regenerated by electron transfer for atom-transfer radical polymerization of (meth)acrylates and related block copolymers. *Angewandte Chemie*, 118(27):4594–4598, 2006.

[10] A.J.D. Magenau, N.C. Strandwitz, A. Gennaro, and K. Matyjaszewski. Electrochemically mediated atom transfer radical polymerization. *Science*, 332(6025):81–84, 2011.

[11] Q. Lou and D.A. Shipp. Recent developments in atom transfer radical polymerization (ATRP): methods to reduce metal catalyst concentrations. *ChemPhysChem*, 13(14):3257–3261, 2012.

[12] K. Matyjaszewski, M. Wei, J. Xia, and N.E. McDermott. Controlled/"living" radical polymerization of styrene and methyl methacrylate catalyzed by iron complexes. *Macromolecules*, 30(26):8161–8164, 1997.

[13] T. Ando, M. Kamigaito, and M. Sawamoto. Iron(II) chloride complex for living radical polymerization of methyl methacrylate. *Macromolecules*, 30(16):4507–4510, 1997.

[14] K. Matyjaszewski, S. Coca, S.G. Gaynor, M. Wei, and B.E. Woodworth. Zerovalent metals in controlled/"living" radical polymerization. *Macromolecules*, 30(23):7348–7350, 1997.

[15] P.V. Mendonça, A.C. Serra, J.F.J. Coelho, A.V. Popov, and T. Guliashvili. Ambient temperature rapid ATRP of methyl acrylate, methyl methacrylate and styrene in polar solvents with mixed transition metal catalyst system. *European Polymer Journal*, 47(7):1460–1466, 2011.

[16] Y. Zhang, Y. Wang, and K. Matyjaszewski. ATRP of methyl acrylate with metallic zinc, magnesium, and iron as reducing agents and supplemental activators. *Macromolecules*, 44(4):683–685, 2011.

[17] C.M.R. Abreu, P.V. Mendonça, A.C. Serra, J.F.J. Coelho, A.V. Popov, and T. Guliashvili. Accelerated ambient-temperature ATRP of methyl acrylate in alcohol-water solutions with a mixed transition-metal catalyst system. *Macromolecular Chemistry and Physics*, 213(16):1677–1687, 2012.

[18] J.F.J. Coelho, P.C. Ferreira, P. Alves, R. Cordeiro, A.C. Fonseca, J.R. Góis, and M.H. Gil. Drug delivery systems: advanced technologies potentially applicable in personalized treatments. *The EPMA Journal*, 1(1):164–209, 2010.

[19] K. Matyjaszewski and N.V. Tsarevsky. Nanostructured functional materials prepared by atom transfer radical polymerization. *Nature Chemistry*, 1(4):276–288, 2009.

[20] A.K.A.S. Brun-Graeppi, C. Richard, M. Bessodes, D. Scherman, and O.W. Merten. Thermoresponsive surfaces for cell culture and enzyme-free cell detachment. *Progress in Polymer Science*, 35(11):1311–1324, 2010.

[21] L. Casettari, D. Vllasaliu, E. Castagnino, S. Stolnik, S. Howdle, and L. Illum. PEGylated chitosan derivatives: synthesis, characterizations and pharmaceutical applications. *Progress in Polymer Science*, 37(5):659 – 685, 2012.

[22] S. Gomes, I.B. Leonor, J.F. Mano, R.L. Reis, and D.L. Kaplan. Natural and genetically engineered proteins for tissue engineering. *Progress in Polymer Science*, 37(1):1 – 17, 2012.

[23] A. Gregory and M.H. Stenzel. Complex polymer architectures via RAFT polymerization: From fundamental process to extending the scope using click chemistry and nature's building blocks. *Progress in Polymer Science*, 37(1):38–105, 2012.

[24] D.J. Siegwart, J.K. Oh, and K. Matyjaszewski. ATRP in the design of functional materials for biomedical applications. *Progress in Polymer Science*, 37(1):18–37, 2012.

[25] H. Tian, Z. Tang, X. Zhuang, X. Chen, and X. Jing. Biodegradable synthetic polymers: preparation, functionalization and biomedical application. *Progress in Polymer Science*, 37(2):237–280, 2012.

[26] J. Zhang, X. Li, and X. Li. Stimuli-triggered structural engineering of synthetic and biological polymeric assemblies. *Progress in Polymer Science*, 37(8):1130–1176, 2012.

[27] S. Park, H.Y. Cho, J.A. Yoon, Y. Kwak, A. Srinivasan, J.O. Hollinger, H. Paik, and K. Matyjaszewski. Photo-cross-linkable thermoresponsive star polymers designed for control of cell-surface interactions. *Biomacromolecules*, 11(10):2647–2652, 2010.

[28] Y.Z. You, D.S. Manickam, Q.H. Zhou, and D. Oupicky. Reducible poly(2-dimethylaminoethyl methacrylate): synthesis, cytotoxicity, and gene delivery activity. *Journal of Controlled Release*, 122(3):217–225, 2007.

[29] J.M. Layman, S.M. Ramirez, M.D. Green, and T.E. Long. Influence of polycation molecular weight on poly(2-dimethylaminoethyl methacrylate)-mediated DNA delivery *in vitro*. *Biomacromolecules*, 10(5):1244–1252, 2009.

[30] S.E. Averick, E. Paredes, A. Irastorza, A.R. Shrivats, A. Srinivasan, D.J. Siegwart, A.J. Magenau, H.Y. Cho, E. Hsu, A.A. Averick, J. Kim, S. Liu, J.O. Hollinger, S.R. Das, and K. Matyjaszewski. Preparation of cationic nanogels for nucleic acid delivery. *Biomacromolecules*, 13(11):3445–3449, 2012.

[31] H.Y. Cho, A. Srinivasan, J. Hong, E. Hsu, S. Liu, A. Shrivats, D. Kwak, A.K. Bohaty, H. Paik, Jeffrey O. Hollinger, and K. Matyjaszewski. Synthesis of biocompatible PEG-based star polymers

with cationic and degradable core for siRNA delivery. *Biomacromolecules*, 12(10):3478–3486, 2011.

[32] J. Robbens, C. Vanparys, I. Nobels, R. Blust, K. Van Hoecke, C. Janssen, K. De Schamphelaere, K. Roland, G. Blanchard, F. Silvestre, V. Gillardin, P. Kestemont, R. Anthonissen, O. Toussaint, S. Vankoningsloo, C. Saout, E. Alfaro-Moreno, P. Hoet, L. Gonzalez, P. Dubruel, and P. Troisfontaines. Eco-, geno- and human toxicology of bio-active nanoparticles for biomedical applications. *Toxicology*, 269(2-3):170–181, 2010.

[33] B.I. Cerda-Cristerna, H. Flores, A. Pozos-Guillen, E. Perez, C. Sevrin, and C. Grandfils. Hemocompatibility assessment of poly(2-dimethylamino ethylmethacrylate) (PDMAEMA)-based polymers. *Journal of Controlled Release*, 153(3):269–277, 2011.

[34] F.L. Baines, S.P. Armes, N.C. Billingham, and Z. Tuzar. Micellization of poly(2-(dimethylamino)ethyl methacrylate-*block*-methyl methacrylate) copolymers in aqueous solution. *Macromolecules*, 29(25):8151–8159, 1996.

[35] F.A. Plamper, M. Ruppel, A. Schmalz, O. Borisov, M. Ballauff, and A.H.E. Müller. Tuning the thermoresponsive properties of weak polyelectrolytes: aqueous solutions of star-shaped and linear poly(N,N-dimethylaminoethyl methacrylate). *Macromolecules*, 40(23):8361–8366, 2007.

[36] B. Nottelet, M. Vert, and J. Coudane. Novel amphiphilic degradable poly(epsilon-caprolactone)-graft-poly(4-vinyl pyridine), poly(epsilon-caprolactone)-graft-poly(dimethylaminoethyl methacrylate) and water-soluble derivatives. *Macromolecular Rapid Communications*, 29(9):743–750, 2008.

[37] K. Sui, X. Shan, S. Gao, Y. Xia, Q. Zheng, and D. Xie. Dual-responsive supramolecular inclusion complexes of block copolymer poly(ethylene glycol)-block-poly[(2-dimethylamino)ethyl methacrylate] with α-cyclodextrin. *Journal of Polymer Science Part A: Polymer Chemistry*, 48(10):2143–2153, 2010.

[38] S. Guo, Y. Huang, T. Wei, W. Zhang, W. Wang, D. Lin, X. Zhang, A. Kumar, Q. Du, J. Xing, L. Deng, Z. Liang, P.C. Wang, A. Dong, and X.J. Liang. Amphiphilic and biodegradable methoxy polyethylene glycol-block-(polycaprolactone-*graft*-poly(2-(dimethylamino)ethyl methacrylate)) as an effective gene carrier. *Biomaterials*, 32(3):879–889, 2011.

[39] Z.L. Yao and K.C. Tam. Synthesis and self-assembly of stimuli-responsive poly(2-(dimethylamino) ethyl methacrylate)-block-fullerene (PDMAEMA-*b*-C60) and the demicellization induced by free PDMAEMA chains. *Langmuir*, 27(11):6668–6673, 2011.

[40] X. Zhang, J. Xia, and K. Matyjaszewski. Controlled/"living" radical polymerization of 2-(dimethylamino)ethyl methacrylate. *Macromolecules*, 31(15):5167–5169, 1998.

[41] F. Zeng, Y. Shen, S. Zhu, and R. Pelton. Atom transfer radical polymerization of 2-(dimethylamino)ethyl methacrylate in aqueous media. *Journal of Polymer Science Part A: Polymer Chemistry*, 38(20):3821–3827, 2000.

[42] N. Pantoustier, S. Moins, M. Wautier, P. Degée, and P. Dubois. Solvent-free synthesis and purification of poly[2-(dimethylamino)ethyl methacrylate] by atom transfer radical polymerization. *Chemical Communications*, 0:340–341, 2003.

[43] B. Mao, L.H. Gan, Y.Y. Gan, X. Li, P. Ravi, and K.C. Tam. Controlled polymerizations of 2-(dialkylamino)ethyl methacrylates and their block copolymers in protic solvents at ambient temperature via ATRP. *Journal of Polymer Science Part A: Polymer Chemistry*, 42(20):5161–5169, 2004.

[44] K.M. Xiu, J.J. Yang, N.N. Zhao, J.S. Li, and F.J. Xu. Multiarm cationic star polymers by atom transfer radical polymerization from beta-cyclodextrin cores: Influence of arm number and length on gene delivery. *Acta Biomaterialia*, 9(1):4726 – 4733, 2013.

[45] W. Zhang, W. Zhang, Z. Zhang, J. Zhu, Q. Pan, and X. Zhu. Synthesis and characterization of AB2-type star polymers via combination of ATRP and click chemistry. *Polymer Bulletin*, 63(4):467–483, 2009.

[46] B.Y. Zhang, W.D. He, W.T. Li, L.Y. Li, K.R. Zhang, and H. Zhang. Preparation of block-brush PEG-b-P(NIPAM-g-DMAEMA) and its dual stimulus-response. *Polymer*, 51(14):3039–3046, 2010.

[47] S.B. Lee, A.J. Russell, and K. Matyjaszewski. ATRP synthesis of amphiphilic random, gradient, and block copolymers of 2-(dimethylamino)ethyl methacrylate and n-butyl methacrylate in aqueous media. *Biomacromolecules*, 4(5):1386–1393, 2003.

[48] A.P. Narrainen, S. Pascual, and D.M. Haddleton. Amphiphilic diblock, triblock, and star block copolymers by living radical polymerization: synthesis and aggregation behavior. *Journal of Polymer Science Part A: Polymer Chemistry*, 40(4):439–450, 2002.

[49] S. Lu, Q.L. Fan, S.J. Chua, and W. Huang. Synthesis of conjugated-ionic block copolymers by controlled radical polymerization. *Macromolecules*, 36(2):304–310, 2003.

[50] L. Chen, M. Zhang, Z. Liu, Z. Gu, Y. Tu, and P. Ni. Fabrication of gene carrier via self-assembly of poly[(dimethylamino)ethyl methacrylate] and poly(aspartic acid)-*grafted*-poly(ethylene glycol). *Journal of Macromolecular Science, Part A*, 48(11):862–871, 2011.

[51] M. Ji, L. Jin, J. Guo, W. Yang, C. Wang, and S. Fu. Formation of luminescent nanocomposite assemblies via electrostatic interaction. *Journal of Colloid and Interface Science*, 318(2):487–495, 2008.

[52] X. Sun, H. Zhang, X. Huang, X. Wang, and Q.F. Zhou. Synthesis of poly(ethylene oxide)-block-poly(methyl methacrylate)-block-polystyrene triblock copolymers by two-step atom transfer radical polymerization. *Polymer*, 46(14):5251–5257, 2005.

[53] K. Jankova, X.Y. Chen, J. Kops, and W. Batsberg. Synthesis of amphiphilic PS-*b*-PEG-*b*-PS by atom transfer radical polymerization. *Macromolecules*, 31(2):538–541, 1998.

[54] M.A. Kryuchkov, C. Detrembleur, R. Jérôme, R.E. Prud'homme, and C.G. Bazuin. Synthesis and thermal properties of linear amphiphilic diblock copolymers of L-lactide and 2-dimethylaminoethyl methacrylate. *Macromolecules*, 44(13):5209–5217, 2011.

[55] S. McDonald and S.P. Rannard. Room temperature waterborne ATRP of *n*-butyl methacrylate in homogeneous alcoholic media. *Macromolecules*, 34(25):8600–8602, 2001.

[56] X. Bories-Azeau and S.P. Armes. Unexpected transesterification of tertiary amine methacrylates during methanolic ATRP at ambient temperature: a cautionary tale. *Macromolecules*, 35(27):10241–10243, 2002.

[57] Nicolay V. Tsarevsky, Tomislav Pintauer, and Krzysztof Matyjaszewski. Deactivation efficiency and degree of control over polymerization in ATRP in protic solvents. *Macromolecules*, 37(26):9768–9778, 2004.

[58] L. Mespouille, P. Degee, and P. Dubois. Amphiphilic poly(N,N-dimethylamino-2-ethyl methacrylate)-*g*-poly(epsilon-caprolactone) graft copolymers: synthesis and characterisation. *European Polymer Journal*, 41(6):1187–1195, 2005.

[59] X. Jin, Y. Shen, and S. Zhu. Atom transfer radical block copolymerization of 2-(N,N-dimethylamino)ethyl methacrylate and 2-hydroxyethyl methacrylate. *Macromolecular Materials and Engineering*, 288(12):925–935, 2003.

[60] D.M. Haddleton, C. Waterson, P.J. Derrick, C.B. Jasieczek, and A.J. Shooter. Monohydroxy terminally functionalised poly(methyl methacrylate) from atom transfer radical polymerisation. *Chemical Communications*, (7):683–684, 1997.

[61] K. Matyjaszewski, Y. Nakagawa, and C.B. Jasieczek. Polymerization of n-butyl acrylate by atom transfer radical polymerization. remarkable effect of ethylene carbonate and other solvents. *Macromolecules*, 31(5):1535–1541, 1998.

[62] S. Coca, C.B. Jasieczek, K.L. Beers, and K. Matyjaszewski. Polymerization of acrylates by atom transfer radical polymerization. homopolymerization of 2-hydroxyethyl acrylate. *Journal of Polymer Science Part A: Polymer Chemistry*, 36(9):1417–1424, 1998.

CHAPTER 3

Novel cationic triblock copolymer
poly[2-(dimethylamino)ethyl
methacrylate]-*block*-poly(*β*-amino
ester)-*block*-poly[2-(dimethylamino)ethyl methacrylate]: a
promising non-viral gene delivery system

3.1   Abstract

This Chapter reports the synthesis of a new cationic triblock copolymer based on poly[2-(dimethylamino)ethyl methacrylate] (PDMAEMA) and poly(β-amino ester) (PβAE) from different polymerization strategies. For the first time, it is proposed a triblock copolymer based only on cationic segments, aiming a high biocompatibility, enhanced buffering capacity and stimuli-responsive character in a single structure. The new block copolymer successfully condensed the plasmid DNA (pDNA) into nanosized (< 200 nm) polyplexes. The polyplexes were tested as non-viral gene delivery systems in two different cell lines revealing ~4-fold and ~6-fold (in HeLa cells), and ~11-fold (in COS-7 cells) higher transgene expression than branched PEI (25,000 g.mol^{-1}) and TurboFect^{TM}, respectively. These results show that the new block copolymer PDMAEMA-*b*-PβAE-*b*-PDMAEMA is a promising candidate to be used as a polymeric non-viral vector.

3.2   Introduction

In the past two decades, cationic polymers have attracted increasing attention for biomedical applications[1,2]. This growing interest is closely related to the fact that these polymers, with high density of positive charges, have been considered as a safer alternative to viral vectors for nucleic acid delivery[1,3]. As examples of the most used cationic polymers for gene delivery are chitosan, poly(L-lysine), polyethylenimine (PEI), poly[2-(dimethylamino)ethyl methacrylate] (PDMAEMA) and, more recently, poly(β-amino ester) (PβAE)[4]. Although much effort have been placed in the development of new synthetic polymeric non-viral vectors, generally they do not possess the transfection activity of the viral vectors[3].

PDMAEMA, a dual-responsive polymer (temperature and pH), has been widely used in the gene delivery area[5–8] since its first use as a gene transfection system in 1996 by Cherng[9]. Since then, several studies were performed to evaluate different aspects on the transfection efficiency of this polymer, such as, the role of molecular weight, polyplex size, and transfection parameters as pH, ionic strength, temperature, viscosity, polymer/plasmid (N/P) ratio, and the presence of stabiliz-

ers[10]. Among these, the molecular weight has been considered as one of the most important aspects on transfection activity[10–12]. It has been reported that PDMAEMA with higher molecular weight leads to smaller polyplexes that are more efficient in transfection. Neverthless, it is also showed to be more cytotoxic than polymers with low molecular weight[10]. In the last two decades, efforts have been made to prepare PDMAEMA with controlled structure and low dispersity (*Đ*) using reversible deactivation radical polymerization (RDRP) methods[13–16]. In Chapter 2 was reported the synthesis of PDMAEMA by atom transfer radical polymerization (ATRP) under mild reaction conditions and using biological relevant initiators, based on poly(ethylene glycol) (PEG) and cholesterol.

Poly(*β*-amino ester) (P*β*AE) is a recently explored synthetic, hydrolytically biodegradable and biocompatible polymer as gene carrier[17;18]. This polymer can be easily synthesized by a Michael addition reaction between primary amine or bis(secondary amine) monomers and diacrylates[18;19]. P*β*AE contains easily hydrolyzable esters linkages in their backbone resulting in bis(*β*-amino acid) and diol fragments[17;18]. The physicochemical properties of the P*β*AE, such as charge density, water solubility, crystallinity, and degradation profile, can be synthetically adjusted to meet the specific requirements of several applications due to the wide range of amines and diacrylates available as monomers buildings[20]. One of the most studied P*β*AE is the one prepared from 1,4-butanediol diacrylate and 5-amino-1-pentanol, usually referred as C32, due to its excellent biocompatibility and both *in vitro* and *in vivo* high DNA transfection activity[17].

Recently, the use of copolymers combining polymers with different properties has been explored in order to achieve novel targeted gene delivery systems[21]. The combination of PDMAEMA and P*β*AE opens the possibility of using a unique polymer as a non-viral carrier with high positive charge density and stimuli-responsive properties. Moreover, the introduction of P*β*AE may bring to the polymeric structure improved degradability characteristics and, consequently, enhanced biocompatibility. As mentioned above, the molecular weight and chain lenght of a cationic polymer have a significant effect on transfection activity, namely in the cellular uptake, endosomal escape, DNA unpacking and nuclear internalization, and mainly, in the

produced cytotoxicity[4;22]. Thus, introducing a degradable cationic segment in middle of the polymeric chain may permit to obtain materials with a low cytotoxicity associated with a high gene delivery capacity.

In this Chapter, it is proposed a simple method for the synthesis of the first entirely cationic triblock copolymer based on stimuli-responsive PDMAEMA and C32-based P*β*AE segments. The cationic block copolymer PDMAEMA-*b*-P*β*AE-*b*-PDMAEMA was assessed as a plasmid DNA delivery system in HeLa and COS-7 cell lines and compared with the gold standard for polymeric gene carriers, the branched PEI (25,000 g.mol⁻¹), and with a commercial linear cationic polymeric non-viral vector, the TurboFect™, in order to demonstrate its suitability for gene delivery.

3.3   Experimental

3.3.1   Materials

5-amino-1-pentanol (Alfa Aesar, 97%), 1,4-butanediol diacrylate (Alfa Aesar, +99%), propargylamine (Sigma-Aldrich), copper (II) bromide (CuBr$_2$) (Acros, +99% extra pure, anhydrous), 2-(2-chloroethoxy)ethanol (Sigma Aldrich, 99%), polystyrene (PS) standards (Polymer Laboratories), (Acros, 99%, ~70 mesh), PMDETA (Aldrich, 99%), iron powder (Fe(0)), *α*-bromoisobutyryl bromide (Sigma Aldrich, 98%), sodium azide (Panreac, 99% PS), 2-propanol (Fisher Chemical), THF (Fisher Chemical), ethyl acetate (Fisher Chemical), diethyl ether (Fisher Scientific), DMSO (Acros Organics, +99.8%, extra pure), deuterated chloroform (CDCl$_3$) (Euriso-top, +1%TMS) and deuterium oxide (D$_2$O) (Euroiso-top, +99.9%D), Dulbecco's Modified Eagle's Medium - high glucose (DMEM-HG) (Sigma-Aldrich), resazurin sodium salt (Sigma-Aldrich), DL-dithiothreitol (Sigma), tris-phosphate (Sigma), ethylenediaminetetraacetic acid (EDTA) (Sigma-Aldrich), magnesium chloride (MgCl$_2$) (Sigma), glycerol (Sigma), Triton™ X-100 (Sigma), bovine serum albumin (BSA) (Sigma), boric acid (Sigma-Aldrich), D-luciferin sodium salt (Synchem, 99%), DC™ Protein Assay (Bio-Rad), plasmids encoding luciferase DNA (pCMV.Luc) (Vical), TurboFect™ (a kind gift from Thermo Scientific), PEI (branched, M$_w$ 25,000 g.mol⁻¹) (Sigma), Hoechst (Sigma-Aldrich), nucleic acid labeling kit Label IT®Cy5™ (Mirus Bio Corporation), Ficoll®

400 (Sigma-Aldrich), bromophenol blue (Sigma-Aldrich), sodium dodecyl sulfate (SDS) (Sigma-Aldrich) were used as received. Triethylamine (Sigma Aldrich, +99%) was dried over CaH_2, distilled and stored over molecular sieves. DMAEMA (Aldrich, 98%) was passed over a sand/alumina column before use in order to remove the radical inhibitor. Milli-Q water (Milli-Q$^®$, Millipore, resistivity >18 MΩ cm) was obtained by reverse osmosis. High-performance liquid chromatography (HPLC) tetrahydrofuran (THF) (Panreac, HPLC grade) was filtered under reduced pressure before use. Dichloromethane (DCM) (Fisher Scientific, +99.6%) was dried and distilled over calcium hydride. Triethylamnine (TEA) (Sigma-Aldrich, 96%) was distilled and stored over molecular sieves. 4-Dimethylaminopyridine (DMAP) (Sigma-Aldrich. +99%) was recrystallized from toluene. 2-(2-Azidoethoxy)ethyl bromoisobutyrate (N_3EiBBr) was prepared according to the procedure described in *Appendix B - Supporting Information*.

3.3.2   Methods

3.3.2.1   Synthesis of poly[2-(dimethylamino)ethyl methacrylate]-*block*-poly(*β*-amino ester)-*block*-poly[2-(dimethylamino)ethyl methacrylate]

Synthesis of α,ω-acrylate-poly(β-amino ester) through Michael addition reaction. 5-amino-1-pentanol (1.5 g, 14.54 mmol) was weighed into an opaque vial and 1,4-butanediol diacrylate (3.20 mL, 17.45 mmol) was added. A teflon-coated stir-bar was added, the vial was sealed with a teflon-lined screw-cap, and the reaction was placed in a pre-heated oil bath at 90 °C with stirring. After 24 h, the reaction was cooled down to room temperature, precipitated and washed three times with cold diethyl ether. Polymer was dried overnight at 40 °C under vacuum. Polymer was stored at -20 °C until use.

Synthesis of α,ω-alkyne-poly(β-amino ester) through Michael addition reaction. 1 g (0.31 mmol) of α,ω-acrylate-poly(β-amino ester) ($M_{n,NMR}$ = 3,212 g.mol^{-1}), and 85.74 mg (1.56 mmol) of propargylamine were dissolved in 1 mL of dry DMSO. The reaction was carried out overnight under magnetic stirring (300 rpm) at room temperature. Afterwards, the polymer was precipitated and washed three times with cold diethyl ether. Polymer was dried overnight at 40 °C under vacuum. Polymer was stored at

-20 °C until use.

Typical procedure for the synthesis of α-azide-poly[2-(dimethylamino)ethyl methacrylate] by atom transfer radical polymerization (DP = 45) - [Fe(0)]$_0$/[CuBr$_2$]$_0$/[PMDETA]$_0$ = 1/0.1/1.1. α-Azide-poly[2-(dimethylamino)ethyl methacrylate] was prepared according to the a previously reported procedure in Chapter 2. The synthesis of 2-(2-azidoethoxy)ethyl bromoisobutyrate (N$_3$EiBBr) is described in *Appendix B - Supporting Information*. A mixture of DMAEMA (6.0 mL, 35.61 mmol), Fe(0) (44.2 mg, 0.79 mmol) and CuBr$_2$ (17.7 mg, 0.079 mmol) was placed in a Schlenk tube reactor. The sample was first stirred and then frozen in liquid nitrogen. Subsequently, a mixture of N$_3$EiBBr (221.7 mg, 0.79 mmol), PMDETA (150.8 mg, 0.87 mmol) and isopropanol/water mixture (9/1, v/v) (6 mL) (previously bubbled with nitrogen for about 15 minutes) was added, under nitrogen atmosphere, to the reactor. The Schlenk tube reactor containing the reaction mixture was deoxygenated with three freeze-vacuum-thaw cycles and purged with nitrogen. The Schlenk tube reactor was placed in a pre-heated bath at 25 °C with stirring (700 rpm) for 2 hours. After the reaction was stopped, the sample was precipitated in cold hexane, dialyzed against distilled water (dialysis membrane, molecular weight cut off (MWCO) = 1,000 g.mol^{-1}) and then lyophilized.

Typical procedure for the preparation of tri-block copolymer poly[2-(dimethylamino)ethyl methacrylate]-block-poly(β-amino ester)-block-poly[2-(dimethylamino)ethyl methacrylate] (PDMAEMA-b-PβAE-b-PDMAEMA) by copper(I)-catalyzed azide-alkyne cycloaddition click chemistry. α,ω-Alkyne-PβAE (M$_{n,NMR}$ = 2,700 g.mol^{-1}, 100 mg, 0.04 mmol) and α-azide-PDMAEMA (M$_{n,NMR}$ = 8,300 g.mol^{-1}, 763 mg, 0.09 mmol) were placed in a Schlenk tube reactor with 5 mL of isopropanol previously bubbled with nitrogen for 15-20 minutes. PMDETA (22.3 mg, 0.128 mmol) and CuBr (18.5 mg, 0.128 mmol) were dissolved in 2 mL of isopropanol and then added to the Schlenk tube reactor. The mixture was deoxygenated with three freeze-vacuum-thaw cycles and purged with nitrogen. The Schlenk tube reactor was placed in a pre-heated bath at 50 °C with stirring (700 rpm) during 48 hours. The product was precipitated into cold ethyl ether and then dialyzed against dry THF (dialysis membrane MWCO 3,500 g.mol^{-1}) during 24 hours. After concentration by rotary evaporation, the mixture was precipitated into methanol. The final product was dried overnight under vacuum at 40 °C.

Block copolymer was storage at -20 °C until use.

3.3.2.2 Size exclusion chromatography

The chromatographic parameters of the samples were determined using high performance size exclusion chromatography (HPSEC; Viscotek (Viscotek TDAmax)) with a differential viscometer (DV); right-angle laser-light scattering (RALLS, Viscotek); low-angle laser-light scattering (LALLS, Viscotek) and refractive index (RI) detectors. The column set consisted of a PLgel 10 μm guard column (7.5 × 50 mm) followed by one Viscotek T200 column (6 μm), one MIXED-E PLgel column (3 μm) and one MIXED-C PLgel column (5 μm). HPLC dual piston pump was set with a flow rate of 1 mL.min^{-1}. The eluent (THF) was previously filtered through a 0.2 μm filter. The system was also equipped with an on-line degasser. The tests were done at 30 °C using an Elder CH-150 heater. Before the injection (100 μL), the samples were filtered through a polytetrafluoroethylene (PTFE) membrane with 0.2 μm pore. The system was calibrated with narrow PS standards. The number-average molecular weight (M$_{n,SEC}$) and Đ of synthesized polymers were determined by multidetectors calibration using OmniSEC software version: 4.6.1.354.

3.3.2.3 Nuclear magnetic resonance spectroscopy

^{1}H NMR (400 MHz) spectra of reaction mixture samples were recorded on a Bruker Avance III 400 MHz spectrometer, with a 5-mm TXI triple resonance detection probe, in CDCl$_3$ or D$_2$O with tetramethylsilane (TMS) as an internal standard. Conversion of monomers was determined by integration of monomer and polymer signals using MestReNova software version: 6.0.2-5475.

3.3.2.4 Fourier transform infrared spectroscopy

Fourier-transform infrared attenuated total reflection (FTIR-ATR) spectra were acquired in the range of 500-4000 cm^{-1}, using a JASCO 4200 FTIR spectrophotometer (Jasco, Japan) equipped with a single horizontal Golden Gate ATR cell, at 128 scans and with a 4 cm^{-1} resolution.

3.3.2.5   Atomic absorption spectroscopy

An atomic absorption spectrometer 3300 (Perkin Elmer, USA) flame atomic absorption spectrometer was used for the analysis of residual copper content. The copper hollow cathode lamp was run under the conditions suggested by the manufacturer (current: 4.0 mA). Also, the wavelength (324.8 nm) and the bandwidth of the slit (0.7 nm) had conventional values. The flame composition was: acetylene (flow rate: 2.0 L.min^{-1}) and air (flow rate: 10.0 L.min^{-1}). Aspiration flow rate was 5.0 L.min^{-1}. At least, eight measurements were taken for each sample.

3.3.2.6   Polymer buffering capacity

Potentiometric titration curves of polymers were obtained in Milli-Q water 3.5 (*Appendix B - Supporting Information*). The initial polymer solutions contain a fixed amount of mass (25 mg) in a volume of 40 mL. Initially, the pH of the solution was acidified with 2.35 mL of 1% HCl aqueous solution. The solution was then titrated with 25 μL aliquots of 0.1 M NaOH. Titration curve of Milli-Q water (without the presence of polymer) was used as background control. Measurements were taken using a Crison Basic 20 pH meter (Crison, Allela, Spain). Buffer capacity was calculated using two different methodologies: by taking the ratio of total protons buffered between pH 7.4 and 5.5 to the total amines of the polymer, and by taking the ratio of protons buffered between 7.4 and 5.5 to total polymer mass. For pK$_a$ determination, a correction of experimental errors during titration was carried out according a previously reported methodology[24] (see corrected potentiometric titration curves in Figure B.6 (*Appendix B - Supporting Information*). Based on corrected curve, plots of the degree of protonation of the amine groups (α) according pH variation (Figure B.6, *Appendix B - Supporting Information*) was estimated using equation α(pH) = {[amine]$_i$.V$_i$ - [NaOH]$_{0,amine}$(pH).V$_{amine}$(pH) + [NaOH]$_{0,water}$(pH).V$_{water}$(pH)}/{[amine]$_i$.V$_i$}, where [NaOH]$_0$ denotes the nominal concentration of added NaOH (after correction) and V the total volume of the solution at a given point of titration, and the subscripts, *amine*, *water*, and *i* represent, respectively, the amine titration measurement, the water titration measurement, and the initial condition of the titration experiments. The pK$_a$ was determined for α(pH) = 0.5.

3.3.2.7 Matrix-assisted laser desorption ionization time-of-flight mass spectroscopy

For the matrix-assisted laser desorption ionization time-of-flight mass spectroscopy (MALDI-TOF MS) analysis, the P*β*AE sample was dissolved in THF at a concentration of 20 mg.mL^{-1} and 2,5-dihydroxybenzoic acid (DHB) was used as the matrix. The dried-droplet sample preparation technique was used to obtain 1/1 ratio (sample/matrix); an aliquot of 2 μL of sample was directly spotted on the MTP AnchorChip TM 600/384 TF MALDI target, Bruker Daltonik (Bremen Germany) and, before the sample dried, 2 μL of matrix solution in THF was added and the sample was allowed to dry at room temperature to allow matrix crystallization. External mass calibration was performed with a peptide calibration standard (PSCII) for the range 700-3000 (nine mass calibration points), 0.5 μL of the calibration solution and matrix previously mixed in an Eppendorf tube (1/2, v/v) were applied directly on the target and allowed to dry at room temperature. Mass spectra were recorded using an Autoflex III smartbeam MALDI-TOF-MS mass spectrometer Bruker Daltonik operating in the linear positive ion mode. Ions were formed upon irradiation by a smartbeam laser using a frequency of 200 Hz. Each mass spectrum was produced by averaging 2500 laser shots collected across the whole sample spot surface by screening in the range *m/z* 421-5030. The laser irradiance was set to 35-40% (relative scale 0-100) arbitrary units according to the corresponding threshold required for the applied matrix systems.

3.3.2.8 Thermogravimetric analysis

Thermogravimetric analysis (TA Instruments, Q500, USA) were carried out, in duplicate, from room temperature up to 600 °C, at a 10 °C.min^{-1} heating rate, under a dry nitrogen atmosphere (at 40 mL.min^{-1}) using approximately 5 mg of the sample.

3.3.2.9 Biological activity

The biological activity and cytotoxicity of the complexes prepared with the cationic block copolymers PDMAEMA-*b*-P*β*AE-*b*-PDMAEMA and pCMV.Luc were evaluated in the HeLa (human epithelial cervical carcinoma) and COS-7 (african green

monkey kidney fibroblast-like) cell lines. Subculturing procedures for these cells are described in *Appendix B - Supporting Information*.

Preparation of polymer-DNA complexes (polyplexes). Polymers were dissolved in Milli-Q water and mixed with 1 μg of pCMV.Luc at the desired polymer/DNA (N/P, +/-) charge ratio. The mixture was further incubated for 15 min at room temperature. Complexes were used immediately after being prepared.

Cell viability assay. Cell viability under the different experimental conditions was assessed, in parallel experiments, by a modified Alamar Blue assay[25]. Forty-seven hours post-transfection, cells were incubated with DMEM containing 10% (v/v) Alamar blue dye, prepared from a 0.1 mg/mL stock solution of Alamar Blue. After 1 hour incubation period at 37 °C, the absorbance of the medium was measured at 570 nm and 600 nm in SPECTRAmax PLUS 384 spectrophotometer (Molecular Devices, USA). Cell viability was calculated, as percentage of the non-transfected control cells, according: (A_{570}-A_{600}) of treated cells $\times$ 100 / (A_{570}-A_{600}) of control cells.

Transfection studies

- For luminescence evaluation of luciferase expression, HeLa (2×10^4 cells/well) or COS-7 (3.5×10^4 cells/well) cells were seeded onto 48-well plates for 24 h prior to incubation with polyplexes. Cells were used at 50-70% confluence and polyplexes containing 1 μg of pCMV.Luc were added to cells previously covered with DMEM-HG (without serum). After 4 h of incubation (in 5% CO_2 at 37 °C), the transfection medium was replaced with DMEM-HG containing 10% (v/v) FBS and antibiotics, and the cells were further incubated for 48 h to allow gene expression. The quantification of luciferase expression in cell lysates was evaluated by measuring light production by luciferase in a Lmax II 384 luminometer (Molecular Devices, USA). Forty-eight hours post-transfection, cells were washed twice with PBS and 100 μL of lysis buffer [1 mM dithiothreitol; 1mM EDTA; 25 mM Tris-phosphate (pH 7.8); 8 mM MgCl$_2$; 15% glycerol; 1% (v/v) Triton^{TM} X-100] was added to each well. The protein content of the lysates was measured by the DC^{TM} Protein Assay reagent using BSA

as a standard. The data were expressed as relative light units (RLU) of luciferase per mg of total cell protein.

- For confocal laser scanning microscopy analysis of intracellular visualization of the polyplexes, pDNA was labeled with the Label IT® Cy5™ labeling kit (Mirus Corp., USA) following to the manufacture's protocols. HeLa cells were seeded at a density of 35,000 cells per well and incubated for 24 h. Polyplexes prepared with Cy5-labeled pDNA at N/P ratio of 25/1 were added to each well. After 4 h, cells were washed with PBS buffer and the nuclear staining was done with the fluorescent dye Hoechst 333258 (1 μg.ml^{-1}) (Invitrogen Life Technologies, UK) for 5 min. The CLSM observation was performed using a Zeiss LSM 510 Meta microscope (Zeiss, Germany) with Plan-Apochromat 63×/1.4 oil DIC objective at excitation wavelengths of 408 nm for Hoechst (blue) and 633 for Cy5 (far red).

3.3.2.10   Physico-chemical characterization of the polyplexes

Ethidium bromide intercalation assay. DNA condensation by PDMAEMA-*b*-P*β*AE-*b*-PDMAEMA polyplexes was analyzed using an ethidium bromide (EtBr) exclusion assay. Polyplexes were prepared and, after 15 minutes, 50 μL of each sample was transferred into a black 96-well plate (Costar, USA). Then, 50 μL of EtBr solution was added to achieve a final EtBr concentration of 400 nM. Following 10 min of incubation, fluorescence was measured in a SpectraMax Gemini EM fluorometer (Molecular Devices, USA) at λ_{exc} = 518 nm and λ_{em} = 605 nm. The fluorescence scale was calibrated such that the initial fluorescence of EtBr (50 μL of EtBr solution were added to 50 μL of Milli-Q water to achieve a final EtBr concentration of 400 nM) was set at residual fluorescence. The value of fluorescence obtained with 1 μg of naked DNA (control) was set as 100%. The amount of DNA available to interact with the probe was calculated by subtracting the values of residual fluorescence from those obtained for the samples and expressed as the percentage of the control.

Agarose gel electrophoresis assay.   To evaluate the complexation of the DNA with the copolymer an electrophoresis in agarose gel was performed. Polyplexes were prepared and, after 15 minutes, 20 μL of each sample was added to 5 μL of loading

buffer (15% (v/v) Ficoll$^®$ 400, 0.05% (w/v) bromophenol blue, 1% (w/v) SDS, 0.1 M EDTA, pH 7.8). 20 μL of each blend were transferred to a 1% agarose gel prepared in TBE solution (89 mM Tris-buffer (pH 8.6), 89 mM boric acid, 2.5 mM EDTA) and containing 1 μg/mL of EtBr. The electrophoresis was set to 40 min at 80 mV. Sample visualization takes place in a GelDoc$^®$ (BioRad$^®$, USA) system using the QuantityOne$^®$ program.

Dynamic light scattering and zeta potential analyses. Dynamic light scattering (DLS) measurements were performed on a Zetasizer Nano-ZS (Malvern Instruments Ltd., UK). The particle size distribution (in intensity), average hydrodynamic particle size average (z-average) and polydispersity index (PDI) were determined with Zetasizer 6.20 software. Measurements were made at 25 °C with a backward scattering angle of 173 °. Zeta-potential measurements were performed using a Zetasizer Nano-ZS (Malvern Instruments Ltd., UK), coupled to laser Doppler electrophoresis and determined using Smoluchovski model. The polyplexes were prepared immediately before analysis and three independent experiments were performed in triplicate for size and zeta potential.

3.3.2.11   Statistical analysis

Data are presented as mean result $\pm$ standard deviation (SD) and analyzed using the IBM$^®$ SPSS$^®$ Statistics software (version 20). Statistical significance of diferences between data was evaluated by one-way ANOVA using Bonferroni or Games-Howell post-hoc tests. A *p*-value < 0.05 was considered as statistically significant.

3.4   Results and discussion

The PDMAEMA-*b*-P*β*AE-*b*-PDMAEMA cationic block copolymer was synthesized via a four-step procedure as presented in Scheme 3.1. Firstly, α,ω-acrylate-P*β*AE was synthesized by a Michael addition reaction between 5-amino-1-propanol and an excess of 1,4-butanediol diacrylate (Scheme 3.1 (a)). Acrylate-terminals were further functionalized with propargylamine through a Michael addition reaction

(Scheme 3.1 (b)) to obtain a *α,ω*-alkyne-P*β*AE homopolymer. PDMAEMA with azide-terminal group was prepared by DMAEMA polymerization throughout ATRP initiated process with N_3EiBBr (Scheme 3.1 (c)). The triblock copolymer, could then be obtained by combination of *α,ω*-alkyne-P*β*AE and *α*-azide-PDMAEMA using copper(I)-catalyzed azide-alkyne cycloaddition[26;27]. In this work, two different block copolymers were prepared: PDMAEMA$_{3000}$-*b*-P*β*AE$_{3000}$-*b*-PDMAEMA$_{3000}$ and PDMAEMA$_{8000}$-*b*-P*β*AE$_{3000}$-*b*-PDMAEMA$_{8000}$.
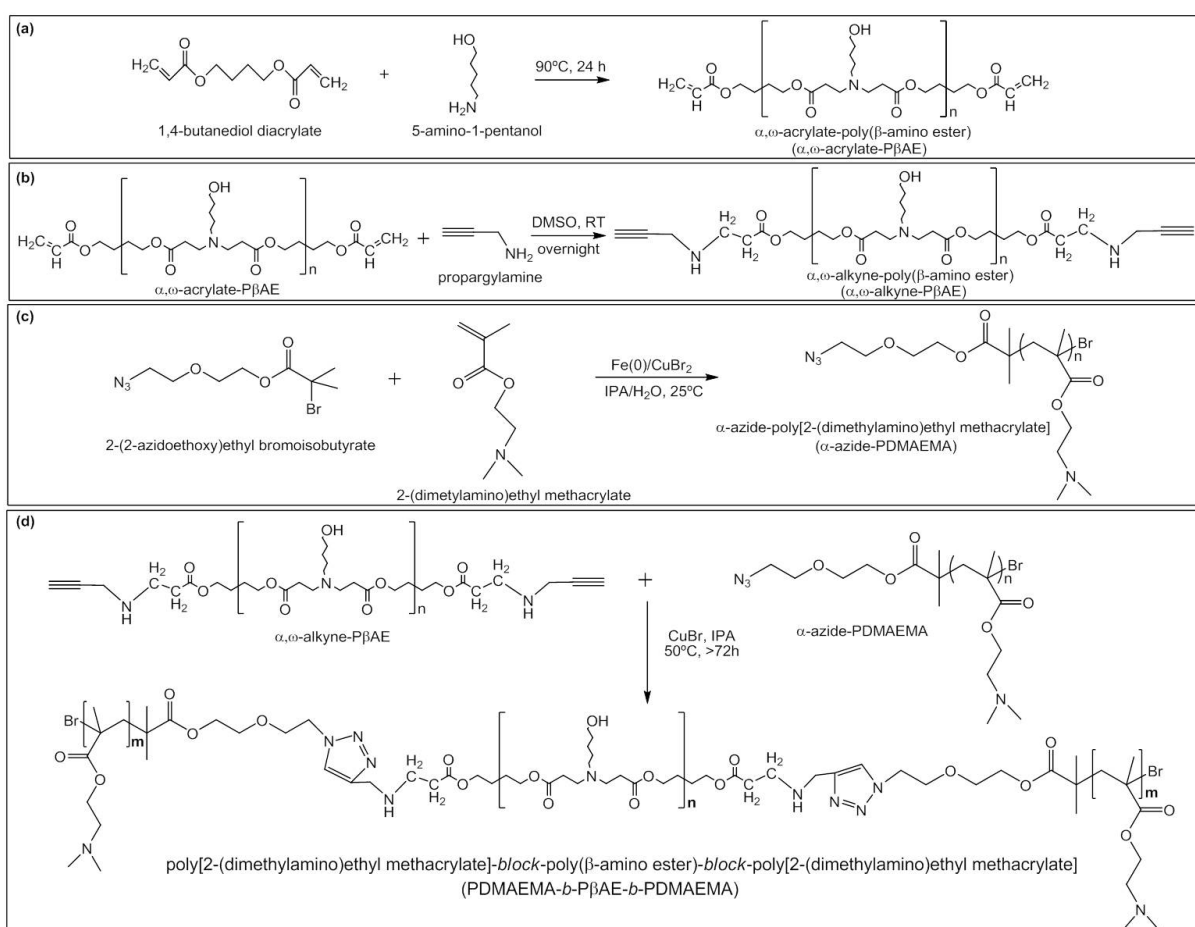
Scheme 3.1: Synthesis of ABA type linear block copolymer via combining Michael addition reaction, ATRP, and Cu-catalyzed click chemistry reactions: (a) Synthesis of *α,ω*-acrylate-P*β*AE by Michael addition reaction; (b) Terminal modification with propargylamine of *α,ω*-acrylate-P*β*AE by Michael addition; (c) Synthesis of PDMAEMA with azide-based initiator through SARA-ATRP method; (d) Cu(I)-catalyzed Huisgen azide-alkyne 1,3-dipolar cycloaddition reaction between *α*-azide-PDMAEMA and *α,ω*-alkyne-P*β*AE.

3.4.1   Synthesis of *α*-azide-PDMAEMA

α-Azide-PDMAEMAs were synthesized by ATRP according to Chapter 2 procedure. A typical chemical structure analysis was assessed by ^{1}H NMR (Figure 3.1) and FTIR-ATR (Figure 3.2) spectra and its molecular weight distribution (Table 3.1) was obtained from the SEC trace.
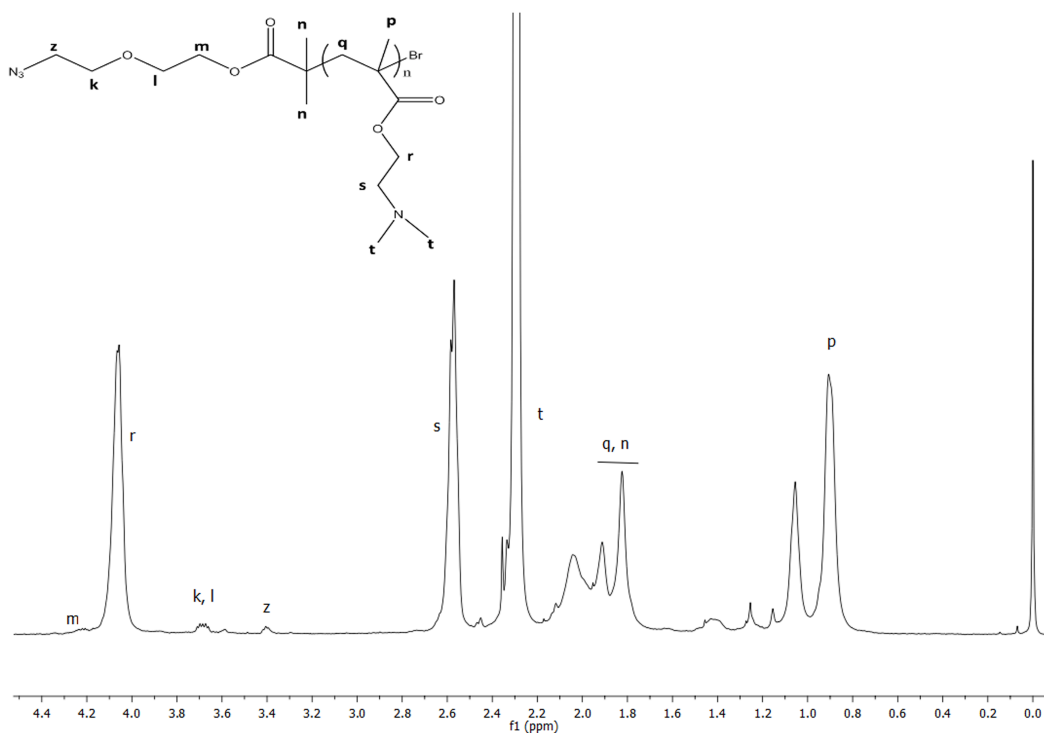
Figure 3.1: ^{1}H NMR spectrum (CDCl$_3$, 400 MHz) of *α*-azide-PDMAEMA.

In Figure 3.1, the signals observed at 4.07 ppm (2H, -OC*H*$_2$CH$_2$N-), 2.58 ppm (2H, -OCH$_2$C*H*$_2$N-), 2.35-2.20 ppm (6H, -N(C*H*$_3$)$_2$), 2.00-1.75 ppm (2H, -CC*H*$_2$C-) and 1.10-0.80 ppm (3H, -CC*H*$_3$Br) are in agreement with the expected PDMAEMA chemical structure[28]. In the FTIR-ATR spectra (Figure 3.2) the absorption peak at 2,083 cm^{-1} is assigned to the azide group of PDMAEMA. Additionally, the terminal methylene protons originally from N$_3$EiBBr initiator at 3.42 ppm in ^{1}H NMR (Figure 3.1) can be used to estimate the number-average molecular weight. On the basis of the integrals ratio of peaks *z* and *s* (Figure 3.1), M$_{n,NMR}$ = 8,298 g.mol^{-1} were calculated, whereas SEC analysis indicated a M$_{n,SEC}$ = 7,973 g.mol^{-1} and Đ = 1.07 (Figure 3.4). These results suggest that a well-controlled structure of *α*-azide-PDMAEMA (N$_3$-PDMAEMA) was successfully achieved.
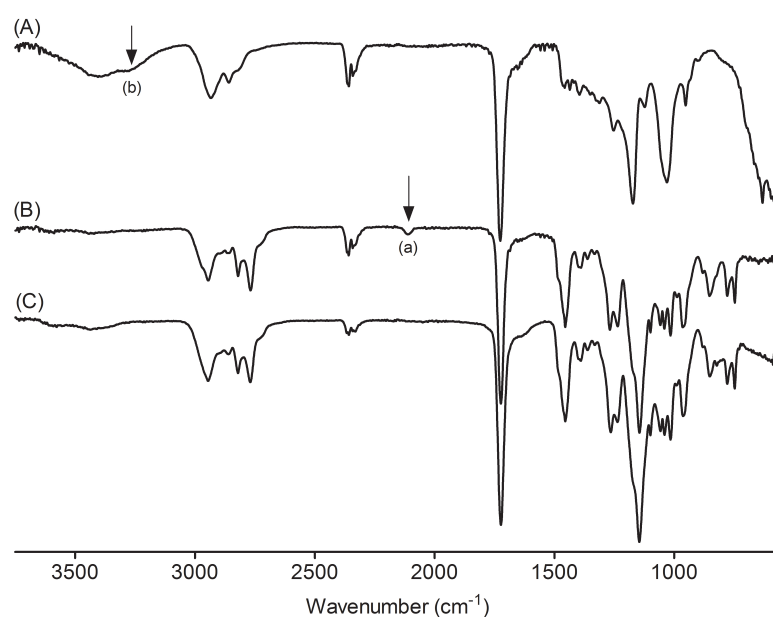
Figure 3.2: FTIR-ATR spectra of α,ω-alkyne-poly(β-amino ester) (A), α-azide-poly[2-(dimethylamino)ethyl methacrylate] (B) and polycationic block copolymer poly[2-(dimethylamino)ethyl methacrylate]-*b*-poly(β-amino ester)-*b*-poly[2-(dimethylamino)ethyl methacrylate] (C). Peak (*a*) at 2083 cm^{-1} is assigned to the azide group of PDMAEMA and peak (*b*) at 3240 cm^{-1} are assigned to the C-H stretch.

3.4.2 Synthesis and post-polymerization functionalization of poly(β-amino ester)

The successful polymerization of acrylate-terminated P*β*AE and its post-polymerization modification to α,ω-alkyne-P*β*AE (Scheme 3.1 (a and b) were confirmed by ^{1}H NMR (Figure B.8, *Appendix B - Supporting Information*), SEC (Table 3.1) and MALDI-TOF MS (Figure 3.3). For the α,ω-acrylate-P*β*AE ^{1}H NMR spectrum (Figure B.8 (A), *Appendix B - Supporting Information*), chemical shifts are in agreement with the expected α,ω-acrylate-P*β*AE chemical structure[29]. The presence of the signals for terminal acrylate groups allows the evaluation of the number-average molecular weight of the polymer. On the basis of the integral ratio of peaks *d* and *j*, M$_{n,NMR}$ was determined as 3,212 g.mol^{-1}. Regarding α,ω-alkyne-P*β*AE, the successful synthesis was confirmed by the disappearance of the signals at 5.81-5.88, 6.06-6.18, and 6.36-6.45 ppm, corresponding to the acrylate protons (Figure B.8 (B), *Appendix B - Supporting Information*). For α,ω-alkyne-P*β*AE, the number-average molecular weight was calculated on the basis of the integral ratio of peaks *d* and *k*, obtaining a value

for $M_{n,NMR}$ = 2,719 g.mol^{-1}. FTIR-ATR spectrum (Figure 3.2) shows an absorption peak at 3,240 cm^{-1} (superimposed to -OH groups absorption), which can be assigned to the C-H stretch. In addition, MALDI-TOF MS spectrum (Figure 3.3) suggests the presence of two alkyne terminal groups. As an example, the highest intensity peak (*m/z* 911.91) corresponds to the two repeating units of the βAE containing the two alkyne terminal unities (2 × *alkyne terminal* + (βAE)$_n$ = 2 × 154.19 + 2 × 301.38 = 911.14).
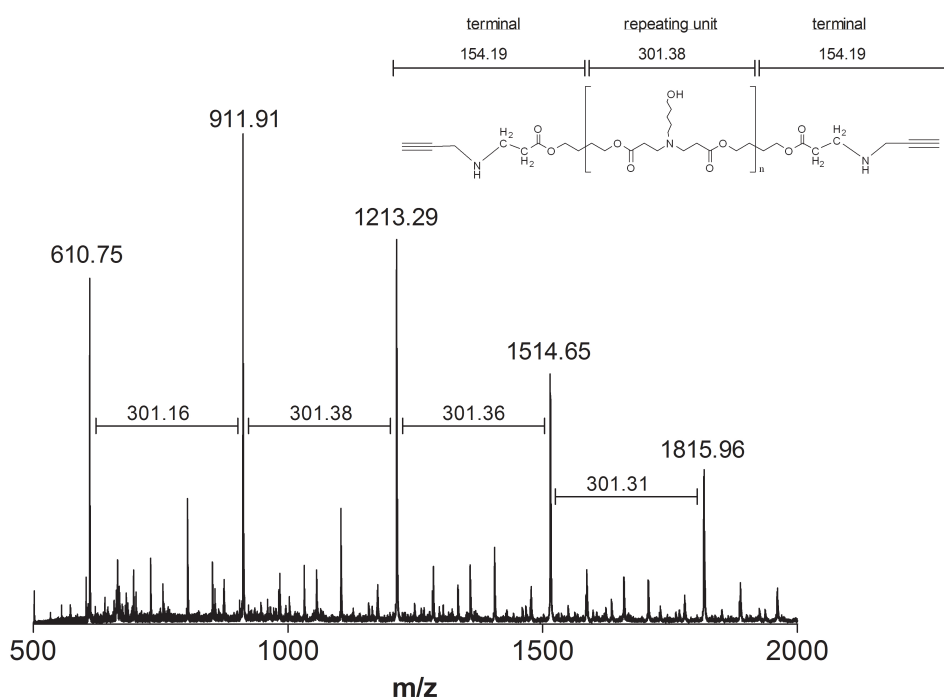
Figure 3.3: Enlargement of the MALDI-TOF MS (using DHB as matrix) from m/z 500 to 2,000 of α,ω-alkyne-PβAE in the linear mode.

3.4.3 Synthesis of PDMAEMA-*b*-PβAE-*b*-PDMAEMA block copolymers

PDMAEMA-*b*-PβAE-*b*-PDMAEMA block copolymers were synthesized in iso-propanol through copper(I)-catalyzed azide-alkyne cycloaddition (CuAAc) click reaction between mono-azide functionalized PDMAEMA and α,ω-alkyne-PβAE. A typical chemical structure of PDMAEMA-*b*-PβAE-*b*-PDMAEMA was confirmed by ^{1}H NMR (Figure 3.4 (b)) and FTIR-ATR (Figure 3.2) analyzes. The ^{1}H NMR spectrum of PDMAEMA$_{8000}$-*b*-PβAE$_{3000}$-*b*-PDMAEMA$_{8000}$ (Figure 3.4 (b)) shows a signal

(**x**) at 7.29 ppm, which can be assigned to the proton of the triazole ring, indicating that the click reaction was well succeeded[30]. In spite of some overlap in the NMR signals and taking into account the profile of SEC chromatograms, the efficiency of the click chemistry reaction seems to be high. The disappearance of the absorption signals at 2,083 (a) and 3,240 (b) cm^{-1} in the FTIR-ATR spectrum (Figure 3.2) of PDMAEMA$_{8000}$-*b*-P*β*AE$_{3000}$-*b*-PDMAEMA$_{8000}$, suggests the reaction of the alkyne groups with the azide groups. In addition, a shift in the SEC traces (Figure 3.4 (a)) was observed towards higher molecular weight, confirming the formation of the triblock copolymer.
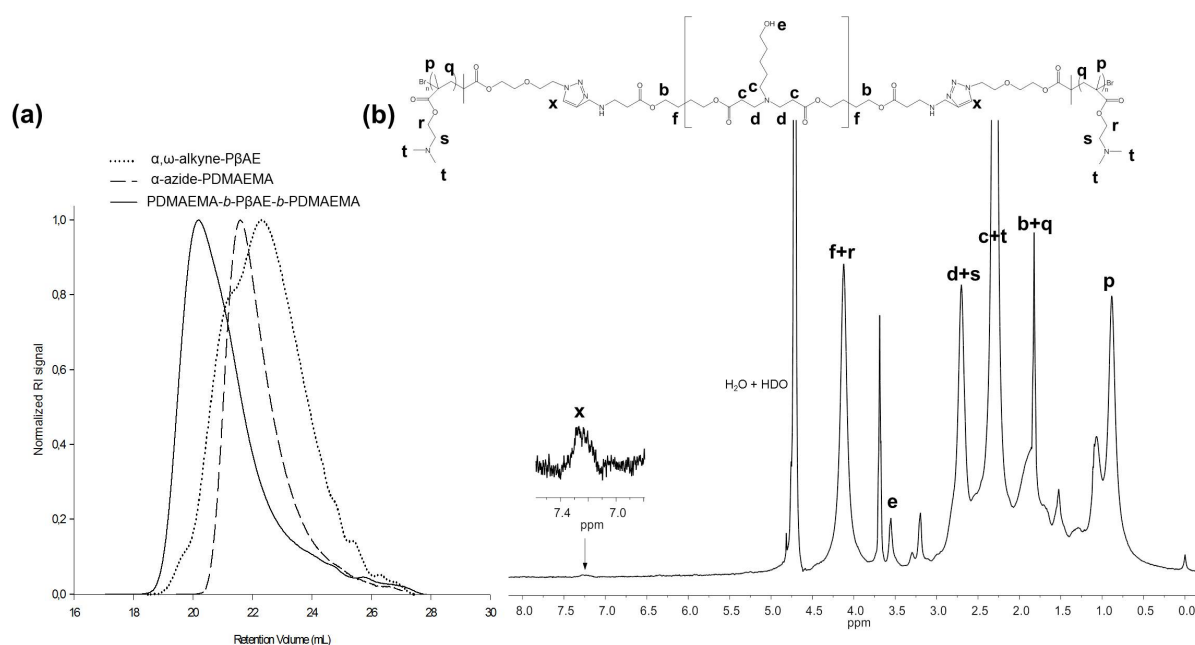
Figure 3.4: SEC refractive index traces overlay (a) and ^{1}H NMR spectrum (D$_2$O, 100 MHz) (b) showing successful click reaction between *α*,*ω*-alkyne-P*β*AE$_{3000}$ and *α*-azide-PDMAEMA$_{8000}$ to give PDMAEMA$_{8000}$-*b*-P*β*AE$_{3000}$-*b*-PDMAEMA$_{8000}$.

In Table 3.1, the molecular weight values obtained from NMR and SEC analyzes of the homopolymers and the triblock copolymers, suggesting the success of the click reaction, since the molecular weight of the copolymer is roughly the sum of the three 'clickable' segments.

During the click chemistry reaction a small amount of copper was used. Therefore, before biological assays, the amount of remaining Cu in PDMAEMA-*b*-P*β*AE-*b*-PDMAEMA after purification was determined by flame atomic absorption spectrometry. The results reveal a very low remaining amount of copper (0.05%).

Table 3.1: Characterization of *α*-azide-PDMAEMA, *α*,*ω*-alkyne-P*β*AE and PDMAEMA-*b*-P*β*AE-*b*-PDMAEMA.

Polymer sample	DP	$M_{n,NMR}$[a]	$M_{n,SEC}$[b]	Đ
α,*ω*-alkyne-P*β*AE$_{3000}$	8	2,700	2,800	3.30
α-azide-PDMAEMA$_{3000}$	21	3,600	3,000	1.28
α-azide-PDMAEMA$_{8000}$	51	8,300	8,000	1.07
PDMAEMA$_{8000}$-*b*-P*β*AE$_{3000}$-*b*-PDMAEMA$_{8000}$	-	18,900	14,900	3.94
PDMAEMA$_{3000}$-*b*-P*β*AE$_{3000}$-*b*-PDMAEMA$_{3000}$	-	8,200	10,000	3.91

[a] Calculated from the integration of *α*-azide-PDMAEMA, *α*,*ω*-alkyne-P*β*AE, and PDMAEMA-*b*-P*β*AE-*b*-PDMAEMA;
[b] Determined by SEC in THF with polystyrene standards.

Thermogravimetric analysis of the PDMAEMA-*b*-P*β*AE-*b*-PDMAEMA was also performed. Figure B.9 (*Appendix B - Supporting Information*) presents the thermoanalytical curves of *α*-azide-PDMAEMA$_{8000}$ and PDMAEMA$_{8000}$-*b*-P*β*AE$_{3000}$-*b*-PDMAEMA$_{8000}$. PDMAEMA shows two distinct degradation stages. The first one up 300 °C corresponds to around 50% of the mass loss, followed by a second stage at 400 °C involving the loss of the remaining mass. These temperatures are in agreement with values available in the literature[31]. The block copolymer PDMAEMA$_{8000}$-*b*-P*β*AE$_{3000}$-*b*-PDMAEMA$_{8000}$ presents a similar degradation profile compared to PDMAEMA$_{8000}$, which suggest that the method used for the synthesis does not jeopardize the thermostability of the final structure. Table B.1 (*Appendix B - Supporting Information*) summarizes the important peak temperatures obtained for the polymers.

3.4.4   Polymer buffering capacity

The release ability of the complexed DNA at intracellular level is a critical parameter for polymers intended to be used for the preparation of gene delivery systems. In this context, endosomal swelling is a non-contact strategy required for endosomal escape[4;32;33]. When internalized by endocytosis, polymers with high buffering capacity prevent acidification of the endosome (by absorbing protons), which leads to passive chloride ions (Cl⁻) influx into the endosome followed by osmotic swelling and eventually rupture of the endosome membrane with consequent cargo release to the cytoplasm. Cationic polymers, which contain secondary and tertiary amino groups, have been shown to have the ability to buffer the endosome, acting as "proton sponge",

and enhancing the release process of materials to cytoplasm[4;32;34]. Thereby, potentiometric titration curves of polymers were carried out in order to evaluate their buffer capacity (Figure 3.5).
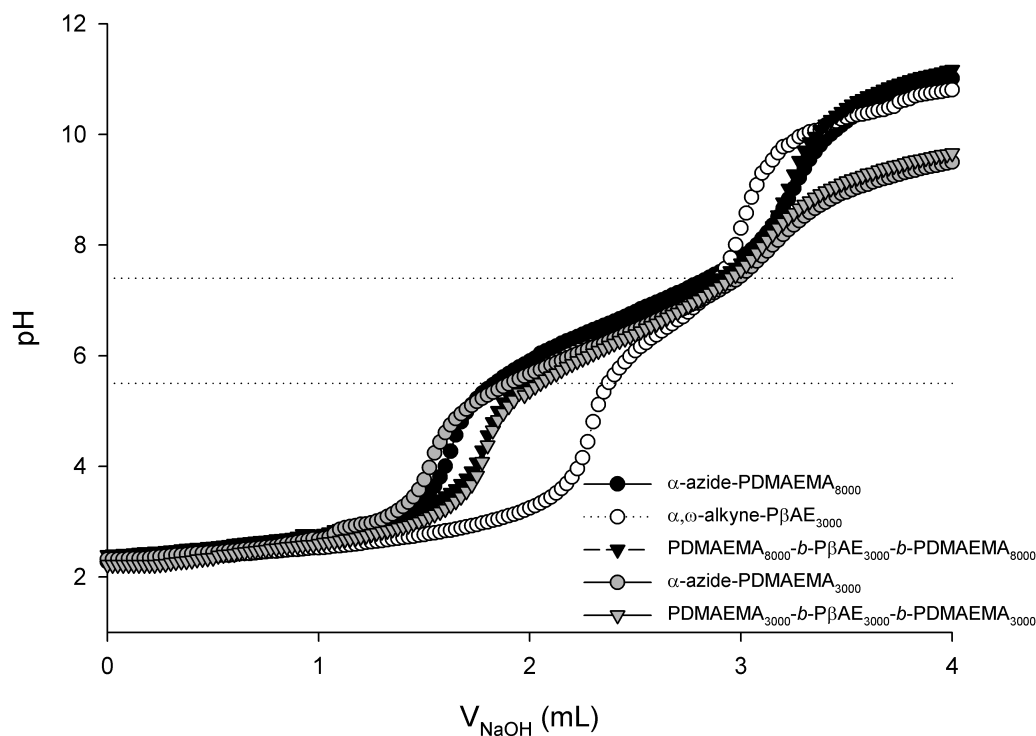
Figure 3.5: Potentiometric titration curves of α-azide-PDMAEMA$_{8000}$ (black circles), α-azide-PDMAEMA$_{3000}$ (grey circles), α,ω-alkyne-PβAE$_{3000}$ (white circles) and block copolymers PDMAEMA$_{8000}$-*b*-PβAE$_{3000}$-*b*-PDMAEMA$_{8000}$ (black triangles) and PDMAEMA$_{3000}$-*b*-PβAE$_{3000}$-*b*-PDMAEMA$_{3000}$ (grey triangles) in Milli-Q water. The *x*-axis label of the plot, V$_{NaOH}$, denotes the total volume of added NaOH. Horizontal lines correspond to pH 5.5 and 7.4 which were used for buffer capacity analysis.

Using the titration curves, for each polymer, the buffering capacity (Table 3.2) was calculated using two different approaches: by taking the ratio of total protons buffered between pH 7.4 and 5.5 to the total amines of the polymer; and by taking the ratio of protons buffered between pH 7.4 and 5.5 to total polymer mass.

From Table 3.2, it can be observed that buffer capacities for all polymer/copolymers are substantially greater than the value reported for PEI (13-26%)[35–37]. Regarding the homopolymers, α,ω-alkyne-PβAE presents the greater buffer capacity, when calculated per amine, and the smaller one, when compared per mass, than α-azide-PDMAEMAs. These results could be explained by the differences in molec-

Table 3.2: Buffer capacities and acid dissociation constant (p*K_a*) values of synthesized block copolymers PDMAEMA-*b*-P*β*AE-*b*-PDMAEMA and the corresponding homopolymers.

Polymer	Buffer capacity		pK_a	$M_{n,NMR}$
	Per amine: protons buffered/ total amines (%)	Per mass: protons buffered/total mass (mmol of H$^+$.g^{-1})		(g.mol^{-1})
α,ω-alkyne-PβAE$_{3000}$	71.37	2.1	6.78	2,700
α-azide-PDMAEMA$_{3000}$	51.17	3.0	6.47	3,600
α-azide-PDMAEMA$_{8000}$	66.71	4.1	6.84	8,300
PDMAEMA$_{3000}$-b-PβAE$_{3000}$-b-PDMAEMA$_{3000}$	65.19	3.8	6.68	8,200
PDMAEMA$_{8000}$-b-PβAE$_{3000}$-b-PDMAEMA$_{8000}$	59.03	3.6	6.85	18,900

ular weight of each repeating unit (both have only one amine group per repeating unit). The repeating unit of the α,ω-alkyne-PβAE has 301.38 g.mol^{-1} of molecular weight while α-azide-PDMAEMA has only 157.21 g.mol^{-1}. Therefore, for the same mass, α,ω-alkyne-PβAE have less amine groups than α-azide-PDMAEMA decreasing the buffer capacity when calculated based on mass of the polymer. This difference become most inconspicuous in block copolymers due to high contribution of PDMAEMA relatively to PβAE in the final structure.

The pK_a value obtained for the block copolymers PDMAEMA-*b*-P*β*AE-*b*-PDMAEMA are in agreement with their cationic nature (with ionizable amine groups). The values between 6.68-6.85 suggest that at a pH below their pK_a (as in endolysosomal pathway), the amine groups will be protonated inducing the endosomal swelling and/or enhancing the interaction with the endosomal/lysosomal membranes, which can be essential to induce membrane rupture and leakage of the transported material to cytoplasm. For pH values higher than its pK_a, the PβAE part becomes hydrophobic (Figure 3.6).
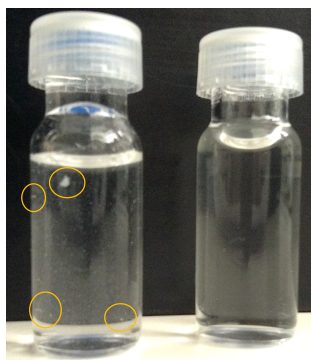
Figure 3.6: Visual solubility at room temperature of α,ω-alkyne-PβAE (left side) and PDMAEMA-*b*-P*β*AE-*b*-PDMAEMA (right side) at the end of the titration (pH ~11). Orange circles highlight insoluble α,ω-alkyne-PβAE.

In the block copolymer, the linkage of the PβAE with an hydrophilic segment like PDMAEMA turns the copolymer stable in water even for high pH values (pH $\gg$ pK$_a$).

3.4.5 Biological activity

The potential of the two developed block copolymers, PDMAEMA$_{3000}$-*b*-PβAE$_{3000}$-*b*-PDMAEMA$_{3000}$ and PDMAEMA$_{8000}$-*b*-PβAE$_{3000}$-*b*-PDMAEMA$_{8000}$, to be used as gene delivery vectors was analyzed. To further evaluate the performance of this new cationic block copolymer as polymeric transfection agents, it was compared with two others commonly used cationic polymers: PEI, considered as a gold standard for polymeric-based gene delivery systems[3;12;38], and TurboFect^{TM}, a recent and promising commercial linear cationic polymeric non-viral vector.

3.4.5.1 Bare polymer and polymer/pDNA complexes toxicity

Since the application of cationic polymers is usually associated with some cytotoxicity[39], preliminary cell viability studies were carried out in different cell lines, using the Alamar Blue assay, to assess the toxicity of the developed block copolymers (Figure 3.7). Cell viability was only significantly reduced for PDMAEMA-*b*-PβAE-*b*-PDMAEMA concentrations higher than 25 μg.mL^{-1}, showing the potential of these novel cationic block copolymers for biomedical applications, since their use in those applications requires a much lower polymer concentration.

Regarding the cytotoxicity of the polymer/pDNA complexes, it was assessed in two different cell types, HeLa and COS-7 cell lines (Figure 3.8). The obtained results, for both cell lines, show that the toxicity of the polyplexes is dependent on their N/P ratio and polymer composition, being observed a higher reduction on cell viability for higher N/P ratios (Figure 3.8). For both block copolymers-based polyplexes no significant cytotoxicity was observed, until 25/1 N/P ratio, for both cell lines. Comparing the results in the two cell lines, it was observed slightly higher viability with COS-7 cells than with HeLa cells, for both block copolymers-based polyplexes.
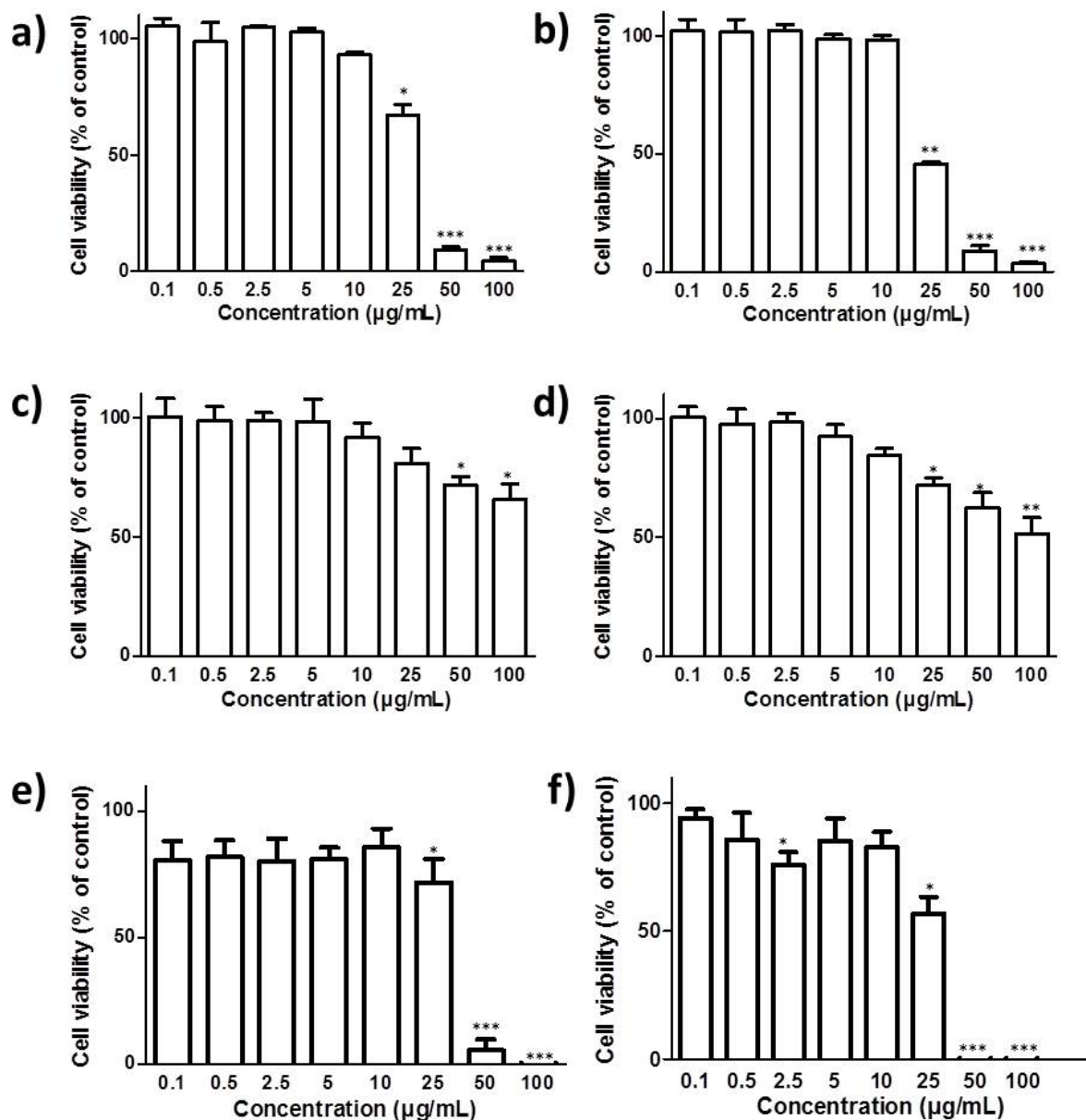
Figure 3.7: Cell viability after 48 hours of incubation with the block copolymer PDMAEMA$_{8000}$-*b*-PβAE$_{3000}$-*b*-PDMAEMA$_{8000}$ in 3T3-L1 (a) and TSA (b) cell lines and PDMAEMA$_{3000}$-*b*-PβAE$_{3000}$-*b*-PDMAEMA$_{3000}$ in 3T3-L1 (c), TSA (d), HeLa (e) and COS-7 (f) cell lines. The data are expressed as percentage of cell viability with respect to the control corresponding to untreated cells (mean $\pm$ SD, obtained from triplicates). Asterisks ($\ast\ast\ast$ p $\leq$ 0.001, $\ast\ast$ p $\leq$ 0.01 and $\ast$ p $\leq$ 0.05) indicate values that differ significantly from those measured in the positive control.
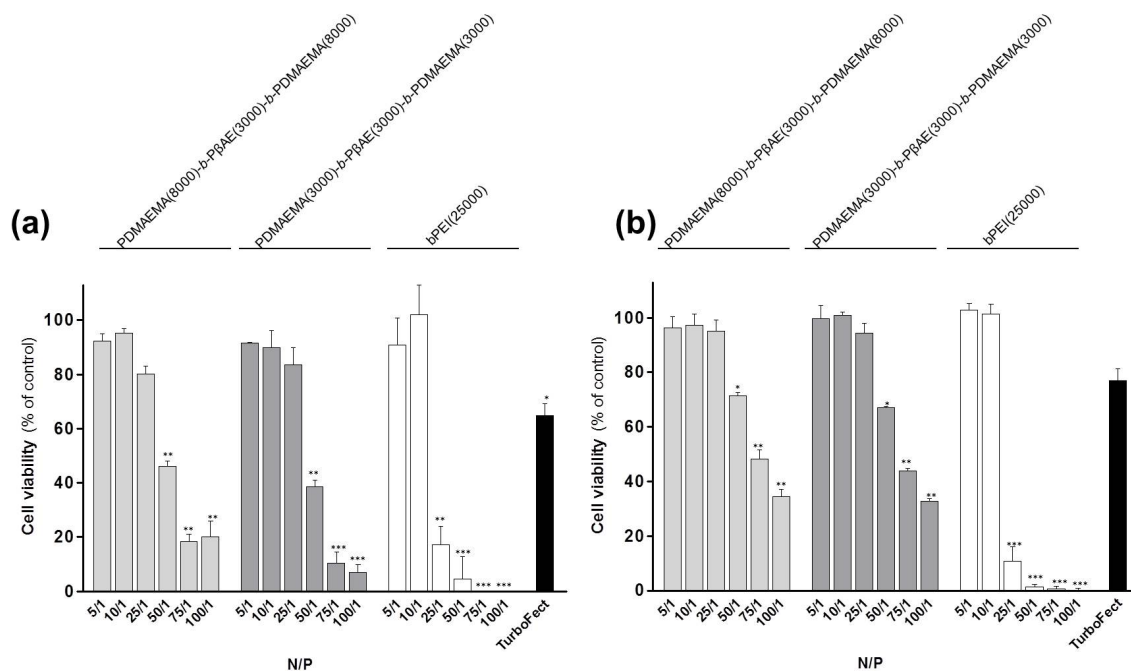
Figure 3.8: Effect of the N/P ratio and composition of polyplexes on their cytotoxicity in HeLa (a) and COS-7 (b) cell lines. The different block copolymers of PDMAEMA-*b*-PβAE-*b*-PDMAEMA and branched PEI were complexed with 1 μg of pCMV.Luc at the indicated polymer/DNA N/P ratios. TurboFect^{TM} was used according to the manufacturer's instructions. The data are expressed as percentage of cell viability with respect to the control corresponding to untreated cells (mean $\pm$ SD, obtained from triplicates). The results are representative of at least three independent experiments. Asterisks ($***$ p $\leq$ 0.001, $**$ p $\leq$ 0.01 and $*$ p $\leq$ 0.05) indicate values that differ significantly from those measured in the positive control.

3.4.5.2   Transfection activity

The new cationic block copolymers were assessed as non-viral vectors for plasmid delivery (Figure 3.9) in HeLa and COS-7 cell lines. The transfection activity was assessed by luciferase assay.

As illustrated in Figure 3.9 PDMAEMA-*b*-PβAE-*b*-PDMAEMA block copolymer-based polyplexes have the ability to successfully deliver the plasmid DNA into HeLa and COS-7 cells. Polyplexes prepared with the block copolymer PDMAEMA$_{3000}$-*b*-PβAE$_{3000}$-*b*-PDMAEMA$_{3000}$ showed much higher transgene (luciferase) expression than that observed with those prepared with PDMAEMA$_{8000}$-*b*-PβAE$_{3000}$-*b*-PDMAEMA$_{8000}$ in both cell lines. This fact is probably due to a more favorable structure of PDMAEMA$_{3000}$-*b*-PβAE$_{3000}$-*b*-PDMAEMA$_{3000}$-based polyplexes both to interact with cells and to deliver genetic material inside them, consequently result-
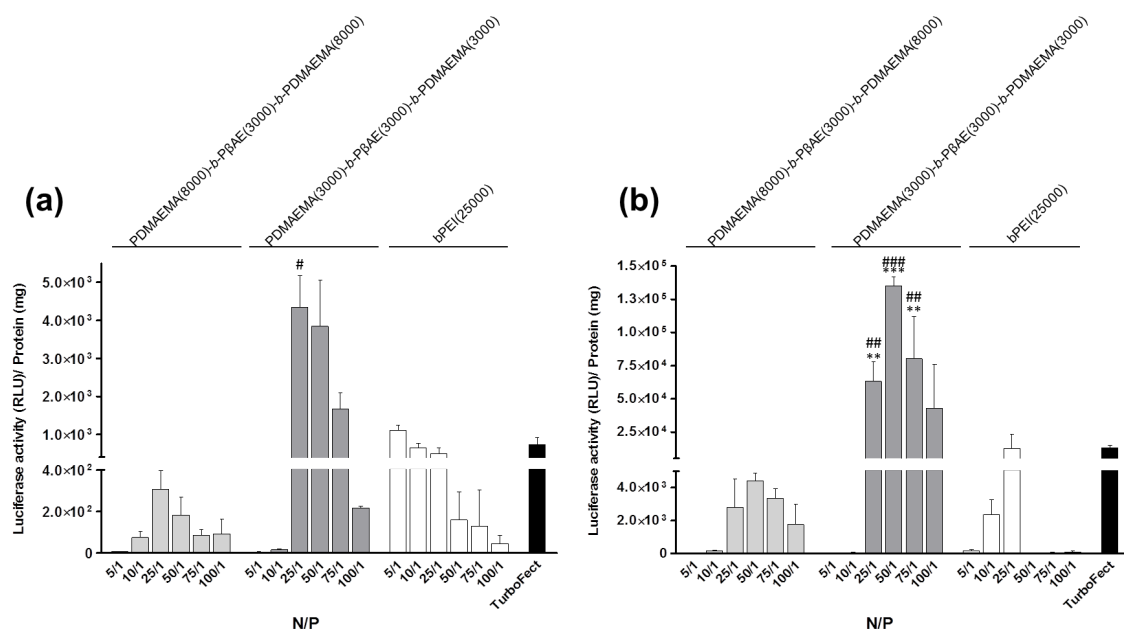
Figure 3.9: Effect of the N/P ratio and composition of polyplexes on their transfection activity in HeLa (a) and COS-7 (b) cell lines. The different block copolymers of PDMAEMA-*b*-PβAE-*b*-PDMAEMA and branched PEI were complexed with 1 μg of pCMV.Luc at the indicated polymer/DNA N/P ratios. TurboFect$^{\text{TM}}$ was used according to the manufacturer's instructions. The data are expressed as RLU of luciferase per mg of total cell protein (mean ± SD, obtained from triplicates). The results are representative of at least three independent experiments. Asterisks (∗∗∗ p ≤ 0.001, ∗∗ p ≤ 0.01) and cardinals (###p ≤ 0.001, ## p ≤ 0.01 and # p ≤ 0.05) indicate values that differ significantly from those measured with polyplexes prepared with bPEI and TurboFect$^{\text{TM}}$, respectively.

ing in a higher biological activity. Therefore, the differences in length of chain of the PDMAEMA revealed to have an important influence on transfection activity. Indeed, it has been reported that polyplexes based on end-modified PβAE with different terminal ends (such as, acrylates or amines) lead to a high variety of responses in terms of gene delivery efficacy [19;29;35].

Figure 3.9 also shows that the transfection activity of the generated polyplexes is dependent on their N/P ratio, being the maximum transgene expression obtained at the 25/1 N/P ratio, for HeLa cells, and at the 50/1 N/P ratio, for COS-7 cells. Accordingly, the increase of the polyplexes N/P ratios, up to these N/P ratios values, resulted in an enhancement of the transfection activity, most probably due to an increased coating/complexation of the pDNA by the polymer, facilitating the binding and uptake of the polyplexes by the cells (Figure 3.10). For N/P ratios higher than 25/1, in HeLa cells, and 50/1, in COS-7 cells, it was observed a luciferase gene

expression decrease that could be due to a stronger interaction between the block copolymer and the pDNA, which could difficult the release of the genetic material from the polyplexes, consequently reducing the transgene expression.
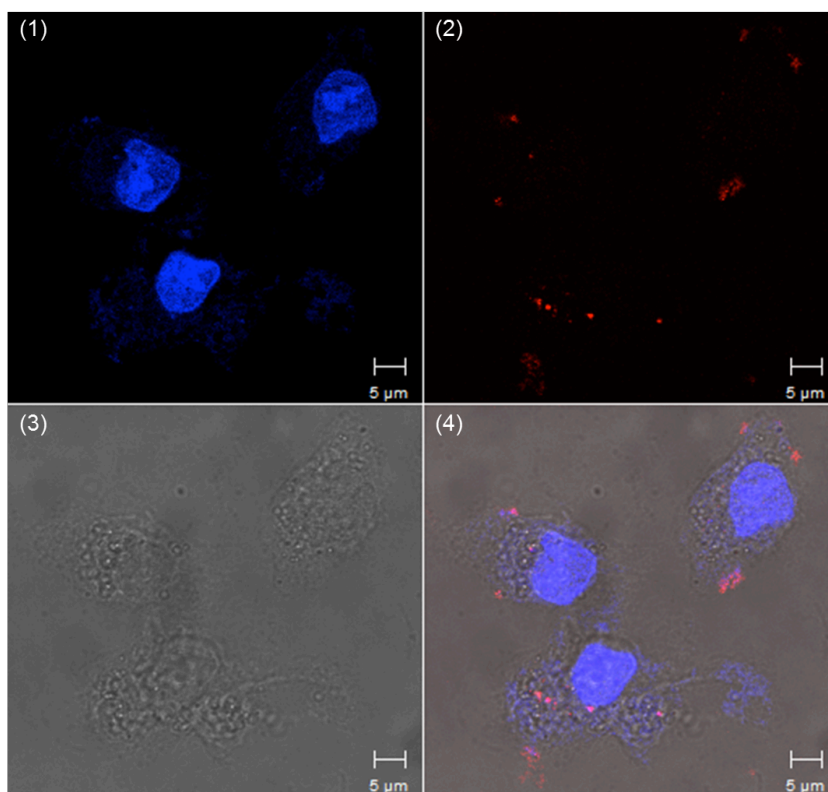
Figure 3.10: Confocal laser scanning microscopic images of HeLa cells transfected with polyplexes prepared with PDMAEMA$_{3000}$-*b*-PβAE$_{3000}$-*b*-PDMAEMA$_{3000}$ at the 25/1 N/P ratio: (a) blue fluorescent image of cell nucleus stained by Hoechst 333258; (b) red fluorescent image of polyplexes prepared with pDNA labeled with Cy5; (c) differential interference contrast (DIC); and (d) overlaying image of (a-c).

These results were compared with those obtained with branched PEI (bPEI) (25,000 g.mol^{-1}), generally accepted as a gold standard non-viral vector presenting high transfection efficiency[3], and TurboFect^{TM}, a novel and promising formulation described as an efficient and non-toxic non-viral vector for *in vitro* delivery of plasmid DNA. As illustrated in Figure 3.9 (a), for HeLa cells, polyplexes prepared at the optimal N/P ratio (25/1) with PDMAEMA$_{3000}$-*b*-PβAE$_{3000}$-*b*-PDMAEMA$_{3000}$ exhibit approximately 4-fold and 6-fold higher transfection activity than that observed with the best formulation of polyplexes generated with bPEI (N/P 5/1) or TurboFect^{TM}, respectively. Concerning the COS-7 cell line, polyplexes prepared at the optimal N/P ratio (50/1) with PDMAEMA$_{3000}$-*b*-PβAE$_{3000}$-*b*-PDMAEMA$_{3000}$ exhibit approx-

imately 11-fold higher transfection activity than that obtained with the best formulation of polyplexes generated with bPEI (25/1 N/P) or TurboFect[TM]. These data suggest that this new block copolymer is more effective as gene delivery system than the current commercial polymeric non-viral vectors, which are considered excellent transfection reagents.

Under the conditions leading to the highest luciferase gene expression (PDMAEMA$_{3000}$-*b*-P*β*AE$_{3000}$-*b*-PDMAEMA$_{3000}$/DNA, for both cell lines), the cell viability was not significantly affected (Figure 3.8). The high transgene expression and the reduced toxicity obtained with this new polyplex formulation, opens the door to a new and efficient non-viral gene delivery system. A very well-known relationship between transfection activity and cytotoxicity, that in the case of polycations is largely caused by the presence of a high charge density at the complex surface, is crucial for the development of effective nucleic acid delivery systems[40;41]. In addition, cell viability and transfection assays were performed in HeLa cells using polyplexes prepared with the P*β*AE and PDMAEMA homopolymers, with molecular weight of 12,000 and 20,000 g.mol^{-1}, respectively (Figure 3.11).
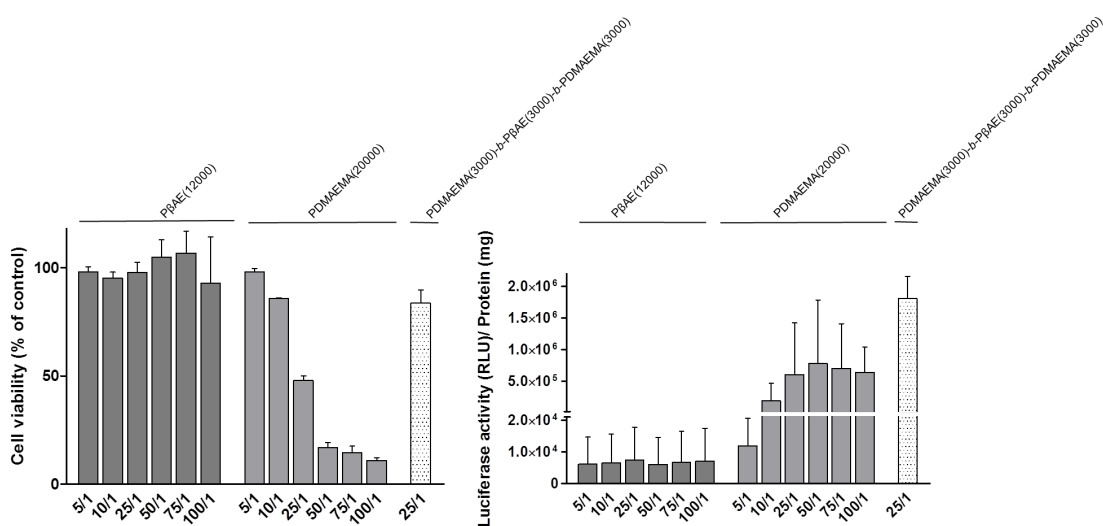
Figure 3.11: Effect of the N/P ratio and composition of PDMAEMA$_{12000}$-, P*β*AE$_{20000}$- and PDMAEMA$_{3000}$-*b*-P*β*AE$_{3000}$-*b*-PDMAEMA$_{3000}$-based polyplexes on their cell viability (a) and transfection activity (b) in HeLa cell line. The different polymers were complexed with 1 μg of pCMV.Luc at the indicated polymer/DNA N/P ratios. The data are expressed as RLU of luciferase per mg of total cell protein (mean $\pm$ SD, obtained from triplicates), for transgene expression, and percentage of cell viability with respect to the control corresponding to untreated cells (mean $\pm$ SD, obtained from triplicates), for cytotoxicity assay. The results are representative of two independent experiments.

The obtained results revealed that these homopolymers-based polyplexes present a low biological activity when compared to PDMAEMA$_{3000}$-*b*-P*β*AE$_{3000}$-*b*-PDMAEMA$_{3000}$-based complexes at the 25/1 N/P ratio. These results suggest that the combination of P*β*AE and PDMAEMA in a single structure produces a new material with improved transfection properties compared to the corresponding homopolymers.

3.4.5.3   Biophysical characterization of PDMAEMA-*b*-P*β*AE-*b*-PDMAEMA-based polyplexes: protection of DNA, size and zeta potential

The physicochemical properties of the carrier systems have an important role on their ability to mediate gene delivery into target cells, namely, the capacity to condense and protect DNA, the size and the surface charge (zeta potential)[4;42].

In order to correlate transfection activity with physicochemical properties, polyplexes based on PDMAEMA$_{3000}$-*b*-P*β*AE$_{3000}$-*b*-PDMAEMA$_{3000}$ were characterized. As a first approach, to determine if the polyplexes were able to condense and protect DNA, the EtBr intercalation and agarose gel electrophoresis assays were used. EtBr is a monovalent DNA-intercalating agent whose fluorescence is dramatically enhanced upon binding to DNA and quenched when displayed by higher affinity compounds or by condensation of the DNA structure. Figure 3.12 illustrates the accessibility of EtBr to DNA carried by PDMAEMA$_{3000}$-*b*-P*β*AE$_{3000}$-*b*-PDMAEMA$_{3000}$-based polyplexes prepared at different N/P ratios.

As observed in Figure 3.12 (b), EtBr fluorescence decreased with increasing the N/P ratio of polyplexes, indicating that an increase in the amount of cationic block copolymer led to a higher degree of DNA condensation and protection. The only significant drop in EtBr access was observed when the N/P ratio of the polyplexes goes from 5/1 to 10/1. The higher EtBr access registered in the 5/1 (N/P) ratio of polyplexes may be explained by the fact that the amount of cationic block copolymer was not enough to create a strong electrostatic interaction with the DNA, allowing the intercalation of the small EtBr molecule due to the weak DNA condensation. For the other N/P ratios of the polyplexes, only 10% of the carried DNA remained accessible to the probe. These results are in accordance with those obtained in the
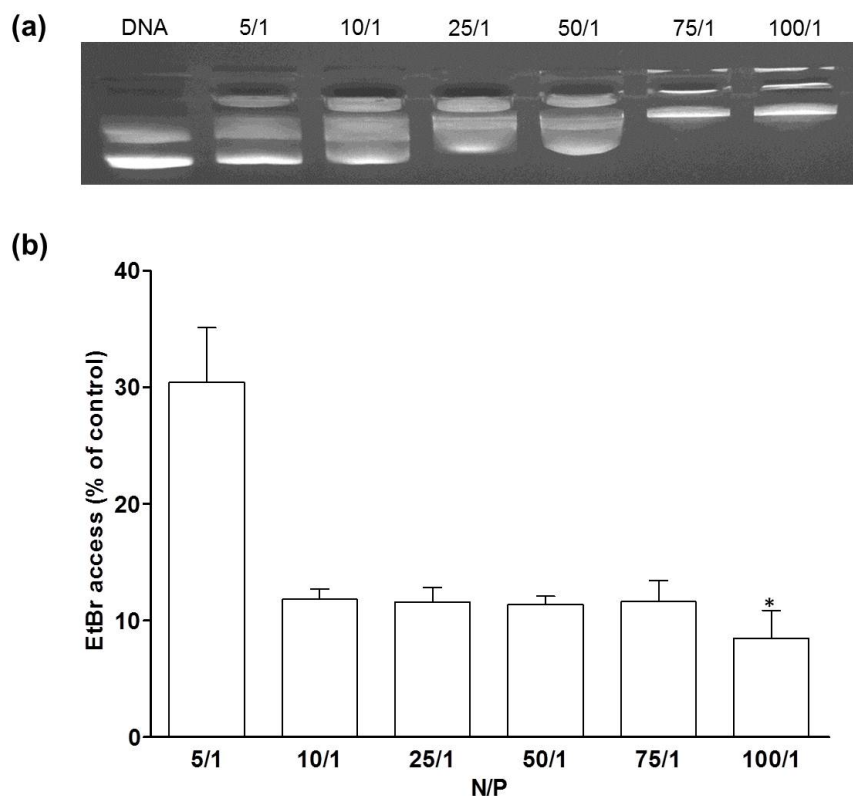
Figure 3.12: Agarose gel electrophoresis (a) and accessibility of ethidium bromide to DNA (b) of the PDMAEMA$_{3000}$-*b*-PβAE$_{3000}$-*b*-PDMAEMA$_{3000}$-based polyplexes prepared at different N/P ratios. The amount of DNA available to interact with the probe was calculated by subtracting the values of residual fluorescence from those obtained for the samples and expressed as the percentage of the control. Control corresponds to free DNA in the same amount as that associated with the complexes (100% of EtBr accessibility). The data are expressed as EtBr access (% of control) and correspond to mean $\pm$ SD of n = 9 (triplicates of three independent experiments). Asterisk ($*$ $p \leq 0.05$) indicates value that differ significantly from those measured (with polyplexes prepared at 5/1 (N/P) ratio) in the positive control.

gel migration assay (Figure 3.12 (a)), where it was observed a lower intensity of the bands and a decrease in their running distance with increasing the N/P ratio of the polyplexes.

Other two major aspects for transfection activity are the size and the zeta potential of the polyplexes, which are dependent on the polymer/DNA ratio. Figure 3.13 depicts the particle size (a) and zeta potential (b) of polyplexes prepared at different N/P ratios.

Polyplexes were formed by simple mixing of the cationic polymer and pDNA in an aqueous solution, which allows the establishment of electrostatic interactions between these two components, generating the polyion pairs. During the
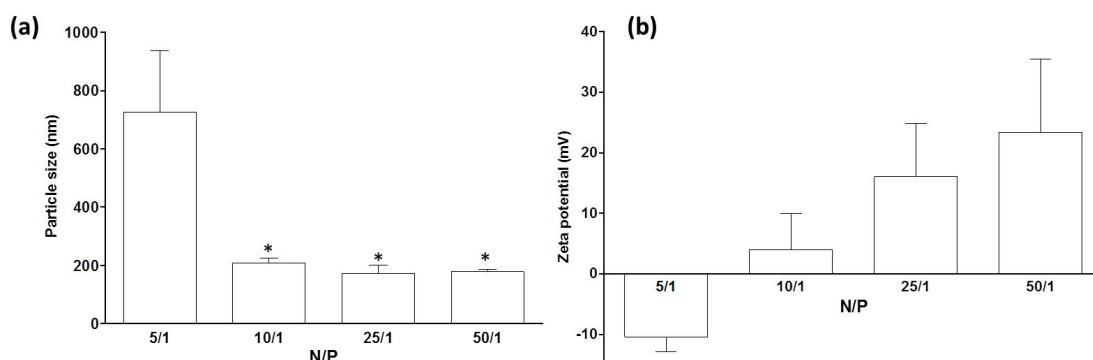
Figure 3.13: Particle size (a) and zeta potential (b) of PDMAEMA$_{3000}$-*b*-P*β*AE$_{3000}$-*b*-PDMAEMA$_{3000}$/DNA polyplexes. The polyplexes were prepared with 1 μg of pCMV.Luc at the indicated polymer/DNA (N/P) ratios. The data are expressed as particle size in nanometers (mean $\pm$ SD, n = 6) and zeta potential in mV (mean $\pm$ SD, n = 6). Two independent experiments were realized in triplicate. Asterisks ($*$ $p \leq 0.05$) indicate values that differ significantly from those measured (with polyplexes prepared at 5/1 (N/P) ratio) in the positive control.

formation process, most probably pDNA undergoes a phase transition from an extended to a globular structure, being condensed by PDMAEMA$_{3000}$-*b*-P*β*AE$_{3000}$-*b*-PDMAEMA$_{3000}$ into nanosized polyplexes (Figure 3.13 (a)). The size sharply decreased when the N/P ratio increased from 5/1 to 10/1. Further increases in the N/P ratio above 10/1 appear to not have influence on the particle size. The higher size ($\sim$725 nm) of polyplexes formed at the 5/1 N/P ratio is most probably due, as described above, to the weak or insufficient electrostatic interactions established between the block copolymer and pDNA, not being able to efficiently constrict/-condense the polyplex. Effective gene delivery into the targeted cells through endocytosis depends on the size of the polyplexes[4;42]. It had been already reported that a size of polyplexes in the order of 200 nm is important for efficient cellular uptake via endocytosis in most cells[43], showing that our best polyplex formulation (PDMAEMA$_{3000}$-*b*-P*β*AE$_{3000}$-*b*-PDMAEMA$_{3000}$/DNA, N/P ratio of 25/1 for HeLa cells and 50/1 for COS-7 cells) presents a mean diameter favorable to a successful gene delivery process.

Figure 3.13 (b) illustrates the zeta potential of polyplexes prepared at different N/P ratios, showing that zeta potential is more positive with the increase of the N/P ratios. In fact, increasing the amount of cationic polymer with respect to a fixed amount of DNA resulted in an increase of the charge of the polyplexes due

to the higher concentration of polymer on their surface. Some authors[3] consider that this high concentration of polymer allows a higher degree of interaction and destabilization of the cellular membrane, thereby facilitating cellular uptake of the polyplexes. Alternatively, this polymer on the nanoparticle surface could destabilize the endosomal membrane resulting in the release of the polyplexes into the cytosol[22].

Correlating these results with those obtained in the transfection activity studies, it can be concluded that for the higher levels of transgene (luciferase) expression, polyplexes have positive surface charge and a particle size around 170 nm, which facilitates their interaction with target cells and their cellular internalization, consequently promoting a high biological activity.

3.5   Conclusion

In the present Chapter, a strategy to prepare a new triblock copolymer composed of poly($β$-amino ester) and poly[2-(dimethylamino)ethyl methacrylate] was reported. The combination of these two types of polycationic blocks made possible to achieve a high buffer capacity associated to a low cytotoxicity profile and favorable physicochemical properties, resulting in an efficient *in vitro* pDNA delivery. Polyplexes prepared using PDMAEMA$_{3000}$-*b*-P$β$AE$_{3000}$-*b*-PDMAEMA$_{3000}$ and pDNA have shown a 4- and 6-fold higher transfection activity in HeLa cells and a 11-fold higher transfection activity in COS-7 cells than the obtained with the best formulation of polyplexes generated with bPEI or TurboFect[TM], respectively. Overall, these results show that PDMAEMA$_{3000}$-*b*-P$β$AE$_{3000}$-*b*-PDMAEMA$_{3000}$ block copolymer presents a great potential as non-viral gene delivery system.

3.6   Acknowledgements

Bibliography

[1] J.H. Jeong, S.W. Kim, and T.G. Park. Molecular design of functional polymers for gene therapy. *Progress in Polymer Science*, 32(11):1239–1274, 2007.

[2] J.F.J. Coelho, P.C. Ferreira, P. Alves, R. Cordeiro, A.C. Fonseca, J.R. Góis, and M.H. Gil. Drug delivery systems: advanced technologies potentially applicable in personalized treatments. *The EPMA Journal*, 1(1):164–209, 2010.

[3] Y. Yue and C. Wu. Progress and perspectives in developing polymeric vectors for *in vitro* gene delivery. *Biomaterials Science*, 1:152–170, 2013.

[4] A. Aied, U. Greiser, A. Pandit, and W. Wang. Polymer gene delivery: overcoming the obstacles. *Drug Discovery Today*, 18:1090–1098, 2013.

[5] Y.Z. You, D.S. Manickam, Q.H. Zhou, and D. Oupicky. Reducible poly(2-dimethylaminoethyl methacrylate): synthesis, cytotoxicity, and gene delivery activity. *Journal of Controlled Release*, 122(3):217–225, 2007.

[6] J.M. Layman, S.M. Ramirez, M.D. Green, and T.E. Long. Influence of polycation molecular weight on poly(2-dimethylaminoethyl methacrylate)-mediated DNA delivery *in vitro*. *Biomacromolecules*, 10(5):1244–1252, 2009.

[7] K.S. Pafiti, C.S. Patrickios, T.K. Georgiou, E.N. Yamasaki, N.P. Mastroyiannopoulos, and L.A. Phylactou. Cationic star polymer siRNA transfectants interconnected with a piperazine-based cationic cross-linker. *European Polymer Journal*, 48(8):1422–1430, 2012.

[8] C. Boyer, J. Teo, P. Phillips, R.B. Erlich, S. Sagnella, G. Sharbeen, T. Dwarte, H.T.T. Duong, D. Goldstein, T.P. Davis, M. Kavallaris, and J. McCarroll. Effective delivery of siRNA into cancer cells and tumors using well-defined biodegradable cationic star polymers. *Molecular Pharmaceutics*, 10(6):2435–2444, 2013.

[9] J.Y. Cherng, P. van de Wetering, H. Talsma, D.J.A. Crommelin, and W.E. Hennink. Effect of size and serum proteins on transfection efficiency of poly((2-dimethylamino)ethyl methacrylate)-plasmid nanoparticles. *Pharmaceutical Research*, 13(7):1038–1042, 1996.

[10] S. Agarwal, Y. Zhang, S. Maji, and A. Greiner. PDMAEMA based gene delivery materials. *Materials Today*, 15(9):388–393, 2012.

[11] A.A. Eltoukhy, D.J. Siegwart, C.A. Alabi, J.S. Rajan, R. Langer, and D.G. Anderson. Effect of molecular weight of amine end-modified poly(*β*-amino ester)s on gene delivery efficiency and toxicity. *Biomaterials*, 33(13):3594–3603, 2012.

[12] Z. Kadlecova, S. Nallet, D.L. Hacker, L. Baldi, H.A. Klok, and F.M. Wurm. Poly(ethyleneimine)-

mediated large-scale transient gene expression: influence of molecular weight, polydispersity and N-propionyl groups. *Macromolecular Bioscience*, 12(5):628–636, 2012.

[13] X. Zhang, J. Xia, and K. Matyjaszewski. Controlled/"living" radical polymerization of 2-(dimethylamino)ethyl methacrylate. *Macromolecules*, 31(15):5167–5169, 1998.

[14] F. Zeng, Y. Shen, S. Zhu, and R. Pelton. Atom transfer radical polymerization of 2-(dimethylamino)ethyl methacrylate in aqueous media. *Journal of Polymer Science Part A: Polymer Chemistry*, 38(20):3821–3827, 2000.

[15] N. Pantoustier, S. Moins, M. Wautier, P. Degée, and P. Dubois. Solvent-free synthesis and purification of poly[2-(dimethylamino)ethyl methacrylate] by atom transfer radical polymerization. *Chemical Communications*, 0:340–341, 2003.

[16] C.M.R. Abreu, A.C. Serra, A.V. Popov, K. Matyjaszewski, T. Guliashvili, and J.F.J. Coelho. Ambient temperature rapid SARA ATRP of acrylates and methacrylates in alcohol-water solutions mediated by a mixed sulfite/Cu(II)Br$_2$ catalytic system. *Polymer Chemistry*, 4:5629–5636, 2013.

[17] G.T. Zugates, S.R. Little, D.G. Anderson, and R. Langer. Poly(*β*-amino ester)s for dna delivery. *Israel Journal of Chemistry*, 45(4):477–485, 2005.

[18] D.M. Lynn and R. Langer. Degradable poly(*β*-amino esters): synthesis, characterization, and self-assembly with plasmid DNA. *Journal of the American Chemical Society*, 122(44):10761–10768, 2000.

[19] J.J. Green, R. Langer, and D.G. Anderson. A combinatorial polymer library approach yields insight into nonviral gene delivery. *Accounts of Chemical Research*, 41(6):749–759, 2008.

[20] H. Devalapally, D. Shenoy, S. Little, R. Langer, and M. Amiji. Poly(ethylene oxide)-modified poly(beta-amino ester) nanoparticles as a pH-sensitive system for tumor-targeted delivery of hydrophobic drugs: part 3. therapeutic efficacy and safety studies in ovarian cancer xenograft model. *Cancer Chemotherapy and Pharmacology*, 59(4):477–484, 2007.

[21] M. Hamidi, M.A. Shahbazi, and K. Rostamizadeh. Copolymers: efficient carriers for intelligent nanoparticulate drug targeting and gene therapy. *Macromolecular Bioscience*, 12(2):144–164, 2012.

[22] M.S. Shim and Y.J. Kwon. Stimuli-responsive polymers and nanomaterials for gene delivery and imaging applications. *Advanced Drug Delivery Reviews*, 64(11):1046–1059, 2012.

[23]

[24] H. Lee, S.H. Son, R. Sharma, and Y.Y. Won. A discussion of the pH-dependent protonation behaviors of poly(2-(dimethylamino)ethyl methacrylate) (PDMAEMA) and poly(ethylenimine-*ran*-2-ethyl-2-oxazoline) (P(EI-*r*-EOz)). *The Journal of Physical Chemistry B*, 115(5):844–860, 2011.

[25] H. Faneca, A. Faustino, and M.C. Pedroso de Lima. Synergistic antitumoral effect of vinblastine and HSV-Tk/GCV gene therapy mediated by albumin-associated cationic liposomes. *Journal of Controlled Release*, 126(2):175–184, 2008.

[26] R. Huisgen. 1.3 - Dipolare cycloadditionen rückschau und ausblick. *Angewandte Chemie*, 75(13):604–637, 1963.

[27] V.V. Rostovtsev, L.G. Green, V.V. Fokin, and K.B. Sharpless. A stepwise Huisgen cycloaddition

process: copper(I)-catalyzed regioselective "ligation" of azides and terminal alkynes. *Angewandte Chemie*, 114(14):2708–2711, 2002.

[28] L. Mespouille, P. Degee, and P. Dubois. Amphiphilic poly(N,N-dimethylamino-2-ethyl methacryl ate)-*g*-poly(epsilon-caprolactone) graft copolymers: synthesis and characterisation. *European Polymer Journal*, 41(6):1187–1195, 2005.

[29] J.C. Sunshine, M.I. Akanda, D. Li, K.L. Kozielski, and J.J. Green. Effects of base polymer hydrophobicity and end-group modification on polymeric gene delivery. *Biomacromolecules*, 12(10):3592–3600, 2011.

[30] S. Sinnwell, A.J. Inglis, M.H. Stenzel, and C. Barner-Kowollik. Access to three-arm star block copolymers by a consecutive combination of the copper(i)-catalyzed azide-alkyne cycloaddition and the RAFT hetero Diels-Alder concept. *Macromolecular Rapid Communications*, 29(12-13):1090–1096, 2008.

[31] M.T. Hunley, J.P. England, and T.E. Long. Influence of counteranion on the thermal and solution behavior of poly(2-(dimethylamino)ethyl methacrylate)-based polyelectrolytes. *Macromolecules*, 43(23):9998–10005, 2010.

[32] D. Lechardeur, A.S. Verkman, and G.L. Lukacs. Intracellular routing of plasmid DNA during non-viral gene transfer. *Advanced Drug Delivery Reviews*, 57(5):755–767, 2005.

[33] N.D. Sonawane, F.C. Szoka, and A.S. Verkman. Chloride accumulation and swelling in endo-somes enhances DNA transfer by polyamine-DNA polyplexes. *Journal of Biological Chemistry*, 278(45):44826–44831, 2003.

[34] A. Daka and D. Peer. RNAi-based nanomedicines for targeted personalized therapy. *Advanced Drug Delivery Reviews*, 64(13):1508–1521, 2012.

[35] J.C. Sunshine, D.Y. Peng, and J.J. Green. Uptake and transfection with polymeric nanoparticles are dependent on polymer end-group structure, but largely independent of nanoparticle physical and chemical properties. *Molecular Pharmaceutics*, 9(11):3375–3383, 2012.

[36] Z. Liu, M. Zheng, F. Meng, and Z. Zhong. Non-viral gene transfection *in vitro* using endosomal pH-sensitive reversibly hydrophobilized polyethylenimine. *Biomaterials*, 32(34):9109–9119, 2011.

[37] D. Zhao, T. Gong, D. Zhu, Z. Zhang, and X. Sun. Comprehensive comparison of two new biodegradable gene carriers. *International Journal of Pharmaceutics*, 413:260 – 270, 2011.

[38] U. Lungwitz, M. Breunig, T. Blunk, and A. Göpferich. Polyethylenimine-based non-viral gene delivery systems. *European Journal of Pharmaceutics and Biopharmaceutics*, 60(2):247–266, 2005.

[39] H. Lv, S. Zhang, B. Wang, S. Cui, and J. Yan. Toxicity of cationic lipids and cationic polymers in gene delivery. *Journal of Controlled Release*, 114(1):100–109, 2006.

[40] C. Alexander. Temperature- and pH-responsive smart polymers for gene delivery. *Expert Opinion on Drug Delivery*, 3(5):573–581, 2006.

[41] A. Pathak, S. Patnaik, and K.C. Gupta. Recent trends in non-viral vector-mediated gene delivery. *Biotechnology Journal*, 4(11):1559–1572, 2009.

[42] C. Scholz and E. Wagner. Therapeutic plasmid DNA *versus* siRNA delivery: Common and

different tasks for synthetic carriers. *Journal of Controlled Release*, 161(2):554–565, 2012.

[43] A. El-Sayed and H. Harashima. Endocytosis of gene delivery vectors: from clathrin-dependent to lipid raft-mediated endocytosis. *Molecular Therapy*, 21(6):1118–1130, 2013.

[44] L. Mespouille, M. Vachaudez, F. Suriano, P. Gerbaux, W. Van Camp, O. Coulembier, P. Degée, R. Flammang, F. Du Prez, and P. Dubois. Controlled synthesis of amphiphilic block copolymers based on polyester and poly(amino methacrylate): comprehensive study of reaction mechanisms. *Reactive and Functional Polymers*, 68(5):990–1003, 2008.

CHAPTER 4

Improvement of transfection efficiency of PDMAEMA-*b*-P*β*AE-*b*-PDMAEMA non-viral vector

4.1   Abstract

Polymeric-based non-viral vectors have been considered a promising strategy in gene therapy area. Previously, in Chapter 3, it was reported the use of a new cationic block copolymer based on PDMAEMA and P*β*AE that revealed high transfection efficiency. During these studies, however, it was also observed that the new block copolymer induced significant levels of cytotoxicity for high polymer/DNA ratios. In this chapter, it is designed a novel synthetic procedure to prepare the poly[2-(dimethylamino)ethyl methacrylate]-*block*-poly(*β*-amino ester)-*block*-poly[2-(dimethylamino)ethyl methacrylate] (PDMAEMA-*b*-P*β*AE-*b*-PDMAEMA) block copolymer without use of metal catalyst to link the different segments. In addition, to better understand the influence of the P*β*AE block length of PDMAEMA-*b*-P*β*AE-*b*-PDMAEMA block copolymer in transfection activity, three different block copolymers were prepared varying the molecular weigth of this segment. Among those, the top polyplexes formulation revealed between 40- and 60-fold higher transgene expression in HeLa and COS-7 cell lines than commonly used polymeric non-viral vectors standards, branched PEI and TurboFect[TM]. The new procedure of synthesis allowed to reach a very low degree of cytotoxicity even for high polymer/DNA charge ratios. These data show that the cytotoxicity previously reported in Chapter 3 could results from the remaining copper catalyst of the click chemistry reaction. The results reported in this chapter confirm the enormous potential of this block copolymer as gene carrier.

4.2   Introduction

Gene delivery arose as a promising strategy to treat inherited and acquired diseases involving genetic factors[1–3]. While most drug-based approaches only treat the symptoms, the gene therapy aims to treat or to eliminate the causes of disease[4]. In this sense, cationic polymers have attracted increasing attention in the past two decades[5;6]. The positive charges of these polymers interact electrostatically with the negative charges of nucleic acids forming structures known as polyplexes. This conformation should protects genetic material from nucleolytic enzymes and, at the

same time, should allows an efficient unpacking and consequent delivery of the genetic material into the target cells[7]. The main advantage of the use of polymeric-based materials for gene delivery is the relative ease fine tuning of physicochemical properties through, for example, controlling their molecular weight or architecture, or by varying their chemical composition[8]. Some examples of the most used cationic polymers as gene carriers are polyethylenimine (PEI), poly(L-lysine), poly[2-(dimethylamino)ethyl methacrylate] (PDMAEMA), chitosan and, more recently, poly(*β*-amino ester) (P*β*AE)[9–11]. Particularly, PDMAEMA and P*β*AE have been widely studied for this purpose[12;13]. In spite of many efforts to develop new polymeric-based non-viral vectors, low gene transfection efficiency and cytotoxicity concerns remains the main weaknesses to overcome to be used at clinical stage[14]. In Chapter 3, PDMAEMA-*b*-P*β*AE-*b*-PDMAEMA block copolymers were prepared by a copper-catalyzed alkyne-azide cycloaddition (CuAAC) reaction and the effect of PDMAEMA segment in transfection activity was studied. The combination between P*β*AE and PDMAEMA revealed a good conjugation in terms of gene transfection activity. However, it was observed that polyplexes induced considerable cytotoxicity for N/P ratios above 25/1. It was envisaged that this observation might be due to the remaining copper catalyst from CuCAAC reaction. In fact, as ester bond of P*β*AE is easily degraded in water environment, purification process of the block copolymer is more difficult. The weak solubility of copper in organic solvents with low boiling point for an easy removal at the end the reactions was another critical point in purification process of the block copolymer prepared by CuAAc reaction (Chapter 3). In order to eliminate the potential copper contamination, this work proposes a new method to prepare PDMAEMA-*b*-P*β*AE-*b*-PDMAEMA free of metal catalysts. In addition, PDMAEMA-*b*-P*β*AE-*b*-PDMAEMA cationic block copolymers prepared with different molecular weight P*β*AE segments were assessed as nucleic acid delivery systems in HeLa and COS-7 cell lines and compared with branched PEI (25,000 g.mol^{-1}) and TurboFect^{TM}, as previously done in Chapter 3, to demonstrate their suitability for gene delivery.

4.3   Experimental

4.3.1   Materials

5-amino-1-pentanol (Alfa Aesar, 97%), 1,4-butanediol diacrylate (Alfa Aesar, 99+%), propargylamine (Sigma-Aldrich), copper (II) bromide ($CuBr_2$) (Acros, +99% extra pure, anhydrous), PS standards (Polymer Laboratories), (Acros, 99%, ~70 mesh), PMDETA (Aldrich, 99%), iron powder (Fe(0)), 2-propanol (Fisher Chemical), diethyl ether (Fisher Scientific), DMSO (Acros Organics, 99.8+%, extra pure), deuterated chloroform ($CDCl_3$) (Euriso-top, +1%TMS) and deuterium oxide (D_2O) (Euroiso-top, 99.9%+D), Dulbecco's Modified Eagle's Medium - high glucose (DMEM-HG) (Sigma-Aldrich), resazurin sodium salt (Sigma-Aldrich), DL-dithiothreitol (Sigma), tris-phosphate (Sigma), ethylenediaminetetraacetic acid (EDTA) (Sigma-Aldrich), magnesium chloride ($MgCl_2$) (Sigma), glycerol (Sigma), Triton^{TM} X-100 (Sigma), bovine serum albumin (BSA) (Sigma), D-luciferin sodium salt (Synchem, 99%), DC^{TM} Protein Assay (Bio-Rad), plasmids encoding luciferase (pCMV.Luc) and green fluorescent protein (pCMV.gfp) DNA (Vical), TurboFect^{TM} (kindly offered by Thermo Scientific), polyethylenimine (PEI) (branched, M_w 25,000 g.mol^{-1}) (Sigma) were used as received. DMAEMA (Aldrich, 98%) was passed over a sand/alumina column before use in order to remove the radical inhibitor. Milli-Q water (Milli-Q$^{®}$, Millipore, resistivity >18 MΩ cm) was obtained by reverse osmosis. High-performance liquid chromatography (HPLC) tetrahydrofuran (THF) (Panreac, HPLC grade) was filtered under reduced pressure before use. Dichloromethane (DCM) (Fisher Scientific, +99.6%) was dried and distilled over calcium hydride. Triethylamine (TEA) (Sigma-Aldrich, 96%) was distilled and stored over molecular sieves. 4-Dimethylaminopyridine (DMAP) (Sigma-Aldrich. +99%) was recrystallized from toluene. 2-(2-Azidoethoxy)ethyl bromoisobutyrate (N$_3$EiBBr) was prepared according to the procedure described in *Appendix B - Supporting Information*.

4.3.2   Methods

4.3.2.1   Synthesis of poly[2-(dimethylamino)ethyl methacrylate]-*block*-poly(*β*-amino ester)-*block*-poly[2-(dimethylamino)ethyl methacrylate]

Synthesis of α,ω-acrylate-poly(β-amino ester) through Michael addition reaction.   α,ω-acrylate-poly(*β*-amino ester) was prepared according to a previously reported procedure in Chapter 3.   Briefly, 5-amino-1-pentanol (1.5 g, 14.54 mmol) was weighed into an opaque vial and 1,4-butanediol diacrylate (3.20 mL, 17.45 mmol) was added.   A Teflon-coated stir-bar was added, the vial was sealed with a Teflon-lined screw-cap, and the reaction was placed in a pre-heated oil bath at 90 °C with stirring.   After 24 h, the reaction was cooled down to room temperature, precipitated and washed 3 times with cold diethyl ether.   Polymer was dried overnight at 40 °C under vacuum. Polymer was stored at -20 °C until use.

Typical procedure for the synthesis of α-azide-poly[2-(dimethylamino)ethyl methacrylate] by atom transfer radical polymerization (DP = 45) - $[Fe(0)]_0/[CuBr_2]_0/[PMDETA]_0 = 1/0.1/1.1$. α-azide-poly[2-(dimethylamino)ethyl methacrylate] (α-N_3-PDMAEMA) was pre-pared according to a previously reported procedure in Chapter 2.   The synthesis of 2-(2-azidoethoxy)ethyl bromoisobutyrate (N_3EiBBr) is described in *Appendix B - Supporting Information*. A mixture of DMAEMA (6.0 mL, 35.61 mmol), Fe(0) (44.2 mg, 0.79 mmol) and $CuBr_2$ (17.7 mg, 0.079 mmol) was placed in a Schlenk tube reactor. The sample was first stirred and then frozen in liquid nitrogen.   Subsequently, a mixture of N_3EiBBr (221.7 mg, 0.79 mmol), PMDETA (150.8 mg, 0.87 mmol) and isopropanol/water mixture (9/1, v/v) (6 mL) (previously bubbled with nitrogen for about 15 minutes) was added, under nitrogen atmosphere, to the reactor.   The Schlenk tube reactor containing the reaction mixture was deoxygenated with three freeze-vacuum-thaw cycles and purged with nitrogen. The Schlenk tube reactor was placed in a pre-heated bath at 25 °C with stirring (700 rpm) for 2 hours.   Afterwards, the sample was precipitated in cold hexane, dialyzed against distilled water (dialysis membrane, molecular weight cut off (MWCO) = 1,000 $g.mol^{-1}$) and then freeze dried.

Synthesis of α-amine-poly[2-(dimethylamino)ethyl methacrylate]. 4 g (1.25 mmol) of α-azide-poly[2-(dimethylamino)ethyl methacrylate] (α-N$_3$-PDMAEMA) ($M_{n,NMR}$ = 3,200 g.mol^{-1}), and 655.73 mg (2.5 mmol) of triphenylphosphine were dissolved in 20 mL of THF under N$_2$ at room temperature overnight. Then, 10 mL of deionized water was added to proceed for another 12 h. After removal of THF in a rotary evaporator, the mixture was centrifuged to remove the precipitate. The solution was dialyzed against deionized water with dialysis membrane (MWCO = 1,000 g.mol^{-1}) and then freeze dried.

Typical procedure for the preparation of tri-block copolymer poly[2-(dimethylamino)ethyl methacrylate]-block-poly(β-amino ester)-block-poly[2-(dimethylamino)ethyl methacrylate] (PDMAEMA-b-PβAE-b-PDMAEMA) by Michael addition reaction. α,ω-acrylate-P*β*AE ($M_{n,NMR}$ = 12,000 g.mol^{-1}, 85 mg, 0.007 mmol) and α-amine-PDMAEMA ($M_{n,NMR}$ = 3,200 g.mol^{-1}, 45.33 mg, 0.014 mmol) were dissolved in a solvent mixture of 1/1 (v/v) DMSO/THF and placed in a vial with a Teflon-lined screw-cap. The reaction was performed at room temperature during 48 h. The resulting solution was precipitated and washed 3 times into cold ethyl ether and then dialyzed against dry THF (dialysis membrane MWCO = 3,500 g.mol^{-1}) during 24 hours. Block copolymer was dried overnight at 40 °C under vacuum. Polymer was stored at -20 °C until use.

4.3.2.2   Size exclusion chromatography

The chromatographic parameters of the samples were determined using high performance size exclusion chromatography HPSEC; Viscotek (Viscotek TDAmax) with a differential viscometer (DV); right-angle laser-light scattering (RALLS, Viscotek); low-angle laser-light scattering (LALLS, Viscotek) and refractive index (RI) detectors. The column set consisted of a PLgel 10 μm guard column (7.5 × 50 mm) followed by one Viscotek T200 column (6 μm), one MIXED-E PLgel column (3 μm) and one MIXED-C PLgel column (5 μm). HPLC dual piston pump was set with a flow rate of 1 mL.min^{-1}. The eluent (THF) was previously filtered through a 0.2 μm filter. The system was also equipped with an on-line degasser. The tests were done at 30 °C using an Elder CH-150 heater. Before the injection (100 μL), the samples were

filtered through a polytetrafluoroethylene (PTFE) membrane with 0.2 μm pore. The system was calibrated with narrow PS standards. The number-average molecular weight ($M_{n,SEC}$) and dispersity index ($Đ$) of synthesized polymers were determined by multidetectors calibration using OmniSEC software version 4.6.1.354.

4.3.2.3   Nuclear magnetic resonance spectroscopy

400 MHz ^{1}H NMR spectra of reaction mixture samples were recorded on a Bruker Avance III 400 MHz spectrometer, with a 5-mm TXI triple resonance detection probe, in CDCl$_3$ or D$_2$O with tetramethylsilane (TMS) as an internal standard. Conversion of monomers was determined by integration of monomer and polymer peaks using MestReNova software version 6.0.2-5475.

4.3.2.4   Fourier transform infrared spectroscopy

Fourier-transform infrared attenuated total reflection (FTIR-ATR) spectra were acquired in the range of 500-4000 cm^{-1}, using a JASCO 4200 FTIR spectrophotometer (Jasco, Japan) equipped with a single horizontal Golden Gate ATR cell, at 128 scans and with a 4 cm^{-1} resolution.

4.3.2.5   Biological activity

The biological activity and cytotoxicity of the complexes prepared with the cationic block copolymers PDMAEMA-*b*-PβAE-*b*-PDMAEMA and pCMV.Luc were evaluated in the HeLa (human epithelial cervical carcinoma) and COS-7 (african green monkey kidney fibroblast-like) cell lines. Subculturing procedures for these cells are described in *Appendix B - Supporting Information*.

Preparation of polymer-DNA complexes (polyplexes). Polymers were dissolved in Milli-Q water and mixed with 1 μg of pCMV.Luc at the desired polymer/DNA (N/P, +/-) charge ratio. The mixture was further incubated for 15 min at room temperature. Complexes were used immediately after being prepared.

Cell viability assay. Cell viability under the different experimental conditions was assessed, in parallel experiments, by a modified Alamar Blue assay[16]. Forty-seven

hours post-transfection, cells were incubated with DMEM containing 10% (v/v) Alamar blue dye, prepared from a 0.1 mg/mL stock solution of Alamar Blue. After 1 hour incubation period at 37 °C, the absorbance of the medium was measured at 570 nm and 600 nm in SPECTRAmax PLUS 384 spectrophotometer (Molecular Devices, USA). Cell viability was calculated, as percentage of the non-transfected control cells, according: (A_{570}-A_{600}) of treated cells $\times$ 100 / (A_{570}-A_{600}) of control cells.

Transfection studies

- For luminescence evaluation of luciferase expression, HeLa (2×10^4 cells/well) or COS-7 (3.5×10^4 cells/well) cells were seeded onto 48-well plates for 24 h prior to incubation with polyplexes. Cells were used at 50-70% confluence and polyplexes containing 1 μg of pCMV.Luc were added to cells previously covered with DMEM-HG (without serum). After 4 h of incubation (in 5% CO_2 at 37 °C), the transfection medium was replaced with DMEM-HG containing 10% (v/v) FBS and antibiotics, and the cells were further incubated for 48 h to allow gene expression. The quantification of luciferase expression in cell lysates was evaluated by measuring light production by luciferase in a Lmax II 384 luminometer (Molecular Devices, USA). Forty-eight hours post-transfection, cells were washed twice with PBS and 100 μL of lysis buffer [1 mM dithiothreitol; 1mM EDTA; 25 mM Tris-phosphate (pH 7.8); 8 mM $MgCl_2$; 15% glycerol; 1% (v/v) Triton^{TM} X-100] was added to each well. The protein content of the lysates was measured by the DC^{TM} Protein Assay reagent using BSA as a standard. The data were expressed as relative light units (RLU) of luciferase per mg of total cell protein.

- For flow cytometry analysis of GFP expression, 8×10^4 and 14×10^4 HeLa and COS-7 cells/well, respectively, were seeded in 12-well culture plates and, after 24 h polyplexes containing 1 μg of pCMV.gfp were added to cells. After 4 h incubation (5% CO_2 at 37 °C), the transfection medium was replaced with DMEM-HG and cells were further incubated for 48 h. Then, cells were washed twice with PBS and detached with trypsin (2-3 min at 37 °C). After that, cells were washed and resuspended in PBS, and immediately analyzed in a FACSCalibur flow cytometer

(Becton Dickinson, NJ, USA). Live cells were gated by forward/side scattering from a total of 20,000 events and data was analyzed using CellQuest software.

- For fluorescence microscopy analysis of GFP expression, 8×10^4 and 14×10^4 HeLa and COS-7 cells/wel, respectively, were seeded in 12-well culture plates (previously covered with a coverslip) and, after 24 h polyplexes containing 1 μg of pCMV.gfp were added to the cells. After 4 h incubation (5% CO_2 at 37 °C), the transfection medium was replaced with DMEM-HG and cells were further incubated for 48 h. Then, cells were washed twice with PBS, fixed with 4% paraformaldehyde, for 15 min at room temperature, and then mounted in Mowiol® mounting medium (Sigma-Aldrich, MO, USA). The images (original magnification: $\times$ 20) were obtained on an AxioCam HRc camera (Zeiss, Munich, Germany). Image acquisition was done at the MICC Imaging facility of CNC.

4.3.2.6   Physico-chemical characterization of the polyplexes

Ethidium bromide intercalation assay. DNA condensation by PDMAEMA-*b*-PβAE-*b*-PDMAEMA polyplexes was analyzed using an ethidium bromide (EtBr) exclusion assay. Polyplexes were prepared and, after 15 minutes, 50 μL of each sample was transferred into a black 96-well plate (Costar, USA). Then, 50 μL of EtBr solution was added to achieve a final EtBr concentration of 400 nM. Following 10 min of incubation, fluorescence was measured in a SpectraMax Gemini EM fluorometer (Molecular Devices, USA) at λ_{exc} = 518 nm and λ_{em} = 605 nm. The fluorescence scale was calibrated such that the initial fluorescence of EtBr (50 μL of EtBr solution were added to 50 μL of Milli-Q water to achieve a final EtBr concentration of 400 nM) was set at residual fluorescence. The value of fluorescence obtained with 1 μg of naked DNA (control) was set as 100%. The amount of DNA available to interact with the probe was calculated by subtracting the values of residual fluorescence from those obtained for the samples and expressed as the percentage of the control.

Agarose gel electrophoresis assay. To evaluate the complexation of the DNA with the copolymer an electrophoresis in agarose gel was performed. Polyplexes were

prepared and, after 15 minutes, 20 μL of each sample was added to 5 μL of loading buffer (15% (v/v) Ficoll® 400, 0.05% (w/v) bromophenol blue, 1% (w/v) SDS, 0.1 M EDTA, pH 7.8). 20 μL of each blend were transferred to a 1% agarose gel prepared in TBE solution (89 mM Tris-buffer (pH 8.6), 89 mM boric acid, 2.5 mM EDTA) and containing 1 μg/mL of EtBr. The electrophoresis was set to 40 min at 80 mV. Sample visualization takes place in a GelDoc® (BioRad®, USA) system using the QuantityOne® program.

Dynamic light scattering and zeta potential analyses. Dynamic light scattering (DLS) measurements were performed on a Zetasizer Nano-ZS (Malvern Instruments Ltd., UK). The particle size distribution (in intensity), average hydrodynamic particle size average (z-average) and polydispersity index (PDI) were determined with Zetasizer 6.20 software. Measurements were made at 25 °C with a backward scattering angle of 173 °. Zeta-potential measurements were performed using a Zetasizer Nano-ZS (Malvern Instruments Ltd., UK), coupled to laser Doppler electrophoresis and determined using Smoluchovski model. The polyplexes were prepared immediately before analysis and three independent experiments were performed in triplicate for size and zeta potential.

4.3.2.7   Statistical analysis

Data are presented as mean result $\pm$ standard deviation (SD) and analyzed using the IBM® SPSS® Statistics software (version 20). Statistical significance of diferences between data was evaluated by one-way ANOVA using Bonferroni or Games-Howell post-hoc tests. A *p*-value < 0.05 was considered as statistically significant.

4.4   Results and discussion

The PDMAEMA-*b*-P*β*AE-*b*-PDMAEMA polycationic block copolymer was synthesized via a four-step procedure as presented in Scheme 4.1. Firstly, *α*,*ω*-acrylate-poly(*β*-amino ester) was synthesized by a Michael addition reaction between 5-amino-1-propanol and an excess of 1,4-butanediol diacrylate (Scheme 4.1 (a))[9].

PDMAEMA with azide-terminal group was prepared by DMAEMA polymerization throughout ATRP initiated process with N_3EiBBr (Scheme 4.1 (b)). Azide-chain ends were further modified through reaction with triphenylphosphine (TPP) (Scheme 4.1 (c)) to afford a α-amine-PDMAEMA homopolymer[17]. The triblock copolymer, could then be obtained by combination of α,ω-acrylate-poly(β-amino ester) and α-amine-PDMAEMA using Michael addition reaction. In this work, three different block copolymers were prepared varying the molecular weight of the PβAE segment: PDMAEMA$_{3000}$-*b*-PβAE$_{3000}$-*b*-PDMAEMA$_{3000}$, PDMAEMA$_{3000}$-*b*-PβAE$_{9000}$-*b*-PDMAEMA$_{3000}$ and PDMAEMA$_{3000}$-*b*-PβAE$_{12000}$-*b*-PDMAEMA$_{3000}$.
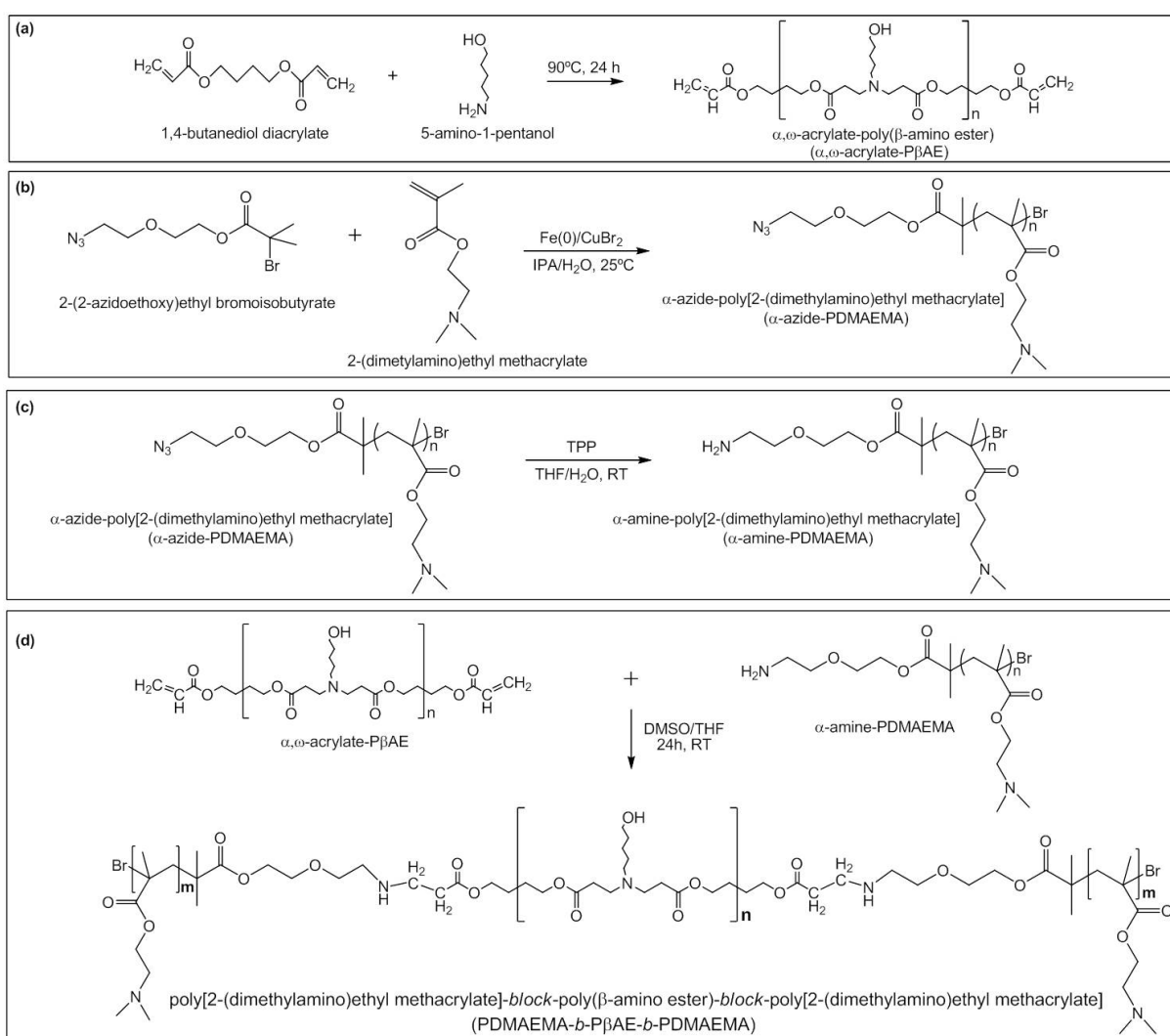
Scheme 4.1: Synthesis of ABA type linear block copolymer via combining Michael addition and ATRP reactions: (a) Synthesis of α,ω-acrylate-PβAE by Michael addition reaction; (b) Synthesis of PDMAEMA with azide-based initiator through SARA-ATRP method; (c) Terminal modification of α-azide-PDMAEMA to α-amine-PDMAEMA; (d) Michael-addition reaction between α-amine-PDMAEMA and α,ω-acrylate-PβAE.

4.4.1 Synthesis and post-polymerization functionalization of PDMAEMA

α-Azide-PDMAEMA was synthesized by ATRP according to the procedure described in Chapter 2 and the post-polymerization end-modification to afford *α*-amine-PDMAEMA was performed according a procedure reported in the literature[17]. The chemical structure analysis was assessed by ^{1}H NMR (Figure 4.1) and its molecular weight distribution (Table 4.1) was obtained by SEC.
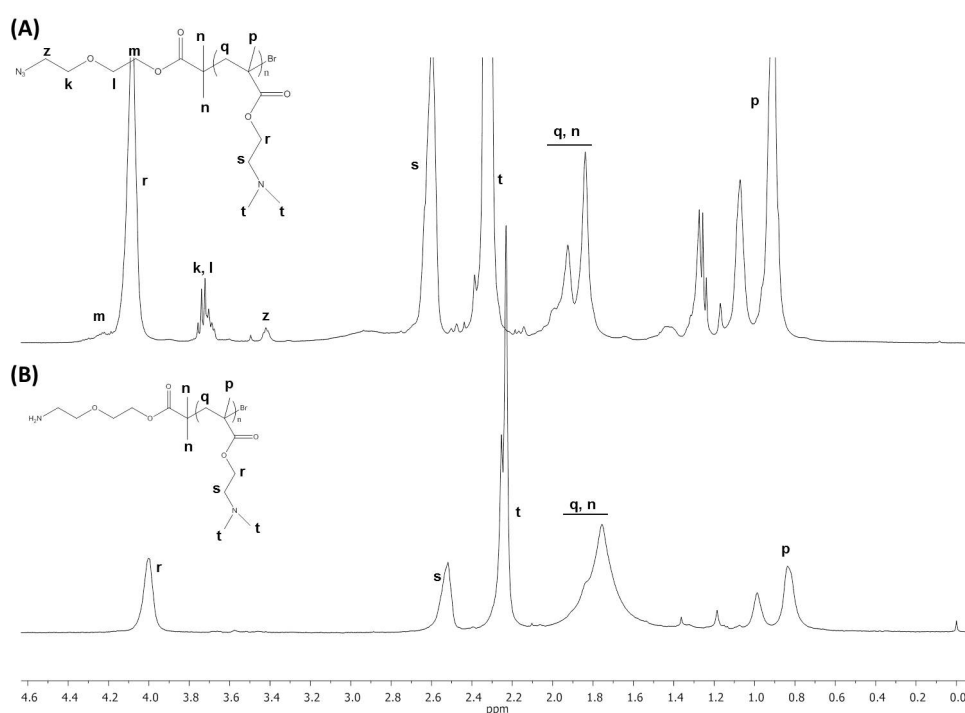
Figure 4.1: ^{1}H NMR spectrum (CDCl$_3$, 400 MHz) of *α*-azide-PDMAEMA.

The signals observed at 4.07 ppm (2H, -OCH_2CH$_2$N-), 2.58 ppm (2H, -OCH$_2$CH_2N-), 2.35-2.20 ppm (6H, -N(CH_3)$_2$), 2.00-1.75 ppm (2H, -CCH_2C-) and 1.10-0.80 ppm (3H, -CCH_3Br) are in agreement with the expected PDMAEMA chemical structure[18]. The estimative of the molecular weight of *α*-amine-PDMAEMA was not possible through NMR spectroscopy (Figure 4.1 (B)) because the signal of the amine proton is not visible in the spectrum. Therefore, as the difference between *α*-amine-PDMAEMA and *α*-azide-PDMAEMA structure is minimal, *α*-azide-PDMAEMA NMR spectrum (Figure 4.1 (A)) was used to determine its molecular weight. On the basis of the integrals ratio of peaks *z* and *s*, M$_{n,NMR}$ = 3,200 g.mol^{-1}

were calculated, whereas SEC analysis indicated a $M_{n,SEC}$ = 3,400 g.mol^{-1} and *Đ* = 1.34 (Figure 4.3). These results suggest that a well-controlled structure of *α*-amine-PDMAEMA (NH$_2$-PDMAEMA) was successfully achieved.

4.4.2   Synthesis of poly(β-amino ester)

The successful polymerization of *α,ω*-acrylate-terminated PβAE (Scheme 4.1 (a)) was confirmed by ^{1}H NMR (Figure 4.2) and SEC (Table 4.1) analyzes. A typical *α,ω*-acrylate-PβAE ^{1}H NMR spectrum is presented in Figure 4.2 and chemical shifts are in agreement with the expected *α,ω*-acrylate-PβAE chemical structure[19]. The presence of the signals for terminal acrylate group allows the evaluation of the number-average molecular weight of the polymer. The molecular weights of the three *α,ω*-acrylate-terminated PβAEs were determined on the basis of the integral ratio of peaks *d* and *j* as described in Table 4.1.
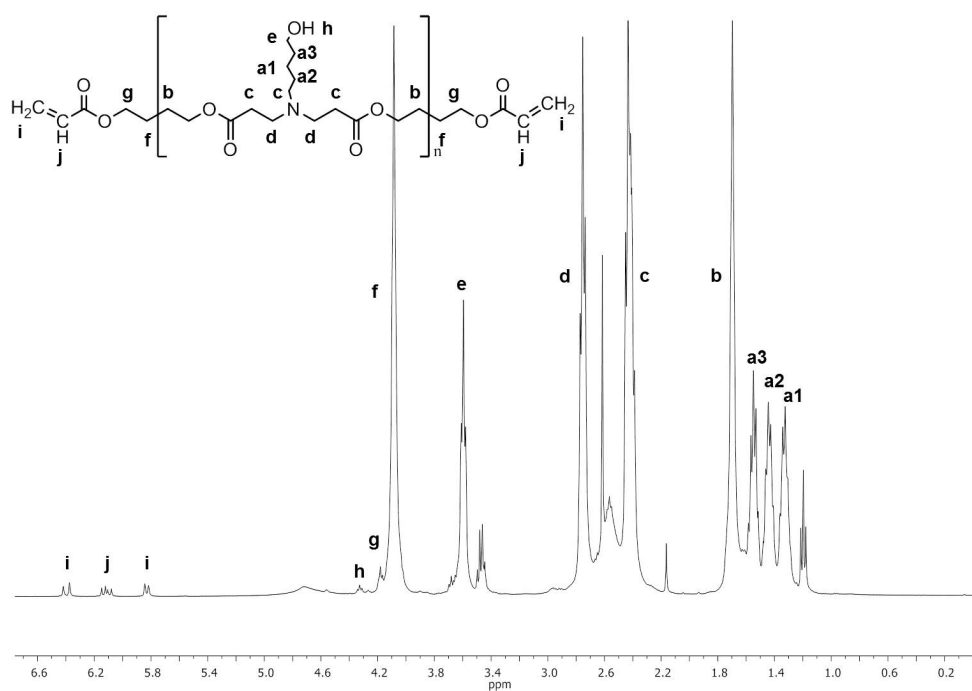
Figure 4.2: ^{1}H NMR spectrum (CDCl$_3$, 400 MHz) of *α*, *ω*-acrylate-PβAE.

4.4.3 Synthesis of PDMAEMA-*b*-P*β*AE-*b*-PDMAEMA block copolymers

PDMAEMA-*b*-P*β*AE-*b*-PDMAEMA block copolymers were synthesized through Michael addition between mono-amine functionalized PDMAEMA and *α,ω*-acrylate-P*β*AE in a mixture of DMSO/THF (50/50) to allow a proper dissolution of the homopolymers.
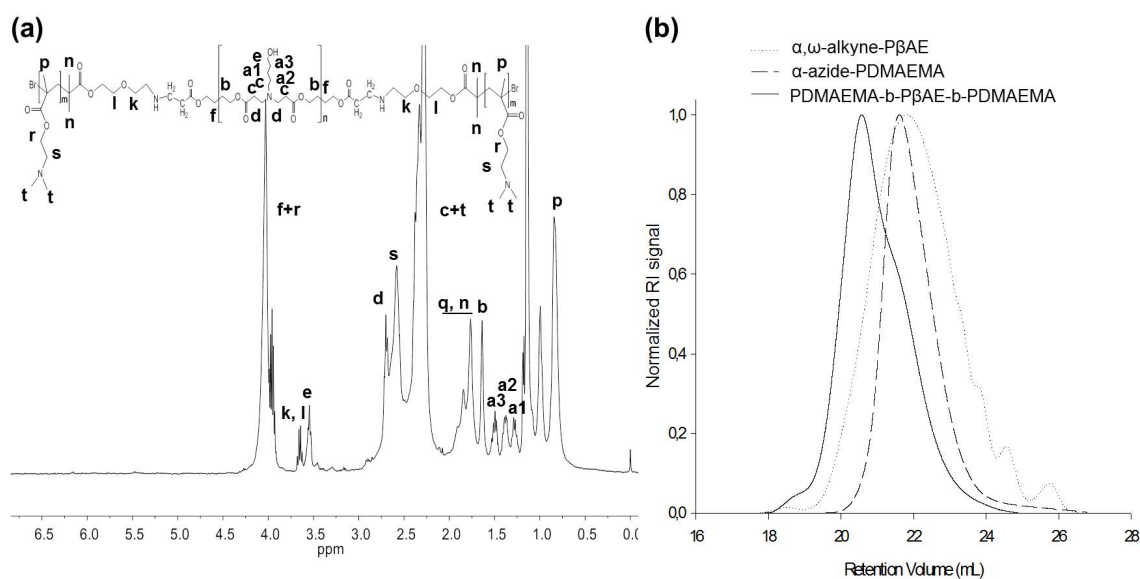
Figure 4.3: ^{1}H NMR spectrum (CDCl$_3$, 400 MHz) (a) and SEC refractive index traces overlay (b) showing successful Michael addition reaction between *α*-amine-PDMAEMA$_{3000}$ and *α,ω*-acrylate-terminated P*β*AE$_{3000}$ to give PDMAEMA$_{3000}$-*b*-P*β*AE$_{3000}$-*b*-PDMAEMA$_{3000}$ block copolymer.

The ^{1}H NMR spectrum of PDMAEMA-*b*-P*β*AE-*b*-PDMAEMA (Figure 4.3 (a)) shows no signals at 5.81, 6.06-6.18, and 6.36-6.45 ppm, corresponding to the acrylate protons of *α,ω*-acrylate-P*β*AE, confirming the success of the Michael addition reaction between amine group of PDMAEMA and acrylate terminal group of P*β*AE. In addition, a shift in the SEC traces was observed toward higher molecular weight, confirming the formation of the triblock copolymer (Figure 4.3 (b)).

In Table 4.1 the molecular weight values obtained from NMR and SEC analyzes of the homopolymers and the triblock copolymers were compared, suggesting a good efficiency of the Michael addition reaction, since the molecular weight of the tri-block copolymer is roughly the sum of the molecular weights of the three homopolymer segments.

Table 4.1: Characterization of α-amine-PDMAEMA, α,ω-acrylate-PβAE and PDMAEMA-*b*-PβAE-*b*-PDMAEMA.

Polymer sample	DP	$\mathbf{M}_{n,NMR}$[a]	$\mathbf{M}_{n,SEC}$[b]	Đ
α-amine-PDMAEMA$_{3000}$	19	3,200	3,400	1.34
α,ω-acrylate-PβAE$_{3000}$	10	3,200	3,500	1.95
α,ω-acrylate-PβAE$_{9000}$	31	9,500	9,800	2.72
α,ω-acrylate-PβAE$_{12000}$	39	11,900	13,100	3.29
PDMAEMA$_{3000}$-*b*-PβAE$_{3000}$-*b*-PDMAEMA$_{3000}$	-	12,000	10,200	1.89
PDMAEMA$_{3000}$-*b*-PβAE$_{9000}$-*b*-PDMAEMA$_{3000}$	-	18,400	17,100	3.59
PDMAEMA$_{3000}$-*b*-PβAE$_{12000}$-*b*-PDMAEMA$_{3000}$	-	20,800	18,900	3.35

[a] Calculated from the integration of α-azide-PDMAEMA, α,ω-alkyne-PβAE, and PDMAEMA-*b*-PβAE-*b*-PDMAEMA;

[b] Determined by SEC in THF with polystyrene standards.

4.4.4   Biological activity

The potential of the three developed block copolymers, PDMAEMA$_{3000}$-*b*-PβAE$_{3000}$-*b*-PDMAEMA$_{3000}$, PDMAEMA$_{3000}$-*b*-PβAE$_{9000}$-*b*-PDMAEMA$_{3000}$ and PDMAEMA$_{3000}$-*b*-PβAE$_{12000}$-*b*-PDMAEMA$_{3000}$ to be used as gene delivery systems was analyzed and compared with two others commonly used cationic polymers: PEI, considered the gold standard for polymeric-based gene delivery systems[14;20;21] and TurboFect^{TM}, a recent and promising commercial linear cationic polymeric non-viral vector. For comparison purpose, the most promising formulation achieved in Chapter 3 was also used during the tests carried out here.

4.4.4.1   Polymer/pDNA complexes toxicity

The cytotoxicity of polymer/pDNA complexes, was assessed in two different cell types, HeLa and COS-7 cell lines (Figure 4.4).

The obtained results, for both cell lines, show that the toxicity of the polyplexes is dependent on their N/P ratio and polymer composition, being observed a higher reduction on cell viability for higher N/P ratios and for PEI-based polyplexes. For the three block copolymer-based polyplexes a low level of cytotoxicity was observed, until 100/1 N/P ratio, for both cell lines. Compared to previous data (Chapter 3), where satisfactory results were observed until 25/1 N/P ratios, these results are a significant improvement in the cell viability. Most probably, this promising data
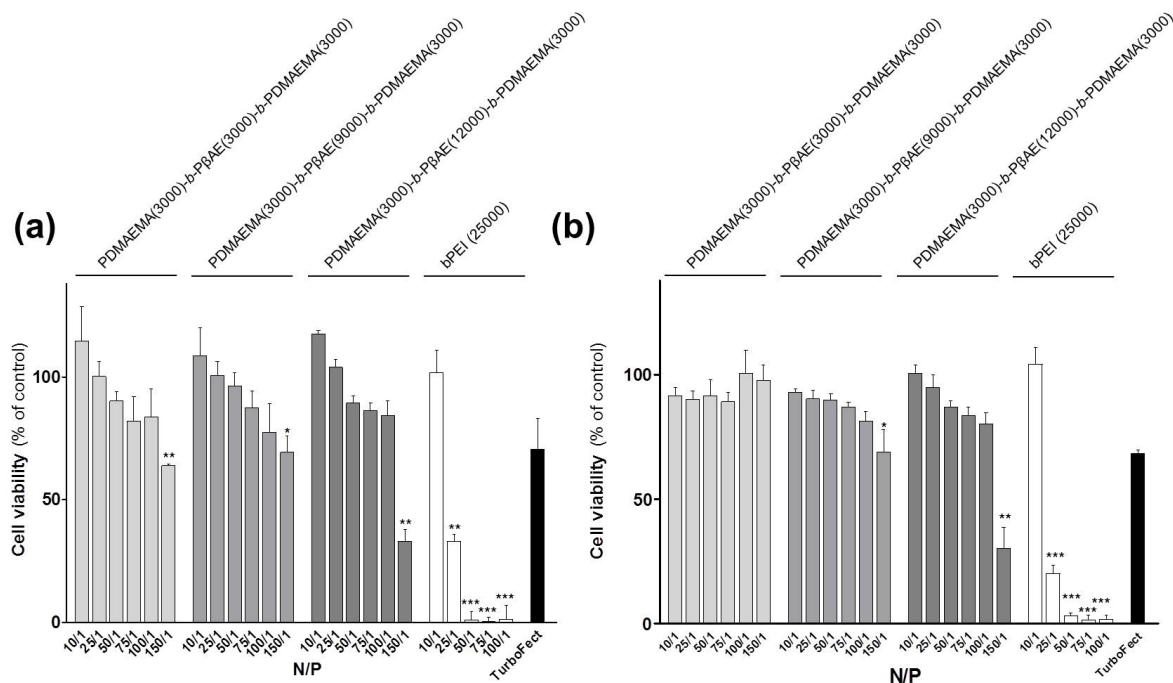
Figure 4.4: Effect of the N/P ratio and composition of polyplexes on their cytotoxicity in HeLa (a) and COS-7 (b) cell lines. The different block copolymers of PDMAEMA-*b*-P*β*AE-*b*-PDMAEMA and branched PEI were complexed with 1 *μ*g of pCMV.Luc at the indicated polymer/DNA N/P ratios. TurboFect^{TM} was used according to the manufacturer's instructions. The data are expressed as percetange of cell viability with respect to the control corresponding to untreated cells (mean $\pm$ SD, obtained from triplicates). The results are representative of at least three independent experiments. Asterisks ($***$ p $\leq$ 0.001, $**$ p $\leq$ 0.01 and $*$ p $\leq$ 0.05) indicate values that differ significantly from those measured in the positive control.

may be directly related to the absence of copper in the synthetic procedure used. These results emphasize the importance of green procedures in biomedical material preparation and manipulation fields.

4.4.4.2 Transfection activity

The three cationic block copolymers were assessed as non-viral vectors for plasmid delivery (Figure 4.5) in HeLa and COS-7 cell lines.

As illustrated in Figure 4.5, all PDMAEMA-*b*-P*β*AE-*b*-PDMAEMA block copolymers-based polyplexes have the ability to successfully deliver the plasmid DNA (pDNA) into HeLa and COS-7 cells. In general, polyplexes prepared with the block copolymer PDMAEMA$_{3000}$-*b*-P*β*AE$_{12000}$-*b*-PDMAEMA$_{3000}$ showed much higher transgene (luciferase) expression than that observed with those prepared

155
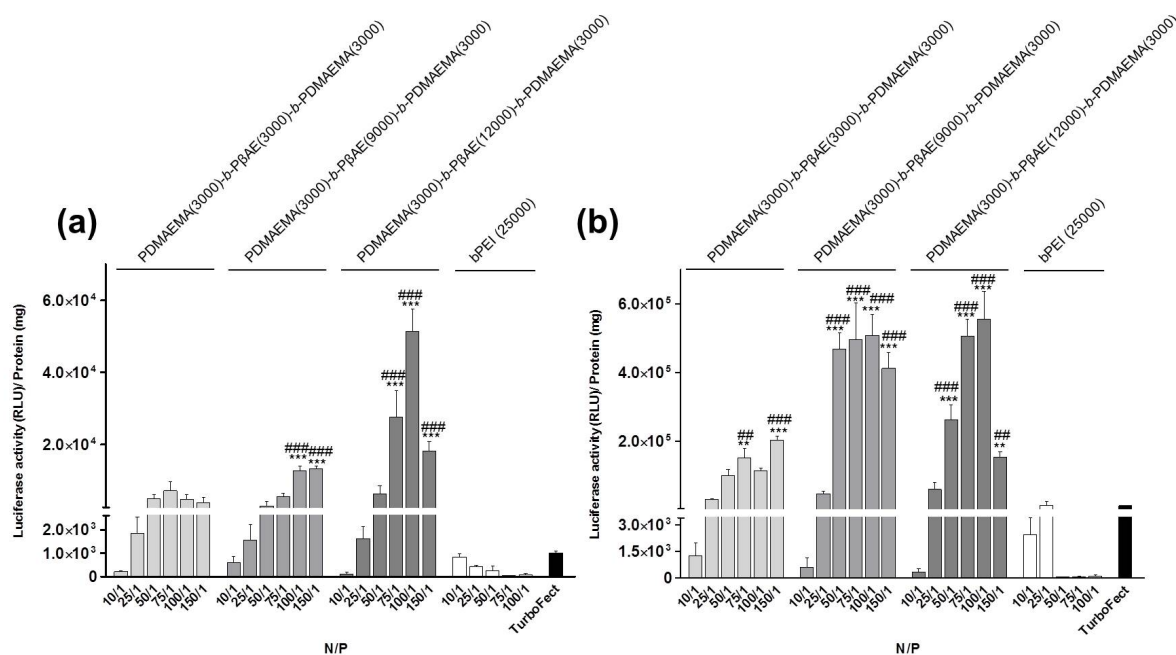
Figure 4.5: Effect of the N/P ratio and composition of polyplexes on their transfection activity in HeLa (a) and COS-7 (b) cell lines. The different block copolymers of PDMAEMA-*b*-PβAE-*b*-PDMAEMA and branched PEI were complexed with 1 µg of pCMV.Luc at the indicated polymer/DNA N/P ratios. TurboFect^{TM} was used according to the manufacturer's instructions. The data are expressed as RLU of luciferase per mg of total cell protein (mean $\pm$ SD, obtained from triplicates). The results are representative of at least three independent experiments. Asterisks ($***$ p $\leq$ 0.001 and $**$ p $\leq$ 0.01) and cardinals (### p $\leq$ 0.001 and ## p $\leq$ 0.01) indicate values that differ significantly from those measured with polyplexes prepared with bPEI and TurboFect^{TM}, respectively.

with PDMAEMA$_{3000}$-*b*-PβAE$_{3000}$-*b*-PDMAEMA$_{3000}$ and PDMAEMA$_{3000}$-*b*-PβAE$_{9000}$-*b*-PDMAEMA$_{3000}$. In spite of in COS-7 cell line PDMAEMA$_{3000}$-*b*-PβAE$_{12000}$-*b*-PDMAEMA$_{3000}$- and PDMAEMA$_{3000}$-*b*-PβAE$_{9000}$-*b*-PDMAEMA$_{3000}$-based polyplexes have, generally, similar transgene expression, the high values of transgene expression of PDMAEMA$_{3000}$-*b*-PβAE$_{12000}$-*b*-PDMAEMA$_{3000}$-based polyplexes in both cell lines make them the more suitable and promising systems. This more suitable structure of PDMAEMA$_{3000}$-*b*-PβAE$_{12000}$-*b*-PDMAEMA$_{3000}$-based polyplexes could probably promote both the interaction with cells and the delivery of genetic material inside them, consequently resulting in a higher biological activity. Therefore, the differences in the length of the PβAE chain revealed to have a decisive influence on transfection activity. In this respect, the arguments found in literature regarding the influence of molecular weight of PβAE-based polyplexes in gene delivery efficiency are contradictory. While some authors argue that different PβAE molecular

weights lead to a high diversity of responses in terms of gene delivery efficacy[22], others claim that more important than molecular weight is their terminal chain ends[23]. Crossing these results with those obtained in Chapter 3, where it was evaluated two PDMAEMA-*b*-P*β*AE-*b*-PDMAEMA block copolymers differing in the molecular weight of PDMAEMA segments, it was observed that molecular weight of both segments significantly influence the transfection activity of polyplexes.

Figure 4.5 also shows that the transfection activity of the generated polyplexes is dependent on their N/P ratio, the maximum transgene expression being generally obtained at the 100/1 N/P ratio for both cell lines. Surprisingly, it is a much high value of N/P ratio when compared to the previous results presented in Chapter 3 (25/1 N/P). This result can be associated to the general lower cytotoxicity of these new block copolymers even for higher N/P ratios in contrast with the higher toxicity for N/P ratios above 25/1 of the synthesized block copolymers of Chapter 3.

Comparing the three new block copolymers, the PDMAEMA$_{3000}$-*b*-P*β*AE$_{12000}$-*b*-PDMAEMA$_{3000}$ is the one that has higher biological activity in both cell lines, as referred above. The enhancement of the transfection activity is most probably due to the fact that polyplexes prepared with this block copolymer have a structure more prone for gene delivery process (which include, the internalization by the endocytic pathway, the release from the endosome, the release of genetic material to cytoplasm and its translocation to the nucleus) resulting in a higher biological activity. For N/P ratio of 150/1, in both cell lines, it was observed a decrease of luciferase gene expression, which could be due to a stronger interaction between PDMAEMA$_{3000}$-*b*-P*β*AE$_{12000}$-*b*-PDMAEMA$_{3000}$ block copolymer and the pDNA. This fact can difficult the release of the genetic material from the polyplexes inside of cells, consequently reducing the transgene expression. Moreover, another reason can be the cytotoxicity observed for this N/P ratio. Indeed, cationic polymers with higher molecular weights are reported to show better DNA binding, cellular uptake and transfection activity, whilst low molecular weight cationic polymers show less cytotoxicity[24]. The results presented here suggest that the balance between molecular weight and cytotoxicity seems to be another important issue that influences the transfection activity.

The transfection activity of the block copolymers was compared to the obtained with

branched PEI (bPEI) (25,000 g.mol^{-1}), generally accepted as a gold standard non-viral vector presenting high transfection efficiency[14], and TurboFect^{TM}, a novel and promising formulation described as an efficient and non-toxic non-viral vector for *in vitro* delivery of plasmid DNA. As illustrated in Figure 4.5 (a), for HeLa cells, poly-plexes prepared at the optimal N/P ratio (100/1) with PDMAEMA$_{3000}$-*b*-PβAE$_{12000}$-*b*-PDMAEMA$_{3000}$ exhibit approximately 60-fold and 50-fold higher transfection activity than the best formulation of polyplexes generated with bPEI (N/P 10/1) or TurboFect^{TM}, respectively. Concerning the COS-7 cell line, polyplexes prepared at the optimal N/P ratio (100/1) with PDMAEMA$_{3000}$-*b*-PβAE$_{12000}$-*b*-PDMAEMA$_{3000}$ exhibit approximately 40- and 50-fold higher transfection activity than that obtained with the best formulation of polyplexes generated with bPEI (N/P 25/1) or TurboFect^{TM}, respectively. These data confirm that the transfection effectiveness of this new copolymer based on PβAE and PDMAEMA is much higher than the obtained with current commercial polymeric non-viral vectors, which are considered excellent transfection reagents.

A comparison between our most promising formulation PDMAEMA$_{3000}$-*b*-PβAE$_{12000}$-*b*-PDMAEMA$_{3000}$ (N/P 100/1) and the previously reported (Chapter 3) best formulation PDMAEMA$_{3000}$-*b*-PβAE$_{3000}$-*b*-PDMAEMA$_{3000}$ (N/P 25/1 and N/P 50/1, in HeLa and COS-7 cells, respectively) is represented in Figure 4.6. As illustrated in Figure 4.6, a notorius improvement in transfection efficiency, in both cell lines, was obtained with the new PDMAEMA$_{3000}$-*b*-PβAE$_{12000}$-*b*-PDMAEMA$_{3000}$-based polyplexes at N/P ratio of 100/1 when compared to that observed with the formulation prepared with the copolymer synthesized previously (PDMAEMA$_{3000}$-*b*-PβAE$_{3000}$-*b*-PDMAEMA$_{3000}$, CuAAC) at N/P 25/1, for HeLa cells, and 50/1, for COS-7 cells. For HeLa cell line, this value reaches 9-fold increase, while for COS-7 cells is 5-fold higher. The increase in transfection efficiency could be explained not only by the increase in the molecular weight of the PβAE segment but also by the decrease of toxicity of the new block copolymer for higher N/P ratio (Figure 4.6). The decrease of cytotoxicity using Michael addition reaction instead of CuAAC click reaction in copolymer preparation is particularly clear with polyplexes prepared at N/P ratio of 100/1 with the block copolymers PDMAEMA$_{3000}$-*b*-PβAE$_{3000}$-

b-PDMAEMA$_{3000}$ (Figure 4.6).
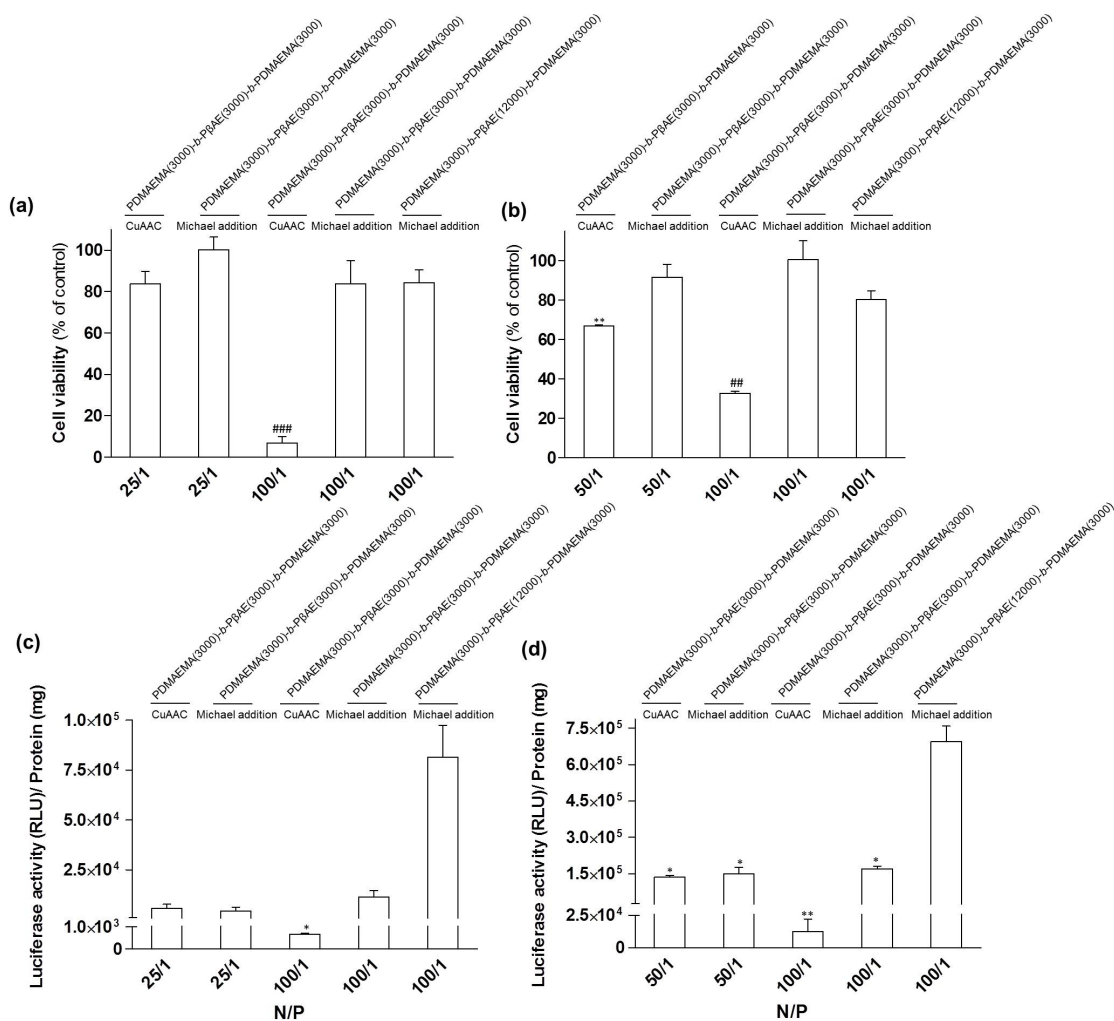
Figure 4.6: Comparison between cell viability and best transfection activity results of polyplexes based on PDMAEMA$_{3000}$-*b*-P*β*AE$_{3000}$-*b*-PDMAEMA$_{3000}$ prepared from copper(I)l-catalyzed azide-alkyne cycloaddition and, PDMAEMA$_{3000}$-*b*-P*β*AE$_{3000}$-*b*-PDMAEMA$_{3000}$ and PDMAEMA$_{3000}$-*b*-P*β*AE$_{12000}$-*b*-PDMAEMA$_{3000}$ prepared from Michael addition reaction in HeLa (a and c, respectively) and COS-7 (b and d, respectively) cell lines. The data are expressed as RLU of luciferase per mg of total cell protein (mean $\pm$ SD, obtained from triplicates). The results are representative of at least two independent experiments. Cardinals (### $p \leq 0.001$ and # $p \leq 0.01$) indicate values that differ significantly from those measured in the control (untreated cells) and asterisks ($\ast\ast$ $p \leq 0.01$ and $\ast$ $p \leq 0.05$) indicate values that differ significantly from those measured with polyplexes prepared at 100/1 N/P ratio based on PDMAEMA$_{3000}$-*b*-P*β*AE$_{12000}$-*b*-PDMAEMA$_{3000}$ copolymer prepared through Michael addition.

In order to examine the effect of PDMAEMA$_{3000}$-*b*-P*β*AE$_{12000}$-*b*-PDMAEMA$_{3000}$ on the percentage of transfected cells, flow cytometry (Figure 4.7) and fluorescence microscopy (Figure 4.8) analyzes were carried out, after cells transfection with poly-

plexes prepared with pGFP.
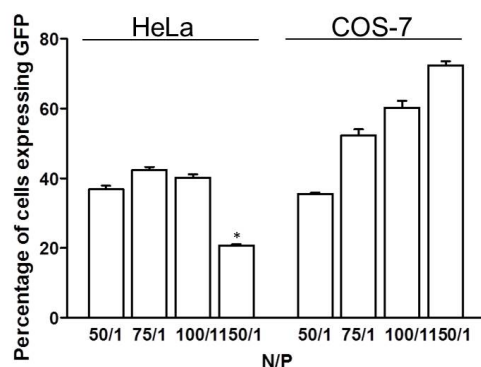
Figure 4.7: Effect of N/P charge ratios of PDMAEMA$_{3000}$-*b*-PβAE$_{12000}$-*b*-PDMAEMA$_{3000}$-based polyplexes on their transfection efficiency in HeLa and COS-7 cells evaluated by flow cytometry. Asterisk ($* p \leq 0.05$) indicates values that differ significantly from those measured with polyplexes prepared at 100/1 N/P ratio.

Flow cytometry analysis was used to evaluate the efficiency of transfection. The results obtained by this analysis (Figure 4.7) show, in general, a good percentage of transfected HeLa and COS-7 cells obtained with the PDMAEMA$_{3000}$-*b*-PβAE$_{12000}$-*b*-PDMAEMA$_{3000}$-based polyplexes for the tested N/P ratios. Comparing cell lines, it was observed a higher percentage of transfected COS-7 cells than HeLa cells. This result confirmed the differences detected in luciferase transgene expression, where it was also observed a higher expression in COS-7 cell line than in HeLa cells. Surprisingly, in COS-7 cell line a high percentage (72%) of transfected cells for polyplexes prepared at 150/1 N/P ratio was also perceived in spite of the low cell viability. This result indicates that despite the polyplexes at this N/P ratio induce high cytotoxicity, the surviving cells are efficiently transfected. The best formulation (100/1 N/P ratio) resulted in ~40% and ~60% of HeLa and COS-7 transfected cells, respectively.

Regarding the fluorescence microscopy study (Figure 4.8), it was observed once again, differences in the number of GFP expressing cells between HeLa and COS-7 cell lines ((c) *vs.* (g) or (d) *vs.* (h)). For both cell lines, it was not observed any fluorescence in cells without treatment ((a) and (e)) and cells treated with only pCMV.gfp ((b) and (f)). The differences between the two distinct N/P ratios (25/1 (g) and 100/1 (h)) used is more evident in COS-7 cell line. Indeed, the number of transfected cells observed with polyplexes prepared at 100/1 N/P ratio was very high, which confirmed the results obtained by flow cytometry (Figure 4.7 (b)).
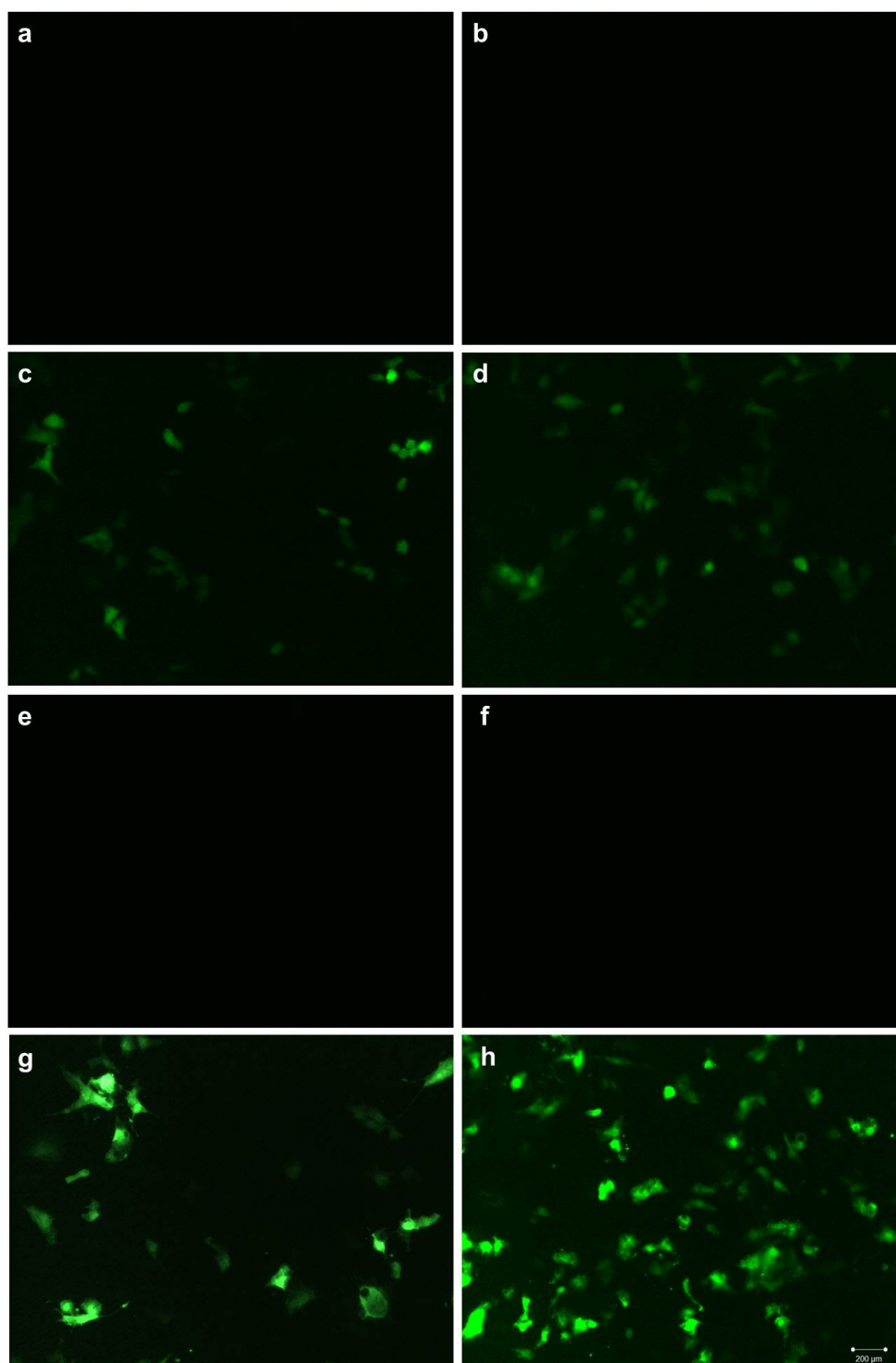
Figure 4.8: Effect of N/P charge ratios on their transfection efficiency evaluated by fluorescence microscopy in HeLa (a, b, c and d) and COS-7 (e, f, g and h) cell lines. Representative fluorescence microscopy images: (a) and (e) cells without treatment; (b) and (f) cells treated with only pCMV.gfp; (c) and (g) cells treated with 25/1 polyplexes; (d) and (h) cells treated with 100/1 polyplexes. Cells without polyplexes treatment and cells treated with only pCMV.gfp were used as controls.

4.4.4.3   Physical characterization of PDMAEMA-*b*-PβAE-*b*-PDMAEMA-based polyplexes: protection of DNA, size and zeta potential

The physicochemical properties of the polymeric-based systems play an important role in their transfection efficiency into target cells. These include the ability to condense and protect DNA, the size and the surface charge (zeta potential) of the polymer/DNA complexes formed[24;25].

Physicochemical properties of the polyplexes based on PDMAEMA$_{3000}$-*b*-PβAE$_{3000}$-*b*-PDMAEMA$_{3000}$, PDMAEMA$_{3000}$-*b*-PβAE$_{9000}$-*b*-PDMAEMA$_{3000}$ and PDMAEMA$_{3000}$-*b*-PβAE$_{12000}$-*b*-PDMAEMA$_{3000}$ block copolymers were determined in order to correlate them with transfection activity. Firstly, EtBr intercalation and agarose gel electrophoresis assays were carried out to determine if prepared polyplexes were able to condense and protect DNA. The monovalent DNA-intercalating agent EtBr fluoresces dramatically upon binding to DNA and quenches the fluorescence when displaced by condensation of the DNA structure or by higher affinity compounds. Figure 4.9 illustrates the accessibility of the EtBr to DNA carried by PDMAEMA$_{3000}$-*b*-PβAE$_{3000}$-*b*-PDMAEMA$_{3000}$- (**a** and **b**), PDMAEMA$_{3000}$-*b*-PβAE$_{9000}$-*b*-PDMAEMA$_{3000}$- (**c** and **d**), and PDMAEMA$_{3000}$-*b*-PβAE$_{12000}$-*b*-PDMAEMA$_{3000}$-based (**e** and **f**) polyplexes prepared at different N/P ratios.

Figure 4.9 (b) shows a decrease of EtBr fluorescence with the increase of the N/P ratio of polyplexes for all block copolymers assessed. The main explanation could be related to the fact that higher amounts of block copolymer results in an increase of positive charge that leads to a higher degree of interaction with negative charges of DNA, which in turn leads to a higher degree of condensation and protection. In general, as found in copolymer tested in Chapter 3, the significant drop in EtBr access was observed when the N/P ratio of polyplexes shift from 5/1 to 10/1. This result could indicate that the amount of cationic block copolymer in 5/1 polyplexes was not enough to create electrostatic interactions that result in an efficient condensation of pDNA, allowing the intercalation of the small EtBr molecule. For the other polyplexes N/P ratios, the different block copolymers show that a very low amount of the carried DNA was accessible to the probe. For 5/1 N/P ratio, it was also ob-
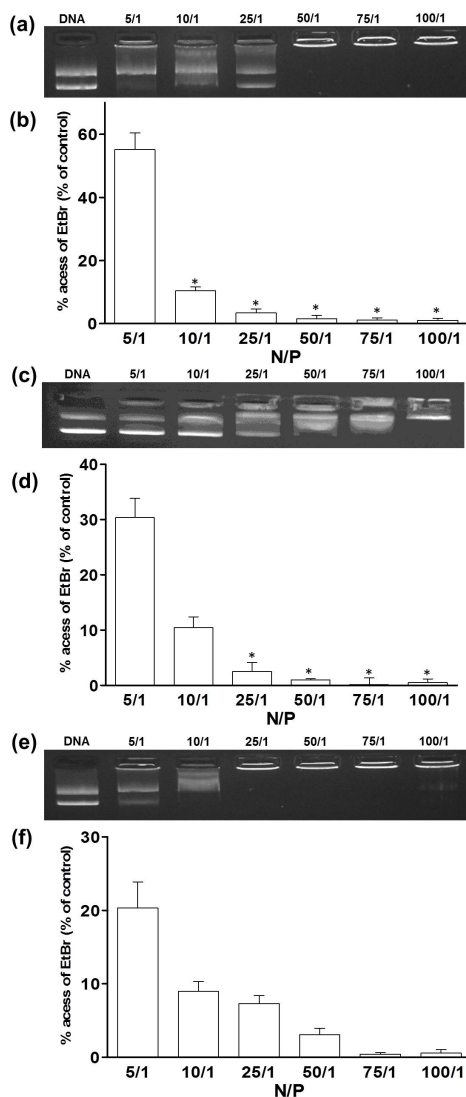
Figure 4.9: Agarose gel electrophoresis and accessibility of ethidium bromide (EtBr) to DNA of the $PDMAEMA_{3000}$-*b*-$PβAE_{3000}$-*b*-$PDMAEMA_{3000}$- (**a** and **b**), $PDMAEMA_{3000}$-*b*-$PβAE_{9000}$-*b*-$PDMAEMA_{3000}$- (**c** and **d**), and $PDMAEMA_{3000}$-*b*-$PβAE_{12000}$-*b*-$PDMAEMA_{3000}$-based (**e** and **f**) polyplexes prepared at different N/P ratios. (**b**, **d** and **f**). The amount of DNA available to interact with EtBr was calculated by subtracting the values of residual fluorescence from those obtained for the samples and expressed as the percentage of the control. Control corresponds to free DNA in the same amount as that associated with the complexes (100% of EtBr accessibility). The data are expressed as EtBr access (% of control) and correspond to mean $\pm$ SD of n = 6 (triplicates of two independent experiments)). Asterisks ($*$ $p \leq 0.05$) indicate values that differ significantly from those measured with polyplexes prepared at N/P 5/1 ratio.

served a decreasing of EtBr accessibility with the increase of the molecular weight of the block copolymers. This result can be explained by a better and higher condensation of pDNA by cationic block copolymers with higher molecular weight at least for polyplexes prepared at 5/1 N/P ratio. The data obtained in these EtBr accessibility

assays are in accordance with those obtained in the agarose gel electrophoresis assay (Figure 4.9 (a)), where it was observed a lower intensity of the bands and a reduction in their migration distance with increasing the N/P ratio of the polyplexes.

Size and the zeta potential of the polyplexes are two other major aspects that influences transfection activity. Figure 4.10 retracts the particle size (a) and zeta potential (b) of polyplexes prepared at different N/P ratios.
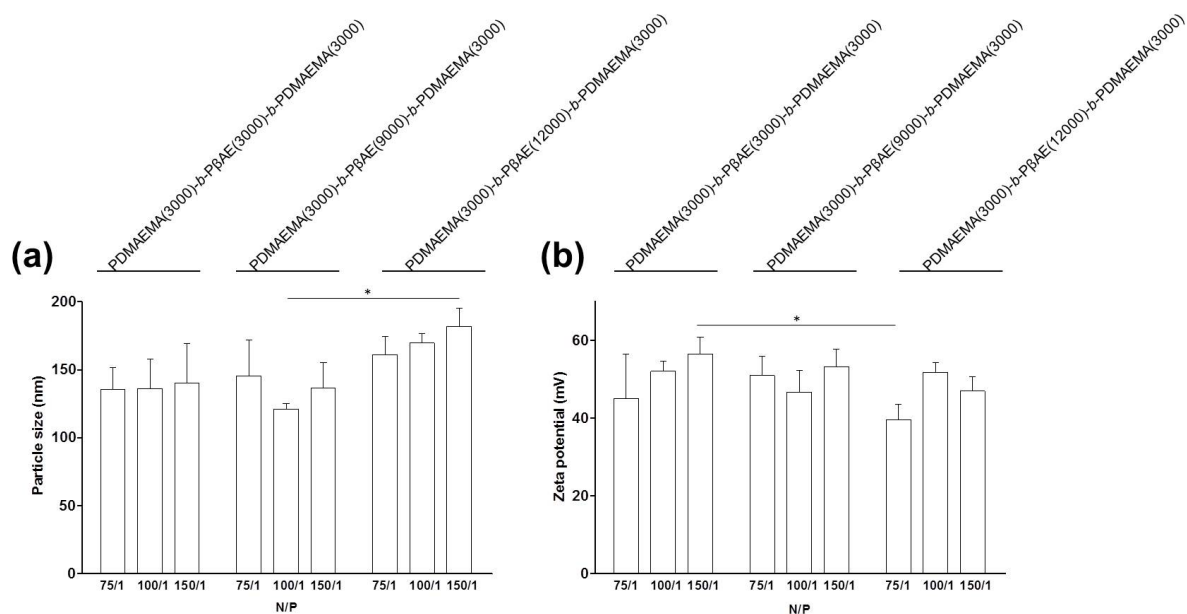
Figure 4.10: Particle size (a) and zeta potential (b) of PDMAEMA$_{3000}$-*b*-PβAE$_{3000}$-*b*-PDMAEMA$_{3000}$-, PDMAEMA$_{3000}$-*b*-PβAE$_{9000}$-*b*-PDMAEMA$_{3000}$- and PDMAEMA$_{3000}$-*b*-PβAE$_{12000}$-*b*-PDMAEMA$_{3000}$-based polyplexes. The polyplexes were prepared with 1 μg of pCMV.Luc at the indicated polymer/DNA (N/P) ratios. The data are expressed as particle size in nanometers (mean $\pm$ SD, n = 6) and zeta potential in mV (mean $\pm$ SD, n = 6). Two independent experiments were realized in triplicate. Asterisks ($*$ $p \leq 0.05$) indicate values that differ significantly.

During polyplexes formation, electrostatic interactions are established between cationic polymer and pDNA by mixing these two components in an aqueous solution. From Figure 4.10, it was observed that all PDMAEMA-*b*-PβAE-*b*-PDMAEMA block copolymers tested were able to efficiently condense pDNA into nanosized (120-180 nm) polyplexes. The entry into the cells, *i.e.*, the endocytosis process, is known to be dependent on the size of the polyplexes[24;25]. For an efficient cellular uptake and effective gene delivery in most cell types, the polyplexes should be in order of 200 nm[26]. Our best formulation, the polyplexes based on PDMAEMA$_{3000}$-*b*-PβAE$_{12000}$-*b*-PDMAEMA$_{3000}$ and prepared at 100/1 N/P ratio, presents a mean diameter of 170

nm, which is favorable to a successful gene delivery process. The similar particle size obtained for polyplexes prepared with block copolymers with different molecular weights may be explained by the fact that at a given N/P ratio a maximum condensation of DNA is reached and, consequently, from there on no significant change in size is observed.

Figure 4.10 (b) depicts the zeta potential (ζ) of polyplexes prepared at different N/P ratios. The assessed three block copolymers-based polyplexes exhibited positive zeta potential, with values ranging from 40 to 57 mV, showing the high content of cationic block copolymer at the polyplex surface. This fact is in agreement with the high level of DNA condensation observed for these polyplexes in the agarose gel and EtBr intercalation assays (Figure 4.9). Moreover, this positive surface charge is most probably associated to a higher degree of interaction with the cellular membrane promoting cellular uptake of the polyplexes[14]. Additionally, the positive charges could be involved in the destabilization of the endosomal membrane resulting in the release of the polyplexes into the cytosol and consequently in an increase in their biological activity[27].

The results presented in this study support the observation that polyplexes based on PDMAEMA$_{3000}$-*b*-PβAE$_{12000}$-*b*-PDMAEMA$_{3000}$ block copolymer with particle size around 170 nm and a positive surface charge have the ability to interact with target cells and induce their cellular internalization and release into the cytosol, consequently promoting high levels of transgene expression.

4.5   Conclusion

In the present study, PDMAEMA-*b*-PβAE-*b*-PDMAEMA triblock copolymers were prepared using a metal-free method to bind the PDMAEMA and PβAE segments. This new synthesis procedure led to an improvement of cell viability in the presence of these materials compared to previous data reported in Chapter 3. Moreover, high transfection efficiency was observed for higher N/P ratios, which are previously (Chapter 3) associated with low transgene expression and high cytotoxicity. Among the different block copolymers synthesized with different molecular weight

of PβAE segment, it was observed that polyplexes prepared using PDMAEMA$_{3000}$-*b*-PβAE$_{12000}$-*b*-PDMAEMA$_{3000}$ and DNA at 100/1 N/P ratio have shown a 60-fold and 50-fold higher transfection activity, in HeLa cells, and a 40-fold and 50-fold higher transfection activity, in COS-7 cells, than the best formulations of polyplexes generated with bPEI or TurboFect^{TM}, respectively. Comparing with the copolymer previously synthesized (Chapter 3), transgene expression increased of 5-fold and 9-fold in COS-7 and HeLa cells, respectively. Overall, these results confirm the high potential of the PDMAEMA$_{3000}$-*b*-PβAE$_{12000}$-*b*-PDMAEMA$_{3000}$ block copolymer as a non-viral gene delivery system.

4.6   Acknowledgements

Bibliography

[1] D.W. Pack, A.S. Hoffman, S. Pun, and P.S. Stayton. Design and development of polymers for gene delivery. *Nature Reviews Drug Discovery*, 4(7):581–593, 2005.

[2] S. Simões, A. Filipe, H. Faneca, M. Mano, N. Penacho, N. Düzgünes, and M. Pedroso de Lima. Cationic liposomes for gene delivery. *Expert Opinion on Drug Delivery*, 2(2):237–254, 2005.

[3] H. Faneca, A.L. Cardoso, S. Trabulo, S. Duarte, and MCP de Lima. Cationic liposome-based systems for nucleic acid delivery: from the formulation development to therapeutic applications. In *Drug Delivery Systems: Advanced Technologies Potentially Applicable in Personalised Treatment*, pages 153–184. Springer Netherlands, 2013.

[4] A. Mountain. Gene therapy: the first decade. *Trends in Biotechnology*, 18(3):119–128, 2000.

[5] J.H. Jeong, S.W. Kim, and T.G. Park. Molecular design of functional polymers for gene therapy. *Progress in Polymer Science*, 32(11):1239–1274, 2007.

[6] J.F.J. Coelho, P.C. Ferreira, P. Alves, R. Cordeiro, A.C. Fonseca, J.R. Góis, and M.H. Gil. Drug delivery systems: advanced technologies potentially applicable in personalized treatments. *The EPMA Journal*, 1(1):164–209, 2010.

[7] H.C. Kang, K.M. Huh, and Y.H. Bae. Polymeric nucleic acid carriers: current issues and novel design approaches. *Journal of Controlled Release*, 164(3):256–264, 2012. The 12th edition of the European Symposium on Controlled Drug Delivery, (ESCDD2012) April 4-6, 2012, Egmond aan Zee, The Netherlands.

[8] Z. Liu, Z. Zhang, C. Zhou, and Y. Jiao. Hydrophobic modifications of cationic polymers for gene delivery. *Progress in Polymer Science*, 35(9):1144–1162, 2010.

[9] G.T. Zugates, S.R. Little, D.G. Anderson, and R. Langer. Poly(*β*-amino ester)s for dna delivery. *Israel Journal of Chemistry*, 45(4):477–485, 2005.

[10] D.M. Lynn and R. Langer. Degradable poly(*β*-amino esters): synthesis, characterization, and self-assembly with plasmid DNA. *Journal of the American Chemical Society*, 122(44):10761–10768, 2000.

[11] H. Devalapally, D. Shenoy, S. Little, R. Langer, and M. Amiji. Poly(ethylene oxide)-modified poly(beta-amino ester) nanoparticles as a pH-sensitive system for tumor-targeted delivery of hydrophobic drugs: part 3. therapeutic efficacy and safety studies in ovarian cancer xenograft model. *Cancer Chemotherapy and Pharmacology*, 59(4):477–484, 2007.

[12] S. Agarwal, Y. Zhang, S. Maji, and A. Greiner. PDMAEMA based gene delivery materials. *Materials Today*, 15(9):388–393, 2012.

[13] Y.K. Kim, C. Zhang, C.S. Cho, M.H. Cho, and H.L. Jiang. Poly(amino ester)s-based polymeric gene carriers in cancer gene therapy. *InTech*, 2013.

[14] Y. Yue and C. Wu. Progress and perspectives in developing polymeric vectors for *in vitro* gene delivery. *Biomaterials Science*, 1:152–170, 2013.

[15] L. Mespouille, M. Vachaudez, F. Suriano, P. Gerbaux, W. Van Camp, O. Coulembier, P. Degée, R. Flammang, F. Du Prez, and P. Dubois. Controlled synthesis of amphiphilic block copolymers based on polyester and poly(amino methacrylate): comprehensive study of reaction mechanisms. *Reactive and Functional Polymers*, 68(5):990–1003, 2008.

[16] H. Faneca, A. Faustino, and M.C. Pedroso de Lima. Synergistic antitumoral effect of vinblastine and HSV-Tk/GCV gene therapy mediated by albumin-associated cationic liposomes. *Journal of Controlled Release*, 126(2):175–184, 2008.

[17] X.B. Dou, Y. Hu, N.N. Zhao, and F.J. Xu. Different types of degradable vectors from low-molecular-weight polycation-functionalized poly(aspartic acid) for efficient gene delivery. *Biomaterials*, 35(9):3015–3026, 2014.

[18] L. Mespouille, P. Degee, and P. Dubois. Amphiphilic poly(N,N-dimethylamino-2-ethyl methacryl ate)-*g*-poly(epsilon-caprolactone) graft copolymers: synthesis and characterisation. *European Polymer Journal*, 41(6):1187–1195, 2005.

[19] J.C. Sunshine, M.I. Akanda, D. Li, K.L. Kozielski, and J.J. Green. Effects of base polymer hydrophobicity and end-group modification on polymeric gene delivery. *Biomacromolecules*, 12(10):3592–3600, 2011.

[20] Z. Kadlecova, S. Nallet, D.L. Hacker, L. Baldi, H.A. Klok, and F.M. Wurm. Poly(ethyleneimine)-

mediated large-scale transient gene expression: influence of molecular weight, polydispersity and N-propionyl groups. *Macromolecular Bioscience*, 12(5):628–636, 2012.

[21] U. Lungwitz, M. Breunig, T. Blunk, and A. Göpferich. Polyethylenimine-based non-viral gene delivery systems. *European Journal of Pharmaceutics and Biopharmaceutics*, 60(2):247–266, 2005.

[22] A.A. Eltoukhy, D.J. Siegwart, C.A. Alabi, J.S. Rajan, R. Langer, and D.G. Anderson. Effect of molecular weight of amine end-modified poly(*β*-amino ester)s on gene delivery efficiency and toxicity. *Biomaterials*, 33(13):3594–3603, 2012.

[23] J.C. Sunshine, D.Y. Peng, and J.J. Green. Uptake and transfection with polymeric nanoparticles are dependent on polymer end-group structure, but largely independent of nanoparticle physical and chemical properties. *Molecular Pharmaceutics*, 9(11):3375–3383, 2012.

[24] A. Aied, U. Greiser, A. Pandit, and W. Wang. Polymer gene delivery: overcoming the obstacles. *Drug Discovery Today*, 18:1090–1098, 2013.

[25] C. Scholz and E. Wagner. Therapeutic plasmid DNA *versus* siRNA delivery: Common and different tasks for synthetic carriers. *Journal of Controlled Release*, 161(2):554–565, 2012.

[26] A. El-Sayed and H. Harashima. Endocytosis of gene delivery vectors: from clathrin-dependent to lipid raft-mediated endocytosis. *Molecular Therapy*, 21(6):1118–1130, 2013.

[27] M.S. Shim and Y.J. Kwon. Stimuli-responsive polymers and nanomaterials for gene delivery and imaging applications. *Advanced Drug Delivery Reviews*, 64(11):1046–1059, 2012.

CHAPTER 5

Final remarks

5.1   Conclusions

Gene therapy provides great opportunity for treating a wide range of diseases from genetic disorders to infections or cancer. To achieve a successful therapy, the design and development of proper gene carrier is one of the most important factors. Polymer-based non-viral gene delivery systems have been extensively studied for this purpose due to their facile tune structure using vast polymer chemistry strategies. However, despite the great effort in this area, efficient polymer-based vectors remain a major challenge.

To overcome this problem, it was proposed a combination of PDMAEMA and PβAE, two of the most used cationic polymers in gene delivery, in a single material. The totally cationic block copolymer would consist in a central segment of PβAE with PDMAEMA as terminal segments (PDMAEMA-*b*-PβAE-*b*-PDMAEMA).

Thus, the first main aim of this thesis was to develop a new block copolymer PDMAEMA-*b*-PβAE-*b*-PDMAEMA. In this direction, the homopolymers were synthesized. While for PβAE was used a reported procedure described in the literature, for PDMAEMA (Chapter 2) was developed a new and more biocompatible and environmentally-friendly catalytic system based on SARA ATRP method comprising Fe(0) and very low amounts of $CuBr_2$ deactivator. In addition, the best reaction performance occurred at room temperature in an alcohol-water solvent mixture. The stringent control reported with this more biocompatible catalytic system combined with the attractive environmental characteristics of alcohol-water media suggests that this may be an interesting system to polymerize other monomers used in biomedical applications. Moreover, the results demonstrated, not only a good control over the PDMAEMA structure concerning to molecular weight and dispersity, but also the possibility to prepare PDMAEMA polymers initiated with biological interest molecules such as cholesterol and PEG.

After homopolymer synthesis, the PDMAEMA-*b*-PβAE-*b*-PDMAEMA block copolymers were prepared by copper(I)-catalyzed azide-alkyne cycloaddition (CuAAC). A preliminary evaluation as pDNA carrier was also assessed in two different cell lines, HeLa and COS-7 cells. At this stage, it was also evaluated the

influence of molecular weight of the PDMAEMA and, for this purpose, two different molecular weights were assessed (3,000 and 8,000 g.mol^{-1}). Surprisingly, the results showed a great difference in transfection activity between PDMAEMA$_{8000}$-b-PβAE$_{3000}$-b-PDMAEMA$_{8000}$ and PDMAEMA$_{3000}$-b-PβAE$_{3000}$-b-PDMAEMA$_{3000}$, revealing the last one better transfection activity. These results highlight the crucial role of the terminal modifications of PβAE on transfection activity. However, a critical issue was observed at this stage, the final block copolymers exhibited remaining copper residues even after purification procedures. The easy degradability of PβAE in water and the weak solubility of copper in organic solvents with low boiling point (for an easy removal at the end of the reaction) make the efficient copper removal extremely difficult. Thus, it has emerged the necessity to develop a new method to prepare the copolymer without the need of any metal catalyst.

Accordingly, Chapter 4 encompasses the other two main objectives of the thesis: a new catalyst-free method for block copolymer preparation and the evaluation of the influence of the molecular weight of the PβAE segment in the transfection activity. Therefore and taking into account the results obtained in Chapter 3, the molecular weight of the PDMAEMA was fixed for 3,000 g.mol^{-1} and the molecular weight of PβAE segments was varied. Concerning to catalyst-free block copolymer preparation, the modification of the terminal-ends of PβAE and PDMAEMA allow to couple them by a metal-free method - Michael addition reaction. These changes on the block copolymer method preparation allowed obtaining higher cell viability results even for high N/P ratios (100/1) of the polyplexes. Shortly, crossing the results obtained by the two methods of block copolymer preparation, it suggests that even residual amounts of copper induce some cytotoxicity. Regarding to molecular weight influence of the PβAE segment on *in vitro* transfection activity, the results showed that the block copolymers with segments of the PβAE with higher molecular weight (PDMAEMA$_{3000}$-b-PβAE$_{9000}$-b-PDMAEMA$_{3000}$ and PDMAEMA$_{3000}$-b-PβAE$_{12000}$-b-PDMAEMA$_{3000}$) have higher transfection activity compared to PDMAEMA$_{3000}$-b-PβAE$_{3000}$-b-PDMAEMA$_{3000}$. In addition, the results of transfection activity of PDMAEMA$_{3000}$-b-PβAE$_{12000}$-b-PDMAEMA$_{3000}$ block copolymer when compared to bPEI$_{25000}$ or TurboFect^{TM}, the two most common

used standard transfection reagents, shown to be between 40- and 60-fold higher. Moreover, when this best formulation is compared to best formulation prepared by CuAAC reaction it was observed, besides the decrease of toxicity for high N/P ratios, an improvement in transfection activity around 5- and 9-fold in COS-7 and HeLa cells, respectively.

To sum up, this PhD work allowed the development of a novel polymeric nucleic acid delivery vector based on biodegradable PβAE and PDMAEMA. The obtained results show improved *in vitro* transfection efficiency and high cell viability compared to PEI, a gold standard for polymeric non-viral vectors, and a commercial polymeric transfection reagent, the TurboFect$^{\text{TM}}$ in two different cell lines (COS-7 and HeLa cell lines).

5.2   Future work

The results presented in this project constitute an important basis to explore new avenues in the area of polymeric vectors. Among several possibilities to continue the work, the following ideas are considered to be of particular relevance:

- To continue the evaluation of the *in vitro* transfection assays will be of the interest (such as, serum-containing cell culture medium transfection assays) in order to evaluate the transfection activity in presence of proteins;

- To evaluate the polyplex stability (such as, against heparin replacement or DNAse I agarose gel) as well as polyplex colloidal stability (*i.e.*, in cell culture medium);

- To evaluate the *in vivo* transfection capacity in an animal model;

- To assess the transfection activity of the PDMAEMA-*b*-PβAE-*b*-PDMAEMA-based polyplexes as carrier of other nucleic acids, such as siRNA or microRNA. In addition, a co-delivery of drug and nucleic acid could also be further studied;

- To evaluate *in vitro* and *in vivo* transfection activity of PDMAEMA-*b*-PβAE-*b*-PDMAEMA-based polyplexes as carrier of a therapeutic gene.

5.3   Final remarks

The work developed introduced a new area - gene therapy - in the group where I have done this project (Polymer Research Group). The establishment of a transfection assay protocol for PDMAEMA-*b*-PβAE-*b*-PDMAEMA block copolymers-based polyplexes was, perhaps, the most challenging difficulty that I needed to overcome. Despite valuable help of Vectors and Gene Therapy research group of Center of Neurosciences and Cell Biology at University of Coimbra, the scarce experience of the group with polymeric vectors, the lack of information about the experimental procedures in the literature, and the fact of pH-responsiveness of the used polymers made it a demanding and laborious task. After all this process, the group gained a new valence and can explore even further in this area.
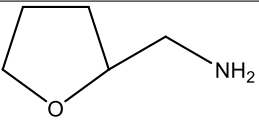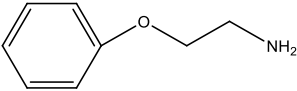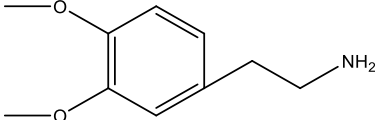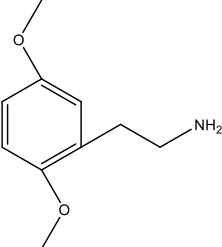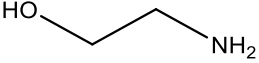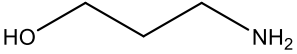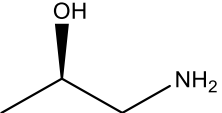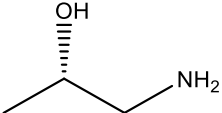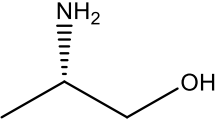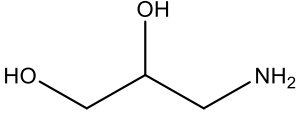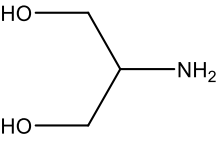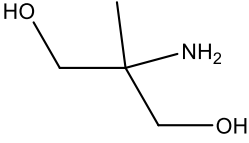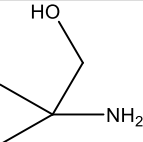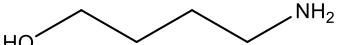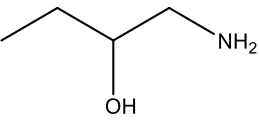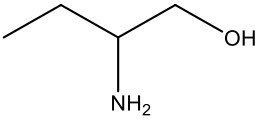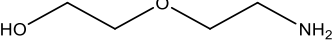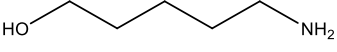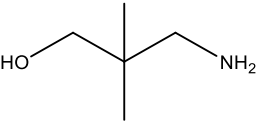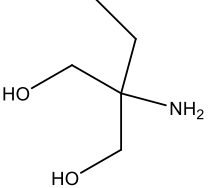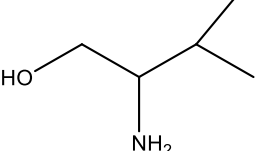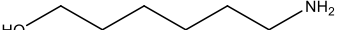
Appendices
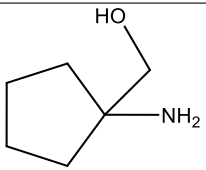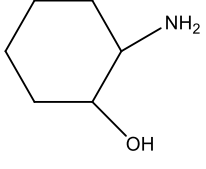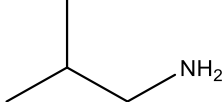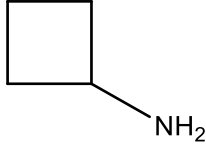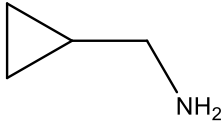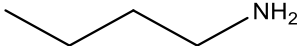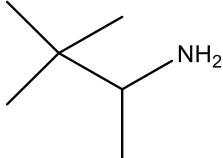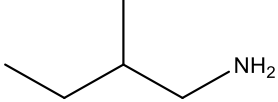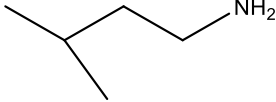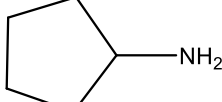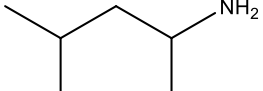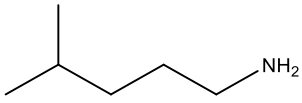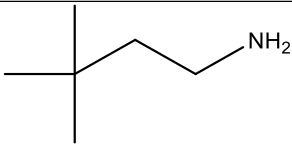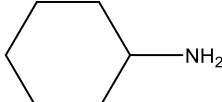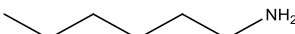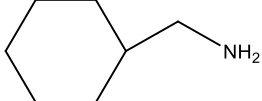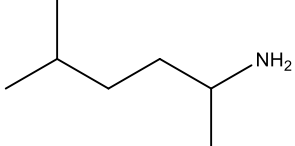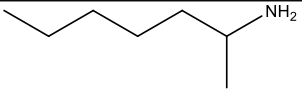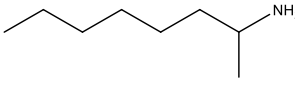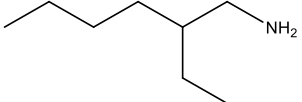
APPENDIX A
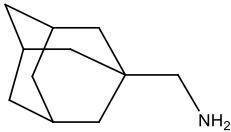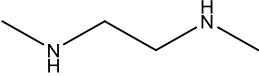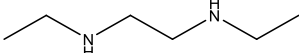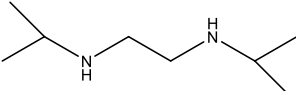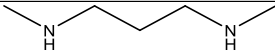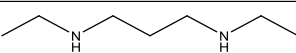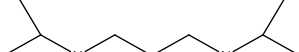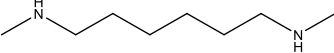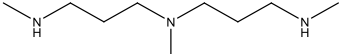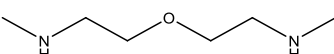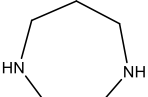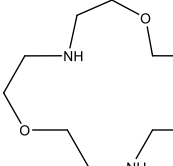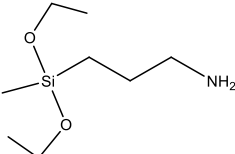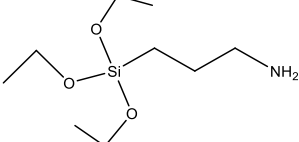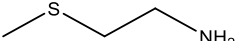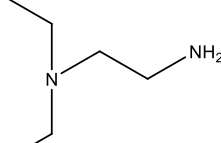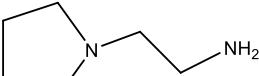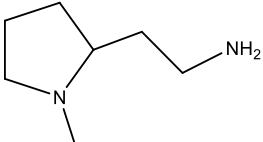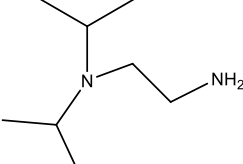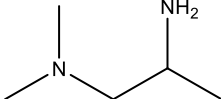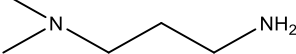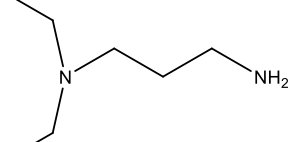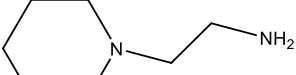
Acrylates/amines library
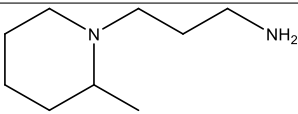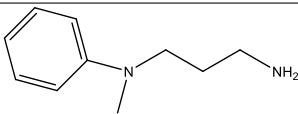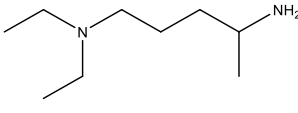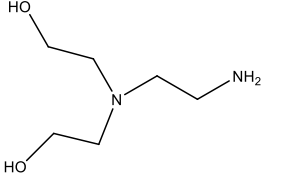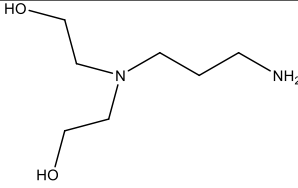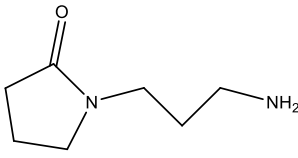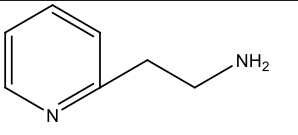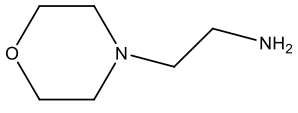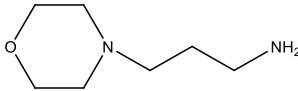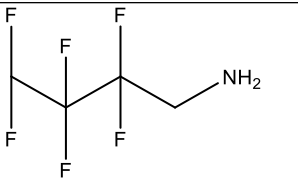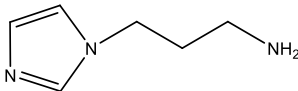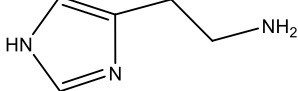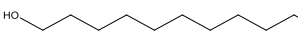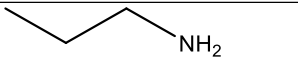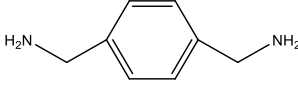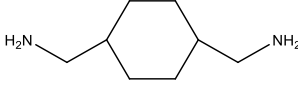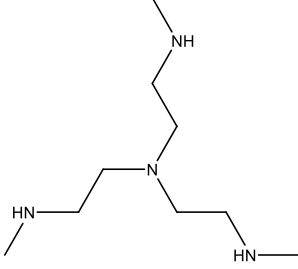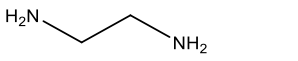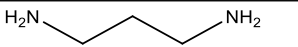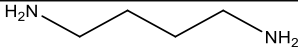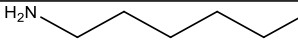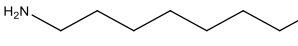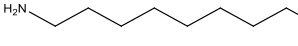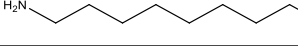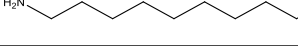
Table A.1: Schematic representation of amines cataloged by Langer lab.

1		2	
3		4	
5		6	
7		8	
9		10	
11		12	
13		14	

15		16	
17		18	
19		20	
21		22	
23		24	
25		26	
27		28	
29		30	
31		32	
33		34	
35		36	

37		38	
39		40	
41		42	
43		44	
45		46	
47		48	
49		50	
51		52	
53		54	
55		56	
57		58	
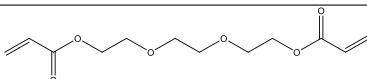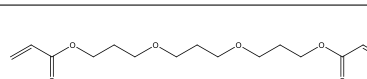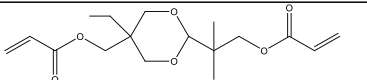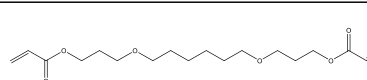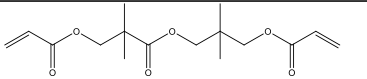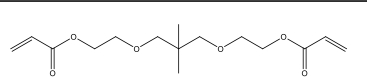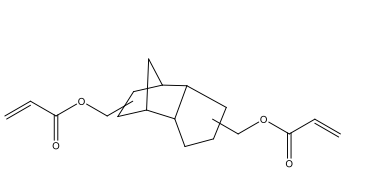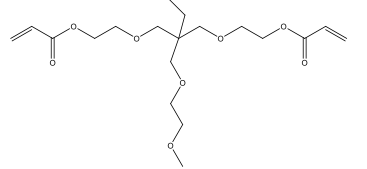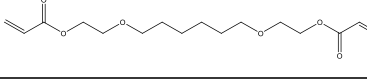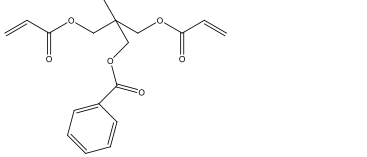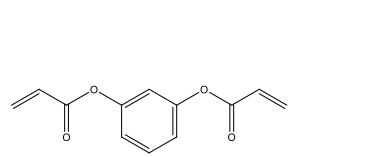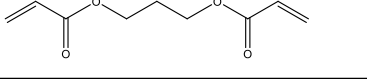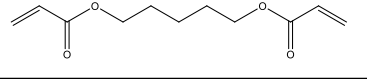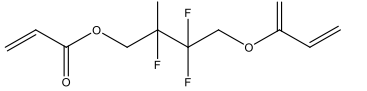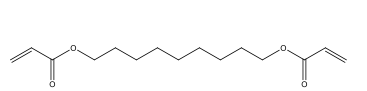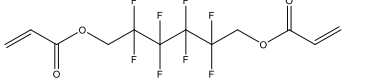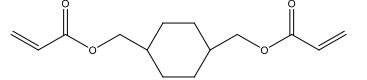
59		60	
61		62	
63		64	
65		66	
67		68	
69		70	
71		72	
73		74	
75		76	
77		78	
79		80	
81		82	

83		84	
85		86	
87		88	
89		90	
91		92	
93		94	
95		96	
98		99	
101		102	
103		104	
105		106	
107		108	
109		110	

111		115	
116		117	
118		121	
122		123	
124		125	
126		127	
128		208	
210		212	
213		221	
225		228	

Table A.2: Schematic representation of diacrylates cataloged by Langer lab.

A		B	
C		D	
E		F	
J		K	

L		M	
O		P	
Q		R	
S		T	
U		Z	
AA		BB	
II		JJ	
KK		LL	
PP			

APPENDIX B

Supporting Information

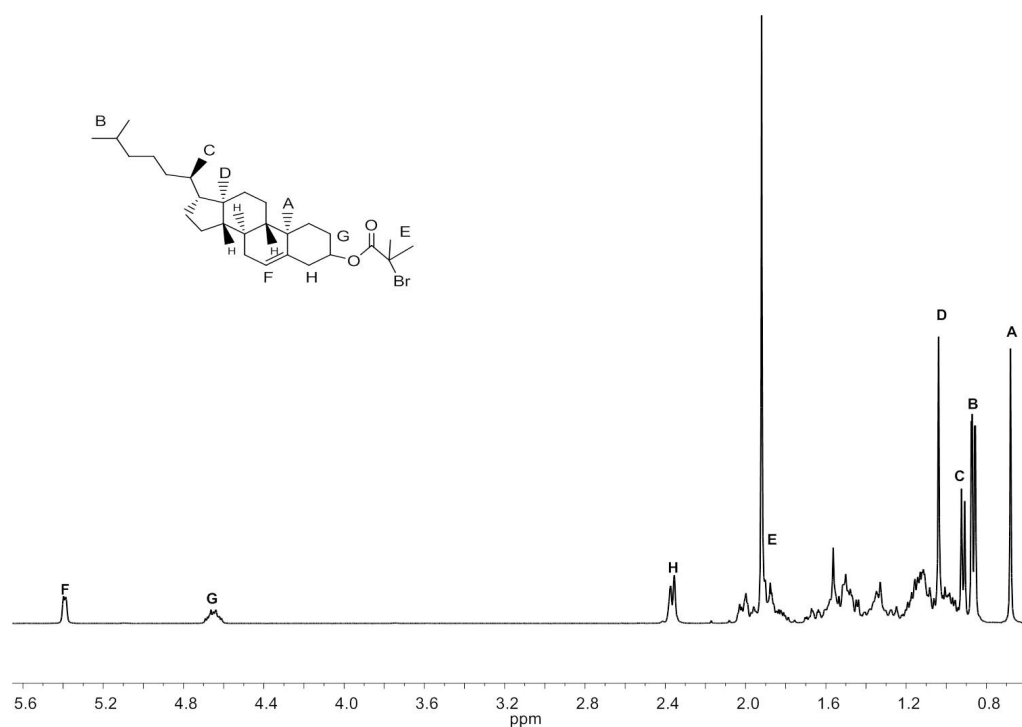The supplementary information of Chapters 2, 3 and 4 will be presented in this appendix.

Figure B.1: ^{1}H NMR spectrum (CDCl$_3$, 400 MHz) and structural assignment of CHO-Br.

Figure B.1 ^{1}H NMR (CDCl$_3$, 400 MHz): δ = 0.68 (s, 3H, cholesteryl CH_3), 0.86 (d, 6H, cholesteryl CH_3), 0.912 (d, 3H, cholesteryl CH_3), 1.046 (s, 3H, cholesteryl CH_3), 0.95-2.00 (m, 28H, cholesteryl CH and CH_2), 1.92 (s, 6H, (CH_3)$_2$-C-Br), 2.37 (d, 1H, CH=C-CH_2), 4.66 (m, 1H, CH-O-COC(CH$_3$)$_2$-Br), 5.39 (s, 1H, CH=C).
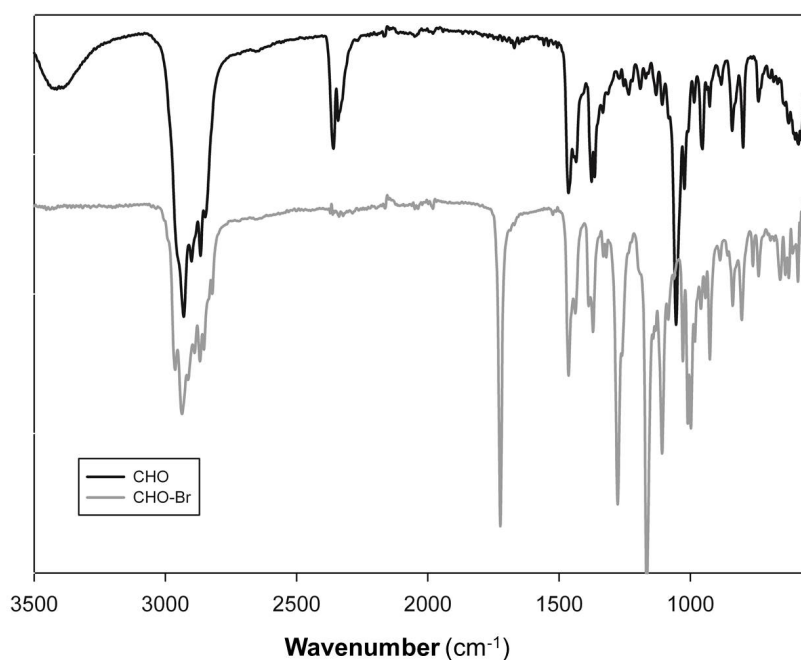

Figure B.2: FTIR-ATR spectrum of cholesterol (black line) and cholesterol initiator (grey line).

Figure B.2 FTIR-ATR (cm^{-1}): 3016-2782(C-H stretching), 1723 (ester, C=O stretch), 1463-1370 (C=C aromatic), 1280-1100 (ester, C-O stretch).

Synthesis of 2-(2-azidoethoxy)ethyl bromoisobutyrate (N$_3$EiBBr)

Azide end-terminal initiator 2-(2-azidoethoxy)ethyl bromoisobutyrate (N$_3$EiBBr) was synthesized based on the procedure described in the literature[1].
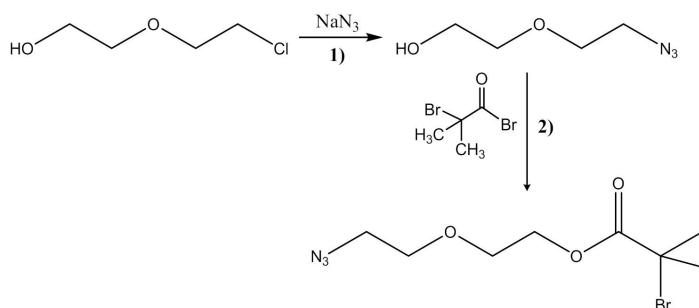
Scheme B.1: Synthesis of 2-(2-azidoethoxy)ethyl bromoisobutyrate (N$_3$EiBBr).

1) Synthesis of 2-(2-azidoethoxy)ethanol. In a round bottom flask surmounted by a reflux column were introduced 5 g of 2-(2-chloroethoxy)ethanol (40.14 mmol), 13.05 g of NaN_3 (200.69 mmol) and 25 mL of distilled water. The mixture was refluxed for 24h at 75 °C, then cooled down and treated with aqueous HCl solution (1 mol.L^{-1}). The aqueous solution was extracted by EtOAC and the organic solvent was evaporated under reduced pressure. The final product was passed over a basic alumina column. Yield: 90%. ^{13}C NMR (100 MHz, D_2O, δ (ppm) (Figure B.3): 50.23 (N_3-CH_2-), 60.38 (-CH_2-OH), 69.12 (N_3-CH_2-CH_2-O), 71.64 (O-CH_2-CH_2-OH).
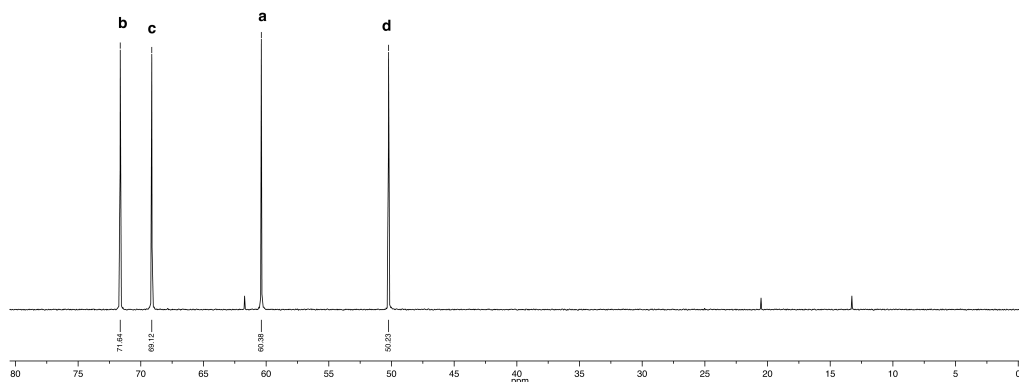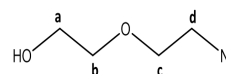

Figure B.3: ^{13}C NMR spectrum (D_2O, 100 MHz) of 2-(2-azidoethoxy)ethanol.

2) Synthesis of 2-(2-azidoethoxy)ethyl bromoisobutyrate (N_3EiBBr). In a round bottom flask were introduced 4 g of 2-(2-azidoethoxy)ethanol (30.50 mmol), 8.5 ml of NEt_3 (61.00 mmol) and 17 ml of THF. A solution of 4.15 ml of 2-bromoisobutyryl bromide (33.55 mmol) in 17 ml of THF was added dropwise at 0 °C. After 48 h at room temperature, insoluble ammonium salts were filtered off and the filtrate was passed over a basic alumina column. The final product was recovered by evaporation of THF. Yield: 74%. ^{1}H NMR (400 MHz, CDCl$_3$, δ (ppm)) (Figure B.4): 1.95 (s, 6H, (CH_3)$_2$C), 3.39 (t, 2H, CH_2N$_3$), 3.70 (t, 2H, N$_3$CH$_2$CH_2O), 3.76 (t, 2H, COOCH$_2$CH_2O), 4.35 (t, 2H, CH_2OCO). ^{13}C NMR (100 MHz, CDCl$_3$, δ (ppm)) (Figure B.5): 30.72 (C(CH$_3$)$_2$), 50.74 (N$_3$-CH_2-), 55.72 (-CH_2-O-C(O)-), 65.01

(C(CH$_3$)$_2$-), 68.79 (N$_3$-CH$_2$-CH$_2$-O), 70.17 (O-CH$_2$-CH$_2$-), 171.63 (O-C(O)-).
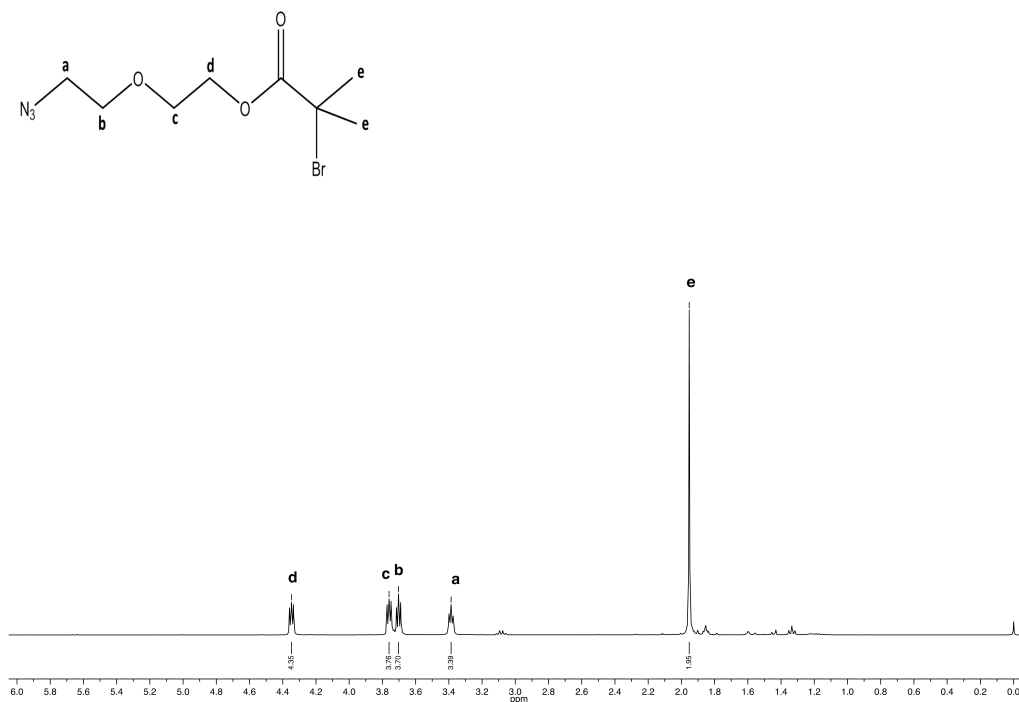

Figure B.4: ^{1}H NMR spectrum (CDCl$_3$, 400 MHz) of 2-(2-azidoethoxy)ethyl bromoisobutyrate.
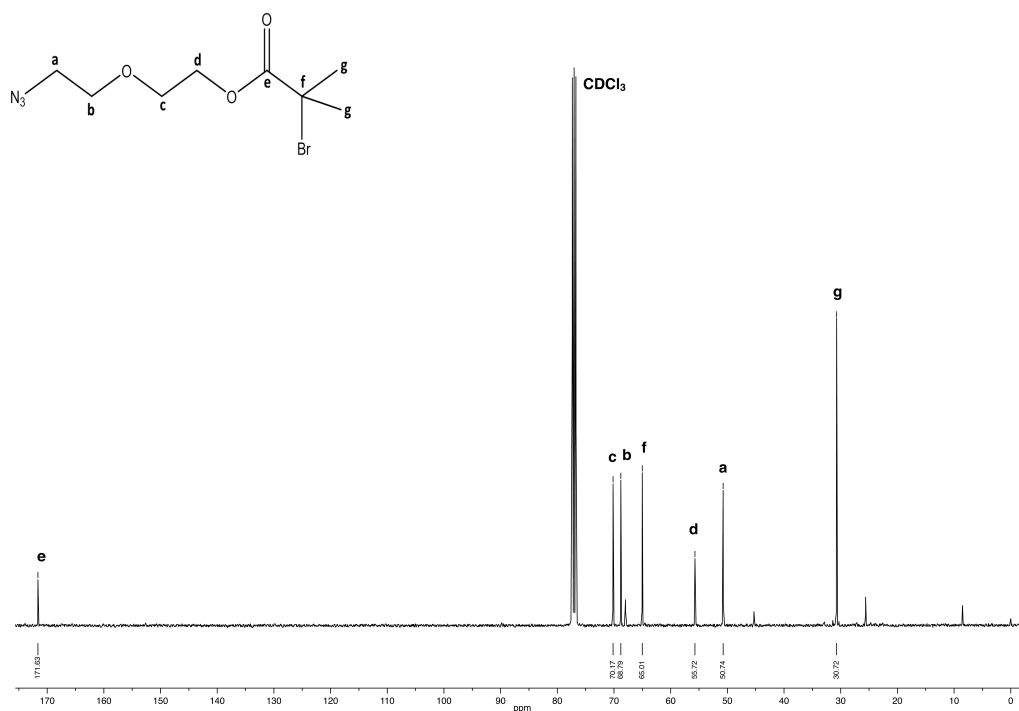

Figure B.5: ^{13}C NMR spectrum (CDCl$_3$, 100 MHz) of 2-(2-azidoethoxy)ethyl bromoisobutyrate.
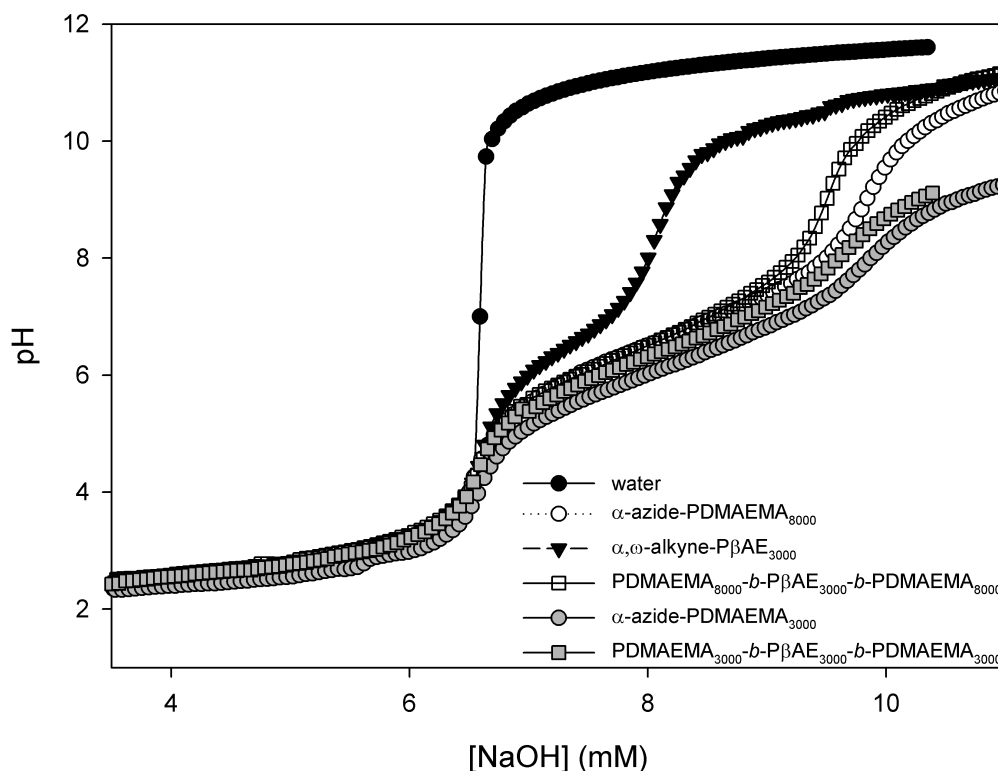
Figure B.6: Potentiometric titration curves of α-azide-PDMAEMA$_{8000}$ (white circles), α-azide-PDMAEMA$_{3000}$ (grey circles), α,ω-alkyne- PβAE$_{3000}$ (black triangles) and block copolymers PDMAEMA$_{8000}$-b-PβAE$_{3000}$-b-PDMAEMA$_{8000}$ (white squares) and PDMAEMA$_{3000}$-b-PβAE$_{3000}$-b-PDMAEMA$_{3000}$ (grey squares) in Milli-Q water. The initial polymer/copolymer solutions were prepared to contain a fixed amount of mass (25 mg) in a total initial volume of 40 mL. Initially, the pH of the solution was acidified with 2.35 mL of 1% HCl aqueous solution. The solution was then titrated with 25 μL aliquots of 0.1 M NaOH. The x-axis label of the plot, [NaOH], denotes the total concentration of added NaOH. The titration data for pure water obtained under an identical set of conditions (black circles) are also shown for reference. For correction of experimental errors, the original titration curves (Figure 3.5) have been shifted by constant factors with respect to water data using the procedure described in literature[2]. Measurements were taken using a Crison Basic 20 pH meter.
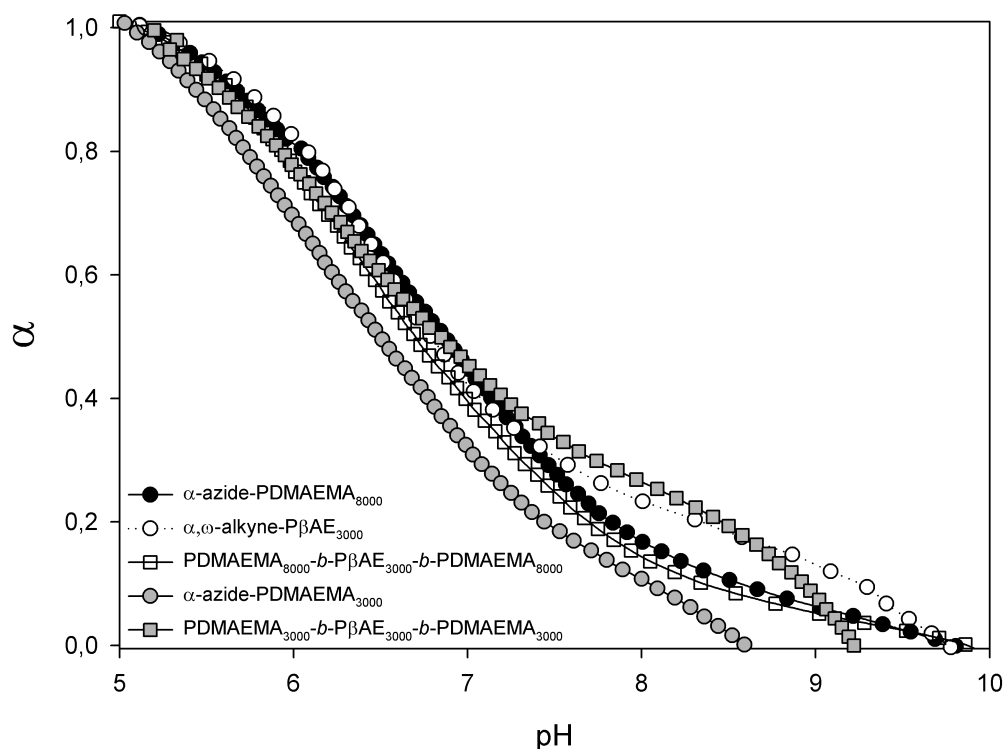
Figure B.7: Plots of the degree of protonation of the amine groups (α) *vs* pH for the α-azide-PDMAEMA$_{8000}$ (black circles), α-azide-PDMAEMA$_{3000}$ (grey circles), α,ω-alkyne-PβAE$_{3000}$ (white circles) and block copolymers PDMAEMA$_{8000}$-*b*-PβAE$_{3000}$-*b*-PDMAEMA$_{8000}$ (white squares) and PDMAEMA$_{3000}$-*b*-PβAE$_{3000}$-*b*-PDMAEMA$_{3000}$ (grey squares) in Milli-Q water, estimated from the data shown in Figure B.6 using equation α(pH) = {[amine]$_i$.V$_i$ - [NaOH]$_{0,amine}$(pH).V$_{amine}$(pH) + [NaOH$_{0,water}$(pH).V$_{water}$(pH)/[amine]$_i$.V$_i$}, where [NaOH]$_0$ denotes the nominal concentration of added NaOH (after correction) and *V* the total volume of the solution at a given point of titration, and the subscripts, *amine*, *water*, and *i* represent, respectively, the amine titration measurement, the water titration measurement, and the initial condition of the titration experiments.
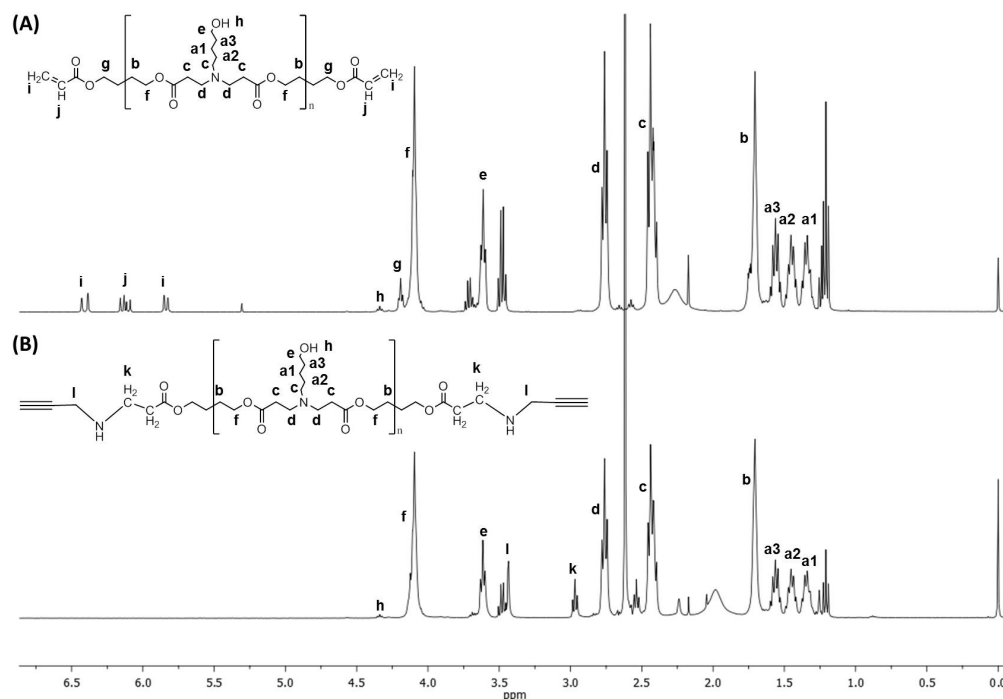
Figure B.8: ^{1}H NMR spectrum (CDCl$_3$, 400 MHz) of α,ω-acrylate-PβAE (A) and α,ω-alkyne-PβAE (B).

Figure B.8 (A). ^{1}H NMR (CDCl$_3$, 400 MHz, δ (ppm)): 1.30-1.38 (2H, br, NCH$_2$CH$_2$C*H*$_2$CH$_2$CH$_2$OH), 1.42-1.49 (2H, br, NCH$_2$C*H*$_2$CH$_2$CH$_2$CH$_2$OH), 1.53-1.60 (2H, br, NCH$_2$CH$_2$CH$_2$C*H*$_2$CH$_2$OH), 1.65-1.77 (4H, br, CH$_2$CH$_2$NCH$_2$CH$_2$(COO)CH$_2$C*H*$_2$C*H*$_2$CH$_2$(COO)), 2.35-2.46 (6H, br, CH$_2$C*H*$_2$NCH$_2$C*H*$_2$(COO)CH$_2$CH$_2$CH$_2$CH$_2$(COO) and NC*H*$_2$CH$_2$CH$_2$CH$_2$CH$_2$OH), 2.68-2.81 (4H, br, CH$_2$C*H*$_2$NC*H*$_2$CH$_2$(COO)CH$_2$CH$_2$CH$_2$CH$_2$(COO), 3.55-3.65 (2H, NCH$_2$CH$_2$CH$_2$CH$_2$C*H*$_2$OH), 4.03-4.14 (4H, br, CH$_2$CH$_2$NCH$_2$CH$_2$(COO)C*H*$_2$CH$_2$CH$_2$C*H*$_2$(COO), 4.18-4.23 (br, C*H*$_2$(COO)CH=CH$_2$), 4.31-4.38 (br, NCH$_2$CH$_2$CH$_2$CH$_2$CH$_2$O*H*), 5.81-5.88 (d, COOCH=C*H*$_2$), 6.06-6.18 (dd, COOC*H*=CH$_2$), 6.36-6.45 (d, COOCH=C*H*$_2$).

Figure B.8 (B). ^{1}H NMR (CDCl$_3$, 400 MHz, δ (ppm)): 1.31-1.38 (2H, br, NCH$_2$CH$_2$C*H*$_2$CH$_2$CH$_2$OH), 1.42-1.49 (2H, br, NCH$_2$C*H*$_2$CH$_2$CH$_2$CH$_2$OH), 1.53-1.60 (2H, br, NCH$_2$CH$_2$CH$_2$C*H*$_2$CH$_2$OH), 1.65-1.78 (4H, br, CH$_2$CH$_2$NCH$_2$CH$_2$(COO)CH$_2$C*H*$_2$C*H*$_2$CH$_2$(COO)), 2.39-2.48 (6H, br, CH$_2$C*H*$_2$NCH$_2$C*H*$_2$(COO)CH$_2$CH$_2$CH$_2$CH$_2$(COO) and NC*H*$_2$CH$_2$CH$_2$CH$_2$CH$_2$OH), 2.70-2.81 (4H, br, CH$_2$C*H*$_2$NC*H*$_2$CH$_2$(COO)CH$_2$CH$_2$CH$_2$CH$_2$(COO), 2.93-2.99 (2H, (COO)CH$_2$C*H*$_2$NHCH$_2$CCH), 3.41-3.45 (2H, CH$_2$NHC*H*$_2$CCH)

3.54-3.66 (2H, NCH$_2$CH$_2$CH$_2$CH$_2$CH_2OH), 4.03-4.18 (4H, br, CH$_2$CH$_2$NCH$_2$CH$_2$(COO)CH_2CH$_2$CH$_2$CH$_2$(COO)), 4.31-4.37 (br, NCH$_2$CH$_2$CH$_2$CH$_2$CH$_2$OH).
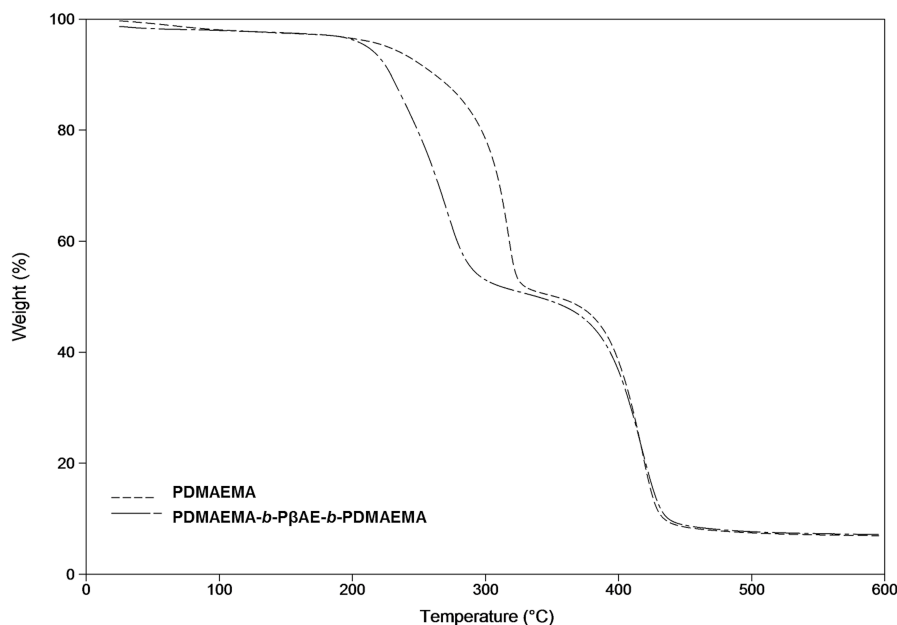

Figure B.9: TGA weight loss curves of α-azide-PDMAEMA (short dashed line) and PDMAEMA-*b*-PβAE-*b*-PDMAEMA (broken dashed line).

Table B.1: Characteristics quantities (average $\pm$ standard deviation) of poly[2-(dimethylamino)ethyl methacrylate] and poly[2-(dimethylamino)ethyl methacrylate]-*b*-poly(β-amino ester)-*b*-poly[2-(dimethylamino)ethyl methacrylate] obtained from TGA data.

Sample	Weight loss ($^\circ$C)		
	$T_{5\%}$ ($^\circ$C)	$T_{10\%}$ ($^\circ$C)	T_{on} ($^\circ$C)
α-Azide-PDMAEMA	226.76 $\pm$ 1.25	263.20 $\pm$ 1.62	294.79 $\pm$ 2.62
PDMAEMA-*b*-PβAE-*b*-PDMAEMA	212.77 $\pm$ 2.51	229.59 $\pm$ 1.36	229.35 $\pm$ 1.26

Subculturing procedure for 3T3-L1, TSA, HeLa and COS-7 cell lines. 3T3-L1 (mouse embryonic fibroblast cell line), TSA (BALB/c female mouse mammary adenocarcinoma cell line), HeLa (human epithelial cervical carcinoma cell line) and COS-7 (african green monkey kidney fibroblast-like) cells were maintained at 37 $^\circ$C, under 5% CO$_2$, in Dulbecco's modified Eagle's medium-high glucose (DMEM-HG) (Irvine Scientific, Santa Ana, CA) supplemented with 10% (v/v) heat inactivated fetal bovine serum (FBS) (Sigma, St. Louis, MO), penicillin (100 U/mL) and streptomycin (100 μg/mL). Both cell lines grown in monolayer and were detached by treatment

with trypsin solution 0.25% (Sigma, St. Louis, MO). For biological activity studies, 2.0×10^4 HeLa cells were seeded in 1 mL of medium in 48-well culture plates, 24 h before study, and used at 70% confluence.

APPENDIX C

Comparative biocompatibility evaluation of poly(β-amino ester) and poly[2-(dimethylamino)ethyl methacrylate]

C.1   Introduction

Polycationic polymers have attracted increasing attention in the past decade for biomedical applications, mainly as non-viral vectors for gene delivery[3]. The optimal polymer structure for gene delivery carrier should combine low cytotoxicity with high transfection efficiency. In this work we compare the cell viability in two different cell lines (3T3-L1 and TSA) for two broadly used polycationic polymers in gene delivery: poly[2-(dimethylamino)ethyl methacrylate)] (PDMAEMA) and a poly(β-amino ester) (PβAE).

C.2   Methods

PDMAEMA was synthesized and purified as previously described[4]. PβAE was synthesized through Michael addition reaction between 5-amino-1-pentanol (1.5 g, 14.54 mmol) and 1,4-butanediol diacrylate (3.20 mL, 17.45 mmol) in dry acetone. After 24 h, the solution was dripped slowly and washed (3 times) into cold diethyl ether. PβAE was dried under reduced pressure and then dried overnight at 40 °C under vacuum. PβAE was stored at -20 °C until use. Cell viability was assessed by a modified Alamar Blue assay, as previously described[5] in two different cell lines (3T3-L1 (mouse embryonic fibroblast cell line) and TSA (BALB/c female mouse mammary adenocarcinoma cell line)). Cell viability (as a percentage of control cells) was calculated according to the equation:

$$Cell\ viability = (A_{570} - A_{600}) / (A'_{570} - A'_{600}) \times 100 \tag{C.1}$$

where A_{570} and A_{600} are the absorbances of the samples, and A'_{570} and A'_{600} those of control cells, at the indicated wavelengths. Values of cell viability measured by the Alamar Blue assay are expressed as a percentage of the untreated control cells (mean $\pm$ SD) obtained from three independent experiments with triplicates.

C.3   Results

The cell viability assays reveal substantial differences between PDMAEMA and PβAE in both studied cell lines. The PβAE shows low cytotoxicity, being observed high levels of viability for both cell lines, even when incubated with high concentrations of PβAE.

C.4   Discussion and conclusions

In this study we have shown that PβAE is much more biocompatible, even at high concentrations, than PDMAEMA as indicated by the viability assays.

C.5   Acknowledgments

APPENDIX D

Evaluation of the biocompatibility of cholesterol-poly[2-(dimethylamino)ethyl methacrylate] synthesized by atom transfer radical polymerization

D.1   Introduction

The use of the reversible deactivation radical polymerization (RDRP) method to prepare tailor made polymers has been proved to be a powerful tool in the synthesis of polymeric structures to biological studies[3,4]. In this work, we report the development of a RDRP method for poly[2-(dimethylamino)ethyl methacrylate)] (PDMAEMA) synthesis using mild conditions initiated with a cholesterol molecule. The viability for *in vitro* applications of the polymer was evaluated in two different cell lines.

D.2   Methods

Cholesteryl-2-bromoisobutyrate and cholesterol-PDMAEMA (CHO-PDMAEMA) were synthesized according to a previously reported method[4]. The final product was characterized by proton nuclear magnetic resonance (^{1}H NMR), size exclusion chromatography (SEC) and in terms of their cytotoxicity, by a modified Alamar Blue assay[5] in 3T3-L1 and TSA cells, 48 hours after incubation with the polymer. Values of cell viability are expressed as a percentage of the untreated control cells (mean $\pm$ SD) obtained from three independent experiments with triplicates.

D.3   Results

The ^{1}H NMR spectrum and SEC trace confirms the well controlled structure of the CHO-PDMAEMA polymer. The polymer also shows promising values of viability in both cell lines studied (Table 1).

Table D.1: Cell viability after 48 h of incubation with the polymer. Values are expressed as a % of control cell and SD are given in brackets.

	Concentration (μg/mL)				
	0.1	**0.5**	**2.5**	**5**	**10**
3T3-L1	98.0 (5.3)	99.3 (5.3)	94.8 (6.7)	51.8 (7.9)	58.5 (6.4)
TSA	94.7 (5.9)	90.0 (8.2)	98.0 (6.0)	81.2 (15.7)	36.6 (23.5)

D.4   Discussion and conclusions

Results suggest a good control over of a CHO-PDMAEMA structure and good bio-compatibility. In addition, the RDRP method used employs mild reaction conditions and sustainable GlaxoSmithKline (GSK)-based solvents[6]. The method developed for the polymer synthesis can be viewed an interesting and attractive solution for pharmaceutical industry.

D.5   Acknowledgments

Bibliography

[1] L. Mespouille, M. Vachaudez, F. Suriano, P. Gerbaux, W. Van Camp, O. Coulembier, P. Degée, R. Flammang, F. Du Prez, and P. Dubois. Controlled synthesis of amphiphilic block copolymers based on polyester and poly(amino methacrylate): comprehensive study of reaction mechanisms. *Reactive and Functional Polymers*, 68(5):990–1003, 2008.

[2] H. Lee, S.H. Son, R. Sharma, and Y.Y. Won. A discussion of the pH-dependent protonation behaviors of poly(2-(dimethylamino)ethyl methacrylate) (PDMAEMA) and poly(ethylenimine-*ran*-2-ethyl-2-oxazoline) (P(EI-*r*-EOz)). *The Journal of Physical Chemistry B*, 115(5):844–860, 2011.

[3] J.F.J. Coelho, P.C. Ferreira, P. Alves, R. Cordeiro, A.C. Fonseca, J.R. Góis, and M.H. Gil. Drug delivery systems: advanced technologies potentially applicable in personalized treatments. *The EPMA Journal*, 1(1):164–209, 2010.

[4] R.A. Cordeiro, N. Rocha, J.P. Mendes, K. Matyjaszewski, T. Guliashvili, A.C. Serra, and J.F.J. Coelho. Synthesis of well-defined poly(2-(dimethylamino)ethyl methacrylate) under mild conditions and its co-polymers with cholesterol and PEG using Fe(0)/Cu(II) based SARA ATRP. *Polymer Chemistry*, 4:3088–3097, 2013.

[5] H. Faneca, S. Simões, and M. C. Pedroso de Lima. Association of albumin or protamine to lipoplexes: enhancement of transfection and resistance to serum. *The Journal of Gene Medicine*, 6(6):681–692, 2004.

[6] R.K. Henderson, C. Jimenez-Gonzalez, D.J.C. Constable, S.R. Alston, G.G.A. Inglis, G. Fisher, J. Sherwood, S.P. Binks, and A.D. Curzons. Expanding GSK's solvent selection guide - embedding sustainability into solvent selection starting at medicinal chemistry. *Green Chemistry*, 13:854–862, 2011.

Appendix D Evaluation of the biocompatibility of cho-PDMAEMA synthesized by ATRP